Proceedings of 5th International Electrical Engineering Conference (IEEC-2020)

Editor:
Dr. Muhammad Mohsin Aman
Associate Professor (NED UET)

2020 5th International Electrical Engineering Conference (IEEC 2020)
Feb, 2020 at IEP Centre, Karachi, Pakistan

Voltage Contingency Ranking of Pakistan National Grid in the vicinity of Nuclear Power Plant

Abdul Ahad, Naila Zareen, Moaz Ahmad, Muhammad Umer, Abdul Rehman Abbasi and Tauseef-ur-Rehman Khan*
Karachi Institute of Power Engineering (KINPOE) College,PIEAS
Karachi ,Pakistan.

*National Transmission & Dispatch Company
Lahore,Pakistan.

abdulahadqu@gmail.com, dr.naila.zareen@paec.gov.pk, moazahmad@ymail.com,
umerlive0@gmail.com, arehmanabbasi@paec.gov.pk, *r.tauseef@ntdc.com.pk

Abstract- To ensure safe control of power system, it is essential to assess the functionality of its components. Thus, to evaluate stability of Pakistan National grid, whole system is implemented in ETAP and Load Flow analysis is done to find the steady state parameters of whole system in normal condition. N-1 contingency analysis is performed to study the parameters after one component failure then voltage stability of region in the vicinity of nuclear power plants is evaluated using performance index which depicts not only voltages but also has relation with reactive power flows. This is done to ensure that nuclear power plant continue to export power in contingency condition as well. Modelled system provides a platform to perform transient stability analysis and fault analysis as well.

Keywords— Load flow; Newton Raphson; Nuclear Power Plant; Voltage Performance Index; N-1 Contingency.

I. Introduction

A. Power System Analysis

Electric energy is the most popular form of energy as it can be transferred easily at reasonable cost and at high efficiency and power system is the network which consists of components which are generating electric energy, transmitting electric energy and distributing electric energy to the consumers [1].

In an ideal power system, generation is always comparable to demand but in actual scenario, there is always an imbalance between power generated and power consumed. This requires certain actions from switching stations to keep the loads and generation equal otherwise system becomes unhealthy and inefficient. These actions may include shedding of loads or changing the state of generators at low power [2]. Thus to nullify these unhealthy condition of power system, grid is configured in such a way that a single variation in some component may not affect the stability of system. [3]

B. Nuclear Power Plant integration with National Grid

Given the complexities of NPP-electric grid interconnection like incapability to respond simultaneously to grid demand changes and requirement of continuous power supply from grid, it is imperative that operators of electric grids perform the proper electric power system simulation studies to study the effects of the system under both normal operating conditions as well as of events for a single faults (sudden losses of key transmission circuits or generating units). Key features to consider for these simulations include identifying the power system response in terms of voltage, physical limitations to prevent overloading transmission circuits, and the effects of automatic features such as automatic load shedding and emergency disconnects. To address concerns with confirming that the physically separate transmission circuits are indeed independent and proper prevention against scenarios in which the NPP is unable to provide long term core decay heat removal, several barriers from nuclear safety regulations and standards have been developed. These barriers include provision of either an immediately accessible power source or independent connection from an off-site electric grid, and/or provision of redundant and reliable on-site power systems based on emergency diesel generators [4].

C. N-1 Contingency Analysis

Contingency is actually an undesirable event in which we remove one component from the system, in case of N-1 contingency, and observe its response on the system [1].

The main focus of this work is the assesment of national power system security in terms of voltages.Therefore, Voltage Peformance Index is calculated on every selected contingency in the vicinity of nuclear power plant by using Newton Raphson Load Flow Method. National grid of Pakistan is analyzed using N-1 contingency analysis and each contingency is ranked using voltage performance index.Most severe contingency is then somewhat nullified by the proposed solution.

The rest of the paper is structured as follows:Literature Review is discussed in section II. Section III details the proposed methodology. The case study and the simulations results are given in section IV. Finally, conclusions and future scope of work are provided in section V.

II. Literature Review

In a power system, successful power system operation under normal three-phase steady-state conditions requires the following [5]:

- Generation supplies the demand (load) plus losses.
- Bus voltage magnitudes remain close to rated values.

- Generators operate within specified real and reactive power limits.
- Transmission lines and transformers are not overloaded.

To assure the above mentioned conditions, load flow analysis is done. In electrical power engineering, load flow analysis refer to power behavior calculation under different circumstances in an interconnected system. It tells us about the healthiness of grid by calculating parameter like bus voltages, real and reactive power flows and line losses. Power system load flow analysis determines the steady state operating condition which gives the idea about in which region generation should be increase and in which region load should be shed [6].

Transfer of power from generation side to load is done in a stable and reliable manner. It can be ensured theoretically by load flow studies. Two iterative method Gauss Siedel and Newton Raphson method are incorporated for load flow studies. These studies are the pre-requisites of all other studies which will be done in a power system afterwards [7].

Contingency Analysis (CA) is the continuation of load flow analysis. Contingency happens for unexpected open circuitry of the power transmission lines, generators tripping condition, sudden changes in power generation and unexpected changes in loads. CA offers tools for analyzing, creating, managing, and reporting lists of contingencies and violations [8].This analysis tells us about the most vulnerable components of grid whose outage may cause severe effects on operating parameters of grid.

In the process of contingency analysis, first we have to create contingency list that may happen in any power system then some of the contingencies are rejected based on their less severity and remaining faults are then quantified and ranked using a suitable performance index [9].

Ejebe and Wollenberg [10] made a huge contribution in contingency analysis in which faults or outages are arranged according to their severity based on the value of their performance index. They have analyzed the 11 bus and 22 bus system with typical thermal generator models.

Followed by the ranking concept, many researchers use different performance indices to rank the outages in their assumed grid as Sandeep Mohantee and Pudi Sekhar [11] use overall performance index to find the severity of any fault in components of their 5 bus system.

Similarly, Hajer Jmii, Asma Meddeb and Souad Chebbi [12] use the summation of active power performance index and reactive power index to evaluate the security assessment of IEEE 39 bus England system in a MATLAB environment.

Line outage Distribution Factor (LODF) is one of the linear sensitive factor which is used in the step of less severe contingency rejection in the process of contingency analysis as described above, is expended by Veenavati Jagadish [13].

In this work, selected region in the vicinity of nuclear power plant is analyzed and stability is evaluated to discover the weak component in that region which may hinder the operation of nuclear power plant.

III. METHODOLOGY

This work includes

- Study of single line diagram of national grid of Pakistan
- ETAP software learning
- Data amendment according to requirement
- Contingency Analysis and Performance Index(PI)-Voltage(V) calculation

Existing national grid of Pakistan has sixteen 500 KV and forty five 220 KV Grid Stations, 5893 km of 500 KV transmission line and 10963 km of 220 KV transmission line in Pakistan [14]. Types of generating units in Pakistan are diverse. There are thermal, nuclear, hydel, solar and wind power plants as well.

Data source required for the analysis of grid can only be available from NTDC previous works done in this regard thus from these sources of data, we have modelled our network. Data cleaning is performed as available data of transmission lines and loads are not in the form required by ETAP for simulation.

The main objective of the proposed approach is to rank all the probable contingencies so that we can identify the most severe ones. We propose the Newton-Raphson load flow based approach which is an offline method for solving the non-linear load flow equations. The results of the resolution provide information about the state of the system in particular the post-contingency buses voltages. Using these values, the voltage performance index (PI) is computed for different conditions particularly line losses in the vicinity of nuclear power plant.

A. Voltage Performance Index

Deviation of voltages on certain contingency in grid can be quantified by using voltage Performance index which is defined as [9]

$$\sum_{i=1}^{n}\left(\frac{W}{2z}\right)\left\{\frac{\left(|V_i|-\left|V_i^{sp}\right|\right)}{\Delta V_i^{lim}}\right\}^{2z} \quad (1)$$

Where,

W and z are constant which are taken as 1 here.

V_i is post contingency voltage of ith bus.

V_i^{sp} is the pre-contingency voltage

ΔV_i^{lim} is the deviation limit of voltage which is 0.05 for standard grid

B. Voltage Contingency Ranking

Different contingencies in our case study are ranked according to algorithm illustrated in Fig. 1.

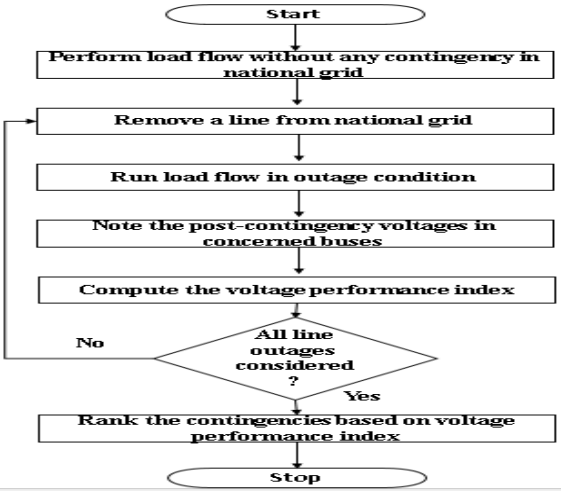

Fig. 1 . Flow chart of methodology

In this case study, we determine the weak links in the vicinity of northern region where four NPPs are located using N-1 contingency analysis. Concerned events where lines are lost are mentioned in table 1 then voltage performance index is evaluated using equation 1.Now lines are ranked according to the values of voltage performance index. Higher the PI-V, severe the contingency is. Once all the possible cases are considered, rank the selected contingencies in the descending order of severity. After ranking the contingencies, a solution is proposed to decrease the severity of contingency which is further validated using the simulation and voltage performance index calculations.

TABLE 1. CONCERNED EVENTS OF CASE STUDY

Event No.	Event Name
1	Line loss from unit1/2 to Ludewala
2	Line loss from unit3/4 to Ludewala
3	Line loss from unit3/4 to unit1/2
4	Line loss from unit1/2 to D.I.Khan
5	Line loss from unit3/4 to D.I.Khan
6	Single Circuit loss from unit1/2 to Daud Khel
7	Single Circuit loss from Daud Khel to Bannu
8	Single Circuit loss from unit3/4 to Bannu
9	Single Line loss from Daud khel to Peshawar

IV. CASE STUDY AND SIMULATION RESULTS

Number of cases were studied in ETAP for the load flow analysis. Each case depict a single circuit loss between two buses in the vicinity of selected region and then voltage profile is analyzed of each bus around that. With the help of pre contingency voltages and post contingency voltage, voltage performance index is calculated to quantify the applied outage. In this way, all events are studied and ranked in order of their severity. In this study, following load buses around the concerned region are considered

- Ludewala
- Daud Khel
- D.I Khan
- Bannu
- Peshawar

Before performance index calculation, load flow analysis is performed and pre-contingency voltages without any line loss in its normal condition are noted. Simulation of load flow analysis of concerned buses in existing network along with bus voltages is shown in Fig. 2.

We have implemented existing grid on ETAP including 132 kV which is illustrated in Fig. 3

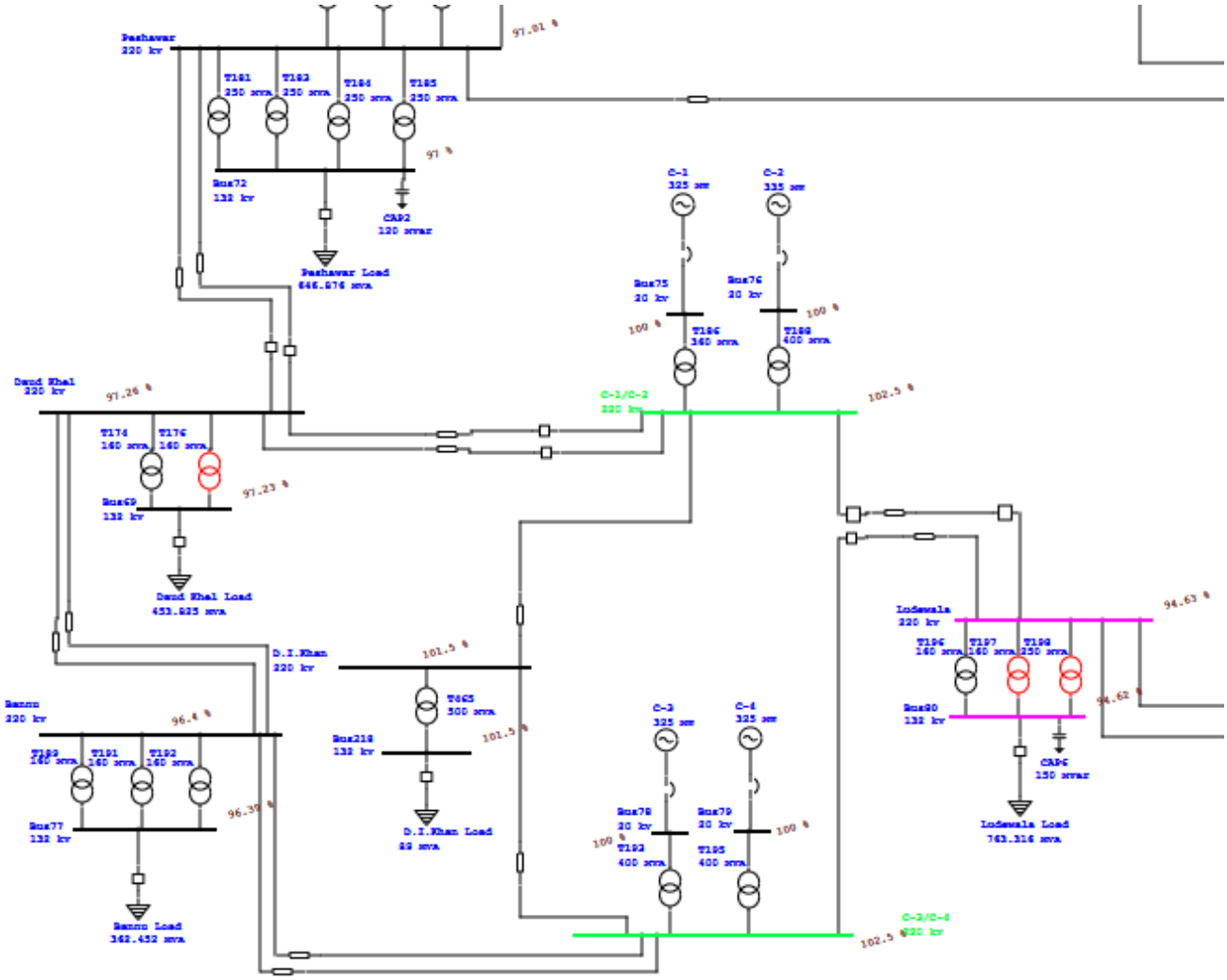

Fig. 2. Concerned Buses Voltages in Normal Conditions

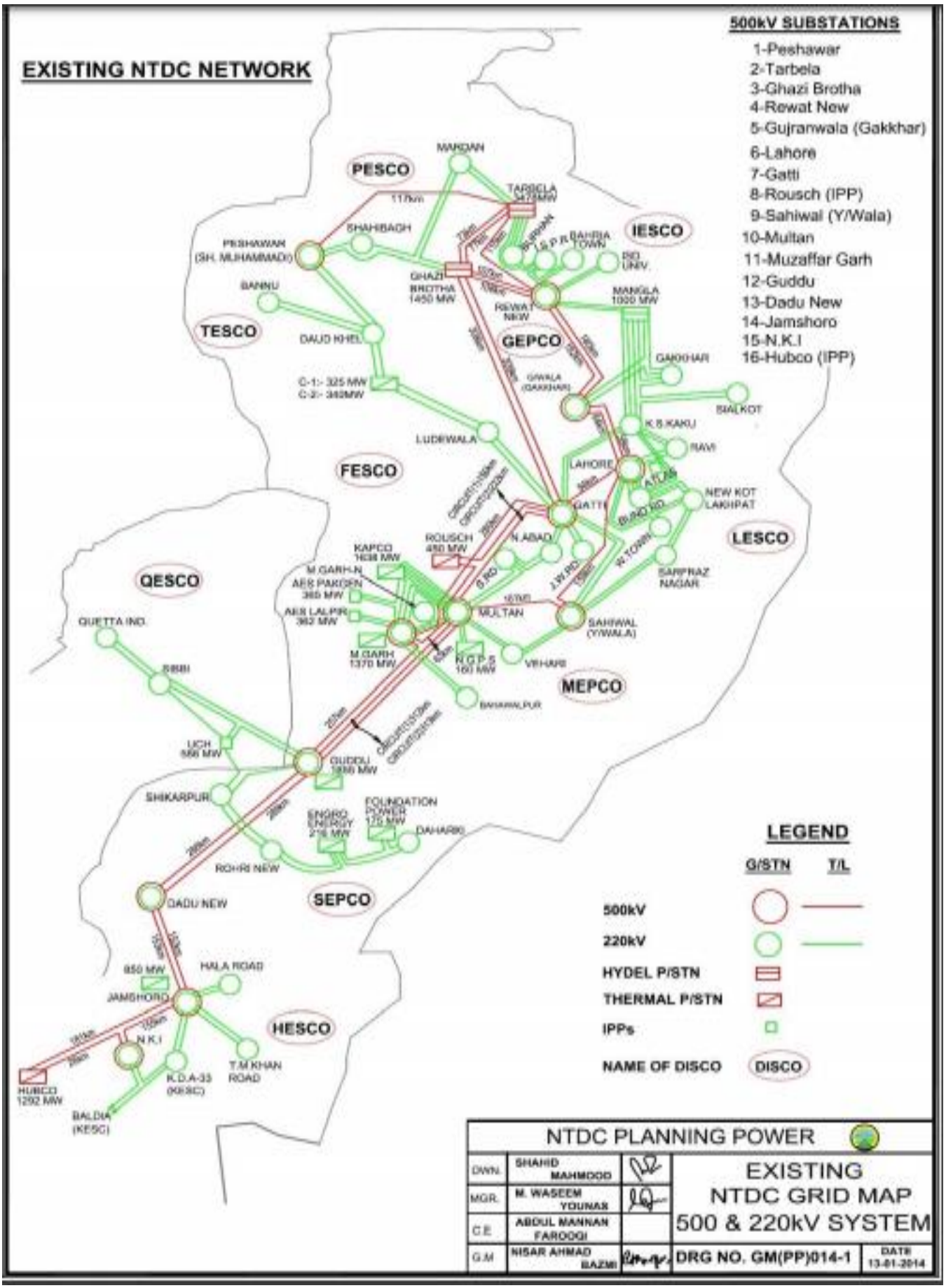

Fig. 3 Existing Transmission Network

A. Voltage Performance Index Evaluation

Calculation of voltage performance index is done by simulating certain line losses and by noting the pre-contingency voltages and post contingency voltages. These line losses or components losses are allotted event numbers which are given in Table 1.

On implementing these events on simulation, computed voltage performance index values are given in Table 2.

TABLE 2. VOLTAGE PERFORMANCE INDEX

Event No.	PI-V	Ranking
1	0.278828	2
2	0.28264	1
3	5.40E-05	9
4	0.05249	6
5	0.080008	5
6	0.161832	3
7	0.006378	7
8	0.159964	4
9	0.000476	8

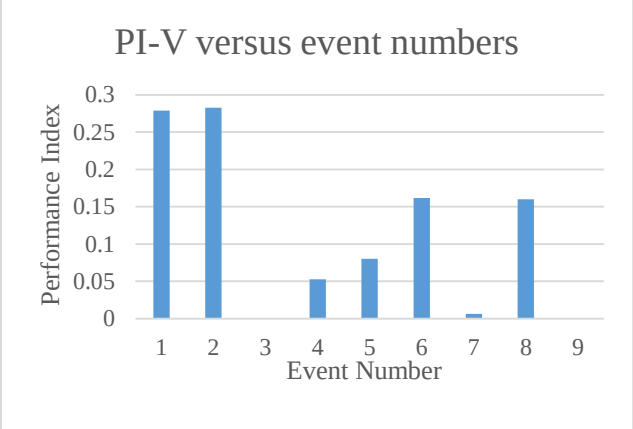

Fig. 4 .Values of voltage performance index corresponding to event number

Table 2 and Fig. 4 shows that according the voltage performance index ranking, the most severe contingency is the line loss from C3/C4 to Ludewala line and then at 2nd position, severe fault is the line loss from C1/C2 to Ludewala which means that Ludewala load bus is the most vulnerable component in the vicinity of nuclear power plant in existing national grid of Pakistan.

For clearly identifying the vulnerability in national grid of Pakistan, [15] explained the method of plotting a graph between index and exponent (z). It is explained that whichever graph for a certain contingency has more slope will be more vulnerable. Thus, to plot the trend, Voltage Performance Index is calculated for each value of z from equation 1 for every event

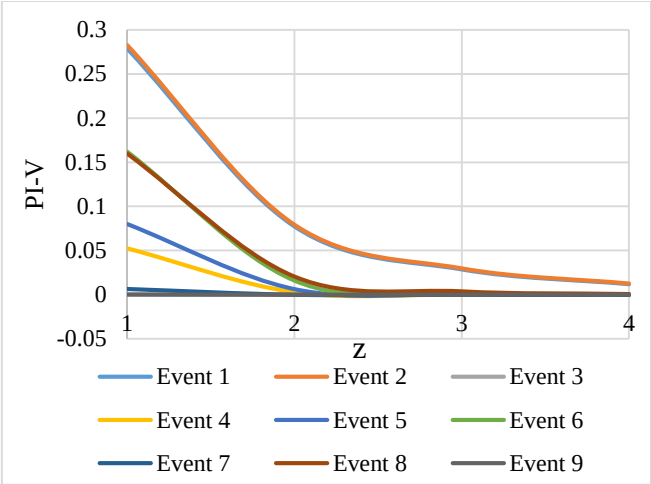

Fig. 5. Graph between Voltage Performance index and exponent

These values are plotted and results support our previous conclusion that event 2 is ranked first in severity while event 1 is ranked second as observed by the slopes in Fig. 5.

B. Proposed Solution

Solution to improve the condition of most vulnerable bus (Ludewala) with respect to voltages as proposed by national transmission and distribution company is the upgradation of Ludewala grid and implementation of transmission line from Ghazi Barotha to Ludewala. To confirm this, we have implemented this solution in simulation and then calculated the voltage performance indices for three most severe contingencies which according to table 2 are event 1,2 and 6. By implementation,we have seen that voltage performance index of three most sever contingencies are reduced as given in Table 3.

TABLE 3. IMPROVEMENT IN PI AFTER PROPOSED SOLUTION

Events		Previous Result	After Modification
Event#	**Event Name**	**PI-V**	**PI-V**
1	Line loss from unit1/2 to ludewala	0.27883	0.02
2	Line loss from unit3/4 to ludewala	0.28264	0.02
6	Single Line loss from unit1/2 to Daud Khel	0.16183	0.1468

Thus by implementation of proposed solution, it is clearly depicted by Table 3 and Fig. 6 that voltage stability has been improved and most vulnerable component which Ludewala load bus is no more vulnerable because voltage performance index is decreased

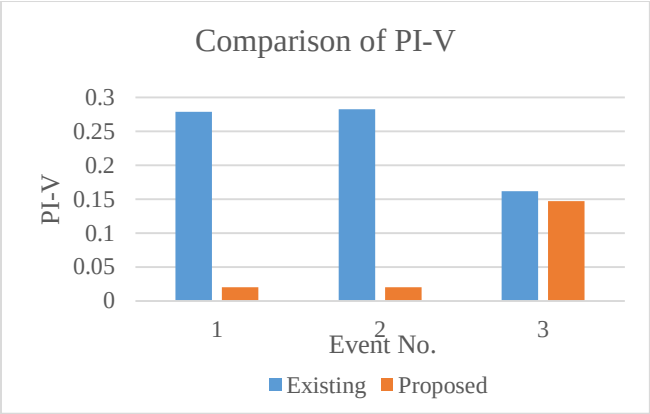

Fig. 6. Values of Voltage Performance Index corresponding to event number before and after event

V. Conclusion and Future Work

For different outages of single transmission lines, voltage performance index are different showing their vulnerability. According to voltage performance index ranking, the most severe contingency is the line loss from unit3/4 to Ludewala line and then at 2nd position, severe fault is the line loss from unit1/2 to Ludewala which means that Ludewala load bus is the most vulnerable component in the vicinity of NPPs which will severely affect the grid condition as well as the operation of selected region. This will cause not only the emergency shutdown of NPP but also decrease the life cycle of nuclear power plant. Most suitable proposed solution is to

- Upgrade the Ludewala grid to 500kV and implement a line from Ludewala 500kV to Ghazi Barotha 500kV .This solution is implemented in our simulation and results show significant improvements in voltage stability.

In future, complete circuit up to 11kV can be simulated and lumped loads at 132kV can further be distributed to get better and less approximated result. Voltage Profiles of buses of circuit can be improved by the optimum capacitor placement and FACTS devices usage. Transient Stability Analysis can be done to analyze the frequency response of nuclear power plants in existing national grid. Based on the study of transient stability within the vicinity of NPPs, its protective system and relaying system parameters can be determined.

References

[1] H. Saadat, Power System Analysis, New York: Mcgraw Hill, 1999.

[2] Archana, "Circuit Globe," [Online]. Available: https://circuitglobe.com/power-system.html. [Accessed 04 09 2019].

[3] "NEPRA," 1997. [Online]. Available: https://nepra.org.pk/Legislation/Rules/Performance%20Standards%20(Transmission)%20Rules%202005.pdf. [Accessed 11 10 2019].

[4] D. J. H. Bickel, "Grid Stability and Safety Issues Associated with Nuclear Power Plants," in *Evergreen Safety and Reliability Technologies*, 2001.

[5] J. Glover, M. S. Sarma and T. J. Overbye, Power System Analysis and Design, Stanford: Global Engineering:Christopher M. Shortt, 2012.

[6] T. Athay, "An Overview of Power Flow Analysis," p. 7, 1983.

[7] Dharamjit, "Load Flow Analysis on IEEE 30 bus system," *Internation journal of science and research*, vol. 2, no. 11, p. 6, 2012.

[8] I. R. Rajesh Ratnamony, "N-1 Contingency analysis in a Congested power system," *Internation Journal of Computer Technology and Applications*, vol. 7, no. 9, p. 11, 2016.

[9] S. Burada, D. Joshi and K. D. Mistry, "Contingency Analysis of Power System by using Active Power Performance Index," in *1st IEEE International Conference on Power Electronics. Intelligent Control and Energy Systems (ICPEICES-2016)*, 2016.

[10] G.C.Ejebe and B.F.Wollenberg, "Automatic Contingency Selection," *IEEE Transactions on Power Apparatus and Systems*, Vols. PAS-98, no. 1, p. 13, 1979.

[11] P. Sekhar and S. Mohanty, "Power system contingency ranking using Newton Raphson Load Flow Method," in *Annual IEEE India Conference*, 2013.

[12] H. Jmii, A. Meddeb and S. Chebbi, "Newton-Raphson Load Flow Method for Voltage Contingency Ranking," in *15th International Multi-Conference on Systems, Signals & Devices (SSD)*, 2018.

[13] V. j. mishra and M. D. Khardenvis, "Contingency Analysis of Power System," in *International Conference on Emerging Frontiers in Technology for Rural Area*, 2012.

[14] M. M. Hamid, "NTDC," 30 06 2017. [Online]. Available: http://www.saarcenergy.org/wp-content/uploads/2018/05/Pakistan-Power-Sector-Country-Presentation-by-Mian.-Muhammad-Hamid.pdf. [Accessed 22 09 2019].

[15] S. Eldeen, A. Abbas and Y.Rahim, "Power System Contingency Analysis to detect Network Weaknesses," in *Zaytoonah University International Engineering Conference on Design and Innovation in Infrastructure 2012*, Amman,Jordon, 2012.

2020 5th International Electrical Engineering Conference (IEEC 2020)
Feb, 2020 at IEP Centre, Karachi, Pakistan

Experimental-Based Performance Evaluation Of Photovoltaic Solar System

Ahmad Rafay Asad[1] , Muhammad Riaz[2*] and Rabia Attiqa[3*]

[1] Department of Electronics and Electrical Systems, The University of Lahore, Islamabad, 44000, Pakistan (ar.scholar2019@outlook.com)
[2,3] Department of Electronics and Electrical Systems , University of Lahore, Islamabad, 44000, Pakistan (Muhammad.riaz@es.uol.edu.pk) * Corresponding author

Abstract: Conversion of solar energy into electrical energy is a very useful technique by knowing that such source of energy is cost-free and environmental friendly in almost all countries of the world. With the increase in demand of electricity, the world is now bending to bring in use renewable energy systems to overcome the shortage of electrical power. The main disadvantage of the photovoltaic (PV) solar system is its lack of performance. Performance and life span of the Photovoltaic module is affected due to rise in temperature. There are so many other factors which affect the performance of the PV system such as shading, wire & inverter losses etc. Now-a-days, the efficiency of a solar panel is not more than 22 percent. It means that a whole system only convert 22% of sun light into electrical energy. This paper analyzed the performance of the PV solar system. We utilize a PV solar system consisting of two arrays of polycrystalline panels inclined at angle of 22˚. This experimental study focuses on various environmental factors and losses like temperature, shading and inverter losses etc. on PV solar system. We present various results on the basis of available data from the metrological department of Pakistan and measurement campaign.

Keywords: Photovoltaic, renewable energy, performance, solar energy, polycrystalline.

I. INTRODUCTION

Energy demand in the world is rapidly increasing day by day. To meet such energy demand, a huge amount of fossil fuels are needed, unfortunately due to limited resources of the fossil fuels it is being very difficult to fulfill such a high energy demand. By taking the advantage of this scenario, renewable energy systems started capturing the world's market rapidly. The renewable energy system has many advantages over fossil fuel as well as disadvantages, but the main disadvantage of the renewable energy system is its performance ratio. While talking about the photovoltaic renewable energy systems, it is the very essential and clean form of energy. It has many advantages such as no by-products, inexpensive, need only capital cost, has no maintenance cost etc. Renewable energy system directly converts the energy into useful form no thermal or any other process is need for conversion. But the worst part, the efficiency of the solar panel is not more than 22% and practically this efficiency rate may not be achievable because of several environmental and system losses such as low irradiance, temperature, dust, shading, inverter and many more.

Several studies has been conducted in past years to analyze the parameters of climate which directly influences the performance of photovoltaic system. González-Longatt, 2005, Gwinyai Dziman 2008, Mustapha et al. 2013, presented the new methodologies and techniques to evaluate and determine the I-V curve characteristics of PV system [1-3]. These all previous studies concluded that the effect of climate parameters on the photovoltaic system such as temperature and solar irradiance has to be measured and examined to increase the performance of the system. In [2], according to the authors, there are two main parameters that effect the performance of a photovoltaic solar system are variation in panel temperature because of climate ambient temperature and variation in solar irradiance. With the increase in temperature it is clearly noticed in the reduction of open-circuit voltage (Voc). And with the increase in cell temperature the significant change can be seen in the output power of the photovoltaic solar system. On the other hand the variation in solar irradiance has major and dominant effect on the performance of solar system. Same as the increase the temperature effect the open circuit voltage, the decrease in solar irradiance will affect the short circuit current which decrease the system performance. [3] Crystalline, amorphous and thin film are the three types of photovoltaic panels which has high performance ratio, efficiencies and most reliable. The performance of the photovoltaic solar modules depends on some climate parameter such as solar irradiance, climate and module temperature. Therefore, during system installation the best knowledge of site and climate parameter are kept in mind. The designing and installing mistake will lead in low performance. Many photovoltaic modules have low performance ratio at site because of variation in climate parameters. Mustapha Used newton rapson method to solve the nonlinear equations. [4]As discussed earlier that the output power of the photovoltaic module depends on the solar irradiation. But during installation the ignorance of shading areas such as trees, fences etc. will affect the output power. The photovoltaic array can also be shaded by the neighbor arrays. These will cause the undesirable effects (a) generated real power from the photovoltaic system will fall [5], [6]. (b) Because of shaded area on the photovoltaic system will cause the long term performance loss [7], [8]. There are many proposed systems to overcome the shading effects on the

photovoltaic solar system by using appropriate configuration [9] or by using a reconfigurable photovoltaic arrays [10]. In order to evaluate the shading effect on photovoltaic solar system, a conventional method has introduced "shading factor" which is defined as the ratio of non-shaded area divided by the total area of the system. But practically it is difficult to accurately calculate the total shading factor. Researchers and scientists are trying to find the accurate method through which the actual shading factor can be calculated. Some uses numerical estimation [9], [10] and photogram metric method [11]. Other methods used neutral networks [12] to relate the climate factors with the output maximum power of the photovoltaic system. Neutral network methods has been proposed to track output maximum power and standalone photovoltaic solar system [13], [14]. Many more researches has been conducted for the assessment of environmental effects on performance of photovoltaic system. The purpose of these researches is to study the effects of dust, shading and color on the performance of the system. As the dust accumulation on the panels is a natural process. The dust on the panels resist the solar irradiation to pass through it. This will cause the decrease in output power and reduced in system efficiency [15]. According to the color assessment it is noticed that photovoltaic panels are more influenced by the red light. Many more researches has been conducted for the assessment of environmental effects on performance of photovoltaic system. The purpose of these researches is to study the effects of dust, shading and color on the performance of the system. As the dust accumulation on the panels is a natural process. The dust on the panels resist the solar irradiation to pass through it. This will cause the decrease in output power and reduced in system efficiency [15]. According to the color assessment it is noticed that photovoltaic panels are more influenced by the red light. Another factor that reduces the efficiency and performance ration of the photovoltaic system is overheating, this is because of high temperature and extreme level of irradiance [16]. The characteristic curve between P-V is obtained when the solar irradiance and the temperature of the module is kept constant. If one of these parameters varies the output power of the system will decrease. To avoid the overheating effect the cooling techniques are used. In this technique water or air circulates through panels to avoid overheating [17].

This paper proposes the methodology for the performance evaluation of the polycrystalline photovoltaic system including the all major losses such as temperature losses, solar irradiance losses, and inverter losses, dust losses, shading losses and overheating losses. The installed solar system is of polycrystalline type with the total capacity of 12Kw. Two arrays of 48 panels with 250 watt of each panel. The 10Kw of hybrid inverter which has the capacity of Data acquisition with grid connected option.

In this research all the climate parameters such as solar irradiance, ambient temperature, module temperature etc. are measured, these are essential for performance evaluation of a photovoltaic solar system. These parameters are examined on daily and monthly basis. Experimental results are generated with the help of measured data which is taken several times at the Climate change alternate energy institute, National Agriculture Research Center Islamabad. The purpose of the research is to analyze the data and try to minimize the amount of losses which influences the decrease in performance ratio of photovoltaic system.

Table 1: Nomenclature

PV	Photovoltaic
PR	Performance ratio
P_out	Output power
Irr	Irradiance
Irr_stc	Irradiance at standard temperature condition
L_T	Temperature losses
L_inv	Inverter losses
L_other	Other losses
Tc	Cell temperature
P_in	Input power
P_max	Maximum power

II. METHEDOLOGY

In order to perform research, the data is directly extracted from the PV solar panels and inverter by using the following equipment's:

- Solar PV analyzer(HT I-V 500)
- Solar-02 and irradiance meter
- Multi-meter and clamp meters
- Temperature sensors

A. Performance ratio calculation

The whole research is carried out for the performance evaluation of the system. The performance of the system can be calculated as the ratio of measured output power to theoretical power at any irradiance.

$$\boldsymbol{PR} = \frac{\sum \boldsymbol{P_{OUT}}}{\frac{\boldsymbol{Irr}}{\boldsymbol{Irr_{STC}}}} \times \sum \boldsymbol{P_{\frac{max}{STC}}} \quad \textbf{(1)}$$

$$\boldsymbol{PR} = \frac{\left(\frac{\boldsymbol{Irr}}{\boldsymbol{Irr_{STC}}}\right) \times \sum \boldsymbol{P_{\frac{max}{STC}}} - (\boldsymbol{L_T} + \boldsymbol{L_{invr}} + \boldsymbol{L_{other}})}{\left(\frac{\boldsymbol{Irr}}{\boldsymbol{Irr_{STC}}}\right) \times \sum \boldsymbol{P_{\frac{max}{STC}}}} \quad \textbf{(2)}$$

B. Losses computation

All the possible losses are computed according to their systems working nature.

a) Temperature losses

Temperature losses plays the significant role in decreasing performance of PV system. The temperature loss can be calculated by the following equation.

$$L_T(\%) = \frac{\left(\frac{\gamma}{100}\right) \times (25 - T_c)}{\left(1 + \frac{\gamma}{100}(25 - T_c)\right)} \times 100 \quad (3)$$

b) Power decrease due to low irradiance

Another main factor in decreasing performance is the low irradiance. Solar irradiance is the input of solar module. As the input decreases automatically the output or efficiency of the system decreases. Theoretically it can be calculated as:

$$\boldsymbol{L_{Irr} = P_{max.STC} - \left(\frac{Irr}{(Irr)_{STC}}\right) \times P_{max.STC}} \quad (4)$$

c) Inverter losses

Power losses are noticeable during the inversion process of DC to AC in inverter. These losses can be calculated by;

$$L_{Inv}(\%) = \left(\frac{\sum P_{OUT}}{\sum P_{IN}}\right) \times 100 \quad (5)$$

d) Other losses

There are also some minute losses due to dust, shading, wiring etc. Sometime these losses are as minute that they can be negligible but in the case of performance evaluation these losses may not be negligible. These can be calculated as follow;

$$\boldsymbol{L_{other} = P_{max} - (P_{out} + L_T + L_{inv} + L_{irr})} \quad (6)$$

The Fig.1 shows the flow chart for the performance evaluation.

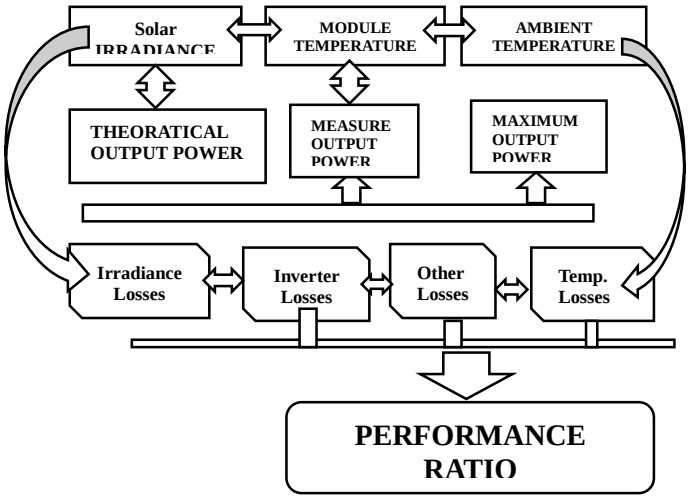

Fig. 1 Performance evaluation flow chart

III. RESUT ANS DISCUSSION

By keeping the above methodology in mind the data was collected and evaluated on daily and monthly basis. After this tiring analysis these results were concluded. Now starting from the module working, the thing come first is filling factor, according to the evaluation it is found that the filling factor of the installed system is 77.5%.

Table 2: Technical specifications of PV panels

1	Capacity of a PV panel=255W
2	Total installed capacity= 12KW
3	Open circuit voltage= 37.9
4	Short circuit current= 8.79
5	Operating voltage = 30.6
6	Operating current = 8.50
7	PV module type Telesun tp-660 255 Wp
8	Weight of a plate = 18.6Kg

The Fig.2 shows the graphical representation between the

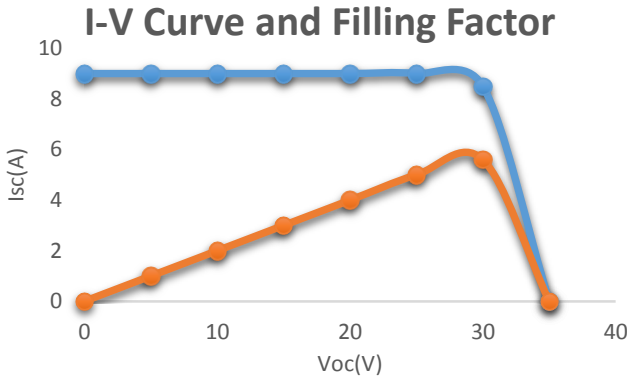

Fig. 2 I-V Curve and Filling Factor

I-V curve and filling factor.

According to the graphical representation the area lies under the P_{max} lines is 77.5% that shows the module lies in the class A w.r.t the filling factor. Similarly, relation between the Module temperature and the solar irradiance are shown in Fig.3. The graph shows the variation of solar irradiance and module temperature on back side. It shows that with the increase in irradiance the module temperature increases. And some points at low irradiance

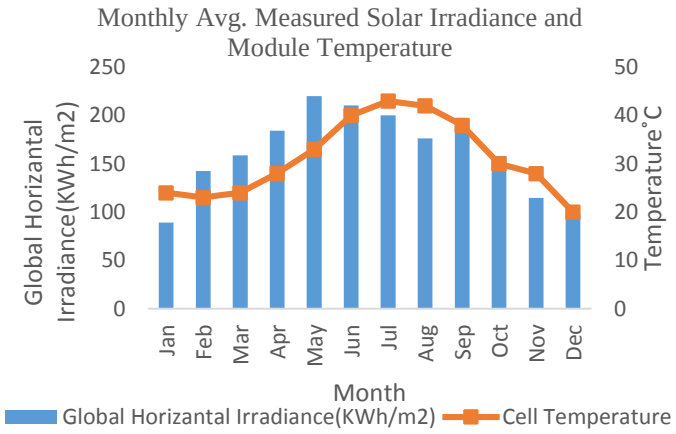

Fig. 3 Global Irradiance and Module Temperature

Table 3: Performance comparison of PV solar systems in different countries

Location	Rated Capacity (KWp)	Type of PV Technology	System Efficiency (%)	Performance Ratio (%)
Khatkar-Kalan, India [18]	190	Polycrystalline	8.3	74
Crete, Greece [19]	171.36	Polycrystalline	-	67.36
Islamabad, Pakistan [proposed]	12	Polycrystalline	15	70.9
Dublin, Ireland[20]	1.72	Mon crystalline	12.6	81.5

has high cell temperature. This is because of the wind speed, wind direction, humidity in air etc.

On the other hand, Fig.4 shows the relation between ambient temperature and cell temperature. It shows the average is module and environment temperature on monthly basis. As it clearly shown that the module temperature is always high from the environment temperature.

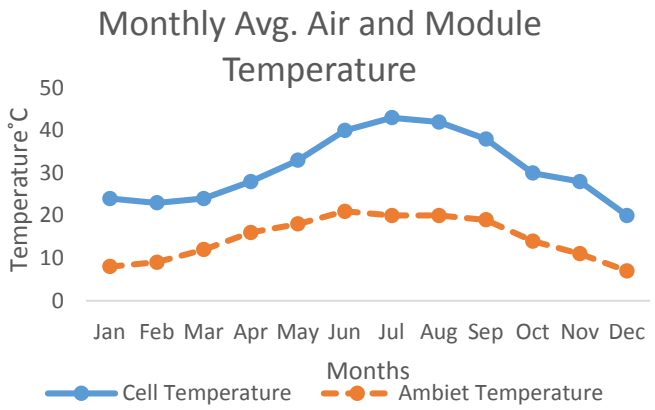

Fig. 4 Ambient Vs Module Temperature

The total capacity of the installed solar system at CAEWRI is 12KW. The below graph shows that the monthly average output of the PV system. And Fig.5 shows the monthly variation on the system and array efficiency.

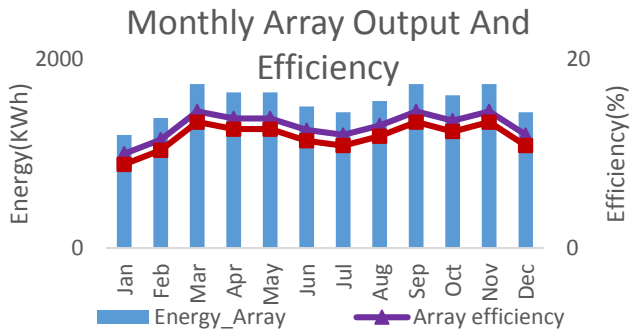

Fig. 5 Monthly Array and Efficiency

With the help of yearly data it is calculated that the average array efficiency throughout the year is not more than 15.8% and the system efficiency is 15%. On the calculation of losses it is found that the temperature and inverter losses has more dominant effect on the performance of a system. Fig.6 shows the graphical representation between the performance ratio and the losses.

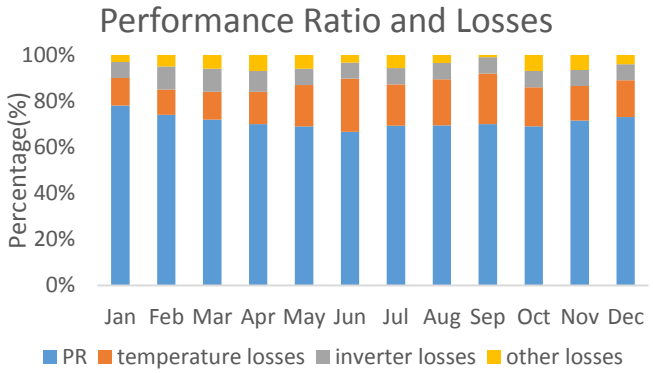

Fig. 6 Avg. Performance Ratio and Losses

With the help of graph, it concluded that the installed system has the maximum performance of the system is 78% and the minimum performance is 66.7% with included losses ranges between 22-33% during the evaluation period. The average performance of the system is 70.9% with the temperature losses are 7.6%, inverter loss are 16.5% and the other losses are 4.8%. The Fig.7 shows the pie chart of performance and losses.

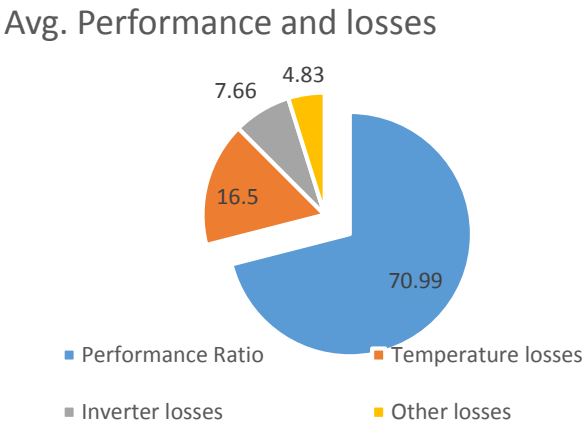

Fig. 7 Avg. Performance and Losses

IV. CONCLUSION

The performance of the particular photovoltaic system is evaluated experimentally under summer days in National Agriculture Research Center, Islamabad. The PV solar system is consist of two arrays, each contains 24 plates of polycrystalline material. The maximum capacity of the installed system is 12KW. Experimental result shows that the temperature, dust on module, wiring material, humidity in air, wind speed and direction are the functions of the performance. Solar irradiance is the important function of the system efficiency but does not play any significance role in the evaluation of system performance. The losses of the system from the nature like solar irradiance cannot be controlled but on the other hand the raising temperature of the module can be controlled by using some effective techniques like cooling mechanism etc. The inverter losses of the system are generally low but they losses can be reduced by using hybrid inverter or by using efficient converters. Accumulation of dust on the panels is a natural process and it cannot be controlled but with continuous monitoring and cleaning of panel's surface the dust losses can be controlled. It is very difficult to monitor and clean the panels from dust in large scale installed system so to overcome this problem the automatic dust remover and panel cleaning system should installed through this system the user is able to solve their time as well as their work load. With continuous monitoring of the system these error and losses occurs because of environment and other factors can be minimized.

REFERENCES

[1] Francisco M. González Longatt, 2005, Model of P hotovoltaic Module in Matlab™,

[2] Gwinyai Dzimano, B.S, 2008, "Modeling of photo voltaic systems", pg 62-68.

[3] Mustapha I., Dikwa M. K., Musa B. U. and Abbag ana M., 2013, Performance evaluation of polycryst alline solar photovoltaic module in weather conditi ons of maiduguri, nigeria.

[4] Dzung D. Nguyen, Brad Lehman, Sagar Kamarthi, Ph.D, Performance Evaluation of Solar Photovolt aic Arrays Including Shadow Effects Using Neural Network

[5] Kosuke Kurokawa "Energy from Desert" 2003, IS BN 1 902916417

[6] V.Quaschning and R. Hanitsch, "Numerical simula tion of current voltage characteristics of photovolt aic systems with shaded solar cells," Solar Energy, vol. 56, no. 6, pp. 513–520, 1996

[7] Ward T. Jewell, M Timothy D. Unruh, "Limits on Cloud-
Induced Fluctuation in Photovoltaic Generation", I EEE Transactions on Energy Conversion, Vol. 5, No. 1, March 1990.

[8] Dan Weinstock, Joseph Appelbaum "Shadow Vari ation on Photovoltaic Collectors in a Solar Filed". 23rd IEEE Convention of Electrical and Electronic s Engineers, 2004.

[9] Narendra D. Kaushika and Nalin K. Gautam "Ener gy Yield Simulations of Interconnected Solar PV Arrays", *IEEE Transaction on Energy Conversion*, vol. 18, no. 1, pp. 127-134, March 2003

[10] Guidelines for Monitoring Stand Alone Photovoltaic Systems: Methodology and Equipme nt iea-pvps.org.

[11] Satsuki Ike , Kosuke Kurokawa ," Photogrammerti c Estimation of Shading Impacts on Photovoltaic Systems", in *Proc. IEEE Conference on Photovolt aic Specialists*, 2005

[12] A. Mellit, M. Benghanem, A. Hadj Arab, A. Guess oum, K. Moulai "Neural Network Adaptive Wavel ets for Sizing of Stand-Alone Photovoltaic System," IEEE International C onference on Intelligent Systems, June 2004.

[13] Nobuyoshi Mutoh, Takaoshi Matuo, Kazuhito Oka da, Masahiro Sakai, "Prediction Data-Based Maximum Power Point Tracking Method fo r Photovoltaic Power Generation System," IEEE P ower Electronics Specialists Conference, Vol. 3, 2 3-27 June 2002.

[14] Takashi Hiyama, Shinichi Kouzuma, Tomofumi Imakubo, "Identification of Optimal Operating Point of PV Modules using Neural Network for Real Time Maximum Power Tracking Control," IEEE Transaction on Energy Conversion, Vol. 10, No. 2, Jun 1995.

[15] Rajeshwari Bhol, Arjyadhara Pradhan, Ritesh Das h, S.M Ali, 2015, Environmental effect assessment on performance of solar pv panel.

[16] A. Akbarzadeh, T. WadowskiHeat-pipe-based cooling systems for photovoltaic cells under concentrated solar radiation, Appl Therm Eng, 16 (1) (1996), pp. 81-87

[17] K.A.Moharram, M.S.Abd-Elhady, H.A.Kandil, H.El-Sherif, 2013, "Enhancing the performance of photovoltaic panels by water cooling".

[18] Vikrant Sharma, S.S. Chandel, Performance analy sis of a 190 kWp grid interactive solar photovoltai cpower plant in India 2013, Elsevier Ltd.

[19] Ahmed YAHFDHOU, Abdel Kader MAHMOUD and Issakha YOUM, Evaluation and determination of seven and five parameters of a photovoltaic ge nerator by an iterative method.

[20] A. A. Zadeh and A. Rezazadeh, Artificial bee swar m optimization algorithm for parameters identifica tions of solar cell modules, Applied Energy 102, 9 43-949, 2013.

2020 5th International Electrical Engineering Conference (IEEC 2020)
Feb, 2020 at IEP Centre, Karachi, Pakistan

Design and Prototype Development of Vehicle Safety Alarm System Using Digital Microchips for Both Seat Belts and Doors

Waqas Ali[1*], Mohsin Jamil[2], Usman Ali[3], Haroon Farooq[4], Muhammad Arslan Yousaf[5] and Samreen Arif[6]

[1,4,5,6] Department of Electrical Engineering (RCET Campus), University of Engineering and Technology, Lahore, 54890, Pakistan (waqas.ali@uet.edu.pk)[1] * Corresponding author, (haroon.farooq@uet.edu.pk)[4], (mughalarslan502@gmail.com)[5], (samreenarif501@gmail.com)[6]

[2] Department of Electrical and Computer Engineering, Memorial University of Newfoundland, St. John's, NL A1C 5S7, Canada (engrdrmohsin@gmail.com)

[3] Department of Electrical Engineering, Information Technology University, Lahore, 54600, Pakistan (usmanali@itu.edu.pk)

Abstract: Motor vehicle accidents or crashes are one of the leading cause of deaths and injuries worldwide and the Pakistani share in the total death toll is extremely high which is about three million per year. One of the main reasons behind this the majority of the automobiles used in the country are lack of safety features and warning system and those who have, do not meet the safety standards. The seat belts and doors safety and their warning systems are an important part of vehicle and research has shown that these safety systems reduce the chances of accidents and decrease the possibilities of fatal injuries. But unfortunately, in Pakistan, some automakers do not provide the safety features including warning systems in their automobiles in order to lessen the price of the vehicle and few that incorporate safety systems in their vehicles, have many limitations. Therefore, the aim of this project is to propose a simple and low-cost design of vehicle safety warning system for both seat belts and doors by using digital microchips. The proposed design is more intelligent than the earlier or that are currently in vehicle's used in Pakistan as it warns and exactly displays which seat belt/belts and door/ doors is/are not buckled up and correctly closed respectively.

Keywords: Vehicle, Road Crash, Accident, Seat Belt, Door, Safety, Alarm, Warning, System, Death, Fatal, Injuries.

I. INTRODUCTION

The motor vehicles are regarded as one of the best ways of transporting human beings from one place to other. But they also have the potential of endangering human lives in the form of road traffic crashes or accidents. The road traffic accidents are the eighth leading cause of deaths and injuries in the world among those aged 15-29 years [1, 2], and they are escalating day by day throughout the world. The World Health Organization (WHO) reported that approximately 3500 lives are lost every day due to road traffic injuries, about 1.24 million deaths each year, globally [3]. Additionally, 20-50 million people sustain non-fatal road traffic injuries and contribute to disability worldwide [4].

The deaths and injuries due to road crashes or accidents leave irreparable financial and social impacts on the communities to which victims belong to. The low and middle income countries are drastically suffered by these road accidents which are estimated to cost 1-2% of their gross national product annually [5]. Pakistan is also among low and middle income countries sharing about 90% of global road death toll, with fatality rates of 17.4 fatalities per 100,000 population per year [6]. Although total prevention of traffic collisions is not possible, minimizing harmful effects of those collisions on motor vehicle users is possible using protective devices like seat belts. Seat belts are one of the primary safety features used in vehicle to avoid major injuries to the driver driving the vehicle as well as other occupants during road crashes. The use of seat belts has been proven to be one of the most effective ways to reduce the risk of fatal injuries for front seat occupants by 40–50% and 25–75% for rear seat occupants during an accident [1, 2, 7, 8]. Studies have also shown that during accidents, the use of seat belts prevents certain types of injuries (especially head and facial injury) to vehicle occupants or mitigates their severity [1]. This is due to the fact that seat belts distribute the forces of rapid deceleration due to any sudden change in direction, stop or crash, over larger and stronger parts of the human body, such as the chest, hips and shoulders [2].

The doors of the vehicles are the significant part of the vehicle that sometime also cause the crash of motor vehicle when not close properly. Upon sudden brake conditions, the improperly closed door easily open and can hit to the nearby vehicle or motor bike and lead to a severe accident. The motor bikes also known as auto bikes are very welcome and popular in Asian countries. According to a report in 2010, in Pakistan alone, motorcycles made up about 50% of the country's registered vehicles [5, 6]. Statistics indicate that many crashes have been happened in Asian countries between the auto bikes and motor vehicles due to suddenly open of vehicle's door which was not properly closed [9].

The research indicates that in the modern world like UK, the inclusion of different safety features and warning system in vehicles reduces the chances of accidents and decreases the possibilities of fatal injuries in case of crashes [10, 11]. But unfortunately, in the low and middle income countries like Pakistan, some vehicle's manufacturer does not provide the safety features including warning systems in their automobiles in order to avoid the increase in the vehicle price and few automakers that incorporate safety systems in their vehicles, have many limitations and do not meet the safety standards. Thus, the purpose of this project is to design and develop an integrated vehicle safety warning system for both seat belts and doors. The proposed system is simple and low-cost due to the use of digital microchips for its implementation. Moreover, the system is propounded, is more intelligent as it warns and exactly shows which seat belt/belts and door/doors is/are not fastened and rightly closed respectively. While, the systems that are currently in vehicle's used in Pakistan, lack of these features in their safety warning systems.

II. PROBLEM STATEMENT AND ITS SOLUTION

The Pakistan, one of the emerging economies in the world has a large number of vehicles running on the roads and many are finding new homes every day. The fifth most populous country also witnesses a lot of accidents daily that claims the highest number of road fatalities in the world. The WHO in 2013 estimated that approximately 30,131 people die in road crashes annually on Pakistani roads [3]. The most casualties are caused to two-wheeler riders and pedestrians, the number of car occupants in fatal crashes too is going up. The one of the reasons for more people dying in a metal box on wheels is that they do not buckle up or wear seat belts and often forget to close the vehicle's door properly. Despite such scary statistics, people can be seen driving without their seat belt on and this ignorant nature not only puts an individual to risk but also endangers his/her family also. The average seat belt use rates in the country is 20% with the highest on motorways (53%) and the lowest on rural roads (5%) [1]. Unawareness of the usefulness, lack of law enforcement, seat belt not fitted, discomfort, forgetfulness, low speed, and careless attitude are the major reasons for not wearing seat belt among Pakistani drivers. It is shocking to note that the automakers in the country offered driver and front seat passenger seat belts only while they did not simply exist for rear passengers [12]. The cheaper options in country market even came without driver seatbelts for a long time. Unfortunately, in the country majority of the vehicles currently in used do not comply with the safety standards. Most of the automobiles do not have warning system for seat belts and doors. While, few have for driver's seat only, but it misses from door safety which is not appropriate and does not meet the standards. This is all because to reduce the price of the vehicle.

The fatality rate due to the vehicle's road collisions has decreased in the last few years in the modern and developed countries because of the combination of a variety of safety factors like vehicle crash safety, seat belt safety, door safety and different types of warning systems [10, 11]. Therefore, this paper presents the simple, low-cost and intelligent design of a vehicle's safety warning system for both seat belts and doors for Pakistani automobile industry and vehicle users.

III. STATISTICAL SURVEY OF SAFETY FEATURES

Table 1 illustrates the data of a survey which is conducted to find the safety features of locally assembled different vehicles that are currently most

Table 1: Statistics of Safety Features of Locally Assembled Vehicles in Pakistan (Model Years: 2012-2016)

Safety Features \ Vehicle			HONDA		TOYOTA		SUZUKI	
			Civic	*City*	*Corolla GLi*	*Corolla XLi*	*Mehran*	*Cultus*
Seat Belt Safety	Seat belt provided	For front seats only	✗	✗	✗	✗	✓	✓
		For both front & rear seats	✓	✓	✓	✓	✗	✗
	Seat belt indication on dashboard display if not fastened	Single indication for front seats only	✓	✓	✓	✓	✗	✗
		Separate indication for each seat belts	✗	✗	✗	✗	✗	✗
	Seat belt warning alarm if not fastened		✓	✓	✓	✓	✗	✗
Door Safety	Door opening indication on dashboard display if not closed including bonnet & dicky	Single indication for all doors including bonnet & dicky	✓	✓	✓	✓	✗	✗
		Separate indication for each door	✗	✗	✗	✗	✗	✗
		Separate indication for bonnet & dicky	✗	✗	✗	✗	✗	✗

(✓) indicates feature exists.
(✗) indicates feature does not exist.

used in Pakistan. In this survey, the vehicles for model year from 2012 to 2016 are considered only because these vehicle's model range are frequently found on Pakistani roads.

IV. PROPOSED SYSTEM DESIGN

A. Design Methodology

For the design of intelligent integrated safety warning system for four seat belts and four doors vehicle (two for front and two for rear seats) including hood (bonnet) and trunk (dicky) lids, the following methodology is adopted which is as follow.

1). For seat belt safety, the two inputs are considered for each seat belt i.e. one from seat pressure and other from seat belt. The signal input for seat pressure is sensed using pressure sensor which is fitted at each seat of the vehicle as shown in Fig. 1(a). While the seat belt signal input is taken through a push button switch which is installed in the buckle of each seat belt as shown in Fig. 1(a). The LED light glows, and buzzer sounds if driver/passenger present on seat and not fastened the seat belt.

2). For door safety, single input is considered for each door including bonnet and dicky. The signal input from door is taken through a push button switch which is installed near the closing lock of each door as shown in Fig. 1(b). The LED light glows, and buzzer sounds if the door is opened.

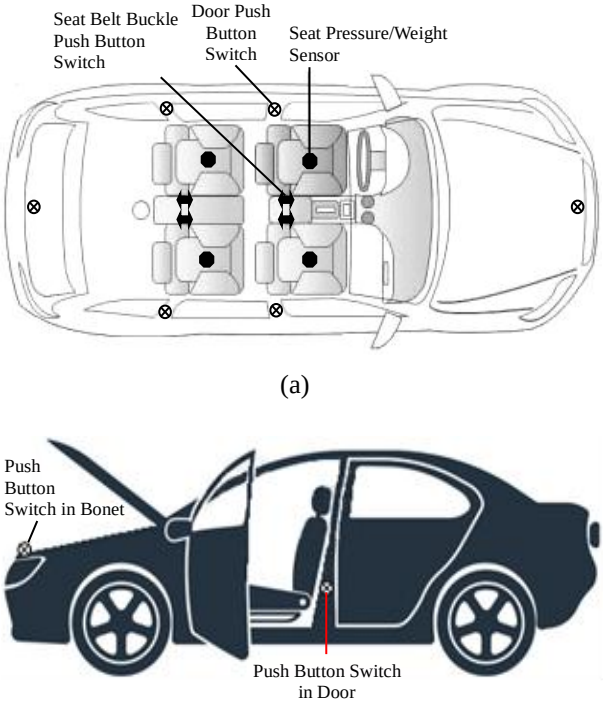

Fig. 1: Sensors and push buttons location in vehicle: (a) Top-veiw of vehicle, (b) Side-veiw of vehicle.

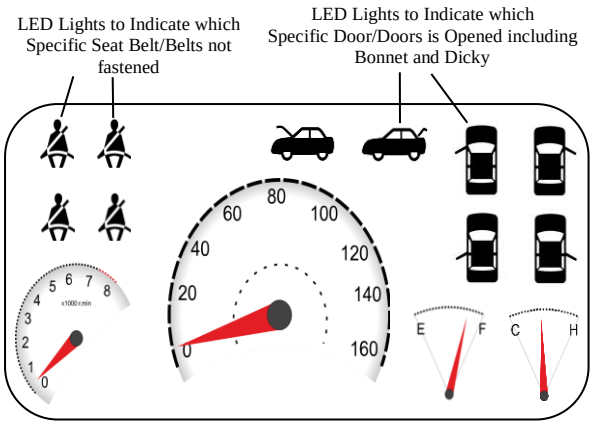

Fig. 2: Dash board display unit proposed for seat belt and door indications.

3). For intelligent indication, the dashboard display unit comprises of separate LEDs for each seat belt and door warning as shown in Fig. 2 to show which seat belt and/or door is not buckled/closed.

4). The seat belt and door safety warning system work if the ignition circuit is turned ON.

B. System Circuitry

The Fig. 3 shows the digital microchips based circuit diagram of the proposed intelligent integrated seat belt and door safety warning system. The circuit consists of following microchips along with few other components.

- IC 7402 x 2 (Two NOR gate ICs).
- IC 7048 x 1 (One AND gate IC).
- IC 7432 x 3 (Three OR gate ICs).
- Six LEDs for doors indications including bonnet and dicky and four LEDs for seat belt indications.
- One buzzer for warning alarm.
- One NPN transistor.

The input signals to circuit for seat belts safety indications and warnings are fed from pressure/weight sensors fitted in the vehicle's seats to sense either driver/passenger seated or not and from push button switches installed in the seat belt buckles to sense either seated driver/passenger buckled up the seat belt or not. For door safety indications and warnings, the input signals to circuit are fed from push button switches installed near the door locks to detect the vehicle's door is closed or not.

The following symbols and notations are used in the circuit and its operation.

1). D1, D2, D3 and D4: input signals from push button switches for door opening for front right-hand side door, front left-hand side door, rear right-hand side door and rear left-hand side door respectively.

2). BN and DK: input signal from push button switches for bonnet and dicky lids opening respectively.

3). L1, L2, L3, L4, L5 and L6: LEDs for indications of door/lid opening for front right-hand side door, front left-hand side door, rear right-hand side door, rear left-hand side door, bonnet lid and dicky lid respectively.

4). B1, B2, B3 and B4: input signals from push button switches for seat belt buckling for front right-hand side seat, front left-hand side seat, rear right-hand side seat and rear left-hand side seat respectively.

5). S1, S2, S3 and S4: input signals from pressure/weight sensors for driver/passenger seating for front right-hand side seat, front left-hand side seat, rear right-hand side seat and rear left-hand side seat respectively.

6). L7, L8, L9 and L10: LEDs for indications of seat belt not fastened for front right-hand side seat, front left-hand side seat, rear right-hand side seat and rear left-hand side seat respectively.

7). Buzzer for warning sound if both or any one or more of the seat belt/belts not fastened and door/doors opening.

8). Pressure/weight sensors generate HIGH input if driver/passenger is present on seat and vice versa.

9). Push button switches for seat belts generate HIGH input if seat belt is not buckled.

10). Push button switches for doors generate LOW input if door is not closed.

C. Working Algorithm

The working algorithm of proposed intelligent

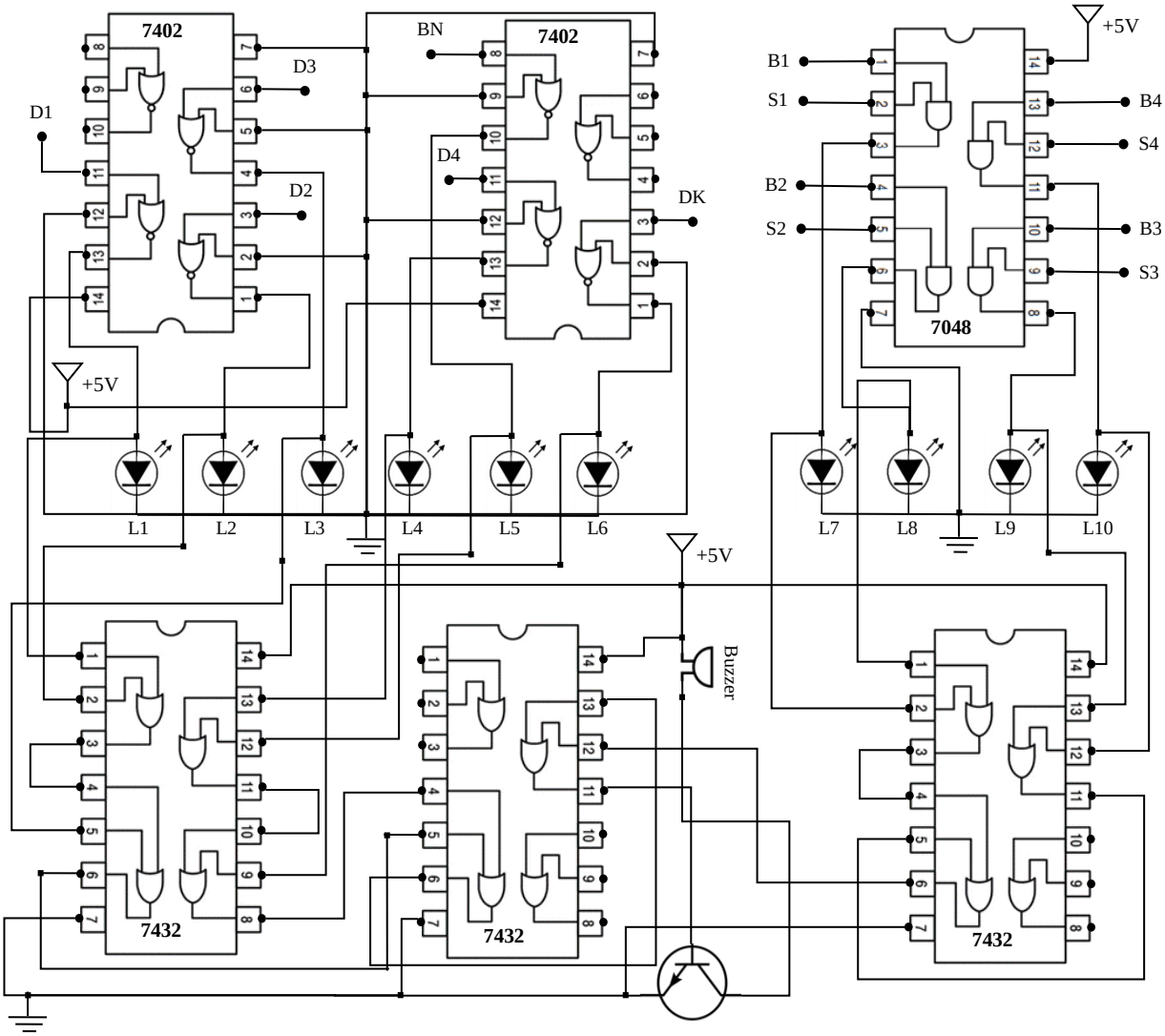

Fig. 3: Proposed system circuit diagram.

integrated seat belt and door safety warning system is shown in Fig. 4. For simplicity, operation for single seat belt and single door is illustrated in the algorithm process. The algorithm is self-descriptive that starts working when the vehicle's ignition circuit is ON.

V. PROTOTYPE DEVELOPMENT FOR SYSTEM TESTING

For the testing of working of the proposed vehicle safety alarm system for its both seat belts and doors, a prototype of a vehicle is developed using Depron foam sheet. Fig. 5 shows the different views of this developed vehicle's prototype. In this prototype, simple push button switches are used in seats to model either driver/passenger(s) is/are on seat or not. Similarly, to model the seat belt buckles to show either seated driver/passenger(s) buckled up the seat belt or not, simple male and female connectors are used in the developed prototype. While, to model the vehicle's doors opening or closing, simple push button switches are used in the vehicle's doors. The circuit diagram of Fig. 3 for proposed safety alarm system is implemented on PCB and installed in this prototype. For the testing of seat belts safety indications and alarms, the input signals are fed to this circuit from simple push button switches, and male and female connectors, fitted in the seats. For the testing of door safety indications and alarms, the input signals to circuit are fed from simple push button switches installed in the door.

The results of experimental testing indicate that the proposed vehicle safety alarm system is working exactly according to the designed specifications.

VI. CONCLUSION

Seat belt and door safety warning system is a good means to remind vehicle's occupants in case of not fastened the belt and/or not properly close the door. The safety warning system as a safety feature reduces the chances of major injuries or even loss of life or lives in an accident. So, to make sure that people wear seat belt and accurately close the vehicle's doors, a simple and low-cost integrated safety warning system has been proposed in this work. The proposed safety warning system is more intelligent than the systems that are currently automobiles comprise in Pakistan as it warns and exactly displays which seat belt/belts is/are not fastened and which door/doors is/are not correctly closed. The prototype of the proposed design is also developed to test its mechanism for safety warnings under different conditions of seat belts and door openings. Hence, the use of the proposed system in Pakistani context is extremely beneficial for automakers in order to avoid the increase in price of vehicle as well as equally valuable to vehicle's users to reduce the chances of accidents and fatal injuries.

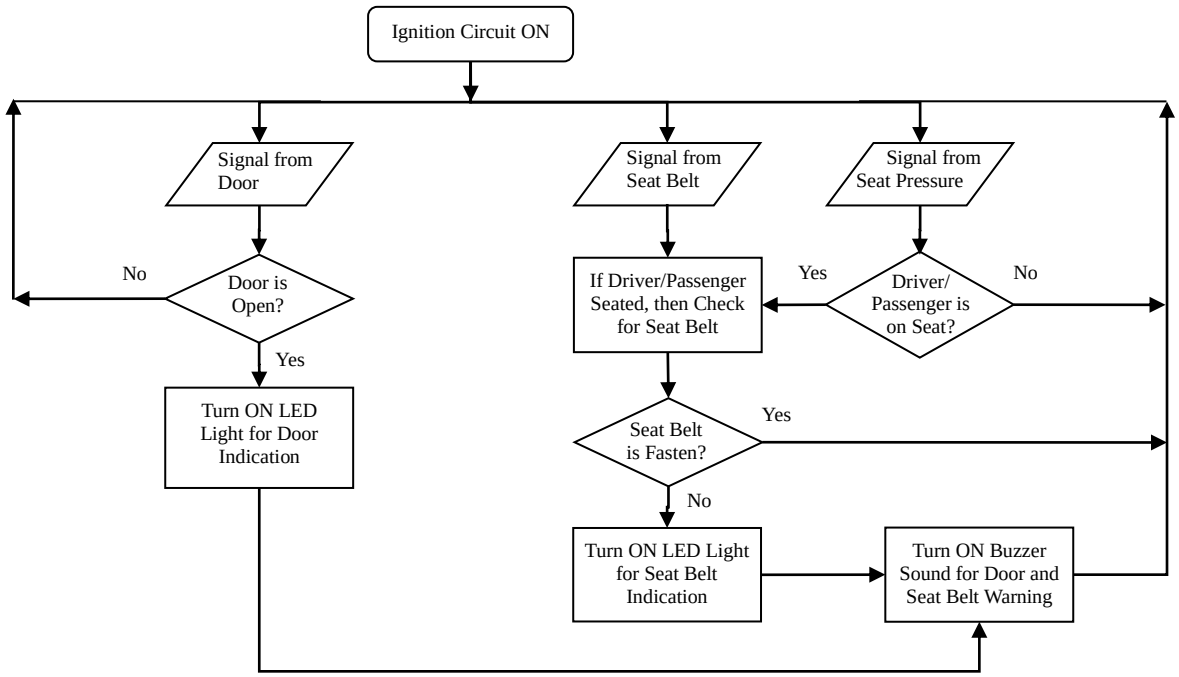

Fig. 4: Proposed system working algorithm for single seat belt and door.

(a)

(b)

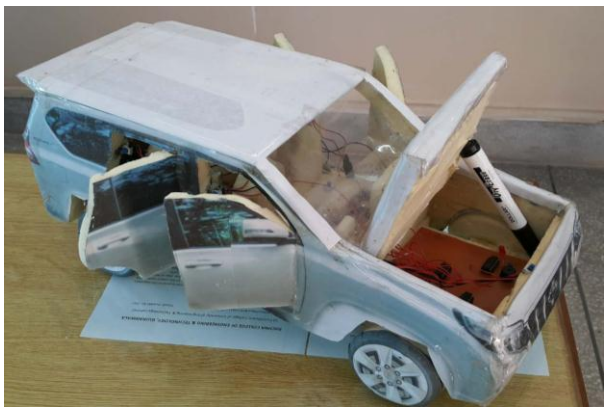

(c)

Fig. 5: Different veiws of vehicle prototype: (a) Complete veiw with doors closed, (b) Side veiw with doors opening, (c) Top veiw with doors opening.

ACKNOWLEDGMENT

We are grateful to Mr. Attique-ur-Rehman from Ahsan Motors Gujranwala for providing the data of vehicles that are currently most used in Pakistan [13-15] and for his help in conducting the survey to get the statistics of the safety features of these vehicles.

REFERENCES

[1] A.A. Klair and M. Arfan, "Use of Seat Belt and Enforcement of Seat Belt Laws in Pakistan," *Traffic Injury Prevention*, vol. 15, pp. 706–710, 2014.

[2] S. Bendak, S.S. Alnaqbi, "Rear Seat Belt Use in Developing Countries: A Case Study from the United Arab Emirates," *WASET International Journal of Transport and Vehicle Engineering*, vol. 11, no.12, pp. 2768-2772, 2017.

[3] World Health Organization, "Global Status Report on Road Safety: Time for Action," Geneva, Switzerland, 2013.

[4] A.A. Khan and Z. Fatmi, "Strategies for Prevention of Road Traffic Injuries (RTIs) in Pakistan: Situational Analysis," *Journal of the College of Physicians and Surgeons Pakistan*, vol. 24, no. 5, pp. 356-360, 2014.

[5] A.A. Klair, M. Arfan and S.S.H. Kazmi, "Determinants of safety helmet use among motorcyclists in Pakistan," *European Academic Research*, vol. 3, no. 5, pp. 5830-5843, August 2015.

[6] R.A. Ghafoor, "Use of Safety Helmet and Issues Related With its Usage in Pakistan," *Scientific Paper, Technische Universität München*, February 10, 2016.

[7] I.M. Abdalla, "Effectiveness of safety belts and Hierarchical Bayesian analysis of their relative use," *Safety Science*, vol. 43, pp. 91–103, 2005.

[8] S. Bendak, "Seat belt utilisation in Saudi Arabia and its impact on road accident injuries," *Accident Analysis and Prevention*, vol. 37, pp. 367-371, 2005.

[9] C.-H. Lai, C.-C. Lin, G.-L. Tsai, Y.-S. Hwang, "The Car Door Safety System with Wireless Alert Transmission," *Proceedings of 7th IEEE International Symposium on Next-Generation Electronics*, Taiwan, 2018, pp. 1-3.

[10] S.D.R Bhardwaj, S.R. Jogdhankar, "Seat Belt Safety Features Using Sensors to Protect Occupant," *International Review of Applied Engineering Research*, vol. 4, no. 4, pp. 349-354, 2014.

[11] P.N. Sheth, A.D. Badgujar, "Developing safety system for monitoring seat belt and controlling speed accordingly to avoid fatal injuries," *Int. Journal of Scientific and Research Publications*, vol. 5, no. 10, pp. 1-5, 2015.

[12] U. Ansari, "Common Excuses: Why People Don't Wear Seatbelts," August 10, 2018. [Online]. Available: https://www.carspiritpk.com/2018/08/10/common-excuses-why-people-dont-wear-seatbelts/. [Accessed: 18 - December - 2019].

[13] https://www.honda.com.pk/.

[14] https://www.toyota-indus.com/.

[15] https://www.paksuzuki.com.pk/.

MINIATURIZED DUAL BAND RFID TAG ANTENNA MOUNTABLE ON METTALIC SURFACE

Sundas Farooq Khan, Sara Bibi and Yasar Amin

Abstract: A miniaturized RFID tag antenna mountable on a metallic surface is proposed which can accommodate dual bands (865-868 MHz, and 899-902MHz) with read range 9.47 m. The antenna has a miniaturized structure achieved by meandering, spiral structure and adjusting the distance between feeding lines. The size of the antenna is 20mm (width) x 30mm (length) x 1.524mm (height).

Introduction: The RFID (Radio Frequency Identification) is a set of technologies used for identification, in which reader sends the electromagnetic waves to the tag placed on any object, for detection [5]. This characteristic of RFID helps to serve a vast variety of objects to identify [1].

RFID is using as a substitute of bar codes as bar codes and other optical marks, can easily be distorted or deface by opaque objects that decrease the readability and reliability of bar codes. The mechanical damage can be avoided by using printed symbols that cannot be easily modified or distorted. Although RFID is a little bit more expensive than optical auto-ID techniques but they have restrained markings and provide more space to store information [4]. To decrease the cost of these tags efforts were made by making passive tags with no battery and standing out of the noise.

RFID tags consist of a microchip that is mountable on antenna that stores the information of the object. Globally RFID tag is used in many applications such as logistics, tracking objects, vehicle identification, and supply chain. RFID tag must be cost effective, have long read range and small enough to place on any object. The frequency should be considered for targeted audience. If the product is used globally than antenna should have the capability to operate in all band 860-960 MHz. The currently the folded dipole structure with parasitic elements, spiral dipole [2], and the slotted planar inverted-F antenna [6] are used on metallic surfaces [3]. However, these antennas acquire a large area and high heights and are complicated, but a half-wavelength resonance length so impedance matching is difficult [7]. Also, when antenna is mounted on a metallic surface its impedance characteristics changed and bandwidth decrease [4].

In this letter a low profile, miniaturized antenna is proposed which do not change its impedance characteristics even on the conductive surface and have high gain and long read range. For worst case scenario, 6 samples of designed antennas are fabricated for the Monte-Carlo analysis.

This antenna has microstrip feeding lines and the meandering length and tip loading technique is used. It can accommodate dual band (865-868MHz and 899-902MHz) with read range 9.47 m.

Antenna design:

Antenna structure has dimensions 20mm (width) x 30mm (length) x 1.524mm (height), whereas Roger's 6010LM substrate is used with dielectric constant of 10.2. Feeding lines are made of copper with thickness 0.035mm. Ansoft HFSS tool is used for antenna optimization. Lengths of the feed lines are decreased by using spiral structure and meandering. Impedance matching is accomplished by tip loading and maintaining the distance between microstrip feedlines. Fig. 1 shows the design of dual-band miniaturized antenna.

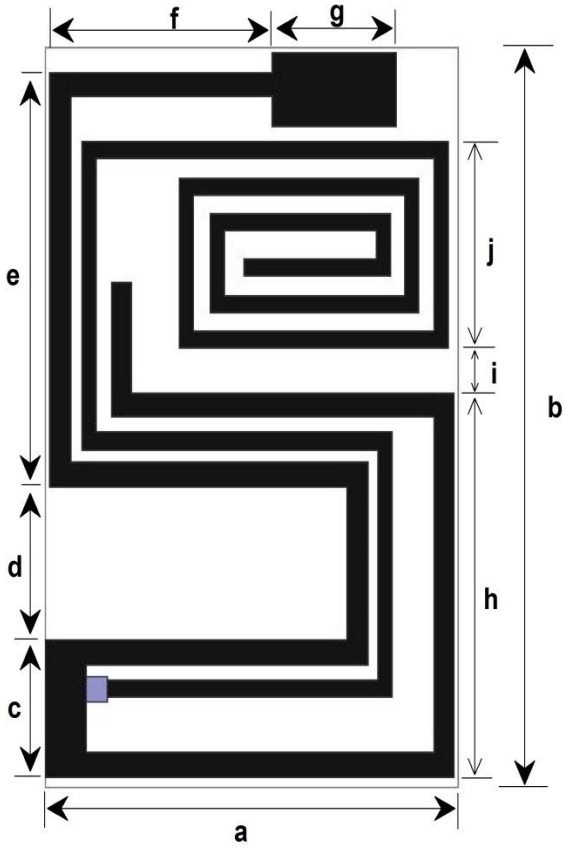

Fig1: Design on Dual-Band Miniaturized Antenna

Variable	Value
a	20
b	30
c	5.6
d	6.2
e	16.8
f	10.75
G	6
H	15.6
I	1.8
J	8.4

Table1: Values of design

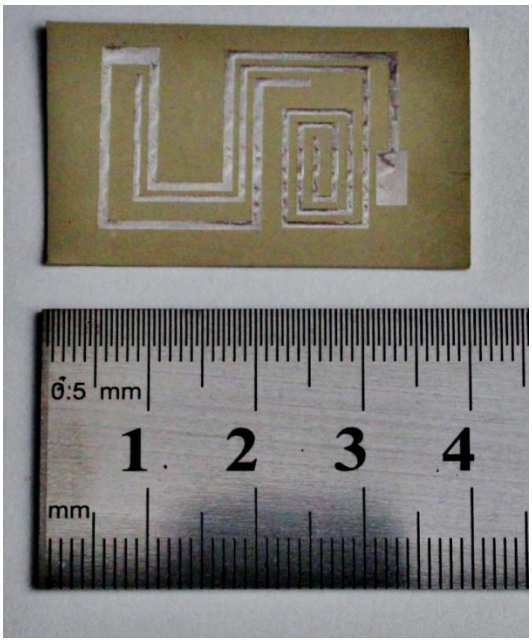

Fig2: Fabricated Antenna Structure

RESULTS: Fig 3 & 4 shows the impedance and S11 values of antenna. The impedance matching is accomplished in Europe band at 866.5 MHz and band of 899-902.5 MHz as shown in the graphs. The design antenna is appropriate to paste on the conductive/metallic surface.

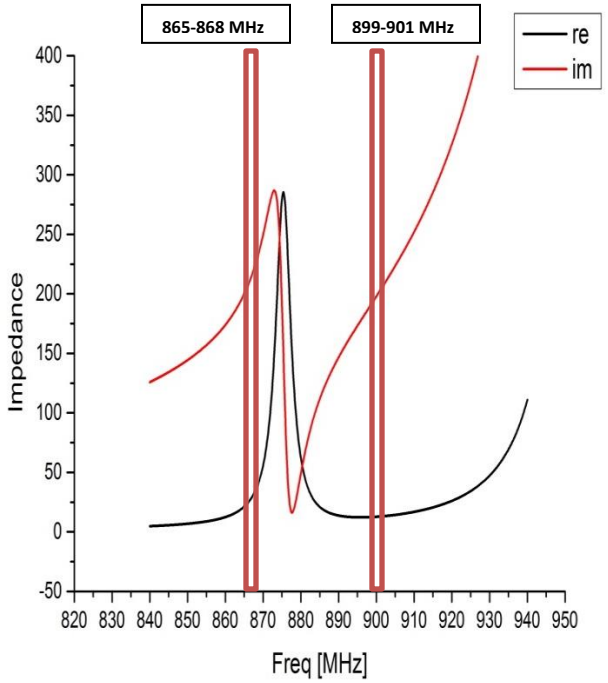

Fig3: Real and Imaginary part of impedance

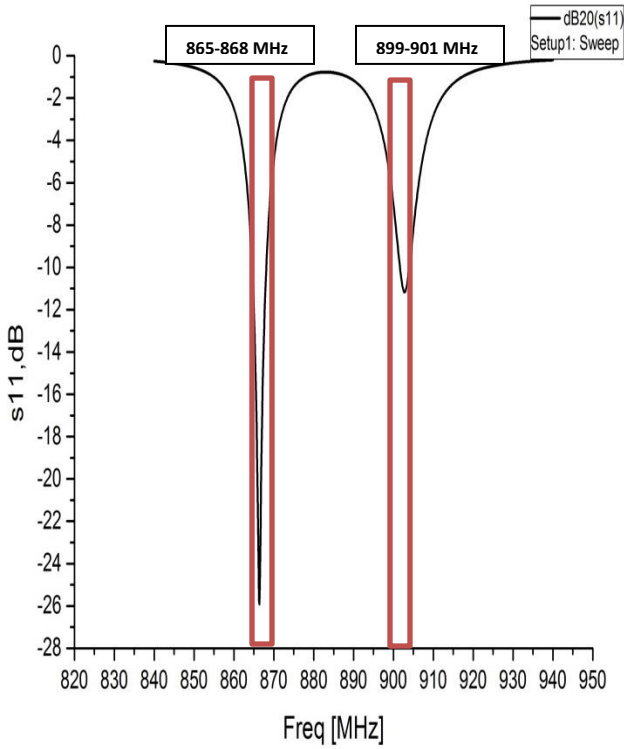

Fig 4: S11 of antenna

	Previous antenna	Proposed antenna
Length	33.5mm	30mm
Width	20mm	20mm
Height	2mm	1.524mm
Read range	1.6m	9.47m
Bandwidth	3MHz	3.5MHz

Table 2: Characteristics comparison of pre-existing antenna in market and proposed antenna in this letter

Conclusion: A dual band miniaturized antenna mountable on a metallic surface with stable impedance characteristics is designed. The tag antenna has a reasonable good read range of 9.47m. Through meandering and spiral structure we achieve this antenna that can accommodate UHF dual band and is much smaller than already existing antennas in the market like spiral dipole, the folded dipole structure with parasitic elements, and the slotted planar inverted-F antenna. The designed antenna can be attached on metallic objects that are exported to and from Europe market.

References

[1] Yasar Amin, Prof. Hannu Tehnuen, Li-Rong Zheng, “Blueprint and integration of Vastly Efficient 802.11a WLAN Front-End”, WSEAS Transaction Electronics, Issue 4 Volume 3, page258 April 2006

[2] Miniaturised dual-band S-shaped RFID tag antenna mountable on metallic surface by J.-Y. Park and J.-M. Woo

[3] Cho, C., Choo, H., and Park, I.: ‘Design of planar RFID tag antenna for metallic objects’, Electron. Lett., 2008, 44, (3), pp. 175–177

[4] Wideband And Dual Band Design Of A Printed Dipole Antenna by Qing-Qiang He; Bing-Zhong Wang; Jun He

[5] Meandered-Slot Antennas for Sensor-RFID Tags by Calabres, C. ; Marracco, G.

[6] Chen H.-D and Y.-H. Tsao ,"Low-profile PIFA array antennas for UHF band RFID tags mountable on metallic objects, "IEEE Transaction on Antennas And Propagation, Vol.58, No.4, 1087-1092,2010

[7] Qing, X., C. K. Goh, and Z. N. Chen, "Impedance characterization of RFID tag antennas and application in tag co-design," IEEE Transactions on Microwave Theory and Techniques, Vol.57, No.5, 1268-1274, 2009

2020 5th International Electrical Engineering Conference (IEEC 2020)
Feb, 2020 at IEP Centre, Karachi, Pakistan

Classification of Pakistani Currency based on Scale Conjugate Gradient (SCG) and Convolutional Neural Network

Bushra Aijaz[1*], Faizan Aadil[2], Zahida Parveen[1] and Muhammad Umair Arif[1]

[1] Department of Electrical Engineering, Bahria University,
Karachi,75260, Pakistan (bushraaijaz.bukc@bahria.edu.pk)*, (zee9848@gmail.com), (umairarif.bukc@bahria.edu.pk)
[2] Intech Process Automation Operations,
Lahore, Pakistan, (faizan_aadil@hotmail.com)

Abstract: Human interactions and manpower is being reduced with the machine automation in every field of technology. Automatic financial services have increased the requirement of automatic currency recognition that have eventually made automatic banking process, a major activity around the world. The paper recognition process is prone to pollution and depreciation of paper currencies due to frequent transactions and cause error during feature extraction. This paper proposes an efficient technique to recognize paper currency for Pakistani currencies. Pakistani currencies differ in color, size and texture and are classified into 7 classes as per the currency values. For feature extraction we have used bounding box technique for length and width extraction and Speed Up Robust Features (SURF) Extractor to extract local point in the images. The currency classifications are done using Scale Conjugate Gradient (SCG) Backpropagation, MobileNets and Inception V3 models and their outcomes are discussed.

Keywords: Currency recognition; SCG; SURF; MobileNets; Inception V3

I. INTRODUCTION

Monetary transactions are of vital importance in everyday transactions. There are more than 200 currencies circulating all over the world, with each of them has different sizes, colors, texture, and template pattern. Automated recognition of paper currency with high processing speed and good accuracy has great importance and today's requirement. Therefore an intelligent pattern recognition system is needed to recognize paper currency. Paper currency recognition can intelligently be done by adopting the Neural Network (NN) approach. NN provides good techniques for solving complex decision boundary problems over multiple variables. They provide good results for solving the currency classification which is complex as they differ in colors, sizes, texture, templates. Neural Network shows limitation as they work on one or two hidden layers. And therefore, they take time for training and have greater number of epoch. These disadvantages can be overcome by Deep Neural Networks (DNN). DNN works on larger number of layers still it consumes less time and contributes more towards efficient performance. Pakistani Currency is known as Rupee. Pakistani Rupee (PKR) has seven dominations as PKR 10, 20, 50, 100, 500, 1000, 5000 [1]. There are many techniques as ZFNet, GoogleNet, ResNet, AlexNet, VGG and others for Deep Neural Networks (DNN) for currency classification [2]. In this paper, three different algorithms are implemented for the currency recognition. First one is based on Scale Conjugate Gradient (SCG) Backpropagation method –a Neural Network (NN) approach, while the other two are based on MobileNets and Inception V3 –a Deep Neural Network (DNN) approaches.

Remaining paper is organized as; section II highlights the related work in the domain of ANN and DNN. Section III and section IV discuss the capturing of dataset and methodology respectively. Section V discusses the experimental analysis and results. And our findings are discussed in section VI ended with future work plans.

II. RELATED WORK

Many techniques of Neural Networks have been practiced in past to recognize paper currencies. Few related works are mentioned below;

In this paper [3] authors have used multiple paper currencies of Chinese Yuan, Euro, Japan Yen, Korean Won, Russian Rubble, and United States Dollar and total of 62 denominations with huge data set of 64,668 images. Their system consists of five convolutional layers for feature extraction and three fully connected layers for classification. The training method used is Stochastic Gradient Descend (SGD). The currency recognition is done by Convolutional Neural Network (CNN) and showed accuracy of 100%. They have extended their work in this paper [4] and have classified the currency fitness as either fit or not fit for recirculation. They have classified fitness into 2 levels i.e., fit or unfit for US$ and into 3 levels i.e., fit, normal or unfit for Korean Won and Indian Rupee. Rectified Linear Unit (ReLU) layer is presented at all eight layers. Softmax function is used to transform the real values at the output of the neuron units. Their proposed method results to 97.16% accuracy. Authors in the paper [5] have done currency recognition of Indian Currency based on texture analysis. They have used Mazda for feature extraction and Fisher linear Discriminant for feature reduction. SVM classifier is used and the accuracy rate is recorded to be 96%. In the paper [6], currency recognition is done using Principle Component Analysis (PCA) classifier. Region of interest (ROI) are shape, numerical value, RBI seal, latent image and micro letter. Mahalanobis distance metric is measured to determine difference between sample and input

images. Their results led to 96% accuracy. The authors in this paper [7] have also used PCA classifier and have compared it with WEKA classifier. They have done comparative analysis of WEKA classifiers as Naïve Bayes, Random Forest and SVM. They have come up that SVM has better accuracy among all. One more technique for feature extraction is to use Fourier Descriptor. This technique is used in paper [8] and classification is done using feed forward Backpropagation neural network (supervised ANN). The testing is done on 115 images with 10,000 iterations and the success rate achieved is 97% with time complexity of 2.52sec. The authors in this paper [9] have performed Backpropagation ANN for Indian Currency recognition. They have adopted Chan-Vase active contours without edges algorithm for the elimination of background noise. They have considered 613 images including 13 soiled images. Training data is 540 images with marginal value of 21 masks. Their results led to the accuracy of 100% for quality notes and 97% for soiled notes. Another paper [10] has adopted SURF descriptor for feature extraction and binary SVM classifier. 10 stage cascaded detector is used by Histogram of Oriented Gradients (HOG) descriptor. The distance between prestored data and input data is calculated using Delta –E distance metric and the results yielded 95.11% for true positive rate and 0.0976% for low false positive rate. A multiclass SVM was adopted in the paper [11] for banknote identification. They have considered currencies from countries Nigerian Naira, US $, Canadian Dollar, Euro and employed HOG for feature extraction and used seven classifiers namely Naïve Bayes, Multinomial, Random Forest, NNge, Hyperpipes, IB1, SMOSVM and MCSVM. The paper has concluded that MCSVM provides the best result overall. They have taken samples of 1800, 1000, 1000, 1400 currencies images respectively. Euler number and image correlation is used for feature extraction and Radial Basis Neural Networks is implemented as classifier in this paper [12] for Saudi Riyal currency recognition system. The average recognition rate is seen as 91.5%. Authors in this paper [13] have also used Euler number for feature extraction, noise removal is done using Wiener filter and KNN classifier is used for Pakistani paper currency classification. Their results are accurate up to 98.57%. In this paper [14] authors have presented a mobile application for currency recognition of Indian Rupee for impaired people. They have used BoW –Bag of Words recognition method and GrabCut algo for feature extraction. For classification, highest vote is declared as result. After testing 2584 images they have got 96.7% accuracy. Scale Invariant Features Transform (SIFT) algorithm is used for feature extraction of Pakistani Coin recognition in this paper [15]. PCA is used to reduce feature space and classification is done using feed forward neural network. Training and testing is done on 50-50 data images and they have achieved an accuracy of 84%. Authors in this paper [16] have proposed the recognition system for SriLankan currency. Feature extraction is done using linear transformation whereas feed forward NN has been used with BP learning with a hidden layer for classification.

III. CAPTURED DATA SET

In this research, we have implemented the selected techniques on seven dominations of Pakistani Rupee (PKR). Images are captured from two different cameras; Samsung SM-J510F and Infinix Zero 3 with specification 1152x2048 (72dpi) and 6144x3456 (72dpi) respectively. The images are taken under best light illumination with black, brown and blue backgrounds with different angles and each image is captured with front and back view.

There are seven denominations of Pakistani currencies, namely PKR-10, PKR-20, PKR-50, PKR-100, PKR-500, PKR-1000 and PKR-5000. The data are organized in classes such as PKR-10 is declared as class 1, PKR-20 as class 2, PKR-50 as class 3, PKR-100 as class 4, PKR-500 as class 5, PKR-1000 as class 6 and PKR-5000 as class 7. Total 1260 images are captured from two different cameras for training phase, 180 images of each class. Similarly, for testing 42 images are taken, 6 images for each class. The captured datasets are recorded in Table 3. The first and second columns show front side and back side of Pakistani Rupee respectively while third and fourth columns show the tilted images of Pakistani Rupee, again front side and back side respectively. Our data set consists of images aligned at zero degree and also with orientations at different angles. Each row represents one class.

IV. METHODOLOGY

A. System Setup

The experimental setup consists of Artificial Neural Network model (ANN) and two Deep Neural Network models (DNN). The training and testing of Neural Networks are performed on MATLAB@ 2016 using "Neural Network Pattern Recognition (nprtool)" on 64 bit Windows 7 operating system and DNN are working by using TensorFlow on Ubuntu 16.04 operating system.

B. Feature Extraction for Identification of Pakistani Currency

To identify the Pakistani Currency, here we have considered three types of features; length (l), width (w) and SURF features by using image-processing techniques. Length and width are taken collectively as one feature. The techniques are explained below:

Length (l) and Width (w) of Pakistani Currencies

Total 1260 samples are used for training in which every class has 180 samples. Same for testing, total 42 samples are used in which six samples are used from

every class. For recognition of particular denomination, the size of every image is determined. The length and width of every class is then converted into pixel format. For calculating length and width, bounding box technique is used. To apply this method, firstly the currency images are converted into binary by using im2bw technique, and then Gaussian filter is applied for removing unwanted noise on the images that appeared during the capturing of images like blurring and more lighting effects. Then region props technique is applied for creating bounding box. Bounding box is a rectangular box.

The length (l) and width (w) of image as shown in Fig. 1. The red line gives the information about bounding box as seen in Fig. 2. Table 1 represents the dimensions of length (l) and width (w) for every currency images in terms of pixels.

SURF Features

Speed Up Robust Features (SURF) is a local feature detector and descriptor in images. It is widely used in computer vision and image processing for object recognition, image registration and classification. In this research paper, SURF is used for object recognition.

SURF uses an integer approximation of the determinant of Hessian blob detector to detect the point of interest, which is then computed with 3 integer operations using pre-computed integral image. Its feature descriptor is based on the sum of the HAAR wavelet response around the point of interest. These can be computed with the aid of integral image.

Fig. 1 Original Image of PKR-100

Fig. 2 Image enclosed in bounding box indicating Length and Width of currency image.

Table 1 The length and width of Pakistani currency images

S No.	Currency (PKR)	Length(l) in pixels	Width (w) in pixels
1	10	688.6538	452.2748
2	20	770.0808	398
3	50	659	398
4	100	832.5413	17.5642
5	500	652.7243	424.4273
6	1000	649.2334	455.6451
7	5000	644.7449	232.9646

C. Scale Conjugate Gradient (SCG) Backpropagation Model Based Classification

The Scale Conjugate Gradient (SCG) is an Artificial Neural Network (ANN), which is used for classification. This algorithm is implemented by using neural network pattern recognition tool (nprtool) of MATLAB 2016 version. This network is trained on SCG Backpropagation Model. It is feed forward neural network, with Sigmoid hidden and Softmax output neurons can classify the currency well and given enough neurons in its hidden layer. Best classification results are obtained by using 10 neurons for length and width feature and 30 Neurons for SURF features training. The correct and incorrect classifications results based on length-width feature extraction and SURF features extraction are given in confusion matrix with target 1 to target 7 during training, validation and testing of the pattern of neural network. Confusion Matrix results are obtained during training process for length-width based (see Fig. 3) and for SURF features based (see Fig. 4). The correct classification of currency samples are presented in green box, incorrect classification is presented in red boxes, while blue boxes represent overall percentage of each confusion matrix of correct and incorrect currency classification for SURF features based and length-width based. The results of ROC for length-width of currencies are obtained (see Fig. 5); also the SURF features results for each class are plotted (see Fig. 6). The best validation performance for SURF features is 0.055028 at 198 epochs and the best validation performance for length-width is 0.068396 at 148 epochs.

D. MobileNets Model Based Classification

MobilNets model is also used for currency recognition in this research. This model is implemented on tensorflow platform belongs to Deep Neural Network (DNN). The architecture of this model is based on streamlined that uses depth wise separable convolution to build up light weight deep Neural Network. The architecture of this model works on convolution techniques. Standard convolutions are performed by MobileNets, which is divided into 3x3 depth wise convolution and a 1x1 point wise convolution. A single filter is to apply on each input channel in depth wise convolution. The point wise convolution is used to apply 1×1 convolution to combine the outputs of depth wise convolution.

2020 5th International Electrical Engineering Conference (IEEC 2020)
Feb, 2020 at IEP Centre, Karachi, Pakistan

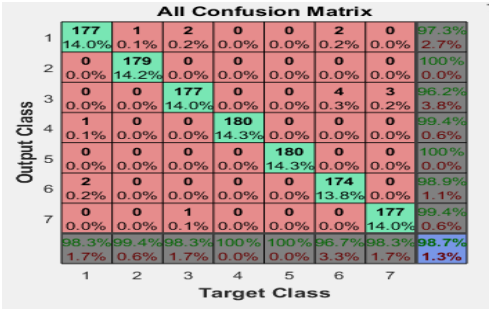

Fig. 3 The confusion matrix obtained by using length and width of the currencies

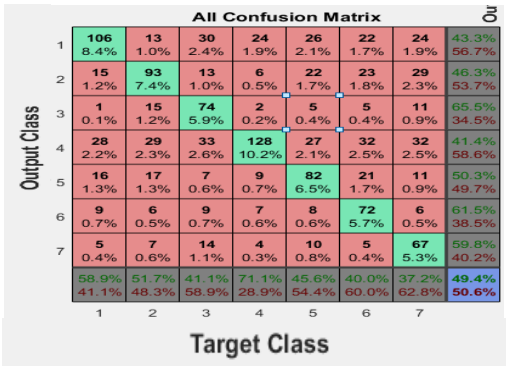

Fig. 4 The confusion matrix obtained by using SURF features

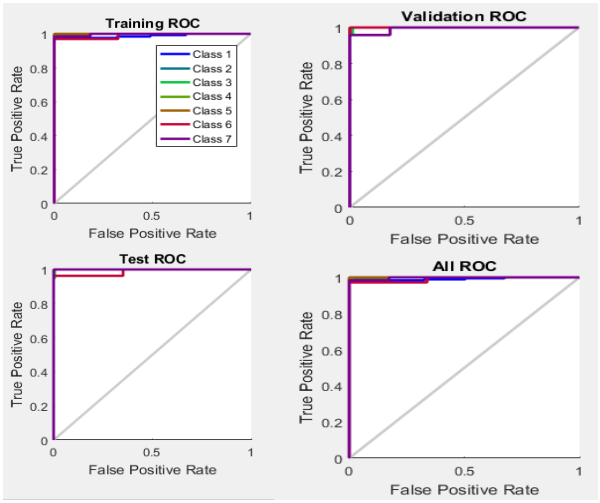

Fig. 5 The ROC plot obtained by using length and width of currencies

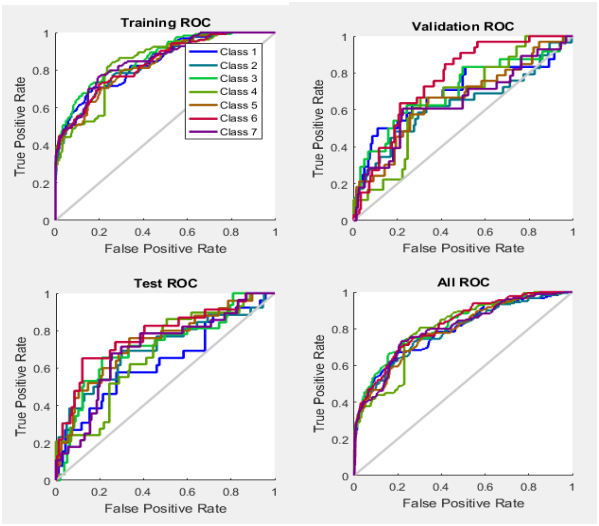

Fig. 6 ROC obtained from SURF features

A special purpose of standard convolution is to use both filters and combined inputs into a new set of output in one-step. The function of standard convolution is to do features filtering based on convolution kernel and combining features in order to produce a new representation. The computation and model size are reduced by using factorization process. Therefore, the filtering and combination of layers break into two steps by using factorized convolution called depth wise convolution. Depth wise convolution creates two layers further, first one is depth wise convolution and second one is point wise convolution. A linear combination of the output of the depth wise layer is produced by point wise convolution. It uses both batch norm and Rectified Linear Unit (ReLU) nonlinearities for both layers. Depth wise convolution is efficient and fast as compared to standard convolution. Although it has only filtered input channel, it also does not combine them to produce any new features. The 3x3 depth wise separable convolution is computationally less time consuming as compared to the standard convolution at low decrement in efficiency. The MobileNets structure is made up of depth wise separable convolutions except for the first layer which is a full convolution. The ROC is also generated in this model. The ROC results of MobileNets convolution is obtained as shown in Fig. 7.

E. Inception V3 Model Based Classification

InceptionV3 technique is implemented using TensorFlow platform and the architecture of inceptionV3 is coded and trained using TensorFlow, Google's deep learning system. In this paper, this model is trained for imageNet large Visual Recognition Currencies data. It is also called Deep Convolution Neural Networks (DCNNs) because this is DNN architecture based technique used for the classification of currencies. In architecture of inceptionV3 model, it uses six standard convolutional layers and total 12 inception layers each with slightly different design. Moreover, InceptionV3 is defined as the transfer

learning that belongs to the concept of machine learning. It is a pre-trained neural network mainly consists of two parts: first part is the extraction of feature by using a convolutional network and the second part has classification portion including Fully connected and Softmax layers. Its basic architecture has the ability to learn nonlinear functions by connecting the convolutional layers through 1x1 convolutions. In this method, fully connected layers get reduced due to the increment in the abstraction power and average of feature maps at the final layer and vectors are directly forwarded to the Softmax layer. The method overall decreases the probability of over fitting because of the less number of fully connected layers. InceptionV3 can also be defined as the variant of inceptionV2, which includes Batch Normalization (BN) auxiliary. In InceptionV3 7x7 convolution is broken into 3x3 convolution. This method is considered as more robust and accurate for the classification of objects. The results of ROC is achieved as in Fig. 8.

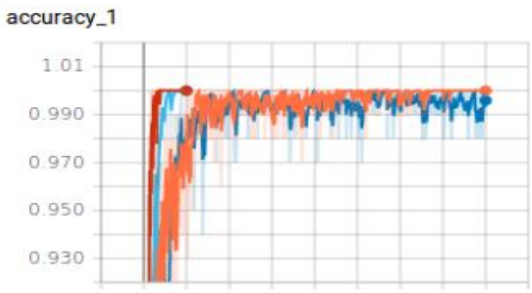

Fig. 7 The overall accuracy of MobileNets Model

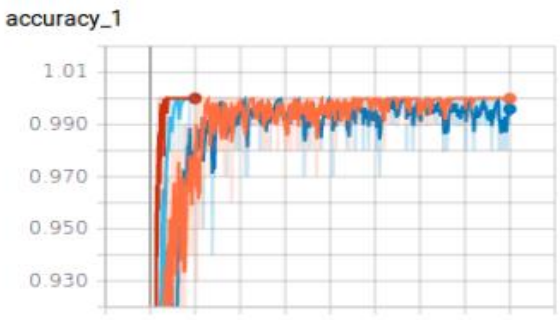

Fig. 8 The overall accuracy of InceptionV3 Model

V. EXPERIMENTAL RESULT

In this paper three different techniques are examined, which are; Scale Conjugate Gradient (SCG) Backpropagation model, MobileNets and InceptionV3. SCG Model belongs to ANN while the other two techniques (MobileNets and InceptionV3) are related to DNN. The results of SCG, MobileNets and InceptionV3 are summarized in Table 2.

- For SURF based classification, random features of currencies images are extracted using SURF command. These features are trained using SCG Backpropagation method. The results of all classes for seven denominations are summarized in Table 2.
- For length-width based classification, length and width of images for all classes are calculated with different orientations. The images are enclosed in in SCG Backpropagation model and results are recorded in Table 2.
- In MobileNets and InceptionV3, inputs are images. The models are trained and tested by using currencies images and results are shown in Table 2.

It can be observed from the result that InceptionV3 and MobileNets model have more accurate true classification as compared to SCG. The highest percentage is obtained from both InceptionV3 and MobileNets models and the interesting observation is that the results of both classifiers are almost same. The same percentages are recorded by both MobileNets and Inception V3 models, for PKR-10 is 89.9 %, for PKR-20 is 98.6%, for PKR-100 is 99.9%, for PKR-500 is 99.9%, for PKR-1000 is 86.6% and for PKR- 5000 is 68.09%. The only PKR-50 is different but have very small difference for both MobileNets and Inception V3 which are 98 % and 97.5% respectively.

In this paper SCG model is implemented twice, Firstly ANN trained and tested by length-width and secondly ANN trained and tested by using SURF features of the currencies. The results for length-width based model are more accurate as compared to SURF based features as observed in Table 2 below.

VI. CONCLUSION AND FUTURE WORK

In this research paper currency recognition is performed by using Scale Conjugate Gradient (SCG), MobileNets and Inception V3 models. For this purpose, we have used Pakistani currencies. There are seven denominations of Pakistani denominations are 10, 20, 50, 100, 500, 1000 and 5000. SCG model is implemented on two different bases i.e., length-width features and SURF feature. Between these two, the best results of SCG are obtained from length-width of currencies then from SURF features during training and testing phases. But the overall comparative study tells that the results from MobileNets and InceptionV3 are almost same for currencies dataset. And is more accurate and more suitable for currency recognition as compared to SCG model.

In future, we will extend our research onto currencies of multiple countries and implement on different platforms like SVM, WEKA, ResNet and InceptionV4. Moreover we will recognize the currencies by extracting multiple features like color, texture and pattern. We will also propose methods to differentiate between fake and real paper currencies.

Table 2 The classifications results of SCG, MobileNets and Inception V3 Models

Class	SCG results based on length-width	SCG result based on SURF features	Mobile Nets model	Inception V3 model
10	100%	70%	89.9%	89.9%
20	64.7%	50%	98.6%	98.6%
50	51.43%	50%	98%	97.5%
100	98%	51.45%	99%	99.9%
500	65.6%	50%	99.9%	99.9%
1000	56.5%	56.5%	86.6%	86.6%
5000	89.8%	50%	68.09%	68.09%

REFERENCES

[1] State Bank of Pakistan Homepage, http://www.sbp.org.pk/Notes/n-note.asp, last accessed 2018/07/25.

[2] Methods of Deep Neural Networks Homepage, https://medium.com/@siddharthdas_32104/cnns-architectures-lenet-alexnet-vgg-googlenet-resnet-and-more-666091488df5 , last accessed 2018/07/25.

[3] Pham TD, Lee DE, Park KR, "Multi-National Banknote Classification Based on Visible-light Line Sensor and Convolutional Neural Network. Sensors", *sensors*, 17(7):1595, 2017.

[4] Pham TD, Nguyen DT, Kim W, Park SH, Park KR, "Deep Learning-Based Banknote Fitness Classification Using the Reflection Images by a Visible-Light One-Dimensional Line Image Sensor", *Sensors*, pp.18(2),2018.

[5] K. Verma, B. K. Singh and A. Agarwal, "Indian currency recognition based on texture analysis", *Nirma University International Conference on Engineering*, pp. 1-5,2011.

[6] R. Vishnu and B. Omman, "Principal component analysis on Indian currency recognition", *International Conference on Computer and Communication Technology (ICCCT)*, pp. 291-296, 2014.

[7] Vishnu R and B. Omman, "Principal features for Indian currency recognition", Annual IEEE India Conference (INDICON), pp. 1-8, 2014.

[8] Gogoi, M., et al.: "Automatic Indian currency denomination recognition system based on artificial neural network", *2nd International Conference on Signal Processing and Integrated Networks (SPIN)*, pp. 553-558, 2015.

[9] Nayak, J. K., et al.: "Neural network approach for Indian currency recognition", *Conference (INDICON)*, pp. 1-6, 2015.

[10] Kamal, S., et al.: "Feature extraction and identification of Indian currency notes", *Fifth National Conference on Computer Vision, Pattern Recognition, Image Processing and Graphics (NCVPRIPG)*, pp. 1-4, 2015.

[11] T. V. Dittimi, A. K. Hmood and C. Y. Suen, "Multi-class SVM based gradient feature for banknote recognition", I*EEE International Conference on Industrial Technology (ICIT)*, pp. 1030-1035, 2017.

[12] Sarfraz M.,"An Intelligent Paper Currency Recognition System,Procedia Computer Science", pp. 65(7):538, 2015.

[13] Ali, Ahmed & Manzoor, Mirfa., "*Recognition System for Pakistani Paper Currency. Research Journal of Applied Sciences, Engineering and Technology*" pp. 3078-3085, 2013.

[14] Singh, S., et al. "Currency recognition on mobile phones", *22nd International Conference on Pattern Recognition (ICPR)*, pp. 2661-2666, IEEE, 2014.

[15] G. Farooque, A. B. Sargano, I. Shafi and W. Ali, "Coin Recognition with Reduced Feature Set SIFT Algorithm Using Neural Network", *International Conference on Frontiers of Information Technology (FIT)*, pp. 93-98, 2016.

[16] Gunaratna, D. A. K. S., N. D. Kodikara, and H. L. Premaratne, "ANN based currency recognition system using compressed gray scale and application for Sri Lankan currency notes-SLCRec", *Proceedings of World academy of sciecne, engineering and technology*, pp. 235-240, 2008.

Table 3 Dataset of different Pakistani currencies with different angles (front and back views)

Denomination (PKR)	Front side	Back side	Front side -tilted	Back side -tilted
10				
20				

50				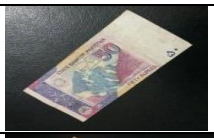
100				
500				
1000				
5000				

2020 5th International Electrical Engineering Conference (IEEC 2020)
Feb, 2020 at IEP Centre, Karachi, Pakistan

Analysis of Hybrid Energy System for Rural Areas:A Case Study of Village Shafiabad District Sanghar Sindh,Pakistan

Suhail Ahmed Shaikh[a], Nayyar Hussain Mirjat[a,b,*], Khanji Harijan[c],Shoaib Ahmed Khatri[a],

[a]Department of Electrical Engineering, Mehran University of Engineering and Technology, Jamshoro, 76062, Pakistan

[b]Energy and Environmental Engineering Research Group, Mehran University of Engineering and Technology, Jamshoro, 76062, Pakistan

[c]Department of Mechanical Engineering, Mehran University of Engineering and Technology, Jamshoro, 76062, Pakistan

Corresponding Author: suhailshaikh393@gmail.com

Abstract: Off-grid renewable energy hybrid systems including solar and wind are the potential solution to replace fossil fuel resources reducing the environment pollution and overcome the consumption of the power. In this study different hybrid configurations including solar and wind for rural areas of shafiabad of district Sanghar have been analyzed by using the HOMER software. The renewable energy sources are considered PV and Wind Energy to meet the demand of the Shafiabad district sanghar. In this study different optimization parameters are considered such as Cost of Electricity (COE),Net present cost (NPC).The result of this study off -grid PV hybrid system are the optimal configurations for the practical aspects to meet the peak demand of 4.4MW.The COE from the PV system is Rs 16.43/kWh. 100% of total kWh production is generated from the which 81.6 kW solar and 100kW of wind and 34.4kW of convertor were optimized for this case study with the total net present cost of Rs 29.4M and the initial capital investment of Rs 17.0M
The sensitivity analysis of the results provides an elaborated understanding of the effect of sensitivity variables on a feasible system configuration. These results suggest that hybrid system is more reliable and useful to overcome the energy crisis for the future work.

Keywords: HOMER, Optimization, HEI, RET, COE, NPC, Sensitivity Analysis.

I. INTRODUCTION

Electricity is an important commodity of modern era. It plays significant role in meeting various human needs and wants. However, production of electricity is generally accompanied with environment emission causing climate change.

The developing countries in particular are facing various challenges of managing energy crises and thus availability of electricity. The Power outages that are continuously increasing due to increasing demand. The demand is increasing because of rapid urbanization in Pakistan includes living standards of people and increasing the population. The planning of electricity infrastructure is collectively linked with demand of the power and increasing of GDP (gross domestic product), particularly in a developing country like Pakistan. Pakistan takes the role of the unidirectional causal bond between electricity consumption and economic activity which indicate increment in electricity demand corresponding to higher economic growth[1].In Pakistan, the power demand of electricity is increasing unexpectedly due to stable 6% growth in GDP per annum from 2002 to 2007 along with negligible planning of infrastructure in power sector. Pakistan faced critical power outages that came up with 2.5% losses in GDP, unemployment of 0.535 million industrial workers and losses in exports worth $1.3 billion in year 2010[2]. Energy economics is a technical approach to analyze and allocate the resources to providing energy to the public. It is excessively dependent on the policies as well as response of demand and supply by the energy market, which being the main source of unreliability for energy planners who mostly focus on developing an environment to invest capitally in energy sector[3].The World Energy Outlook (2016) insights that no less than 51 million individuals in Pakistan or 27% of the population live without any electricity access[4]. As indicated by IFC (International Finance Corporation), the energy rate for poor and needy individuals is much higher with roughly 36% or 67 million out of 185 million without any electricity access. The buildings consume 40% of total energy supply. Similarly, at national level, Pakistan is going through the worst energy crisis of its history. In Pakistan,

the building sector consumes about 27.4% of total energy supply and it is increasing rapidly due to energy intensive life style. Non-residential buildings consume significant amount of commercial energy non-residential consumers include industries, shopping plazas, hospitals and higher educational institutes[5]. Focusing on higher educational institutes which consumes more power than other buildings, it is necessary to have knowledge about how these institutes consume energy and what appliances they use, how much these appliances are efficient, and how can they reduce their cost of electricity consumption. The technologies of Renewable energy are essential in the growth of economic of any country. However, due to rapid increment in the cost of fuel and the problems associate with the energy crisis in the Country. Utilization of renewable energy resource becomes important now a days. These resources of energy and technologies such as PV cells, biomass and wind are pollution free also they can be utilized at very small scales. The Renewable energy which is dependent on very small-grid systems these are the desirable for agriculture buildings which is not based on conventional grid systems and can supply continuously electricity without causing any disturbance[6]. In this study, HOMER (Hybrid Optimization of Multiple Energy Resources) tool is used to undertake the techno economic feasibility analysis of village shafiabad (District Sanghar). HOMER software is appropriate to simulate technical and economical consideration of solar and wind off grid systems created by US National Renewable Energy Laboratory (NREL). HOMER software not only ensures the users to estimate various design options according to the technical and economic principles, but also give the possible changes and many uncertainties in inputs. There are sufficient literature reviews pertaining the utilization of renewable energy resources for the commodities. It is shown in the Literature Review that different studies have been conducted using the HOMER Software. Limited studies for the Pakistan contents are described following. M Kashif et al. [5] studied the hybrid system containing PV solar/Biomass generation system which is elaborated to carry out the needs of an agriculture sector for purpose of irrigation by using the HOMER software. Omar hafeez et al.[7] Studied the four different cases: Case I (a diesel only), case II (a fully renewable based), Case III (a diesel and renewable mixed), Case IV (External grid connected microgrids configurations by using HOMER Software). Alierazaet el al.[8] studied the solar panel technical and economic of hybrid systems containing the solar and wind to wind turbine to supply the electrical energy by using HOMER software. He obtained the results of PV cells and wind systems with 896 kWh/year and 343 kWh/year, respectively. Abolfaz et al. [9] studied the analysis of techno-economic of stand-alone hybrid PV diesel battery systems pertaining to remote rural areas electrification in the eastern part of Iran, where 5kWh/m^2 solar radiations is an essential quality. A number of studies have been conducted using HOMER software based on hybrid energy systems until now such as the investigation of feasibility of hybrid system using hydrogen as main source in Newfoundland made by Khan M. and Iqbal M.[10]. Munuswamy S. et al.[11] performed the comparison between electricity cost from fuel cell-based electricity generation and supply cost from grid using HOMER software.The results demonstrate that a distance greater than 44km from the grid, the off-grid electricity cost is inexpensive. The study mainly focuses on a small group not on a rural community. Olatomiwa et al.[12] studied different models of electricity generation based on hybrid systems such as solar, wind, and diesel generators in the different areas located in Nigeria using HOMER software. The results elaborate that hybrid model based on hybrid systems such as solar, wind diesel and batteries are the most economical with lowest carbon emissions. The limitations of this study that it doesn't include productive usage of electricity and only focuses on the basic rural community needs. Y. Himari et al.[13] studied the economical feasibility of an exciting diesel power plant which is supplying the electrical energy to remote village located in Algeria. Wind turbine was to be added in the exciting power system in order to mitigate the consumption of diesel and environment pollution. HOMER software was to be used for simulation. In this study it was found to be the hybrid system includes wind and diesel becomes more suitable at speed of 5.48m/s or more. Iyad et al.[14] studied the Hybrid Optimization of Multiple Energy Resources to carry out the optimum design of hybrid-micro power energy system for reducing the cost of energy, based on the different capacity shortage percentages. Chongi et al. [15] studied the techno-economic practical study of autonomous hybrid system including wind/ solar

photovoltaic (PV)/battery power system for a house located in Urumqi, China. HOMER software is used for the simulation. The purpose of the study is to decrease the total net present cost about 9% and 11% comparing with solar PV/ battery and wind/battery power systems. Gul and Qureshi et al.[16] have forecasted electricity demand by using multiple regression analysis and observed the result through LEAP software with a 8% of multiple growth rate of the electricity demand increase from 68 GWh in 2008 to 368 Gwhi n 2030.M Aslam uqalli et al.[17] has forecasted the electricity demand of Pakistan for study period 2013- 2035. Pervez and sohail et al.[18] have forecasted electricity demand from 2011-2030.Which they observed 1312 TWh in 2030.Ishaque et al.[19] has also been forecasted electricity demand in government policy (GP), Demand side management (DSM) and renewable energy (REN) scenarios over the period (2014-2035) which is to be 303.7 TWh. The above literature Review suggests that there is considerable work done towards the utilization of renewable energy resources globally, However, there is limited evidence in the literature on any study undertaking for renewable energy enrich Sindh province. Hybrid model provides flexibility to consider many options for electricity production in a cost-effective manner.

II. METHODOLOGY

There are various methodologies have been reported in the literature to undertake techno-economics feasibility analysis. In this study HOMER (Hybrid Optimization of Multiple Energy Resources) tool will be used. The methodological framework of this study is shown in figure 1. HOMER software, created by NREL (National Renewable Energy Laboratory, USA), which is used to carry out the optimal sizing to undertake the techno-economic feasibility of solar and wind off grid systems. Different models are simulated through this powerful tool. This software can be used for electric and heating loads to analyze the simulations depending on the different structures of solar and wind off grid systems. HOMER is also used to carry out the simulate the hybrid systems to balance the energy for each hour and carry out electric and thermal loads per hour to get the supply for the system[15].

A. Input Data

HOMER takes data of types as input including Technical data, Meteorological data, Economic data, Search Space, Load Profile and Equipment Characteristics as shown in Figure 1.in Technical Data Some technical data is required in HOMER which including strategy of dispatch for the simulation purpose, MACS, MREF, and operating reserve. Meteorological Data contains the solar radiation, wind speed, stream flow and temperature that are used as time series data or on the basis of monthly averages in the software. This software estimates the power output of wind turbines, photovoltaic array and hydro by using these inputs.

In Economic data Every equipment that HRES (Hybrid Renewable Energy Sources) uses, includes the cost data based on the Operation, Maintenance, Replacement and capital costs. To estimate these cost simulation and optimization is done for that purpose NPV (Net Present Value) is calculated. Load profile is an essential parameter regarding both the simulation as well as optimization. A few places like hospitals, industrial town sand higher studies institutes contain data of actual load consumption that are suitable to simulate. HOMER utilizes these data as time series data. Whereas, in few areas, particularly rural and remote regions where the actual time data is not promptly accessible, the load profile is, then determined as per the specifications of that area. Such data are then used in this software as daily profile and it utilizes the data in power balancing limitations.

In Search space HRES's (Hybrid Renewable Energy Sources) parameters contain the Wind turbine, Photovoltaic array, Generators and convertors of different sizes, for which there is requirement of search-space, to simulate and optimize the data. Search space contains different combination of equipment's, so, for that purpose Simulation and Optimization is needed.

In Equipment Characteristics Based on the characteristics or properties of individual equipment's, designed in the HOMER, in HRES its operation is more efficient[20].

B. Simulation and Optimization

The stages of optimization and simulation are done for each plan using search space. The key function is to minimize constraints. The main purpose of individual plan is to find the total NPC that represents the sum of revenues subtracted from the current value of the cost's summation. These costs contain the energy cost, which is bought from grid, operational cost, initial cost, cost of maintenance and cost of replacement along with fuel

2020 5th International Electrical Engineering Conference (IEEC 2020)
Feb, 2020 at IEP Centre, Karachi, Pakistan

cost. The energy revenue is bought by the grid. Also, the salvage values are shown by the revenues. These limitations include the charging and discharging limitations of battery, power balance limitations, limitations of energy transaction to the grid and generator technical limitations, etc. To get possible results, the output needed, is estimated containing NPC along with the outcomes of operational sources such as battery, converter and generator in time step,energy transaction with grid and emissions produced. The main purpose of feasibility is that in every step, the power balance constraints must be satisfied. For this, demand of each time step is supplied. Finally, these plans are arranged in accordance with the least net present cost (NPC). The plan with the least NPC is considered as the best. After using input data in HOMER, as discussed in former section, HOMER determines the suitable sizes of equipment of HRES in three stages which contain optimization, simulation and sensitivity analysis. Simulation, optimization stages are conducted concurrently.

C. Sensitivity Analysis

In optimum sizing methodology of HRES's values of few variables are not deterministic like cost of fuel, solar radiation, wind speed, price of electricity and component cost. The unreliability of these variables shows the main impact on the stage 's simulation and optimization. These variables are used in HOMER with various values. After simulating and optimizing results the resulting possible plans are calculated according to the NPC, the sensitivity is done. The stages of simulating and optimizing are repeated; the new more suitable plans are obtained for every uncertain parameter. For the evaluation of the effect of these uncertain parameters on results, two criteria including robust planning and risk planning are proposed in different studies. This software also produces adequate results to find how the most feasible plans output will be varied with those unreliable variables.

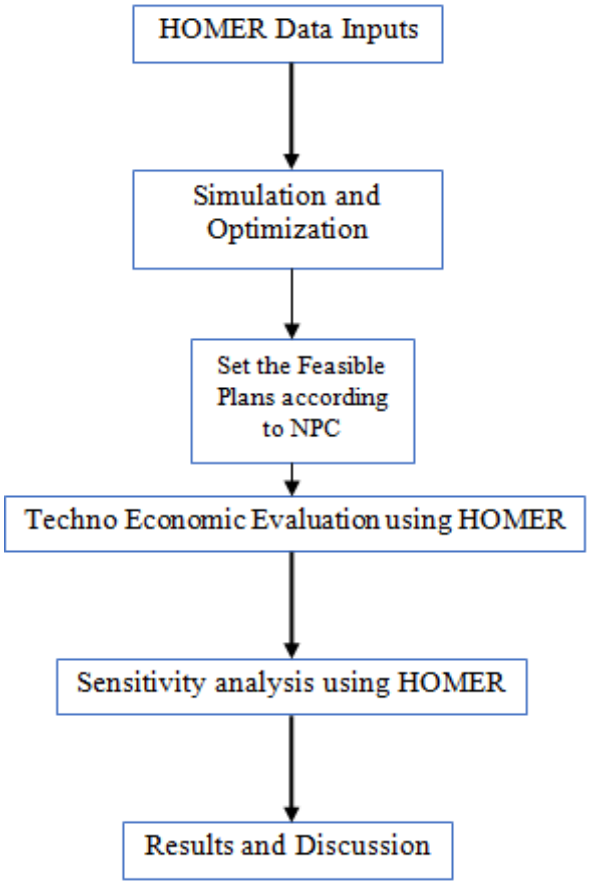

Fig.1. Modeling Framework of HOMER

the modeling procedure followed in HOMER to design a feasible system configuration as shown in the figure1. The input data required by the HOMER and uncertain variables involved in a sensitivity analysis that affects the feasible system configuration are given in the modeling framework of HOMER.

III. Results and Discussion

This study presents the optimization and sensitivity results. Different configurations were obtained in HOMER; energy balance calculations are performed by HOMER for each system configuration to find the optimal solution. The system must be capable of meeting the energy demand under specified conditions. HOMER sort out all the system configurations according their NPC. The system cost includes the initial capital, O&M cost, replacement cost, and interest rate. The optimization, sensitivity results, cost, technical details, and monthly electricity production by considering the sensitivity parameters. PV and Wind are designed to develop an optimal system configuration as

shown in figure 2 of PV-Wind hybrid system. Different configurations have been considered for off -grid electrification and most of system including least COE and NPC.

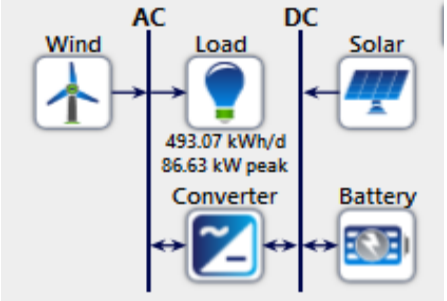

Fig.2. PV-Wind Hybrid System Configuration

A. Optimization Results

In the optimization process, distinctive optimal configurations are obtained, and the most prudent one is selected in the wake of running the simulation Different system configurations are able to meet the energy demand. Homer neglects all infeasible system configurations and sorts out the optimized results in ascending order according to the NPC and COE Different system configurations were analyzed to obtain an optimized hybrid energy system. Taking NPC as a selective parameter for comparison, most optimized result for HOMER is PV based system as first choice because it is the most economical option.

Table 1 Optimization Result of Hybrid System

Solar	Wind	Battery	Converter	NPC	COE
81.6kW	100kW	449	34.4kW	Rs29.4M	Rs16.43

With 81.6KW of PV, 100kW of wind, 34.4KW of converter were the most optimal configuration to fulfill the required energy demand. The total NPC and COE for the hybrid system are 29.4 M$,16.43M$ respectively. The NPC and COE of this configuration is much less as compared to all other configurations.

The electrical output of the proposed hybrid system in shown in Table 1. The excess electricity generated by the hybrid system and unmet are also given in Table 1. It shows that PV and wind penetration reduces electricity consumption from the grid and greenhouse gas emissions. Table 2 shows the technical details of optimal configurations.

Table 2 Technical Details of the Optimal Configuration

Architecture

PV- Array	Wind	Converter
81.6kW	100kW	34.4kW

Electrical Output

Quantity	PV-array	Wind
Production (kWh/yr.)	147,589	52,733
Fraction	73.7%	26.3%

Excess Electricity and Unmet Load

Quantity	kWh/yr.	Percentage
Excess Electricity	19119	9.54
Unmet Load	14756	8.20

The power output generated by the PV array is given eq.(1).

$$P_{PV} = Y_{PV} f_{PV} \left(\frac{\overline{G}_T}{\overline{G}_{T,STC}}\right)\left[1 + \alpha_P\left(T_c - T_{c,STC}\right)\right] \quad (1)$$

Where:

Y_{PV} is the rated capacity of PV array

f_{PV} is the derating factor [%]

$\overline{G}_T$ is the solar irradiance in the current time step [kW/m^2]

$\overline{G}_{T,STC}$ is the incident solar radiation at STC[1kW/m^2]

α_P is the temperature coefficient of power

T_c is the PV cell temperature in the current time step

The output power generated by the wind turbine is given by eq. (2) as given below

$$P_{WTG} = \left(\frac{\rho}{\rho_0}\right) P_{WTG,STP} \quad (2)$$

Where:

P_{WTG} is the power output [kW]

$P_{WTG,STP}$ is the wind turbine power output at STP[kW]

ρ is the density [kg/m^3]

ρ_0 is the air density at standard temperature and pressure (1.225 kg/m^3)

B.Sensitivity Analysis

In component sizing, some parameters are not known because they varied with the time. For the proposed hybrid system, the sensitivities variables considered are

solar irradiance and wind speed. The main variables included the system configurations are often not certain. the output of the system is affected by these uncertain variables These uncertain variables are considered to help the designer to find the most optimized and economic system configuration. The uncertainties are considered for the system are solar irradiance which is varied from 5.64kWh/m^2/day to 7.00kWh/m^2/day and wind speed which is varied 6.47m/s to 7.50m/s as shown in Table 3. The sensitivity results of the analysis show the how NPC and COE change with these sensitivity variables.

Table 3 Sensitivity Analysis Results

Solar Scaled Average	Wind Speed	Solar	Wind	NPC	COE
5.64kWh/m^2	6.47m/s	81.6kW	100kW	Rs29.4M	Rs16.43
6 kWh/m^2	6.8m/s	81.6Kw	100kW	Rs27.7M	Rs16.43
6.5 kWh/m^2	7.0m/s	76.3kW	100kW	Rs28.7M	Rs15.44
7.0 kWh/m^2	7.50m/s	88.0kW	100kW	Rs28.7M	Rs16.08

IV.CONCLUSION

This study undertakes the Techno-economic Feasibility Analysis of Hybrid off grid system for remote area of Shafiabad District Sanghar. There are different system configurations of PV-wind off grid system have analyzed by using HOMER Software.100% of total kWh production is generated from the which 81.6 kW solar and 100kW of wind and 34.4kW of convertor were optimized for this case study with the total net present cost of Rs 29.4M and the initial capital investment of Rs 17.0M. This hybrid off grid system provides the electricity at the low cost of Rs 16.43/kWh. The hybrid off grid renewable energy system is more reliable source of energy for case the study for remote areas. The COE obtained from such solar-wind systems can be reduced further. instead of utilizing the single RET, Hybridization of RETs must be given for the future projects because usage of single RET results in oversizing of the system. Sensitivity variables may affect the system performance and reliability; efforts should be made while designing such systems nullify the effect of sensitivity variables.

REFERENCES

1. Jamil, F. and E. Ahmad, *The relationship between electricity consumption, electricity prices and GDP in Pakistan.* Energy policy, 2010. **38**(10): p. 6016-6025.
2. Perwez, U. and A. Sohail, *Forecasting of Pakistan's net electricity energy consumption on the basis of energy pathway scenarios.* Energy Procedia, 2014. **61**: p. 2403-2411.
3. Sadeghi, M. and H.M. Hosseini, *Energy supply planning in Iran by using fuzzy linear programming approach (regarding uncertainties of investment costs).* Energy policy, 2006. **34**(9): p. 993-1003.
4. Reda, H.T., et al., *On the application of IoT: Meteorological information display system based on LoRa wireless communication.* IETE Technical Review, 2018. **35**(3): p. 256-265.
5. Shahzad, M.K., et al., *Techno-economic feasibility analysis of a solar-biomass off grid system for the electrification of remote rural areas in Pakistan using HOMER software.* Renewable Energy, 2017. **106**: p. 264-273.
6. Sen, R. and S.C. Bhattacharyya, *Off-grid electricity generation with renewable energy technologies in India: An application of HOMER.* Renewable Energy, 2014. **62**: p. 388-398.
7. Hafez, O. and K. Bhattacharya, *Optimal planning and design of a renewable energy based supply system for microgrids.* Renewable Energy, 2012. **45**: p. 7-15.
8. Gheiratmand, A., R. Effatnejad, and M. Hedayati, *Technical and economic evaluation of hybrid wind/PV/battery systems for Off-Grid areas using HOMER Software.* International Journal of Power Electronics and Drive Systems, 2016. **7**(1): p. 134.
9. Ghasemi, A., et al., *Techno-economic analysis of stand-alone hybrid photovoltaic–diesel–battery systems for rural electrification in eastern part of Iran—A step toward sustainable rural development.* Renewable and Sustainable Energy Reviews, 2013. **28**: p. 456-462.
10. Khan, M. and M. Iqbal, *Pre-feasibility study of stand-alone hybrid energy systems for applications in Newfoundland.* Renewable energy, 2005. **30**(6): p. 835-854.
11. Munuswamy, S., K. Nakamura, and A. Katta, *Comparing the cost of electricity sourced from a*

fuel cell-based renewable energy system and the national grid to electrify a rural health centre in India: A case study. Renewable Energy, 2011. **36**(11): p. 2978-2983.

12. Olatomiwa, L., et al., *Economic evaluation of hybrid energy systems for rural electrification in six geo-political zones of Nigeria.* Renewable Energy, 2015. **83**: p. 435-446.
13. Himri, Y., et al., *Techno-economical study of hybrid power system for a remote village in Algeria.* Energy, 2008. **33**(7): p. 1128-1136.
14. Muslih, I.M. and Y. Abdellatif. *Hybrid micro-power energy station; design and optimization by using HOMER modeling software*. in *Proceedings of the International Conference on Modeling, Simulation and Visualization Methods (MSV)*. 2011. The Steering Committee of The World Congress in Computer Science, Computer ….
15. Li, C., et al., *Techno-economic feasibility study of autonomous hybrid wind/PV/battery power system for a household in Urumqi, China.* Energy, 2013. **55**: p. 263-272.
16. Gul, M. and W.A. Qureshi. *Modeling diversified electricity generation scenarios for Pakistan*. in *2012 IEEE Power and Energy Society General Meeting*. 2012. IEEE.
17. Valasai, G.D., et al., *Overcoming electricity crisis in Pakistan: A review of sustainable electricity options.* Renewable and Sustainable Energy Reviews, 2017. **72**: p. 734-745.
18. Perwez, U., et al., *The long-term forecast of Pakistan's electricity supply and demand: An application of long range energy alternatives planning.* Energy, 2015. **93**: p. 2423-2435.
19. Ishaque, H., *Is it wise to compromise renewable energy future for the sake of expediency? An analysis of Pakistan's long-term electricity generation pathways.* Energy strategy reviews, 2017. **17**: p. 6-18.
20. Lambert, T., *Micropower System Modeling with Homer", in Integration of Alternative Sources of Energy by Felix A. Farret and M. Godoy Simoes.* 2006.

2020 5th International Electrical Engineering Conference (IEEC 2020)
Feb, 2020 at IEP Centre, Karachi, Pakistan

Design and Analysis of Controller for Non Isolated High Gain DC-DC converter

Saad Ahmad[1*] , Abasin Ulasyar[2] , Haris Sheh Zad[3] , Abraiz Khattak[4] , Kashif Imran[5]

[1,2,4,5] Department of Electrical Power Engineering, USPCASE, National University of Sciences and Technology (NUST), Islamabad, Pakistan.
(saadahmad331@yahoo.com) * Corresponding author
[3]Department of Electrical Engineering, Riphah International University, Islamabad, Pakistan.

Abstract: This paper discusses the control of Non Isolated High Gain (NIHG) DC-DC Converter through a PID Controller. Traditional DC-DC converters cannot give high voltage gain because of efficiency drop on high duty ratios. To overcome this, NIHG converters have been developed which shows good efficiency on high voltage gains. In this paper NIHG Converter is controlled through a PID controller in a closed loop system. State space equations for the converter has been developed and the equations are used to determine the controller parameters. The NIHG Converter is implemented in Simulink and the performance is observed for load variations, input voltage variations and change in reference voltage.

Keywords: Non-Isolated High Gain DC-DC Converter, State Space Average Model, PID Controller.

I. INTRODUCTION

DC-DC converters have many applications in Power supplies, LED Drives, DC motor drives, integration of renewable energy sources with the grid. Conventional converters used for the above applications are Buck, Boost, Buck-Boost and some isolated converters. Sometimes a very high voltage gain is required which cannot be achieved by the conventional converters as their efficiency on high duty ratios drops down significantly [1]. New topologies have been developed to address this issue [2-4].

NIHG converter is one of them which is proposed recently. The term "NIHG converter" used in this paper refers to the converter proposed in [5]. It shows good efficiency when operates with high voltage gain. It has less voltage stresses on switches as compared to conventional converters. It can be used in DC micro grids if an appropriate controller is designed for it. No work has yet been done to apply either conventional or advance control to this converter. Applying any kind of control to NIHG converter is different from other converters as it has three switches which is operated by two different duty ratios.

Many controllers are used for controlling DC-DC converters [6]. PID controller is one of them which is used widely. [7] proposes a PID controller for boost converter. The design of PID for enhanced performance of Boost converter is explained in [8].

This paper presents the PID control of NIHG converter. SSA equations of NIHG converter are derived. They are utilized to find the PID parameters for NIHG converter. Duty ratio for one switch is kept constant while other two switches which are run by pulses with the same duty ratios are controlled using PID controller. PID controller is applied to NIHG converter in Simulink. The output voltage is analyzed for different operating conditions i.e changing input voltage, varying load and change in reference voltage. NIHG converter with PID controller shows good performance in improvement of transient response and steady state voltage regulation.

II. OPERATION AND MATHEMATICAL MODELLING OF NIHG CONVERTER

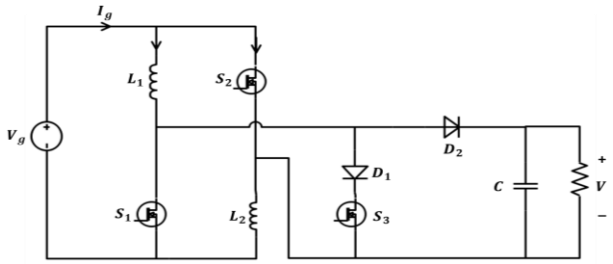

Fig. 2. NIHG converter

NIHG converter has 3 modes when operates in continues conduction mode (CCM). It has three switches S_1, S_2, S_3 and two diodes D_1, D_2. There ON OFF pattern is shown in the table below.

TABLE 1: ON OFF pattern of switches and diodes

Mode	Switches			Diodes	
	S_1	S_2	S_3	D_1	D_2
I	ON	ON	OFF	OFF	OFF
II	OFF	OFF	ON	ON	OFF
III	OFF	OFF	OFF	OFF	ON

SSA model of converter can be developed using detailed approach explained in [9]. The average model can be obtained by averaging the inductor voltages and capacitor currents. Some assumptions are made while

deriving the equations which are stated below.

- All components are assumed to be ideal.
- Inductor is large enough to make the converter operate in CCM operation.
- Capacitance is large enough to hold the output voltage constant.

Inductor currents and capacitor voltages are considered state space variables for typical converters. As this converter contains two inductors and a single capacitor therefore the state vector $\boldsymbol{x}$ contains three variables $i_1(\mathrm{t})$, $i_2(\mathrm{t}), \mathrm{v}(\mathrm{t})$ where i_1 = Current through L_1, i_2 = Current through L_2, v = Output voltage. The input vector u contains v_g while the output vector y contains source current i_g and output voltage v.

$$\boldsymbol{x} = \begin{bmatrix} i_1(\mathrm{t}) \\ i_2(\mathrm{t}) \\ \mathrm{v}(\mathrm{t}) \end{bmatrix} \quad \boldsymbol{u} = \begin{bmatrix} v_g(\mathrm{t}) \end{bmatrix} \quad \boldsymbol{y} = \begin{bmatrix} i_g(\mathrm{t}) \\ \mathrm{v}(\mathrm{t}) \end{bmatrix} \qquad (1)$$

The general State Space equations are shown below:

$$\dot{\boldsymbol{x}} = A\boldsymbol{x} + B\boldsymbol{u} \qquad (2)$$

$$\boldsymbol{y} = C\boldsymbol{x} + E\boldsymbol{u} \qquad (3)$$

Matrix form of equations during three modes of operation are shown below:

Mode 1:

$$\dot{\boldsymbol{x}} = \underbrace{\begin{bmatrix} 0 & 0 & 0 \\ 0 & 0 & 0 \\ 0 & 0 & -\frac{1}{\mathrm{RC}} \end{bmatrix}}_{A_1} \boldsymbol{x} + \underbrace{\begin{bmatrix} \frac{\mathrm{I}}{L_1} \\ \frac{\mathrm{I}}{L_2} \\ 0 \end{bmatrix}}_{B_1} \boldsymbol{u} \qquad (4)$$

$$\boldsymbol{y} = \underbrace{\begin{bmatrix} 1 & 1 & 0 \\ 0 & 0 & 1 \end{bmatrix}}_{C_1} \boldsymbol{x} + \underbrace{\begin{bmatrix} 0 \\ 0 \end{bmatrix}}_{E_1} \boldsymbol{u} \qquad (5)$$

Mode II:

$$\dot{\boldsymbol{x}} = \underbrace{\begin{bmatrix} 0 & 0 & 0 \\ 0 & 0 & 0 \\ 0 & 0 & -\frac{1}{RC} \end{bmatrix}}_{A_2} \boldsymbol{x} + \underbrace{\begin{bmatrix} \frac{1}{L_1+L_2} \\ \frac{1}{L_1+L_2} \\ 0 \end{bmatrix}}_{B_2} \boldsymbol{u} \qquad (6)$$

$$\boldsymbol{y} = \underbrace{\begin{bmatrix} 1 & 0 & 0 \\ 0 & 0 & 1 \end{bmatrix}}_{C_2} \boldsymbol{x} + \underbrace{\begin{bmatrix} 0 \\ 0 \end{bmatrix}}_{E_2} \boldsymbol{u} \qquad (7)$$

Mode III:

$$\dot{\boldsymbol{x}} = \underbrace{\begin{bmatrix} 0 & 0 & -\frac{1}{L_1+L_2} \\ 0 & 0 & -\frac{1}{L_1+L_2} \\ \frac{1}{C} & 0 & -\frac{1}{RC} \end{bmatrix}}_{A_3} \boldsymbol{x} + \underbrace{\begin{bmatrix} \frac{1}{L_1+L_2} \\ \frac{1}{L_1+L_2} \\ 0 \end{bmatrix}}_{B_3} \boldsymbol{u} \qquad (8)$$

$$\boldsymbol{y} = \underbrace{\begin{bmatrix} 1 & 0 & 0 \\ 0 & 0 & 1 \end{bmatrix}}_{C_3} \boldsymbol{x} + \underbrace{\begin{bmatrix} 0 \\ 0 \end{bmatrix}}_{E_3} \boldsymbol{u} \qquad (9)$$

Using SSA technique $A\,B\,C\,E$ parameters can be obtained by [8]:

$$A = A_1 D_1 + A_2 D_2 + A_3 D' \qquad (10)$$

$$B = B_1 D_1 + B_2 D_2 + B_3 D' \qquad (11)$$

$$C = C_1 D_1 + C_2 D_2 + C_3 D' \qquad (12)$$

$$E = E_1 D_1 + E_2 D_2 + E_3 D' \qquad (13)$$

Where D_1 is the duty ratio of switches S_1, S_2 . D_2 is the duty ratio of switch S_3 , $D' = 1 - D_1 - D_2$ and A_n, B_n, C_n, E_n are the matrices in mode "n" of the converter. By putting the values of A_n, B_n, C_n, E_n in Eqs. (10) ~ (13), the following matrices are obtained:

$$A = \begin{bmatrix} 0 & 0 & -\frac{\mathrm{D}'}{L_1+L_2} \\ 0 & 0 & -\frac{\mathrm{D}'}{L_1+L_2} \\ \frac{\mathrm{D}'}{C} & 0 & -\frac{1}{RC} \end{bmatrix} \quad B = \begin{bmatrix} \frac{D_1}{L_1} + \frac{1-D_1}{L_1+L_2} \\ \frac{D_1}{L_1} + \frac{1-D_1}{L_1+L_2} \\ 0 \end{bmatrix}$$

$$C = \begin{bmatrix} 1 & D_1 & 0 \\ 0 & 0 & 1 \end{bmatrix} \quad E = \begin{bmatrix} 0 \\ 0 \end{bmatrix}$$

III. PID CONTROLLER DESIGN FOR NIHG CONVERTER

PID controller can be connected in the circuit as shown in Fig. 1.

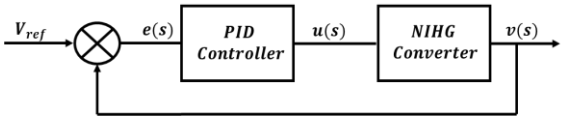

Fig. 1. PID controller in circuit

Reference Voltage (V_{ref}) is compared with the output voltage. The difference is called error (e). Controller takes the error signal as an input and its output (u) changes the duty ratio of PWM to keep the output voltage constant. Its transfer function is as under.

$$G(s) = \frac{u(s)}{e(s)} = K_p + \frac{K_i}{s} + K_d s \qquad (14)$$

Proportional gain (K_p) improves the response time of the control system. Integral gain (K_i) decreases the steady state error but may worsen the transient response. Derivative gain (K_d) decreases the overshoot and improves the system stability [10]. Various methods are used to find the parameters for PID controller. Parameters for PID controller can be found using SSA equations. SSA equations derived in this paper are implemented in Simulink. PID controller is connected to D_1 while D_2 is kept constant at 0.4. The parameters for the simulation are kept as $L_1 = L_2 = 0.0005H$, $C = 0.001F$, $R = 150ohm$. The PID controller is auto tuned to find the gains of the controller which comes out as shown in table 2.

TABLE 2: PID Gains

Proportional Gain (K_p)	Integral Gain (K_i)	Derivative Gain (K_d)
0.0523	2.6519	0.00023

The controller is tuned once and it works for different loads and input voltage variations.

IV. SIMULATION RESULTS AND DISCUSSION

For all simulations the values of converter parameters used are, $L_1 = L_2 = 500uH, C = 1000uF, f_s = 25khz$. NIHG converter is implemented in Simulink. Special

PWM generator is developed to ensure the switching sequence of the converter does not change with changing duty ratio D_1. The Simulink models of PWM generator and PID controlled NIHG converter are shown in Fig. 3 and Fig. 4 respectively.

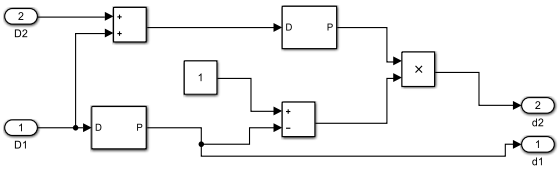

Fig. 3. Special PWM generator

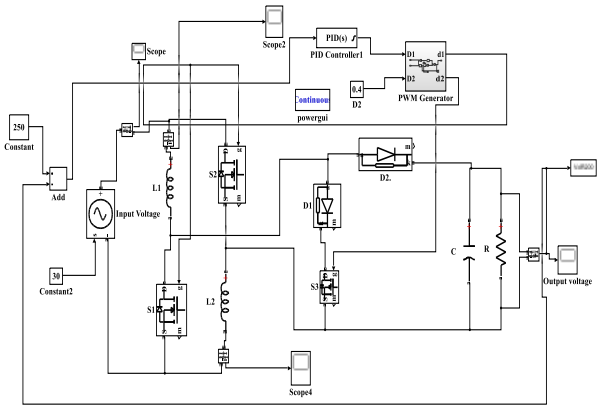

Fig. 4. Simulink Model of NIHG converter

For open loop simulation the duty ratios D_1 and D_2 are kept as 0.48 and 0.4 respectively. For closed loop simulation D_2 is kept constant at 0.4 while controller is connected to D_1 through PWM generator. Ref Voltage is taken as 250V. The performance is observed for three different scenarios i.e Load variations, input voltage variations and change in reference voltage.

A. Load Variations

Different Loads are applied to NIHG converter with PID controller. V_g and V_{ref} are taken as 30V and 250V respectively. The simulations results are shown in Fig. 5.

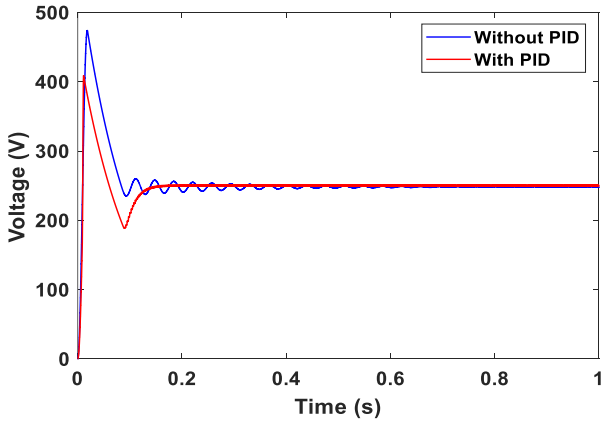

(a)

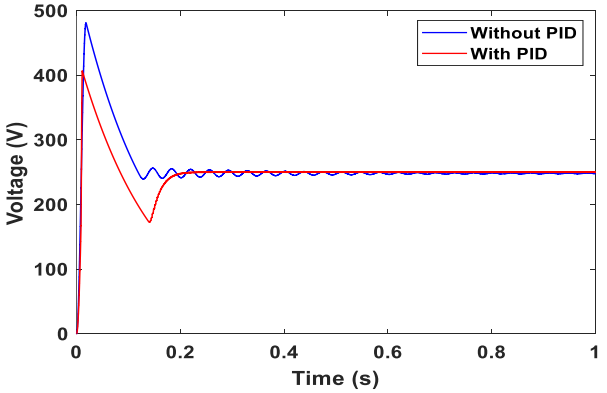

(b)

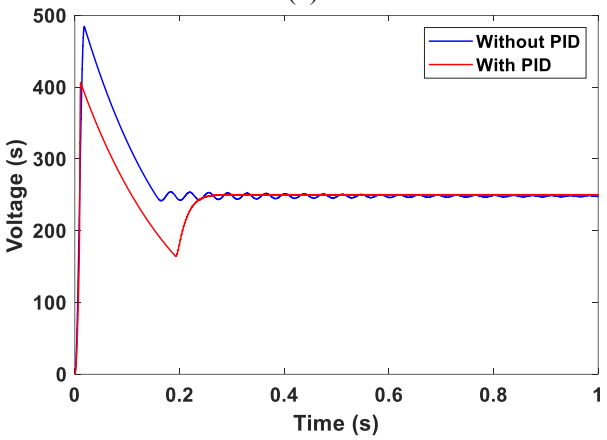

(c)

Fig. 5. Output voltage of NIHG converter for a) R=100ohm, b) R=150ohm, c) R=200ohm.

TABLE 3: Simulation results for load variations

Load (R)	Percent Overshoot		Settling Time	
	Without PID	With PID	Without PID	With PID
100 Ω	89.64%	63.52%	0.4s	0.14s
150 Ω	92.4%	62.80%	0.4s	0.19s
200 Ω	93.8%	62.60%	0.4s	0.24s

The results show that the PID controller reduced the overshoot by 29% 30% and 33% and settling time by 65%,52.5% and 40% for load of 100ohm, 150ohm and 200ohm respectively.

B. Input voltage variations

A step change of 5V in input voltage after every second is applied. V_{ref} and load are kept as 250V and 150ohm. The simulation is run for 3 seconds. The voltage waveform is shown in Fig. 6.

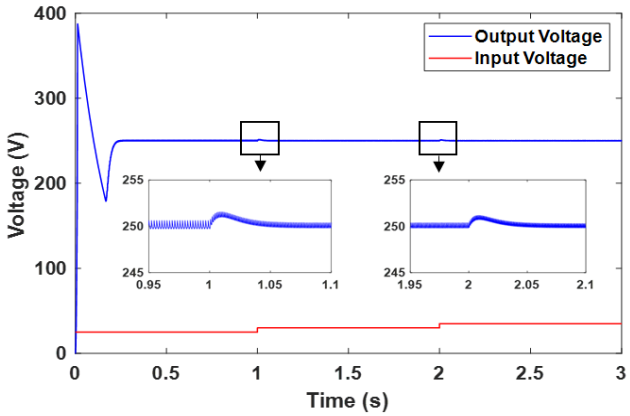

Fig. 6. Voltage waveforms for varying input voltage

The graph shows that after the initial transient, the step change in input voltage causes a change of 1.5V in output voltage but it returns back to its initial value in just 45ms.

C. Change in Reference Voltage

The input voltage is kept constant at 30V and load at 200ohm. Reference voltage with a step change of 50V after every second is applied. The simulation results are shown in Fig. 7.

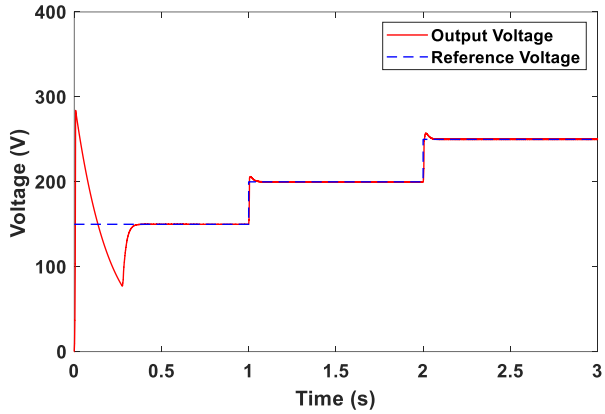

Fig. 7. Voltage waveforms for change in V_{ref}

It is observed that after the initial transient the output voltage followed the reference voltage. The response time to follow the V_{ref} after the change was 55ms.

V. CONCLUSION

PID controller for NIHG converter is designed. Its performance is evaluated for different operating conditions such as: varying input voltage, load changes and reference voltage tracking. The results show that the PID controller reduced the overshoot by 29% 30% and 33% and settling time by 65%,52.5% and 40% for load of 100ohm, 150ohm and 200ohm respectively. For step input voltage variations the response time to make the output voltage follow the reference voltage was just 45ms. For a 50V step change in reference voltage, the output voltage takes 55ms to follow the reference voltage. This converter can be used in DC micro grids where high voltage gain is required. Advance control techniques can be applied to this converter in future for more improvement in performance.

REFERENCES

[1] L. S. Yang, T. J. Liang and J. F. Chen, "Transformer less DC–DC Converters With High Step-Up Voltage Gain," IEEE Trans. Ind. Electron., vol. 56, no. 8, pp. 3144-3152, Aug. 2009

[2] A. Ajami, H. Ardi and A. Farakhor, "A Novel High Step-up DC/DC Converter Based on Integrating Coupled Inductor and Switched Capacitor Techniques for Renewable Energy Applications," IEEE Trans. Power Electron., vol. 30, no. 8, pp. 4255-4263, Aug. 2015.

[3] S. M. Chen, M. L. Lao, Y. H. Hsieh, T. J. Liang and K. H. Chen, "A Novel Switched-Coupled-Inductor DC–DC Step-Up Converter and Its Derivatives," IEEE Trans. Ind. Appl., vol. 51, no. 1, pp. 309-314, Jan.Feb. 2015.

[4] M. Forouzesh, K. Yari, A. Baghramian and S. Hasanpour, "Singleswitch high step-up converter based on coupled inductor and switched capacitor techniques with quasi-resonant operation," IET Power Electron., vol. 10, no. 2, pp. 240-250, Oct. 2017.

[5] M.LakshmiandS.Hemamalini,"Nonisolated high gain DC–DC converter for DC microgrids," IEEE Trans. Ind. Electron., vol. 65, no. 2, pp. 1205– 1212, Feb. 2018.

[6] H. M. Solaiman, M. M. Hasan, A. Mohammad, S. R. Kawsar and M. A. Hassan, "Performance analysis of DC to DC boost converter using different control methods," *2015 IEEE International Conference on Electrical, Computer and Communication Technologies (ICECCT)*, Coimbatore, 2015, pp. 1-5.

[7] L. Mitra and N. Swain, "Closed loop control of solar powered boost converter with PID controller," *2014 IEEE International Conference on Power Electronics, Drives and Energy Systems (PEDES)*, Mumbai, 2014, pp. 1-5.
doi: 10.1109/PEDES.2014.7041973

[8] Adnan, Mirza & Oninda, Mohammad & Nishat, Mirza & Islam, Nafiul. (2017). Design and Simulation of a DC-DC Boost Converter with PID Controller for Enhanced Performance. International Journal of Engineering Research & Technology (IJERT). 6. 27-32. 10.17577/IJERTV6IS090029.

[9] Erickson, R. W.; Maksimovic, D. Fundamentals of Power Electronics.2ed. Springer, 2001.

[10] R. K. Chauhan, B. S. Rajpurohit, R. E. Hebner, S. N. Singh and F. M. G. Longatt, "Design and analysis of PID and fuzzy-PID controller for voltage control of DC microgrid," *2015 IEEE Innovative Smart Grid Technologies - Asia (ISGT ASIA)*, Bangkok, 2015, pp. 1-6

2020 5th International Electrical Engineering Conference (IEEC 2020)
Feb, 2020 at IEP Centre, Karachi, Pakistan

Reactive Power Compensation in the Vicinity of Multiunit Nuclear Power Plant with P-V and Q-V Curves Analysis

Muhammad Umer, Naila Zareen, Abdul Ahad, Moaz Ahmad, Abdul Rehman Abbasi and Tauseef-ur-Rehman Khan*

Karachi Institute of Power Engineering (KINPOE) College, PIEAS
Karachi, Pakistan.
*National Transmission and Dispatch Company (NTDC)
Lahore, Pakistan.
umerlive0@gmail.com, dr.naila.zareen@paec.gov.pk, abdulahadqu@gmail.com, moazahmad@ymail.com, arehmanabbasi@paec.gov.pk, *r.tauseef@ntdc.com.pk

Abstract: Inadequate reactive power support at the load side results in poor voltage profile at load end as well as line over loading, especially under peak load condition. Line overloading increases the probability of line loss contingency. Over frequency surge is observed at generators of base load nuclear power plants in case of line loss contingency due to failure in successful dispersal of generated power. That results in tripping of generators and subsequent tripping of reactors. These problems can be addressed by installation of SVCs (Static VAR Compensators) at load end as a source of reactive power and simulated in ETAP. P-V and Q-V curve analysis is used for voltage stability assessment of system and determine required reactive power compensation. Reactive power from SVCs will improve voltage profiles of load buses as well as reduce line flows. That reduces the probability of line loss due to over loading conditions.

Keywords: NPP, VAR, P-V and Q-V Curves, Voltage Stability, SVCs.

I. INTRODUCTION

Power System Security Assessment is method of identifying, whether the system stays in secure (typical) or shaky (crisis) state in case of any pre-defined list of possible contingences. The most well-known operational issues in case of these contingencies are transmission gears overloading and poor voltage levels at different buses of system. Static security issue assesses the system steady state performance for all possible proposed contingencies, while dynamic investigation is related to behavior of the system of the order of few minutes under transient influences [1].

Society's expanding reliance on a reliable power supply, the significance of avoiding huge aggravations and appropriately identifying the distance to the stability limits is growing. So, the primary phase of maintaining reliable operation of power system is to keep parameters within the satisfactory range.

Voltage Stability of a load bus depends upon two factors, transmission network and load connecting to bus. If demand increases, and transmission network supplying power to load bus is suitable to deliver required power then bus voltage will remain within the stability limit. And if transmission network is weak, with increasing load, not only voltage profile will be affected, there will be chances of line loss due to thermal constraints. And that will jeopardize overall stability of system.

Same situation is observed in the vicinity of 1330MW Nuclear Power Complex when there is transmission line loss between Ludewala 220kV Grid Station and power plants in peak load conditions at Ludewala Grid. Peak load condition not only affects the voltage of Ludewala bus, but also results in subsequent loss of transmission lines due to overloading and over frequency surge at NPP. One solution of avoiding over frequency is flexible operation of NPP. But it is not possible because under discussion nuclear power plants are base load power plants. This entire scenario not only severely effects the operation of NPP but also affects the reliability of power supply.

A. Voltage Stability

Voltage stability is a part of power system stability. Absence of voltage stability in a power system prompts a wild drop (or ascend) in voltages following an aggravation. It is initially a local phenomenon, yet the results can spread to a more extensive region due to falling impacts, referred to as a voltage break down.

Voltage break down or voltage instability phenomena are the ones wherein the receiving end voltage diminishes well beneath its ordinary level and doesn't return considerably after the operation of remedial systems, for example, VAR compensators, or keeps on fluctuating for absence of damping against the instability. Voltage collapse is the phenomena by which the voltage falls to a low unacceptable value as a result of an avalanche of events accompanying voltage instability [2].

As a result of voltage instability, a power system may experience voltage breakdown, if the post disturbance voltages close to load are lower than the defined limit. Voltage breakdown is additionally characterized as a process by which voltage insecurity prompts exceptionally low voltage profile in a noteworthy part of system. The fundamental driver of voltage breakdown might be because of the failure of the power system to supply the reactive power or an excessive ingestion of the reactive power by the power system itself. The voltage stability can be examined either on static (slow time period) or dynamic (long time allotment) considerations [3]. The steady state voltage stability strategies are for the most part relies upon steady state model in the

examination, for example, power flow model. Several methods [4] have been used in static voltage stability analysis such as the,

- PV and QV curves,
- Model Analysis,
- Optimization Method,
- Continuation Load Flow Method.

B. Methods of Improving Voltage Stability

The power system voltage instability can be improved using the following methods [2],

- Generator AVRs
- Under-Load Tap Changers
- Load shedding during contingencies
- Reactive Power Compensation.

In this paper reactive power compensation is used as a method of improving voltage profile

C. Reactive Power Compensation

Actually, voltage instability is the result of required and available reactive power imbalance. Load bus is affected by voltage collapse. To avoid voltage instability reactive power compensation is provided locally. Different methods [5] are used for reactive power support,

- Series Capacitor
- Switched Shunt-Capacitor and Reactor
- Transformer LTC
- Phase Shifting Transformer
- Synchronous Condenser
- FACTS (Flexible AC Transmission Systems).

D. Benefits of Improving Voltage Stability

Once a suitable solution is determined for improving voltage stability, following benefits can be observed in system,

- Increased Loading and More Effective Use of Transmission Corridors
- Improved Power System Stability
- Increased System Security
- Increased System Reliability
- Added Flexibility in Starting New Generation
- Elimination or Deferral of the Need for New Transmission Lines

Vancha Abhilash, Kamlesh Pandey have performed load flow analysis of 400kV substation in [6], with an approach to overcome the problem of harmonics and to increase the flexibility of the system. And determine the optimum size and location of capacitors to surmount the problem of an under voltage. Also, determining the system voltages, under conditions of suddenly applied or disconnected loads.

C. T. Vinay Kumar, P. Bhargava Reddy in [7], suggested a novel approach for optimal placement of FACTS devices based on Bacterial Foraging Optimization (BFO) algorithm. The simulations are carried on the IEEE 30-bus system. The optimization technique results of TCSC (Thyristor Controlled Series Capacitor) are compared with the results of UPFC (Unified-Power-Flow Controller). Results indicate that the placement of FACTS devices leads to improve in voltage stability margin of power system and reduce losses.

Nguyen Nhut Tien in [8], studied the voltage stability of Vietnam power system with the effect of upcoming nuclear power plant. Through P-V and Q-V analysis, it is resulted that the power system in Vietnam operates stably in normal condition with the integration of the large nuclear power plant. Besides, weak buses in the system and contingencies that potentially affect the voltage stability are identified. With the installation of STATCOMs at different load buses, Vietnamese power system and the area around the nuclear power plant are more stable because the maximum power transfer ability, reactive power limit and voltage values of weak buses are risen significantly at various operation modes.

The purpose of this paper is to estimate the stability limits of load buses at different loading conditions and suggest some appropriate remedy to avoid static instability. For static stability analysis P-V and Q-V curves of varies load buses are determined. These plots give voltage profile of load buses at different loading conditions. These P-V and Q-V plots give information about amount of reactive power compensation so that voltage profile remains within the acceptable range. This reactive power compensation will be provided by using SVC and the effect of SVC will be observed by improved P-V and Q-V plots. For the simulation of all scenarios ETAP Software is used.

II. METHODOLOGY

A. Mathematical Modeling

Voltage instability is generally a result of a load response to a disturbance that will cause the maximum power transfer level of the system to be exceeded. The maximum power transfer level is determined by several factors, and can be illustrated by considering a simple network consisting of a transmission line with a generator in one end supplying a load in the other end, as shown in Figure.

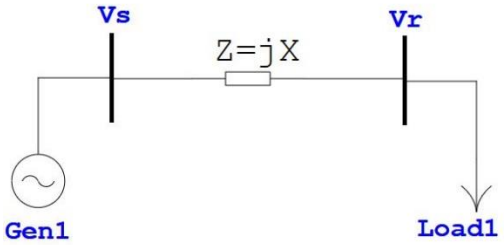

Figure 1: Two Bus Power System.

The active and reactive power consumed by the load is determined by the power flow equations of the system,

$$P_L = \frac{V_S V_R}{X} \sin\delta \qquad (1)$$

$$Q_L = \frac{V_S V_R}{X}\cos\delta - \frac{V_R^2}{X} \quad (2)$$

Where,
P_L = Load Real Power,
Q_L = Load Reactive Power,
V_S = Sending end or generation bus voltage,
V_R = Receiving end or load bus voltage,
X = Transmission line reactance and,
δ = Voltage angle difference between V_S and V_R.

By using equation (1) and (2), following relation is determined between receiving end voltage and active power flow,

$$V_R = \sqrt{\frac{V_S^2}{2} - P_L\tan\phi X \pm \sqrt{\frac{V_S^4}{4} - V_S^2 P_L X\tan\phi - P_L^2 X^2}} \quad (3)$$

Equation (3) can be further simplified by converting it into per unit.

$$v_R = \sqrt{\frac{1}{2} - p\tan\phi \pm \sqrt{\frac{1}{4} - p\tan\phi - p^2}} \quad (4)$$

Equation (4) represents the P-V Curve of power system.

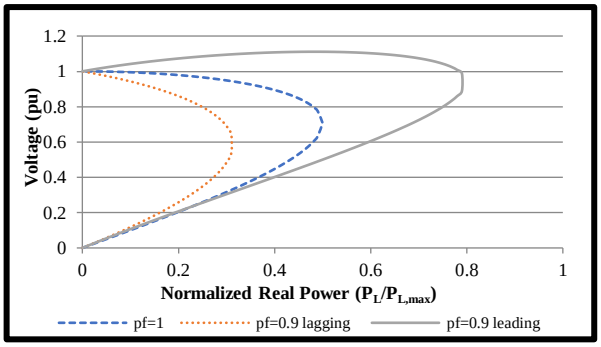

Figure 2: P-V Curve of 2 Bus System at Various Load Power Factors.

Figure 2 indicates P-V curve of the system at different load (resistive, inductive and capacitive). Due to the characteristic shape of the curves, they are also called nose curves, and the tip of the curve represents the maximum power transfer level of the system for a given load.

The part of curve above maximum power transfer level represents the stable system and below that point represents the unstable system and load flow don't converge in the lower section of curve. The distance from maximum power transfer level point represents the stability margin of the system.

Converting (1) and (2) into per unit system,

$$p = v_R\sin\delta \quad (5)$$

$$q = v_R\cos\delta - v_R^2 \quad (6)$$

For specific value of p, equation (5) is used to find power angle δ. And for different values of v_R, equation (6) will provide Q-V curve of system.

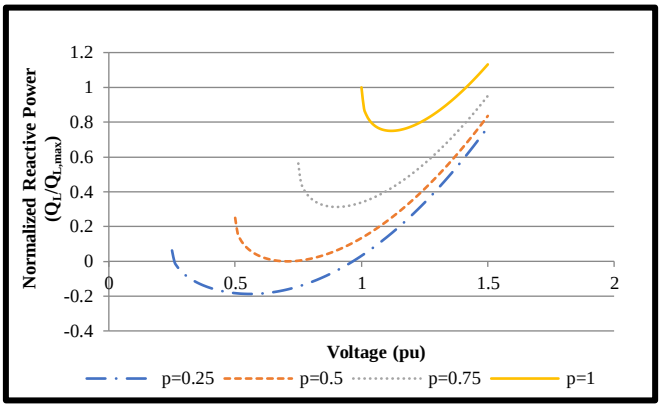

Figure 3: Q-V Curve of 2 Bus System at Various Load Active Power Demands.

Figure 3 represents Q-V Curve of two bus power system at different values of active power supplied to the load. The curves above x-axis represents reactive power deficiency in system. The distance between minimum point of curve and x-axis represents the amount of reactive power required to avoid voltage collapse. For curve that cuts x-axis, it represents surplus reactive power in the system and can be provided to the system at low voltage condition.

B. Voltage and Frequency Stability Limits

As per National Electric Power Regulatory Authority (NEPRA) Performance Standards (Transmission) Rules (PSTR) 2005, allowable range of system voltage variation is described in following subsections.

System Voltage

i. Under normal conditions the voltage variations of plus or minus ±5% of the nominal voltage for voltages of 132kV (where applicable) and above shall be permitted.

ii. Under (N-1) contingency conditions voltage variations of plus or minus ±10% of the nominal voltage for voltages of the 132kV (where applicable) and above shall be permitted [9].

C. ETAP Simulation

NTDC Network (2018) is implemented in ETAP. Figure 4 shows load flow analysis of plants region region. In peak load condition most of the load buses are under voltage. This under voltage due to high load condition causes transmission line to be over loaded. As a solution to this over loading, load shedding and reactive power compensation will be used. Peak Load and voltage of different buses is shown in Table 1.

Table 1: Percentage Voltages of Load Buses at Peak Load.

Bus Name	P (MW)	Q (Mvar)	S (MVA)	%V
Shahibagh	479.45	268.89	549.71	84.75
Daud Khel	401.27	211.99	453.82	89.02
Peshawar	560.97	322.12	646.88	91.41
Bannu	310.37	187.20	362.45	87.55
Ludewala	689.50	327.47	763.32	84.091

To improve voltage profile and to avoid line loss, first P-V and Q-V analysis will perform for each of the above buses. And then remedy will be selected and effect will be observed.

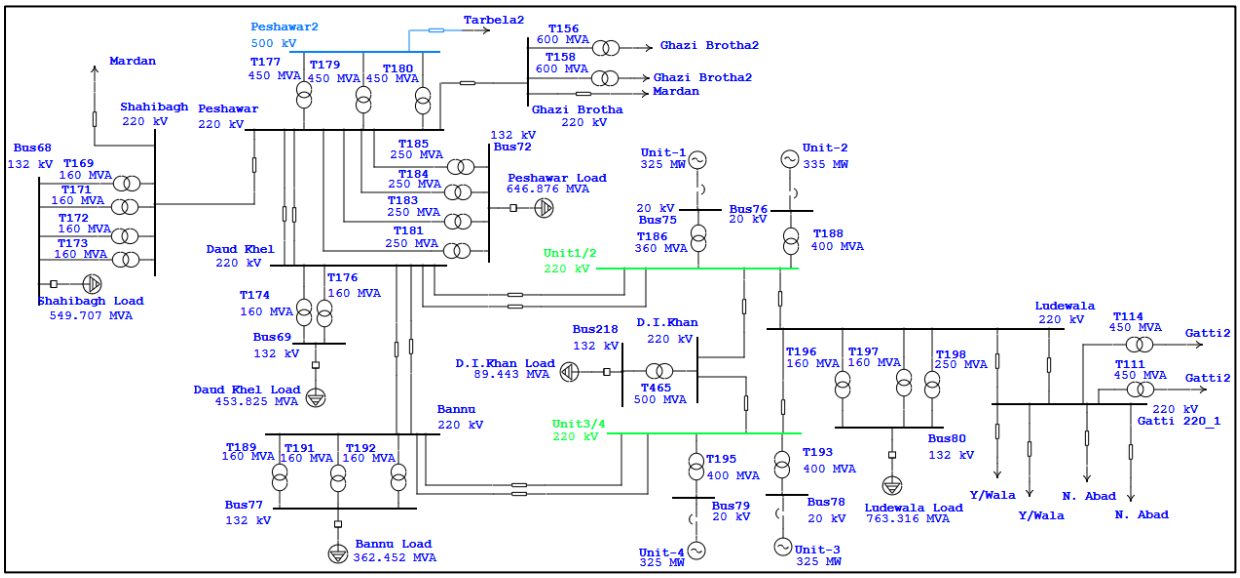

Figure 4: ETAP Simulation (Plants Region).

III. DETERMINING REACTIVE POWER COMPENSATION

A. Voltage Profile at Various Loading Conditions

To plot P-V and Q-V profiles of Ludewala, Daud Khel, Peshawar and Bannu, static voltage response of these buses will be obtained at various loading conditions. Load of will be varied from 100% to 50% of peak load for all buses. It will also give an idea of system voltage profile variation on seasonal basis.

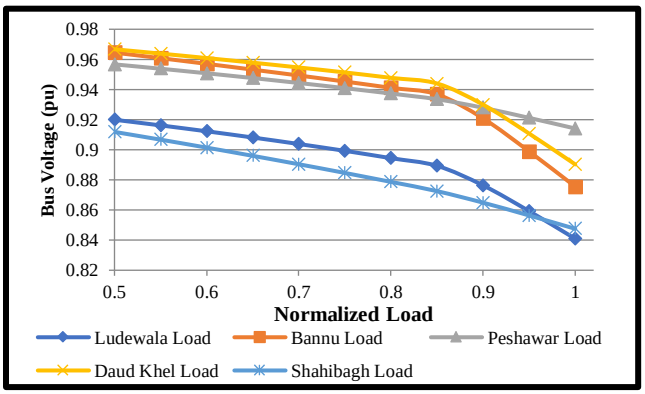

Figure 5: Voltage Profile of Load Buses of Plants Region at Various Loading Conditions.

By increasing load, voltage of load buses decreases, but load buses of Shahibagh and Ludewala are highly effected. Reasons for such poor low are,

i. Ludewala bus is highly overloaded bus and transmission network is weak. Power supply from Gatti to Ludewala is very low.

ii. Shahibagh bus is an isolated bus and power supply is from Peshawar and Mardan and both are load buses.

B. Ludewala Load Bus Reactive Power Compensation

Table 2: Effect of Reactive Power Demand Reduction at Ludewala Bus.

Q (Mvar)	Q	%V	V (kV)	pf
350	1	82.957	182.5054	89.44
300	0.85	85.13	187.286	91.91
250	0.71	87.2	191.84	94.17
200	0.57	89.17	196.174	96.15
150	0.43	91.06	200.332	97.78
100	0.28	92.43	203.346	98.99
50	0.14	93.52	205.744	99.75
0	0	94.6	208.12	100
-50	-0.14	95.66	210.452	-99.8

So, from Table 2, the amount of reactive power that should be provided locally will be,

$$350 - (-50) = \mathbf{400\ Mvar} \qquad (7)$$

To keep voltages within the range defined by NEPRA. By reactive power compensation or alternative saying by power factor improvement line flows are also reduced.

By power factor improvement at load end, reactive power and line currents are reduced as a result lines are less over loaded or in other word lines are now far below thermal margin. Negative sign of power flow indicates the reverse power flow as compared to base case, as shown in Table 3.

Table 3: Flows in Transmission Lines Connected to Ludewala with improving Power Factor.

pf	Unit-1/Unit-2 to Ludewala		Unit-3/ Unit -4 to Ludewala		Gatti to Ludewala	
	Q (Mvar)	I (kA)	Q (Mvar)	I (kA)	Q (Mvar)	I (kA)
89.44	131.9	837.6	132.6	839.9	110.6	367.4
91.91	123.7	818.5	124.5	820.8	88.2	315.7
94.17	115.5	801.1	116.5	803.4	66.6	271.8
96.15	107.5	785.2	108.5	787.5	46	237.1
97.78	99.5	770.7	100.7	773	26.1	213.9
98.99	87.3	759.5	88.3	761.6	11.8	204.7
99.75	72.9	751.4	73.6	753.1	0.226	202.6
100	58.8	745.2	59.3	746.7	-11.2	205.6
-99.8	45	740.9	45.1	742.3	-22.4	213.4

C. Required Size of SVCs

So, the required amount of reactive power compensation at the load buses in the vicinity of nuclear power complex is shown in Table 4. This compensation is suggested to be provided by SVCs. But in actual system some of the compensation has must be provided at load end by some other means like capacitor banks. So, the remaining compensation can be provided by SVCs. Specially load buses of Ludewala and Shahibagh require reactive power compensation. It will not only improve the voltage profile of load buses but also decrease line flows and currents, and line loss probability will reduce as the margin from thermal limit will increase.

Table 4: Calculated Size of SVCs.

SVC Size	
Buses	Q_C (Mvar)
Shahibagh	500
Daud Khel	200
Peshawar	400
Bannu	150
Ludewala	400

D. Effect of SVCs on Voltage Profile

Table 5, shows the voltage improvement of load buses after the implementation of SVCs. After installation of SVCs, voltage of load buses is within the limits defined by NEPRA, even in case of peak load condition.

Table 5: Voltage Profile of Load Bus with and without SVCs.

Buses	Without SVC		With SVC	
	%V	V (kV)	%V	V (kV)
Shahibagh	84.75	186.45	96.03	211.266
Daud Khel	89.02	195.844	96.71	212.762
Peshawar	91.41	201.102	97.36	214.192
Bannu	87.55	192.61	96.35	211.97
Ludewala	84.09	184.998	95.66	210.452

E. Line Flows with and without SVCs

After implementing SVCs, much of the reactive power has been supplied locally near the load end. As a result, reactive power flow reduced in lines and transmission corridors are efficiently used for active power flow, as indicated in Tables 6, 7 and 8.

Table 6: Transmission Lines Flows without SVCs.

Lines	Without SVC			
	P (MW)	Q (Mvar)	S (MVA)	I (kA)
Unit-1/Unit-2 to Ludewala	268.9	127.6	297.64	823.3
Unit-3/ Unit-4 to Ludewala	269.7	128.3	298.66	825.7
Gatti to Ludewala	67.5	99.4	120.15	335.4
Unit-3/Unit-4 to Bannu	133.8	78.1	154.93	428.3
Peshawar to Shahibagh	334.2	239.3	411.04	1180
Ghazi Brotha to Peshawar	152.8	150.8	214.68	563.7
Peshawar to Tarbela	735.9	520.9	901.60	1041
Unit-1/Unit-2 to Daud Khel	212.7	112.7	240.71	666

Table 7: Transmission Lines Flows with SVCs.

Lines	With SVC			
	P (MW)	Q (Mvar)	S (MVA)	I (kA)
Unit-1/Unit-2 to Ludewala	276.8	45.1	280.45	736.1
Unit-3/Unit-4 to Ludewala	277.4	45.1	281.04	737.5
Gatti to Ludewala	70.4	-21.9	73.73	203.6
Unit-3/Unit-4 to Bannu	133.7	32	137.48	360.8
Peshawar to Shahibagh	354.1	24.6	354.95	956.7
Ghazi Brotha to Peshawar	160.8	33	164.15	430.9
Peshawar to Tarbela	791.9	133.4	803.06	927.4
Unit-1/Unit-2 to Daud Khel	204.3	57.6	212.26	557

Table 8: % Reduction in Q and I with SVCs Installed.

Lines	% Reduction	
	Q (Mvar)	I (kA)
Unit-1/Unit-2 to Ludewala	64.655	10.5915
Unit-3/Unit-4 to Ludewala	64.848	10.6818
Gatti to Ludewala	122.032	39.2964
Unit-3/Unit-4 to Bannu	59.027	15.76
Peshawar to Shahibagh	89.720	18.9237
Ghazi Brotha to Peshawar	78.117	23.5586
Peshawar to Tarbela	74.390	10.9126
Unit-1/Unit-2 to Daud Khel	48.891	16.3664

IV. Ludewala Line Loss Contingency

Despite of installation of SVCs to reduce lines overloading and decrease probability of line loss due to line overloading, if there is a line loss contingency occurs then still system voltage profiles is within the defined limit of NEPRA that is now ±10 of nominal voltage. Table 9, show the voltage of Ludewala bus in case of line loss between UNIT-1/UNIT-2 and Ludewala bus. With SVCs installed post contingency voltage is 94.12% that is still within the acceptable limit. And % reduction in line flows with and without SVC is shown in table 10.

Table 9: Ludewala Bus Voltage in case of Line Loss Contingency.

Unit-1/Unit-2 to Ludewala Line Loss		
Ludewala bus Voltage %V	Without SVC	With SVC
Pre-Contingency Voltage	84.09	95.66
Post Contingency Voltage	77.69	94.12

Table 10: %Reduction in Line Flows in case of Line Loss.

Transmission Lines	% Reduction	
	Q	I
Unit-3/ Unit -4 to Ludewala	61.90	10.55
Gatti to Ludewala	107.07	39.23
Unit -3/ Unit -4 to Bannu	59.03	15.04
Daud Khel to Bannu	106.32	36.47
Peshawar to Shahibagh	90.17	17.97
Peshawar to Daud Khel	48.20	46.67
Ghazi Brotha to Peshawar	77.39	28.76
Peshawar to Tarbela	74.77	12.49
Unit-1/Unit-2 to Daud Khel	51.73	15.40
Daud Khel to Bannu	106.32	36.47
Daud Khel to Peshawar	151.80	46.67

CONCLUSION

Response of the system elements is observed by using P-V and Q-V curve analysis. In case of peak load condition power flows through transmission lines are high enough that can breach the allowable thermal limit of lines. And lines can trip due to over loading. This problem is much severe for transmission lines connected to highly loaded buses like Ludewala, Peshawar and Shahibagh in the vicinity of 1330MW nuclear power complex. To avoid line tripping due to over loading, reactive power flow through lines is reduced by supplying reactive power locally by installing SVC (Static Var Compensators). Reactive power supply from SVC is adjusted by automatic control of thyristors. Significant reduction in line flows is observed through lines. And by supplying reactive power locally voltage profile of buses is also improved. Voltage Stability is used as an indicator to observe the health of system. Once we have successfully avoided line loss due to overloading the over frequency surge at Base Load Nuclear Power Plants. Finally, despite of this remedial measure if there is a line loss because of any reason then still the bus voltage is with the defined limits of NEPRA and line flows are also significant low then the line loss contingency case without installation of SVCs.

REFERENCES

[1] J. P. V. A. Prabha Kundu, "Definition and Classification of Power System Stability," *IEEE TRANSACTIONS ON POWER SYSTEMS*, vol. 19, pp. 1387-1400, 2004.

[2] P. A. T. Neha Parsai, "PV CURVE – APPROACH FOR VOLTAGE STABILITY ANALYSIS," *International Journal of Scientific Research Engineering & Technology (IJSRET)*, vol. 4, no. 4, pp. 373-377, 2015.

[3] A. A. Khan, "A Simple Method for Tracing P -V," *International Journal of Electrical, Computer, Energetic, Electronics and Communication Engineering*, vol. 2, 2008.

[4] C.W.Taylor, Power System Voltage Stability, McGrawhill, 1993.

[5] A. K. B. Alok Kumar Mohanty, "Power System Stability Improvement Using Fact Devices," *International Journal of Modern Engineering Research (IJMER)*, vol. 1, no. 2, pp. 666-672.

[6] K. P. Vancha Abhilash, "Power Devices Implementation & Analysis in ETAP," *International Journal of Engineering and Technical Research (IJETR)*, vol. 2, no. 5, pp. 273-277, 2014.

[7] P. B. R. C. T. Vinay Kumar, "Comparison of Facts Devices to Reduce Power System Losses and Improvement in Voltage Stability by Using Optimization Technique," *International Journal of Science and Research (IJSR)*, vol. 4, no. 10, pp. 2246-2250, 2015.

[8] N. N. Tien, "Application of STATCOMS to improve static voltage stability for Vietnam Power System with grid connection of large nuclear power plant.," *Can Tho University Journal of Science*, vol. 2, pp. 50-60, 2016.

[9] N. E. P. R. Authority, "Performance Evaluation Report," 2016-2017.

2020 5th International Electrical Engineering Conference (IEEC 2020)
Feb, 2020 at IEP Centre, Karachi, Pakistan

Transients Fault Analysis using nonlinear state space model of Synchronous Generator

Muhammad Suleman, S Sajjad H Zaidi, Nauman Memon and Bilal Muhammad Khan
tuniosuleman@yahoo.com, sajjadzaidi@pnec.nust.edu.pk, nauman.m@yahoo.com, bmkhan@pnec.nust.edu.pk
Department of Electronics & Power Engineering, Pakistan Navy Engineering College, Karachi, National University of Sciences and Technology, Islamabad ,

Abstract: The focus of this paper is based on analyzing the transient faults of synchronous generator SG. The third order state space nonlinear model for the synchronous generator is designed in MATLAB and faults were discussed. The state space modeling of the system is obtained and then system is applied on the synchronous Generator. Different types of faults were observed by applying disturbances to the system and they are compared to the actual system. Nature of faults currents determine the type of faults. The faults currents analysis give us the details about the health of generator. Further, the health is predicted with the help of transients in the system. This system works well for diagnosing the transient faults of synchronous generator.

Keywords: Synchronous Generator, Nonlinear State Space Model, MATLAB.

NOMENCLATURE

V	Bus Voltage
E_F	Field Voltage
e'_q	transient internal generated voltage
J	rotor inertia
T_m	input mechanical torque
T_e	input electrical torque
P_e	mechanical input power
D	Damping factor
T'_{do}	transient time constant
V_t	generator terminal voltage
X_d	direct axis reactance
X'_d	direct axis transient reactance
I_d	stator axis currents
X_q	quadrature axis reactance
δ	rotor angle of synchronous generator
ω	angular speed for rotor

I. INTRODUCTION

As the demand for power supply is increasing rapidly due to the advancement in the technology. Without the supply of power, technology is useless. The main source of power is generator. Therefore the health of generator is prime concern. There are many methods have been designed to monitor the health of generator. The most power plants use the synchronous generators for the power supply. The main unit of power plants is generator which is to be monitored continuously to check its performance.

Different techniques have been implemented to protect the generators from faults and monitoring the faults currents. The stator ground faults are common in synchronous Generators [1]. The other faults also occur in generators which are generator unbalance, field ground faults, loss of excitation and generator unbalance [2], [3]. These faults mostly affects the generator operations. It is necessary to determine the effects of faults on the system in order to protect them so that the life of generator can be extended. It all depends upon the methods how they are implemented to monitor generator health. Therefore the first step towards the protection of system we need to determine the characteristics of generator. Hence the generators are modeled according to the system demand. There are mainly two types are modeling are available either low order synchronous generators are high order synchronous generators [4]. The more the order of generator, the better will be its performance in regard with protection. The standard generators are available at seventh order [5], they become very complex to design their model while the simpler models are also available which can easily be designed and can determine the stability of system. The models are mostly designed in the state space for determining the systems inputs and outputs. The state space modeling is best way to determine the systems stability and determine the response of system for different kinds of inputs. The synchronous generators health is determined by the faults currents and how they behave for the particular time and then the steady state is observed.

In this paper third order modeling of the synchronous generator is obtained [6]. They are simple and provide few computations for the systems. There are some power systems where flux linkage of field winding cannot be ignore therefore flux is taken in the third order model [4]. Third order model is useful when analysis and synthesis of excitation system is taken for synchronous generators [5]. The dynamic behavior is well explained in this model but not all physical behaviors of synchronous generators are explained. The third order model can be linear or nonlinear but linear model has few variable which can be difficult to observe the system. Hence the nonlinear model is taken which gives greater feasibility to manipulate the variables and to determine the systems outputs more accurately. The third order nonlinear model is designed and simulations is performed on matlab. The different inputs are applied to the model and variations in

outputs are obtained. The range of input must cover the all dynamics of the system. The mostly inputs to the synchronous generator are field voltages and mechanical power and outputs are rotor angle and electrical power [7]. The response is obtained on the matlab to observe the operations of generator and their curves for various outputs are checked. Then the different faults are inserted into the system to check variations in the outputs. The change of curves in the outputs can predict the health of generator. The different responses when different faults are inserted into the synchronous generator are obtained and their transients are calculated. These transients describe how long the subject fault occur in the synchronous generator and what its curve will be at the particular time. The health of synchronous generator can be determined by knowing the response of system at fault different conditions.

II. THE MATHEMATICAL MODEL OF SYNCHRONOUS GENERATOR

Consider the synchronous generator which is connected to bus system whose voltage and frequency does not change regardless of the values of stator currents. This may be called as infinite bus bar as shown in figure.1. The characteristic of infinite bus bar does not alter regardless of power supplied and consumed by any device connected to it [8]. The field voltage V_F, rotor angle δ and electrical power P are measurable. The dynamics of the system are defined by nonlinear set of equations. [4], [9], [10].

$$\dot{\delta} = \omega \quad (1)$$

$$\dot{\omega} = \frac{1}{J}(T_m - T_e - D\omega) \quad (2)$$

$$\dot{e}' = \frac{1}{T'_{do}}(V_F - e' - (xd - x'd)i_d) \quad (3)$$

From above equations, it is cleared shown that

$$i_d = \frac{1}{x'_d}(e' - V\,cos\delta) \quad (4)$$

$$i_q = \frac{1}{x_q}(V\,sin\delta) \quad (5)$$

$$T_e = P_e \cong \frac{V}{x'_d} e'_q sin\delta + \frac{V^2}{2}(\frac{1}{x_q} - \frac{1}{x'_d})sin(2\delta) \quad (6)$$

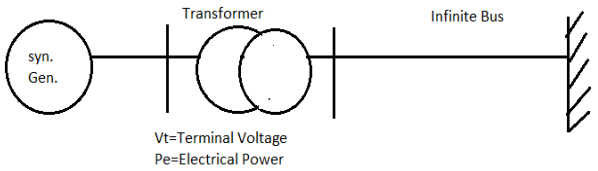

Fig.1 Simple Power System [10]

.The states of synchronous generator and its inputs:

$$X = \begin{bmatrix} x_1 \\ x_2 \\ x_3 \end{bmatrix} = \begin{bmatrix} \delta \\ \omega \\ e'_q \end{bmatrix}, u = \begin{bmatrix} u_1 \\ u_2 \end{bmatrix} = \begin{bmatrix} E_F \\ T_m \end{bmatrix} \quad (7)$$

System nonlinear model will be:

$$\begin{bmatrix} \dot{x}_1 \\ \dot{x}_2 \\ \dot{x}_3 \end{bmatrix} = \begin{bmatrix} 0 & 1 & 0 \\ 0 & K_2 & 0 \\ 0 & 0 & K_5 \end{bmatrix} \begin{bmatrix} x_1 \\ x_2 \\ x_3 \end{bmatrix} + \begin{bmatrix} 0 \\ 0 \\ K_6 \end{bmatrix} u + \begin{bmatrix} 0 \\ \frac{1}{J}\left(T_m - \frac{V}{x'_d} x_3 sinx_1 - \frac{V^2}{2}\left(\frac{1}{x_q} - \frac{1}{x'_d}\right) sin2x_1\right) \\ -(K_5 + K_6)cosx_1 \end{bmatrix} \quad (8)$$

$$y = \begin{bmatrix} x_1 \\ \frac{V}{x'_d} x_3 sinx_1 + \frac{V^2}{2}\left(\frac{1}{x_q} - \frac{1}{x'_d}\right) sin2x_1 \end{bmatrix} \quad (9)$$

The variables mentioned above are measured through identification method which consist of discrete state space model, Prony method and steady state response analysis. These methods helps to solve linear as well as nonlinear models of synchronous generators.

III. METHODOLOGY

The flow chart of the research work is shown in Fig. 2. The real model data of synchronous generated is taken, which is given in Table. 1. Then the value of model is simulated in MATLAB. The short circuit and ground faults are generated as pules and applied to the model during run time. The faults are just the reactances values which area decreased or increased depends upon the type of fault. These fault values of synchronous generator determine the how generator responses during short and ground faults. The transient faults are analyzed in our flow chart.

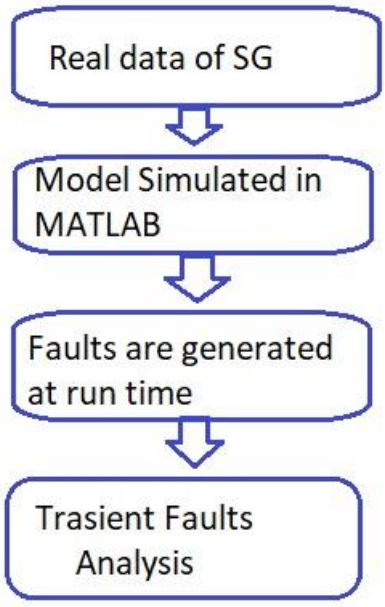

Fig. 2 Flow chart of system

IV. SYNCHRONOUS GENERATOR SIMULATIONS

A. The System Simulation Model

The systems defined in Eq. 8 and Eq. 9 are simulated on matlab Simulink with the values of variables given in the table.1. The natural response of Synchronous Generator output Power and the Terminal Voltage is shown in Fig. 3 and Fig. 4 respectively. The system is simulated with initial conditions, defined as δ_o = 0.9145 rad and $e'_{qo}=0.9653$ pu [7].

Table 1. Parameters of a Synchronous Generator (pu)

K_2	K_5	K_6	J
-1.7375	-29.0524	7.6336	0.0259
X_d	X'_d	X_q	V
2.072	0.568	1.559	1.02

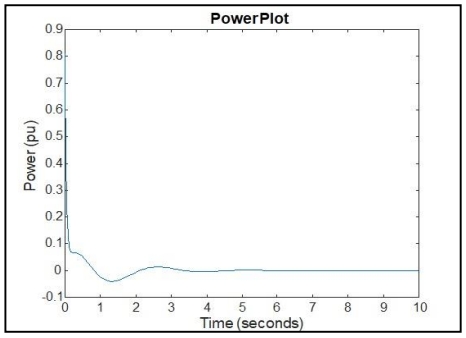

Fig.3 Power of Synchronuos Generator

The Fig. 3 shows the simple natural repsonse of power of synchronous generatorwhen initial conditions of the systems are applied. It shows that synchronous generator goes to steady state after three seconds of time.

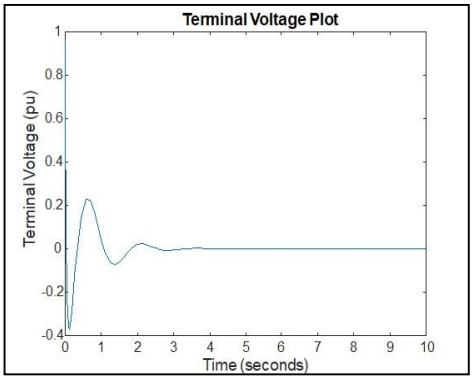

Fig.4 Terminal Voltage of Synchronuos Generator

Fig. 4 represents the graph of terminal voltage of synchornous generator in free response. It also shows the stability of synchronous generator.

B. Generating faults into the Synchronous Generator

Since we are running the simulations of synchronous generator, therefore we want to show how the system responses due to different faults condition. Here we have to put faults into the system on the run time. Therefore mostly faults that occur are short circuits and ground faults [11]. In our simulations, short circuit and open circuit faults are introduced. During the short circuit, the reactance of synchronous generator is decreased 10% to 20 % whereas the transient reactance of system is decreased to 10% to 15% of its normal value. As per our modeling, the value of X'_d is taken as 0.568 so when the transient short circuit fault occurs, it value is taken as 0.0568 of its original value. The transient fault generated as shown in the Fig. 5 and Fig. 6.

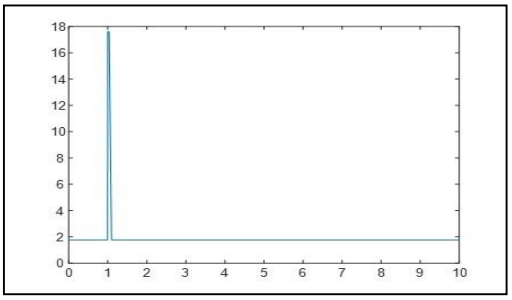

Fig.5 The value of fault is added (short circuit fault)

Fig. 5 and 6 shows that the pulse is generated for short circuit and ground fault. The value of reactance and transeint reactances of synchornous generator(x_q and $1/x'_d$) is decreased and increaed at t=1 s to 10% of its orginal value respectively.

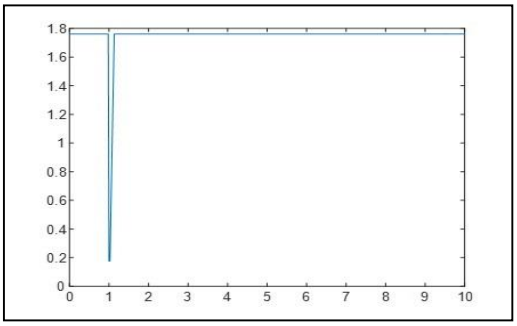

Fig.6 The value of fault is added (Open circuit fault)

C. Faults Occur on the infinite bus

The short circuit fault and ground fault occurs on the synchronous generator bus voltages at t=1 s (third cycle) [12]. The fault current lasts for 50ms and then it has terminated after six cycles at t=1.05 s which is shown in Fig.7 and Fig. 8 [13], [14].

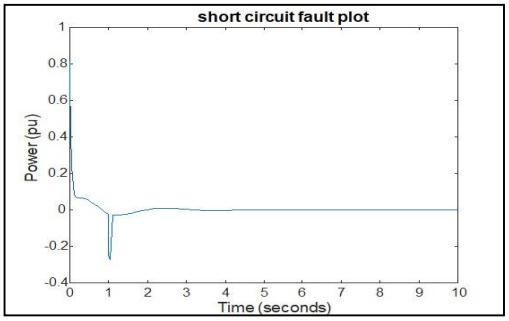

Fig.7 The fault occurred at t=1s

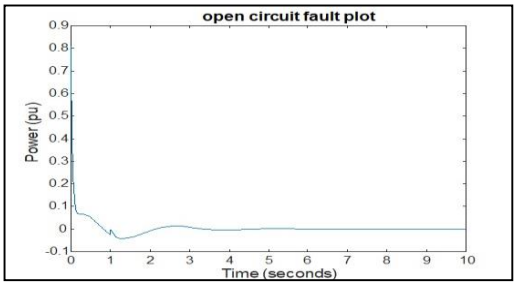

Fig.8 Output power is constant

D. The faults current analysis

The natural reponses of current is taken due to initial conditions as shown in Fig. 9 [15]. Initially it is rising then it goes to its steady state value. When short circuit is observed, the value of current has overshooted and then it finally come to steady state level as shown in the Fig. 10.

On the other hand, when the stator ground fault has occurred [16], the value is deceased then finally it becomes stable as shown in Fig. 11

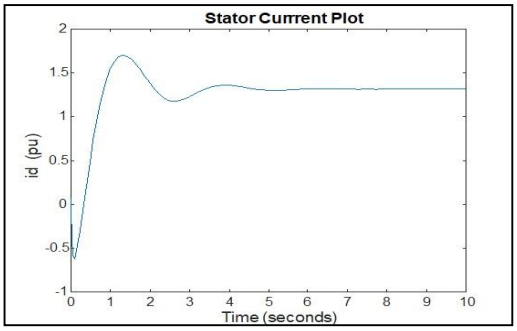

Fig.9 Stator current (I_d)

Fig. 9 shows the natural response of synchronous generator. It is clear that starting generator taken high current then it geos to steady state after 4 seconds of time.

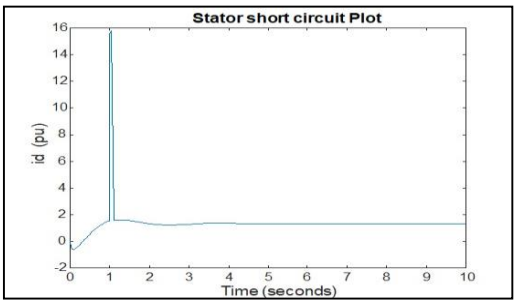

Fig.10 Stator Short circuit current (I_d)

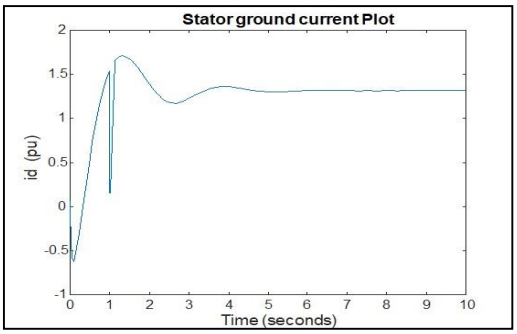

Fig.11 Stator ground current

From Fig. 10 and Fig.11 it is shown that during the short circuit fault the value of current overshoot its actual value and during ground fualt it decreases.

V. DISSCUSSION

In this research work the response of synchronous generator is observed with different kind of faults. The value of the transient reactance of the system is decreased for the short circuit fault and the value is increased for open circuit fault. The variable X'_d is adjusted as per the fault induced. The modeling is done in the nonlinear state space and system is simulated on MATLAB. The same work is carried out in [5, 11] but they have used the built in blocks of matlab for synchronous generator and 3-Phase Fault. In our paper, the state space modeling is used and fault is generated into the system by generating the pulse for transient fault analysis. The third order nonlinear synchronous generator model is simulated therefore, only synchronous reactance and transient reactance is taken. The transient reactance is varied for short circuit and open circuit fault analysis. The power, terminal voltage and stator currents are observed during the fault. Further, the synchronous generator here is assumed to be connected with the infinite bus. From figures [3] & [7], it is observed that the power of synchronous generator has major effect when short circuit has occurred. It will create overshoot into the system, causing the instability of synchronous generator. But the terminal voltage has minor effect on synchronous generator during open circuit. The stator current has

increased drastically for the short interval of time during the short circuit. The time is taken as 50 ms for the short circuit faults.

VI. CONCLUSION

The difference in our paper is that natural response of system is observed and different fault currents are induced into the synchronous generator which shows instability in its operations.
Furthermore, in our system there is no need to use any of matlab sim blocks. The results are directly taken from state space variables. Third order nonlinear model of synchronous generator is easy to implement and different faults current responses can be obtained.
For future work, it can be extended to seventh order synchronous generator which can be modeled like standard synchronous generator model.

REFERENCES

[1] Monia Ben Khader Bouzid, *Member, IEEE*, G´erard Champenois, *Member, IEEE*, Ahmed Maalaoui, and Slim Tnani, Efficient Simplified Physical Faulty Model of a Permanent Magnet Synchronous Generator Dedicated to the Stator Fault Diagnosis Part I: Faulty Model Conception, IEEE TRANSACTIONS ON INDUSTRY APPLICATIONS, 53(3):2752-2762, 2017.

[2] M.V. Sudhakar and Lumesh Kumar Sahu" Simulation of Generator Protection using Matlab'' 2017 IEEE International Conference on Smart Technologies and Management for Computing, Communication, Controls, Energy and Materials (ICSTM), Veltech Dr.RR & Dr.SR University, Chennai, T.N., India. 2 - 4 August 2017 pp.463-469.

[3] M V Sudhakar and Lumesh Kumar Sahu," Simulation of Generator Over-Flux Protection using MATLAB" in International Journal of Innovative Research in Science, Engineering and Technology Vol. 6, Issue 5, May 2017.

[4] Y.-N. Yu, Electric Power System Dynamics, Academic Press, 1983.pp 23-63.

[5] Spoljaric, Zeljko, Miklosevic, Kresimir and Jerkovic, Vedrana," Synchronous Generator Modeling Using Matlab" in University of Osijek, Croatia.

[6] E. Ghahremani, M. Karrari and O.P. Malik, '' Synchronous generator third-order model parameter estimation using online experimental data" IET Gener. Transm. Distrib., 2008, Vol. 2, No. 5, pp. 708–719.

[7] M. Dehghani and S.K.Y. Nikravesh, "Nonlinear State Space Model Identification of Synchronous Generator" in Amikabir University of Tehnology, Sience Direct, B.V. Elsevier, Ed. Teheran: University of Tehnology, Iran 2008, pp. 926–940.

[8] Roozbeh Eshraghnia and Randy J Kleen" Dynamic Modeling and Analysis of LM6000 Gas turbine Synchronous Generator in Proceedings of the 2014 IEEE IEEM.

[9] P. Kundur, Power System Stability and Control, McGraw-Hill Inc., 1994.

[10] M. Karrari and O.P. Malik, Identification of physical parameters of a synchronous generator from on-line measurements, IEEE Trans. Energy Convers. 19 (2) (2004) 407–415.

[11] G60 Generator Protection System Instruction Manual, Available: http://www.gegridsolutions.com/products/manuals/g60/g60man-ab1.pdf

[12] Stephen J. Chapman, Electric Machinery. Fundamentals fifth Ed McGraw-Hill Inc., 2012, pp. 191-271.

[13] Ying Na Zhu, and Jian Xun Jin, ''Simulation Analysis of a Synchronous Generator System under Fault Conditions'" Proceedings of 2013 IEEE International Conference on ID3066 Applied Superconductivity and Electromagnetic Devices Beijing, China, October 25-27, 2013.

[14] LIU Xuezhi, LIU Dichen and HUANG Yong, '' Simulation of Three-phase Short-circuit at the Terminals of Synchronous Machine ''

[15] IEEE Guide: Test Procedures for Synchronous Machines.

[16] Manish Jha, S.Chakrabarti and E. Kyriakides, ''Estimation of the Rotor Angle of a Synchronous Generator by using PMU Measurements''.

2020 5th International Electrical Engineering Conference (IEEC 2020)
Feb, 2020 at IEP Centre, Karachi, Pakistan

Carried Baggage Detection and Classification using Joint Scale LBP

Shahbano[1], Wakeel Ahmad[2], S. M. Adnan Shah[3] and Madiha Ashfaq[4]

[1,2,3,4] Department of Computer Science, University of Engineering and Technology, Taxila, 47080, Pakistan
(shahbano.ather@gmail.com[1], wakeel.ahmad@uettaxila.edu.pk[2], syed.adnan@uettaxila.edu.pk[3], mady.9393@gmail.com[4])

Abstract: As crime rate has been increased in the 21st century, the automatic video surveillance system has gained significant importance in computer vision community. The crucial objective of surveillance is monitoring and security in public places and the system that are used for surveillance entail more intellect and more robust technical directives. This research proposed a detection and classification framework of baggage, that can be achieved by analyzing the human in different postures while carrying bag and it deals with various texture patterns of baggage. The descriptor like SHOG and JLBP is displayed to extract features of different human body parts including head, trunk, and limbs. Then support vector machine (SVM) classifier is used to further train the features. The proposed approach has been widely assessed by using public datasets like INRIA, ILIDS and MSMT. The experimental results have discovered that the system is satisfactorily accurate and faster as compared to the other well-known approaches.

Keywords: Carrying baggage detection and classification, Joint Scale Local Binary Pattern, Scalable Histogram of oriented gradients, Support Vector Machine, Video Surveillance.

I. INTRODUCTION

These days, crime rate has been increased dramatically and it threatens the human lives and resources. These scenarios are often faced by carrying the explosive substance in the carried baggage or placed it as unclaimed one. By installing the CCTV cameras, the detection system monitors the threat and warn the security team. They have a potential impact on many intelligent surveillance systems that involve knowledge integration and management [1,2]. The challenges in the detection procedure include illumination conditions, complex backgrounds, articulate poses, and outdoor scenes [3]. To deal with these problems several approaches in the past had been proposed. In this study as a new branch of automatic video surveillance system, an effort is contributed which avails the dimensional information of the baggage with respect to the body of the human carrying it. This approach distinguishes humans from carried baggage from humans without carrying baggage and it deals with various texture patterns of the baggage. Following are the major contributions this study offers:

- To handle the diverse texture patterns based on the body part information.
- By using a Scalable Histogram of Oriented Gradients (SHOG) and Joint Scale Local Binary Pattern (JSLBP), features of the human body parts and baggage are extracted. The SHOG results in high accuracy by allowing the selection of highly discriminative features. Joint Scale Local Binary Pattern is used for multitier solution analysis. The features of different body parts and baggage are extracted by using the SHOG and JLBP.
- Finally, interpolate the results and substantiate the presence of baggage in the human region.

This paper is divided into the following sections. Section 2 explains the literature review of the study; Section 3 explains the Preprocessing Techniques. Section 4 explains the Feature Descriptors which are used in the framework. Section 5 explains the training strategy and experimental results of the proposed scheme. Section 6 concludes the results.

II. RELATED WORK

For the detection and classification of abandoned baggage, numerous approaches have been offered. D. Raju et al. and S. Smeureanu et al. [4,5] proposed an approach for the automatic surveillance system that provide alert in the presence of threat. With the help of multiple image processing techniques and convolutional neural network the objects are detected. Studies [6-8] proposed a novel approaches for detection and classification of baggage. These techniques utilize three-dimensional information based on the human body carrying baggage. For the baggage detection Fuzzy-Model based integration framework is used to check the baggage screening in order to make sure that either the bag carried threat or not. T. Khanam et al. and R. K. Tripathi et al. [9–13] proposes a detection and classification framework for the baggage using the boosting strategy along with dynamic body parts. The techniques like background subtraction, HSI model, RSD-HOG features are used to deal with the challenges faced. There are few studies [14,15] which used colony optimization and deep belief networks for the efficient object detection method. These techniques are assessed on a simple and uncomplicated criterion, but the results shown are effective and promising in detection of different kinds of objects. Similarly there are many other [16-19] studies which proposed a system for the detection of abandoned objects and human blob in uncluttered scene. Background subtraction and chamfer matching are used, and if the object is successfully

detected it will generate an alarm. Few other studies like [20-22] presents a technique based on the Local Binary Pattern descriptors for the facial recognition. Van Dung H. et al [23] proposed a framework called the Joint component model based on extended feature descriptor for the detection of humans. H. Wang et al and Y. Peng et al [24, 25] proposed a segmentation method of Object of Interest (OOI) which includes Gaussian Distribution and Laplace operator. In [26–28] authors present two contributions like Scalable Histogram of Oriented Gradients and Laser Data Information. The author claims 3% higher accuracy as compared to standard HOG which is 77.02%.

III. THE PROPOSED METHOD

A. An Overview

This section presents the context for the detection of human and baggage in an image which is shown in Fig. 1. The first step is to extract the object like a human with or without carrying bag from the input image. For this purpose, background subtraction is used. The images used in this detection framework are resized into 130*66. So that we can create a window of 16 pixels from the margin of all four sides. If we reduce the margin by about 8%, the performance is decreased by about 6%. And if we increase the window size, again a loss of performance occurred. But by increasing the window size the resolution of the images increased to some extent. The information which we get from the margins provide contextual information that helps in detection.

The foreground region, which is extracted from the input image, is enhanced by using the histogram equalization technique. It enhances the contrast and removes noise to increase image visual quality. After that human body proportional model is used to divide the body from the center of the region called the horizontal axis. Then Scalable histogram of oriented gradients is applied on the human body part samples and baggage samples to extract features.

On these two divided regions and baggage samples, then Joint Scale LBP is applied for adjusting the multi-scale sampling parameters. The final decision involves fusing the features obtained from both descriptors.

B. Background Subtraction and Contrast Enhancement

As sliding window generates time complexity, so to overcome this background subtraction is used and extensively detect moving objects from static and dynamic cameras. For this, a memory of background images is created to deal with uneven illumination conditions and noise. Here we simply segment out the foreground region by simply subtracting the foreground P[I] from the background P[B].

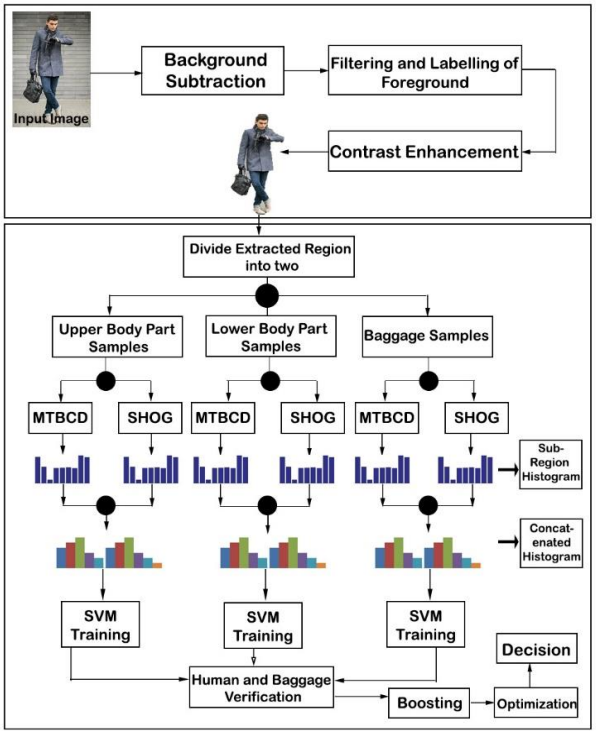

Fig. 1. Overview of the Proposed Method

$$P\left[F\left(t\right)\right] = P\left[I\left(t\right)\right] - P\left[B\right] \quad (1)$$

$$P\left[F\left(t\right)\right] - P\left[F\left(t+1\right)\right] > threshold \quad (2)$$

For the contrast enhancement histogram equalization is used and it involves probability theory, and it is treated as the probability distribution of the gray levels. The histogram of a digital image is a discrete function because intensities are all discrete values,

Histogram h is defined as

$$h(I_k) = n_k, \quad for\ k = 0, 1, 2, \ldots, L-1 \quad (3)$$

For normalization and to find the probability value use following Eq. (4) and Eq. (5) [29].

$$Z_x = \mathrm{I}_x - \mathrm{I}_x / S \quad (4)$$

$$Pk = pixels\ with\ intensity\ k / total\ pixels \quad (5)$$

IV. FEATURE DESCRIPTOR

A. Scalable Histogram of Oriented Gradient

This section of study presents feature descriptor with different block sizes called Scalable Histogram of oriented gradients (SHOG). The SHOG procedure follows the given phases as:

First calculate the histogram of gradients and then compute the magnitude and direction of the gradient by applying the following formulas:

$$g = \sqrt{g_x^2 + g_y^2} \quad (6)$$

$$\theta = \arctan \frac{g_y}{g_x} \quad (7)$$

To extract the features of the image, the concept of layering is applied. It demonstrates the erection of image layers from the image gradient and orientation values. For calculating the histogram of gradients, image is alienated into 8x8 cells (against this patch) as shown in Fig. 2.

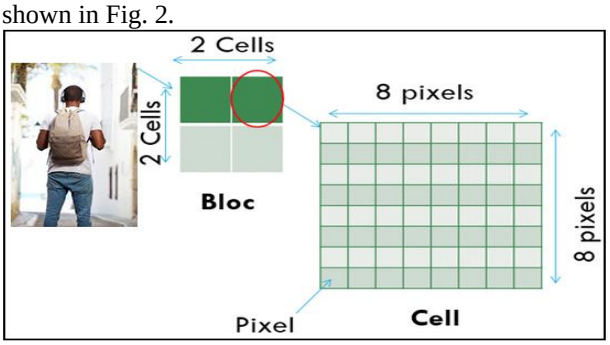

Fig. 2. Cell and Block size Performance

The SHOG is evaluated based on the HOG features, computed by variant block sizes. Like we compute features of block sizes 2x2 to 16x16 (2x2, 4x4, 8x8, 10x10, 12x12, 14x14 and 16x16) [30]. After extracting the features of different block sizes, concatenate them into one feature vector. For normalization take 16x16 block of cells, and values are normalized by using L2-Norm.

$$L2-norm\ : v \rightarrow \frac{v}{\sqrt{\| v \|^2_2 + \in^2}} \quad (8)$$

B. Joint Scale LBP

In Joint Scale Local Binary Pattern, by using some simple arithmetic operations multiple features are blended. And then multiple integration of local patches is extracted based on LBP. Let's suppose B_1 and B_2 are the two neighboring pixels as LBP, so by using K as number of sampling points, the new composition for JLBP is written as (K, B1, B2) as shown in Fig. 3.

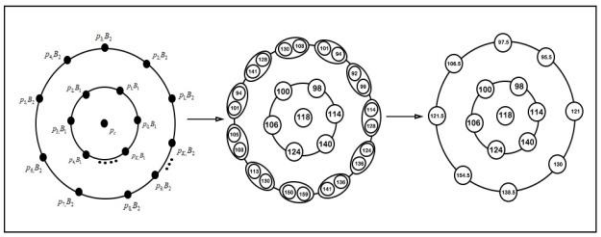

Figure 3: The Principle of JLBP

The Generic impression of JLBP indicates as:

$$JLBP_{(K,B_1,B_2,\ldots,B_L)} = \sum_{i=0}^{K-1} s\left(\sum_{l=1}^{L} p_i, B_1 - L \times p_c\right) \times 2^i \quad (9)$$

V. FEATURE DESCRIPTOR

A. Training of SVM

As a training strategy, Support Vector Machine (SVM) is used for the erudition of different human body parts and the baggage part. Here, we preferred SVM over other models like Neural Network (NN) e.t.c. because these (NN based) models requires huge data sets which was not available every time. Secondly, these models are very hard to train, and they require huge computational resources. While on the other hand SVM can be trained on personal machines and do not require resources like GPU's. Also, neural nets often coverage on local minima rather than global minima, and if training goes too long it overfits, and might start to consider the noise as a part of the pattern. In this study, the evaluation of the proposed descriptor is performed on three standard datasets like INRIA [30], ILIDS [31], MSMT [32] dataset and some other samples which are collected from Google. The training set includes those which contains human with carrying bag or human without carrying bag. Fig. 4 shows samples of placements of baggage on the human body.

Fig. 4: Baggage Placement Samples

For training and testing, image samples are manually classified as testing samples and training samples. For training purposes, 500 images are used which are divided into 3 categories (223 Bag Packs, 171 Duffel Bags, and 68 Wheeling Bags). Fig 5 illustrates the samples used for training purposes and all these samples are resized to 130x66 and then feature descriptors are applied to them.

Fig. 5. Samples used for Training

B. Classification and Results

The presented approach was first analyzed to classify that the image regions having human are either with baggage or without baggage. The samples with carrying bag are positive samples and those image samples in which human without carrying bag are negative samples. For instance, given a training data 'n' and it belongs to 1 or -1 depends upon which class of the feature vector. It can be considered as a body with baggage 1 and body without baggage -1.

To classify the regions, we take 500 positive sample images and 127 negative sample images. To investigate the samples, we randomly take 30 SHOG features and 30 Joint Scale LBP features. Then the classification for the baggage and non-baggage samples is carried out through the trained classifier. The proposed model gives the detection rate of 95.4% with false detection rate of 5% which is shown in Table 1.

2020 5th International Electrical Engineering Conference (IEEC 2020)
Feb, 2020 at IEP Centre, Karachi, Pakistan

Table 1: Evaluation of Training Dataset and comparison with other state of the art methods

Category	Accuracy	Precision	Recall/ TPR	Specificity	FPR	Prediction Speed	Training Time
Proposed Method	95.4%	0.9889	0.9511	0.8333	0.1666	~2700obs/sec	5.7268sec
F. B. Kamal et al., (2019) [12]	90.26%	0.9179	0.703	0.7764	--	--	--
D. Raju et al., (2019) [4]	90.00%	0.90	0.90	0.8252	0.1732	--	--
D. G. Altunay et al., (2018) [1]	87.5	0.87	0.87	0.89			
E. A. Wahyono (2017) [7]	81%	0.81	0.77	0.79	--	--	--
Wahyono et al., (2017) [6]	79.86%	0.8121	0.82	--	--	--	--

VI. CONCLUSION

In this study, an approach is proposed for the detection of human and baggage with the vision of ensuring security in public places. This approach deals with the human body parts and the baggage and utilizes a strong relationship between them. The proposed approach gets the spatial information of the baggage from the body of the human carrying it. On the extracted regions Scalable Histogram of Gradient (SHOG) and Joint Scale Local Binary Pattern (JLBP) are applied and get feature vectors. Finally, the extracted feature vectors are concatenated into one feature vector and trained by the boosting Support Vector Machine (SVM). After conducting extensive experiments, the proposed system shows a satisfactory classification accuracy rate of 95.4%. One of the limitations of this framework is that, it fails to detect baggage in much occluded state where objects are not visually separable. Basically, in such occluded state it is not possible to detect the edges. However, potential promotion of these limitations will improve the system performance in a very notable time.

REFERENCES

[1] E. a. Damla Gül Altunay, "Intelligent Surveillance System for Abandoned Luggage", IEEE, 2018.

[2] E. a. Widodo Budiharto, "Fast Object Detection for Quadcopter Drone using Deep Learning", in 3rd International Conference on Computer and Communication Systems., 2018.

[3] E. a. Hideaki Yanagisawa, "A Study on Object Detection Method from Manga Images using CNN", IEEE, 2018.

[4] D. Raju et al., "Efficient Abandoned Luggage Detection in Comple x Surveillance Videos", International Conference on Innovative Data Communication Technologies and Application (ICIDCA), 2019.

[5] S. Smeureanu et al., "Real-Time Deep Learning Method for Abandoned Luggage Detection in Video", 26th European Signal Processing Conference (EUSIPCO), 2018.

[6] W. et al., "Body part boosting model for carried baggage detection and classification", Neurocomputing, 2017.

[7] E. a. Wahyono, "A Fuzzy Model-based Integration Framework for Vision-based Intelligent Surveillance Systems", in International Conferrence on Mechatronics (ICM), IEEE, 2017.

[8] X. Nie, "The impact of conditional dependence on checked baggage screening", European Journal of Operational Research, Volume 278, Issue 3, 1 November 2019, Pages 883-893.

[9] T. Khanam et al., "Baggage Detection and Classification using Human Body Parameter & Boosting Technique", in 10th international conference on human system ineractions (HSI), 2017.

[10] T. Khanam et Al., "Human and carried baggage detection & classification based on RSD-HOG in video frame", in 9th international conference on electrical and computer engineering (ICECE), 2014.

[11] T. Khanam and K. Deb, "Baggage Recognition in Occluded Environment using Boosting Technique", KSII Transactions on internet and information systems, vol. 11, 2017.

[12] F. B. K. et Al., "Human Detection Based on HOG-LBP for Monitoring Sterile Zone", in International Conference on Electrical, Computer and Communication Engineering (ECCE), 2019.

[13] P. A. et Al., "Abandoned Object Identification and Detection System for Railways in India", in international conference on emerging trends in computing and communication technologies (ICETCCT), 2017.

[14] A. kaur and N. Kaur, "Performance evaluation of object detection algorithm using Ant Colony Optimization based image segmentation", in Third International Conference on Computing, Communication, Control And Automation (ICCUBEA), 2017.

[15] K.-C. C. et Al., "Parallel Design of Background Subtraction and Template Matching Modules for Image Objects Tracking System", International Computer Symposium, 2016.

[16] Q. Hu et al., "Fast Detection of Multiple Objects in Traffic Scenes With a Common Detection Framework", Transactions On Intelligent Transportation Systems, Ieee., 2016.

[17] M. J. Er et al., "A Novel Vision System for Baggage Localization", in International Conference on Intelligent Control Power and Instrumentation (ICICPI), 2016.

[18] S. Hargude et al., "i-surveillance : Intelligent Surveillance System Using Background Subtraction Technique", in International conference on computing communication control and automation (ICCUBEA), 2016.

[19] L. Lui et al., "Extended Local Binary Patterns for Face Recognition", Informatics and Computer science intelligent system applications, 2016.

[20] Q. Lin, "Multi-Scale Local Binary Patterns Based On Path Integral For Texture Classification", IEEE, 2015.

[21] R. Hu et al., "Feature reduction of multi-scale LBP for texture classification", in International Conference on Intelligent Information Hiding and Multimedia Signal Processing, 2015.

[22] V. Dung H. et al., "Joint components based pedestrian detection in crowded scenes using extended feature descriptors", Neurocomputing, Dec 2015.

[23] H. Wang et al., "A two-stage image segmentation via global and local region active contours", Neurocomputing, 2016.

[24] Y. Peng et al., "Object(s)-of-interest segmentation for images with inhomogeneous intensities based on curve evolution", Neurocomputing, 2016.

[25] W. Wahyono et al., "Carried Baggage Detection and Classification Using Part-Based Model", in 11th International Conference ICIC, August 2015.

[26] Wahyono et al., "Hybrid cascade boosting machine using variant scale blocks-based HOG features for pedestrian detection", Neurocomputing, July 2014.

[27] V. D. Haong et al., "Scalable histogram of oriented gradients for multi-size car detection", 10th France-Japan/ 8th Europe-Asia Congress on Mecatronics (MECATRONICS2014- Tokyo), 2014.

[28] B. Youn et al., "Carried object detection in short video sequences", in 12th International Conference on Signal Processing (ICSP), 2014.

[29] R. E. Woods and R. C. Gonzalez, "Digital Image Processing", 4th Edition.

[30] N. Dalal, B. Triggs, "Histograms of oriented gradients for human detection", in: Proceedings of the CVPR, Vol. 1, 2005, pp. 886–893.

[31] i LIDS Team, "Imagery library for intelligent detection systems (i-lids); a standard for testing video-based detection systems", in: Proceedings of the 40th Annual IEEE International Carnahan Conferences Security Technology, 2006, pp. 75–80.

[32] MSMT-17, "Torchreid Image Dataset".

2020 5th International Electrical Engineering Conference (IEEC 2020)
Feb, 2020 at IEP Centre, Karachi, Pakistan

Automatic License Plate Detection

Muhammad Zohaib Sohail and Muhammad Hassan Shah
Department of *Electronics and Power Engineering*
Pakistan Navy, Engineering College, PNEC NUST
Karachi, Pakistan

zohaib.sohail@hotmail.com, mhshakpk@gmail.com

Abstract: Automatic License plate recognition is an important phase in the recognition of vehicle's license plate for intelligent transport systems. In this paper a technique and method for license plate recognition is presented. The proposed algorithm consists of several stages. In the first stage, we extract vertical edges of the input image using Sobel mask. In the next stage, histogram analysis is used for finding the candidate regions of license plate. Candidate regions are also verified by defined compact factor. In the last stage, we locate the license plate exactly with some morphological operators. Experiments have been conducted for validation of this algorithm.

Keywords: *morphological operation, erosion, dilation, canny edge detection, compact factor.*

I. INTRODUCTION

Common problem related to traffic in present days are the check and balance in traffic i.e. monitoring and surveillance of traffic. In order to overcome these issues regarding surveillance and monitoring of traffic some techniques have been proposed by different researches in past such as to detect to license plate of vehicles, location of vehicles through GPS and many different ways to detect and monitor vehicles for surveillance or other purposes.

Automatic License plate recognition (ANPR) is a technique implemented to detect the vehicles number plate for different applications such as for parking of certain vehicles, toll fees collect, for the enforcement of traffic rules, surveillance purposes etc. In the license plate recognition first the license plate has been captured form a digital camera as this is a computer vision application so camera, light and scene are the necessary conditions. After image capturing different operation have been applied on the image for the recognition of license plate having desired applications. Captured image having the license plate will go through further processing steps for the detection and recognition of exact alphanumeric characters of the license plate.

In [1] authors implemented a robust number plate detection as well as segmentation of characters algorithm based on the combine feature extraction model and Block Propagation neural network (BPNN). Using BPNN technique for training the feature vector results better results for number plate recognition.

By incorporating connected component analysis and template matching authors in [2] have perform Analysis of Vehicle Number Plate Recognition System used for feature extraction on 90 sample images. And got meaningful phase correlation and cross correlation for number plate.

In [3] authors have presented a license plate recognition system by using ANN (Artificial Neural Networks). LPR system segregated into different processes, in first stage the license plate region has been pointed out then in second stage character segmentation has been carried out afterwards character recognition. In some other applications, different constraints have been taken into account such as the speed of vehicle, distance between the vehicle and the capturing element (camera), background variations, lighting effects, day or night conditions, glare effect etc. [4], [5].

To make the algorithm robust all these constraints must be overcome for the recognition of actual characters and numbers of the license plates. Moreover some other constraints have also been confronted such as variation in size, font, colors, plate size, and different nonstandard plates including fancy license plates. In designing the algorithm we have made some restrictions in order to implement ANPR on Karachi based standard license plates, having the standard license plate and character size, standard fonts, color etc.

Different types of methods have been followed in the License Plate Localization. Various edge detection techniques have been implemented i.e. Prewitt, Sobel, Log Gabor, Laplacian of Gaussian, Gradient of Gaussian and Canny edge detection.

Detection of edges from an image is not beneficial technique since it contain all the edges of an image i.e. not gives the specific and desired location edges (license plate). On the other hand edge detection technique has some advantages which is fast and simple method. Another technique called Hough Transform can also be used to localize the desired region (in this case license plate) but issue in this technique is that this process is slow and required an efficient amount of memory. Using morphological technique will also works but it reflects out time delay in the output, that's why only dependent on morphological technique is not suitable for license plate detection.

In paper [13], the authors have implemented useful techniques consisting of several steps. In step one the license plate's vertical edges has been extracted using some detection technique, then in step two the image noise image has been removed using the required algorithm. In third step the actual or desired region for localization i.e. the rectangular shaped area of image has segmented out from the initial image of the car. In [9] color based detection technique is implemented using the background subtraction of the image and extracting the desired color portion of rectangular li-cense plate from the whole image.

II. PROPOSED LPL SYSTEM

Our proposed algorithm is based on different steps inter-connecting with each other i.e. results obtained from one step becomes the input (initial state) of the next step. As we are not following the color base detection proposed in [9], so we are not concerned about the specific colored license plates. Since our approach does not need color information, the system is able to locate license plates with different colors. Figure 1 mentioned below is the basic block diagram of our algorithm which we will implement to localize the li-cense plate (first) then recognize the exact alphanumeric license plate.

The overview of the algorithm is shown in figure 1. In this figure first the image is captured from a device (camera) it is the initial stage of it, after capturing the image license plate localization part comes out, in which the localization of particular plate region has been carried out for finding the exact location of the license plate.

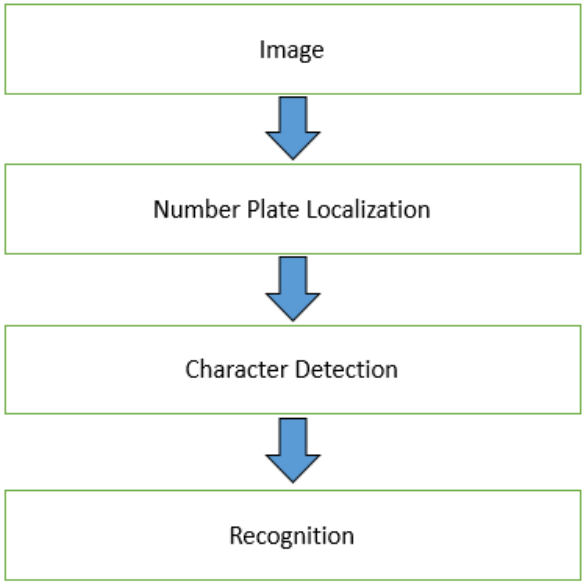

Fig. 1. Basic Block Diagram

After plate localization next block is for character detection of character segmentation. In this step we segment out the detected numbers and alphabets of the license plate, this is significantly important part for the next step i.e. recognition of characters. In recognition block the segmented alphanumeric value will be matched or compared with the database for the recognition of exact characters and numbers of license plate. Figure 2 is the block diagram of proposed algorithm for the localization and then extraction of the license plate of the input image.

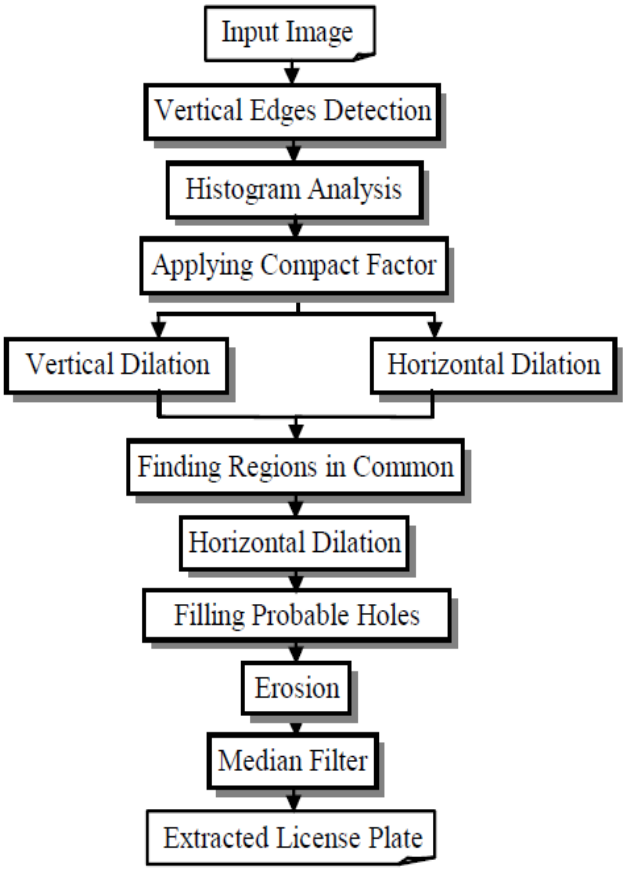

Fig. 2. Overview of the proposed algorithm

After the image captured from camera the image has been converted to grayscale for further processing. Figure 3 is the gray scale image of the captured image

Fig. 3. Gray Scale Image

A. Vertical edges detection

Now for finding the edges in an image, some edge detection technique will be required for the desired purpose. First we will find the vertical edges of image

2020 5th International Electrical Engineering Conference (IEEC 2020)
Feb, 2020 at IEP Centre, Karachi, Pakistan

(grayscale image). Since number plate contains different characters and numbers so vertical edges must be detected. We have implemented sobel edge detection technique to find the vertical edges of the license plate.

Figure 4 shows the vertical edge detection of gray scale image using sobel edge detection technique. Equation 1 is the gradient estimation along the vertical axis of image.

$$g_y = h_y * f(x, y) \quad (1)$$

Fig. 4. Sobel Edge Detection

B. Histogram Analysis

Now image histogram analysis is being carried out. For histogram we have to find the number of ones occurring for each of the row in an image. In histogram vertical projection having the two axis in which vertical axis contains the rows in an image while the horizontal axis consist of the white pixels in each of the row.

Fig. 5 Normalization & Thresholding

C. Dilations

Now dilations will be used as a morphological operator. Obtained image of figure 5 is once dilated horizontally first then vertically dilated too. Now again implement the horizontal dilation in the bright pixels of an image. Dilation operations which can be implemented by using the structural element size on the image, will thickens the object in an image. In vertical dilation the vertical objects have been thickened while in horizontal dilation same process will be done, but now in horizontal direction.

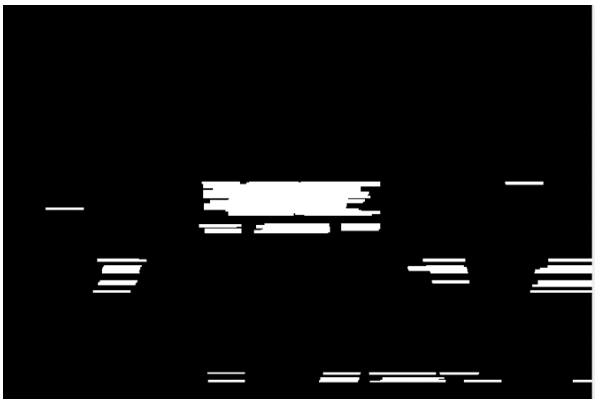

Fig. 6. Morphology Dilation Horizontal

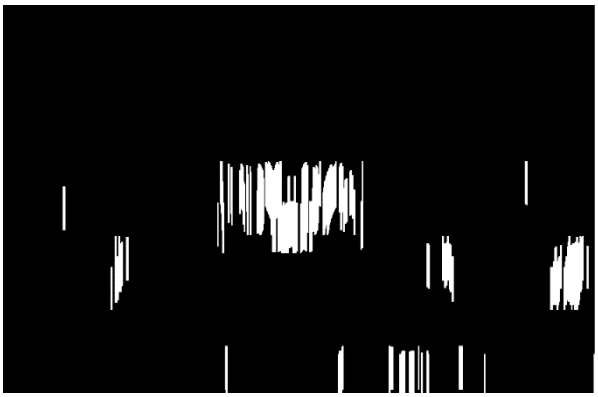

Fig. 7. Morphology Dilation Vertical

D. Filling the probable holes

As we want to obtain a continuous region as the plate location, in this part of algorithm, the probable holes are filled. Figure 8 illustrates the filling operator result.

Fig. 8. Filled holes in Morphological dilation

E. Erosion and Median Filter

Now next step is to find the erosion of the image having holes in morphological dilation. In erosion all the areas in license plate i.e. all the extra regions will be removed. Figure 9 shows the Erosion in an image.

Fig. 9. Erosion of Image

E. License plate extraction

Now in this step, we have detected the surroundings of the rectangle of filtered image. By zoom in (enlarge) of this rectangular image, the plate is located in the image. Figure 10 contain the border of the rectangular license plate image.

Fig. 10. Rectangle border of plate

Now on multiplying the original image i.e. (gray scale) image with the previous obtained image having the rectangular border of plate, we will get the region of plate containing the alphabets as well as numbers of it.
Figure 11 shows the plate localization.

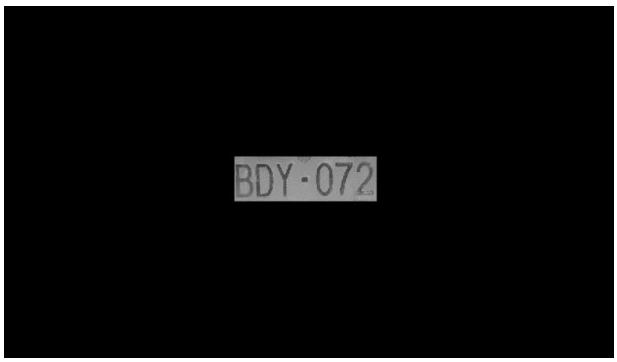

Fig. 11. Detected License Plate

III. CHARACTER SEGMENTATION

Now the half part i.e. localization of license plate region has been completed, so next phase is about segmentation. In segmentation there are a lot of methods available for performing segmentation of characters. We have use the region properties having the bounding boxes algorithm on matlab software. Figure 12 shows out the segmented characters and numbers of ANPR.

Fig. 12. Segmented License Plate

IV. CHARACTER RECOGNITION

In character recognition text in image is identified and con-verted into editable/readable text. Various techniques are available for image to text conversion most of the algorithm use single technique. Some of them are discussed in this section.

A. Template matching

Template matching is used to detect objects in images like in medical image processing, face detection. It can also be used in recognition of characters in image that have fixed size. Resizing of characters in done after section 3, after the segmentation. Template matching can further be divided into two parts, template based matching and feature based matching. If the template image have strong features, feature based technique is used is better approach. Otherwise, template based matching is useful.

Recognition rate of 85% is achieved by statistical feature extraction method. In some other algorithms computation of salient features is per-formed after extraction from training data. Images are readjusted to uniform size using linear normalization algorithm. 1176 images provided recognition rate of 95.7%.

Support Vector Machine (SVM) based approach is used for feature extraction of Chinese and English, Numeric characters. The authors achieved success rate of 97.8% - 99.5% in numerals and character recognition. A template based approach is proposed also proposed, author detected similarity between the patterns using similarity function on very low resolution images such as 4x8.

In this algorithm, correlation is used in matching of segmented with the template image both are resized to 24x42.

B. Other methods

Some algorithms used Optical Character Recognition (OCR) tool. A number of software are available to process OCR. Google has maintained a tool of this purpose, Tesseract, which is available multilingual support. Some people has modified it to achieve recognition rate of up to 98.7%. Markov Random Field used randomness to model uncertainty in assignment of pixels.

V. RESULTS

The Database contains 150 images different in size, background, camera angle, distance, and illumination conditions. This algorithm is approximately 70% accurate, and detecting standard Karachi based license plates.
In future we will implement different training tools such as NPR (Neural Pattern Recognition) and Deep Learning for better performance of our algorithm. Figure 13 is the result of detected license plate.

Fig. 13. Detected Number Plate

Figure 14 is the final GUI (Graphical User Interface) of our algorithm in which load image button will browse the data-base images. Any image selected will be converted to gray-scale on pressing second button. Then edge detection of gray scale image will be done on pressing the button. In the end localization button will process further until the recognition of license plate numbers will be done.

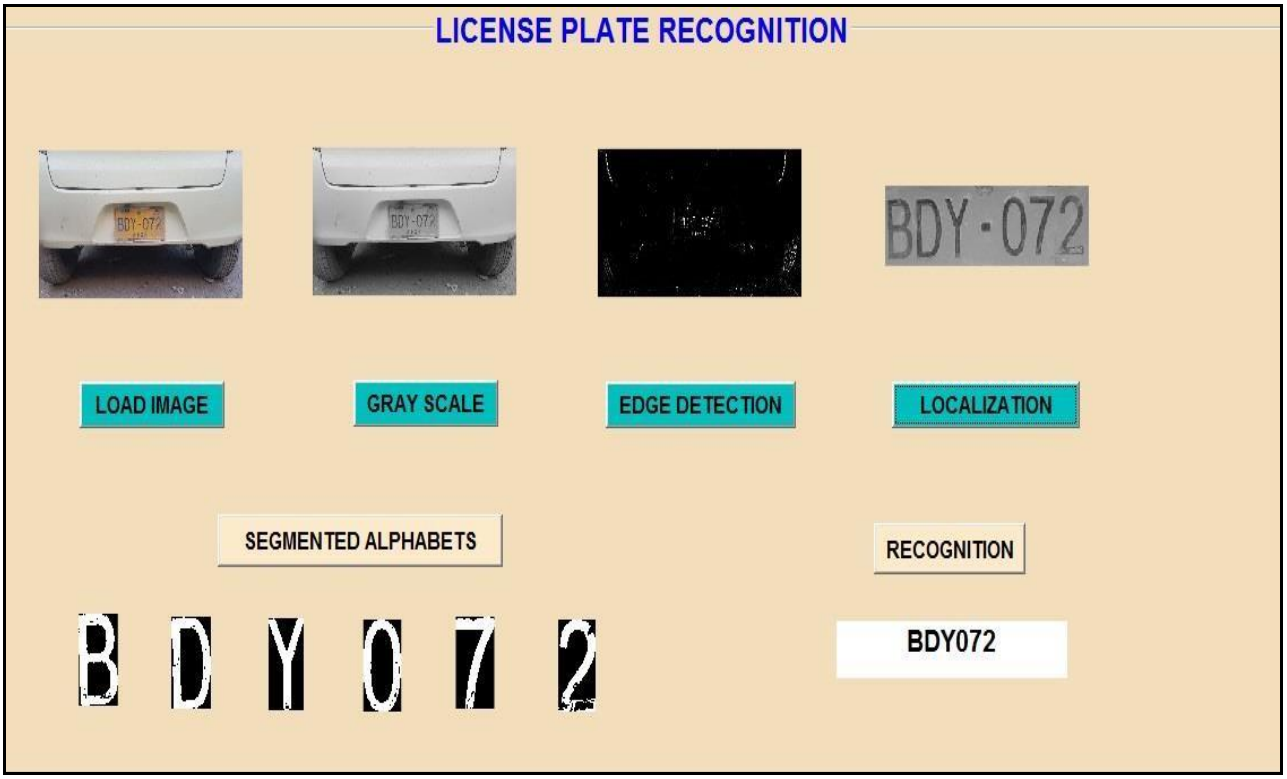

Fig. 14 Formed GUI of ANPR System

VI. CONCLUSION

ANPR is an interesting and challenging research area in which there are a number of complexities in the license plate like colour, size, font style, lighting condition and environment etc. i.e. to detect the area of license plate and then segment out the characters and numbers from the license plate, after wards its recognition. Currently, algorithm has been designed for the standard license plates having Karachi based local number plates. It can also been implemented on the other standard license plates as well. In future, detection and recognition of non-standard license plate will be done on the basis on Neural Network and similar techniques in order to make the algorithm more generic.

REFERENCES

[1] F. Xie, M. Zhang, J. Zhao, J. Yang, Y. Liu and X. Yuan, A Robust License Plate Detection and Character Recognition Algorithm Based on a Combined Feature Extraction Model and BPNN, Journal of Advance Transportation, Vol. 2018.

[2] G. Sharma, Performance Analysis of Vehicle Number Plate Recognition System Using Template Matching Techniques, Journal of Inf. Technol. Softw. Eng., vol. 08, no. 02, 2018.

[3] Ibrahim Turkyilmaz and Kirami Kacan, "License Plate Recognition System Using Artificial Neural Networks", Electronics and Telecommunications Research Institute Journal, Volume39, Issue2 April 2017 Pages 163-172

[4] G. Adorni, F. Bergenti, and S. Cagnoni, "Vehicle license plate recognition by means of cellular automata," in Proc. IEEE Int. Conf. Intelligent Vehicles, pp. 689–693, 1998.

[5] P. Davies, N. Emmott, and N. Ayland, "License plate recognition technology for toll violation enforcement," Inst. Elect. Eng. Colloquium Image Analysis for Transport Appli cations, pp. 7/1–7/5, 1990.

[6] T. Naito, T. Tsukada, K. Yamada, K. Kozuka, and S.Yamamoto, "Robust license-plate recognition method for passing vehicles under outside environment," IEEE Trans. Veh. Technol., vol. 49, pp. 2309–2319, Nov. 2000.

[7] R. Parisi, E. D. D. Claudio, G. Lucarelli, and G. Orlandi, "Car plate recognition by neural networks and image processing," in Proc. IEEE Int. Symp. Circuits and Systems, vol. 3, pp. 195–198,1998.

[8] L. Salgado, J. M. Menendez, E. Rendon, and N. Garcia,"Automatic car plate detection and recognition through intelligentvision engineering," in Proc. IEEE Int. Carnahan Conf. Securit Technology, pp. 71–76, 1999.

[9] Hum Yan Chai. (2014). Non- Standard Malaysian CarLicense Plate Recognition2014 IEEE Symposium on Computer Applications & Industrial Electronics (ISCAIE), April 7 - 8, 2014, Penang, Malaysia.

[10] Mohammad Zakariya Siam (2014). Practical Design of an Automatic License Plate Recognition Using Image Processing Technique. International Journal of Engineering and Innovative Technology (IJEIT) Volume 4, Issue 4, October 2014

[11] Susmita A. Meshram (2013) Traffic Surveillance by Counting and Classification of Vehicles from Video using Image Processing. International Journal of Advance Research in Computer Science and Management Studies. Volume 1, Issue 6, November 2013.

[12] Ali Javed, (2013) Video Analytic Algorithm for License Plate Recognition System. I.J. Image, Graphics and Signal Processing, 2013, 11, 61-67

[13] Farhad Faradji, Amir Hossein Rezaie, Majid Ziara ban (2007) A Morphological-based license plate location, ICIP 2007

Exploring CO_2 emissions and Economic growth in Pakistan

Tahir Ayaz Memon[1], Zubair Ahmed Memon[2], Syed Feroz Ali Shah[1], Faheemullah shaikh[2,3], Munwar Ayaz Memon[4]

1. *Energy Systems Engineering Program, Directorate of Post Graduate Studies Mehran University of Engineering & Technology Jamshoro.*
2. *Department of Electrical Engineering, Mehran University of Engineering & Technology Jamshoro.*
3. *Mehran University Center for Energy And development (MUCED), Mehran University of Engineering & Technology Jamshoro.*
4. *Department of Electrical engineering, Quaid-E-Awam University of Engineering, Science & Technology NawabShah.*

***Abstract*- Energy coupled CO_2 emissions in Pakistan are major sources to global warming. To mitigate the CO_2 emissions in Pakistan, it is important to investigate the elements that affects the carbon dioxide emissions changes. The aim of this paper is to analyze the energy coupled carbon dioxide emissions to decrease the emissions and conduct the decoupling, energy coupled CO_2 emissions, economic development and recommend the policies for reducing the energy coupled CO_2 emissions in Pakistan over the period 1990-2016. The decomposition technique used to examine the four factors: CO_2 emissions intensity (CO_2I), energy intensity (ECI), structural changes (ES) and economic activity (G) using log mean divisia index (LMDI) method, which is divided into three economic sectors: industrial, services and agriculture sectors. The results show that the economic development is the main contributor towards increasing the CO_2 emissions in all three sectors of economy in Pakistan. Whereas as per trend analysis of decoupling, it indicated that for most of years shows the different values of decoupling index and that values shows the different type of coupling and decoupling types.**

Keyword- Sectorial Energy Consumption, Decomposition, Decoupling.

1. INTRODUCTION

Energy has made a significant contribution to the world economy over the last four decades with insufficient energy resources. In the 21st century, energy consumption in developing countries has increased with population growth, industrialization and economic development[1]. According to the IEA, 2017, Global energy growth by 30% in 2040, Which is equal to adding current energy consumption of another India and China. The global economy has an average growth rate of 3.4% every year and the population increases from the current 7.4 billion to more than 9 billion in 2040 [2]. Therefore, understanding the relationship between energy utilization and economic development is important for developing effective energy and environmental policies. Energy consumption in the fields of environment and economic development has been discussed in recent years. Several studies in recent years have examined the relationship between economic growth and energy utilization[1]. The greenhouse gases (GHHs) especially CO_2 emissions in the atmosphere responsible for global warming. The greenhouse gases (GHGs) includes methane, nitrogen oxide carbon dioxide, water vapor and ozone, optimizing the use of fossil fuels as a major factor in climate change[3]. Another problem that is closely related to agriculture and human health is the lack of an environment caused by global warming, huge amounts of waste and sewage, especially rivers, canals and wetlands, which could lead to environmental disasters in the coming years especially in developing countries. In Pakistan, climate change pressures have a direct impact on our socioeconomic sectors, including water supply, crops, forests, biodiversity, livestock and coastal areas. In Pakistan, the consumption of energy has increased significantly due to the inefficiency of environmental policies and standards and can be considered as a potentially contaminating site for stress-intensive activities. Pakistan consumes more than 98% of non-renewable energy (fossil fuels) that pollute the environment[4].

Pakistan is considered to be one of the worst affected countries due to climate change and energy-related CO_2 emissions are considered to be prime reason. Pakistan's contribution to CO_2 emission is although minimum but it is increasing due to current energy policies. Therefore, it is important to evaluate the factors related to the CO_2 emissions to design various energy and environmental policies to reduce the worse impacts of climate change.

The Paris Agreement is intended to intensify the universal response to climate change warnnings, make the sustainable development environment and to eliminate the poverty. The aims and objectives of Paris agreement are:

(a) Raise the average universal temperature between 1.5 ° C to 2 ° C this will minimize the risks and the impact of weather change.

(b) Increase the ability to convert the harmful results of climate change, stimulate the climate resilience and the development of low CO_2 emissions will not threaten the food production.

c) Harmonization of financial flows with low greenhouse gas emissions and adaptive Climate Development[5].

Pakistan is also signatory of Paris Agreement. Pakistan approves its strong objectives and purposes of the Climate Convention. It also emphasized Pakistan's determination to continue fully committed to the implementation of the Paris Agreement[6].

Pakistan has agreed to promote economic growth and reduce energy poverty in the face of climate change. To improve the balance of payments and energy security, the Pakistani government has done a lot in the past decade to extract the country's rich coal reserves. The $ 46 billion China-Pakistan Economic Corridor (CPEC) mainly includes energy projects ($ 33.8 billion). In the first phase, energy projects include coal-fired power plants and renewable energy.

Given the high carbon content of coal, compared to renewable energy projects, a higher proportion of coal production projects will have a serious impact on the environment, which will be a major problem caused by climate change (Pakistan Vision, 2014) [8].

The situation of global climate change is even more important because of the past energy structure in Pakistan and its current and future performance. Therefore, Pakistan's commitment to COP21 has not yet established the specific plans to decrease CO_2 emissions. In addition, the commitment to carbon reduction depends on "affordability, providing international technology transfer, climate finance and capacity building[9].

In this context, it is important role can be played by analyzing the human factors that affects the CO_2 emissions changes. In the past few decades, many studies have used decomposition techniques to evaluate the mechanisms that links the technological advances, economic growth and energy utilization to carbon dioxide emissions. [10]–[15].

In addition, a relevant decomposition analysis is conducted to evaluate the decoupling pathways of developed and undeveloped countries[16], [17].

This study aims to answer the following questions.

Is the increase in carbon dioxide emissions caused by economic development inevitable?

Can energy utilization be separated from economic revolution by achieving energy efficiency?

Will G_{effect} affect emissions of conventional sector to modern sector?

To what level does this research help to find the answers to these questions, a question mark?

Therefore, the basis of this work is to identify the issues responsible for changing Pakistan's carbon dioxide emissions.

2. Literature Review

Global warming has become a serious problem worldwide. The energy needs of every country depends on many things (population, economic and social, culture and climate, wealth) that can be met by dissimilar kinds of energy, such as primary fuels, current technologies and electricity[18]. Energy consumption is required for all sectors because of the rapid increase in economic growth and the social revolution during the past decades[19].

Energy shortages, pollution and climate change were becoming challenging in the world. This is the most common cause of CO_2 emissions with the development of industry around the world and the maximum use of energy[20]. The use of fuel energy and other greenhouse gases has emitted carbon dioxide emissions and has led to climate change[21]. The Intergovernmental Panel on Climate Change found that some forms of energy have different CO_2 emission factors and these emissions depend on the energy source[22]. A decomposition method was used for the power decomposition analysis and was developed in 2001[23].

According to IDA method asses the factors in order to improve the CO_2 emissions and current policy impacts. There are two types of IDA method, The Laspeyre and the Divisia Index method. These methods are used in different literature works. LI method divides the primary prevalence of each section of overall sign and categories into a base year, while the DI method uses statistics based on weighted logarithms of changes in related variables to measure the results for each unit and introduced the LMDI method based on IDA[24]–[26].

A method introduced by Ang and Liu (2001) found on decomposition properties and aggregation reliability. The method is specified by LMDI-II[23]. While the former is specified by LMD-I. This method is valuable for all decomposition methods, i.e "0" or alternate values[25], [27]. LMDI method is an advantage, that can break the changes in carbon dioxide emissions and analysis the factors to predict the fossil fuel emissions[3].

After [3], [28]–[30] LMDI method is used to decompose and solve the zero-value problem and the general analysis of CO_2 emissions. In addition, LMDI method is used to determine CO_2 emissions changes in China's non-metallic industry during the period

1986-2010. They show that productivity is a key factor in increasing CO_2 emissions. As a result, LMDI method is considered to be a decomposition technique that can solve many problems without residual problems. It can be divided into two methods. Addition and multiplicative method[31].

According to [26], [32] the additive method breaks down the difference by changing the real GDP to multiple origins related to the change, while the multiplicative method measures the change in the relationship. So it is useful for time series analysis [23]. The existing literature review provides three relations between the energy consumption, economic development and CO_2 emissions for developed and undeveloped countries. In future this study breaks these relationships between the series into three parts as:

Relation between economic development, energy and CO_2

Relation between energy consumption and economic growth.

Relation between CO_2 and economic growth [8].

The latest information and causal relationship of the empirical literature are summarized in [33], [34], [17], [35], [15], [14], [13], [36], [16], [12], [11], [37]

In the context of Pakistan's development, performed a Simple political forgery of subsidies and carbon dioxide emissions to combat pollution. subsidies will not only be a useful tax credit, but also have a greater momentum of development. By comparing the production of liquefied petroleum gas with the production of natural gas in pipelines, the production of liquefied petroleum gas should be favored, as this would result in a significant reduction in the solid power sources. If the administration only supports clean fuels to reduce the air pollution and LPG by natural gas. As a result, alternative energy technology is the substitute between electricity demand and supply in Pakistan[38]–[40].

3.Data Source

The collection of data is taken from International Energy Agency (IEA) World Energy Balance from 1990 to 2016; it select a specific period based on the time series data. Carbon dioxide emissions from fossil fuel consumption of three main economic sectors of Pakistan are considered in million tone (Mt). Economic growth (GDP) of Pakistan have been obtained from world development indicators (WDI), By summarizing economic growth and investigating sectors, information on economic accounting can be provided. In this article, Pakistan's GDP is expressed in terms of US dollars and energy consumption in tera joules (TJ) through three economic sectors.

For a comprehensive decomposition analysis a case study of Pakistan based on three different sectors agriculture, industrial and services are taken.

4. LMDI Method

In order to determine the contribution of various components of specific variables decomposition method is used. This method can be utilized in numerous extents other than economics. For example, conservational and economic sciences have led to major factors leading to CO_2 emissions and techniques that affect the energy utilization. It uses in policy development and is often used to enhance the viable management, promote energy and technology efficiency, reduce economic impact on the environment and develop decoupling policies. When conducting decomposition techniques. There are two common methods of decomposition in energy consumption and used to measure the carbon dioxide emissions to calculate their effecting factors: First method is the (SDA) Structural Decomposition Method. Originally the structural decomposition problems solved by the Indian scientist Debesh and proposed the SDA method in 2006. Shang and Jiang introduced the same method used for the decomposition of energy consumption in 2009 in China. Then this procedure has been generally used for the evaluation of CO_2 emissions and structural decomposition in China. Structural Decomposition Method is based on the input/output tables and needs input/output data. The second method is (IDA) Index Decomposition Method is based on the sectoral data (statistics) and is capable for time series evaluation. In addition, this method is more viable in real applications. The IDA-based, LMDI method presented in 2004 and introduced for the energy decomposition. This method can break down the several factors (elements) and the result of decomposition also explain the problem of the remaining elements. Therefore, it is widely used in the establishing and analyzing the decomposition model of CO_2 emitters. Which is based on the LMDI method, CO_2 emission measurements and affected factors examined by local, regional, provincial, industrial, municipal, and national levels. This research work not only has important theoretical significance, but also has practical significance for the future development of the world[41]. Conducting decomposition technique to investigate the changes in CO_2 emissions into the following four components.

CO_2 Emissions Intensity (CO_2Ieffect): is the ratio of CO_2 emissions and energy utilization. CO_2 emissions intensity reflects the technological evolution of reducing CO_2 emissions, fuel quality and fuel conversion.

Energy Intensity (ECI_{effect}): is the ratio of energy utilization and GDP. Energy intensity reflects the changes in the structure and efficiency of the energy system.

Structural Changes Effect (ES effect): is the ratio of GDP of a sector and the total GDP. Structural changes reflect the change in the relative position of a sector in the economy.

Economic Activity Growth Effect (Geffect): is the economic activity growth effect, this evaluate the theoretical carbon dioxide emissions originated by economic activity.

5. Methodology

This paper based on the Pakistan's energy consumption, performs a decomposition evaluation to evaluate the main factors that influence the energy coupled carbon dioxide emissions, conduct the decoupling analysis of energy coupled CO_2 emissions and economic development and recommend the policies for reducing the energy coupled CO_2 emissions. However, this is the first time the decomposition technique has been used to examine the contribution of important factors affecting energy coupled CO_2 emissions in Pakistan over the period 1990-2016, which is divided into three economic sectors: industrial, services and agriculture[42].

5.1 Carbon dioxide emissions accounting:

Investigating the sectoral energy-related CO_2 emissions of Industrial, Services, and Agriculture sectors of Pakistan. First collect the different fuels for each sector in kilo tone of oil equivalent and calculate the energy consumption in kilo tone of oil equivalent of all three sectors then converted into a common unit that is Tera Joule (TJ) by applying conversion factor TJ=Ktoe/41.9, get the energy consumption of each sector in Tera Joules (TJ) and get the total energy consumption by adding all three sectors. By multiplying the energy consumption (TJ) of each sector for each year with CO_2 emissions factor for each type fuel which are given in table 1. Because each type fuel contain different amount of CO_2 emissions and divided by 10^6 for all three sectors, we get the CO_2 emissions in Million tones (Mt) and each fuel CO_2 emissions are summed to get the year wise and sector wise CO_2 emissions in Million tones (Mt) by adding CO_2 emissions of all three sectors get the total CO_2 emissions.

With the help of LMDI method, we find the CO_2 emission of three sectors Industrial, Services and Agriculture sectors of Pakistan.

carbon dioxide emissions can be decomposed into several affecting variables:

$$Ct = \sum_i \frac{CO2_i^t}{EC_i^t} \times \frac{EC_i^t}{G_i^t} \times \frac{G_i^t}{G^t} \times G^t$$

$$= \sum_i CO2I_i^t \times ECI_i^t \times ES_i^t \times G^t \quad \textbf{(1)}$$

Where CO_2 is the emissions of three sectors (1) at time (t) ($CO_2t = \sum_i CO2_i^t$) can be evaluated as the product of CO_2I, ECI, ES and G.

$CO2_i^t$ = is the emissions of ith sector (MT), for a specific time (year).

EC_i^t = is the energy utiliation of ith sector (TJ), for a specific time (year).

GDP_i^t = is the gross domestic product of ith sector (USD), for a specific time (year).

GDP^t = the total gross domestic product for specific time(year).

Expression (I) runs from a base year zero means next to previous year we obtained change in carbon dioxide emissions as:

$$\Delta CO2 = CO2^t - CO2^0 \quad \textbf{(2)}$$

Fig 1. Shows the relationship between the energy consumption in kilo tone of oil equivalent, CO_2 emissions in kilo tone (Kt) and GDP in US Dollars of industrial sector of Pakistan. Every country needs to grow with high GDP and the GDP increases when the country produces lot of products in their sectors and the main thing for the growing sectors is the energy consumption to produce lot of products to increase the economy for a country and the energy consumption also increases by population growth, industrialization and economic development, living standards and urbanization when the consumption of energy increases in economic sectors it produces more CO_2 emissions. The greenhouse effect is the main source of global warming, optimizing the use of fossil fuels as a major factor in climate change, In Pakistan climate change pressures have a direct impact on our socioeconomic sectors, including water supply, crops, forests, biodiversity, livestock and coastal areas. So it is significant to know the connection between the energy related CO_2 emissions and economic development to design actual energy and environmental policies. In Fig 1 we see that the CO_2 emission continuously increases from 1990 to 2016, it depends upon the energy consumption because the energy utilization also increases, this energy consumption depends upon the economy and make the relation between GDP, energy and CO_2 emissions as; GDP is directly proportional to energy and the energy consumption is directly proportional to CO_2 emissions (GDP α E α CO_2), it means the GDP of a industrial sector increases, the energy and the CO_2 emissions also increases.

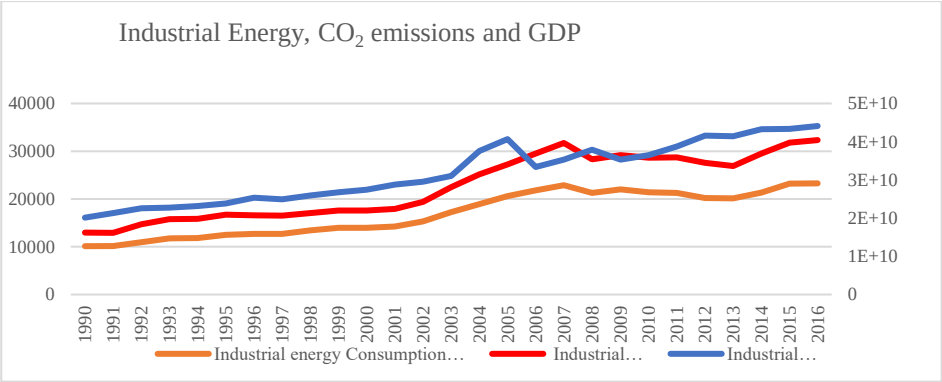

Fig 1. Energy, CO_2 and economic relationship in industrial sector of Pakistan.

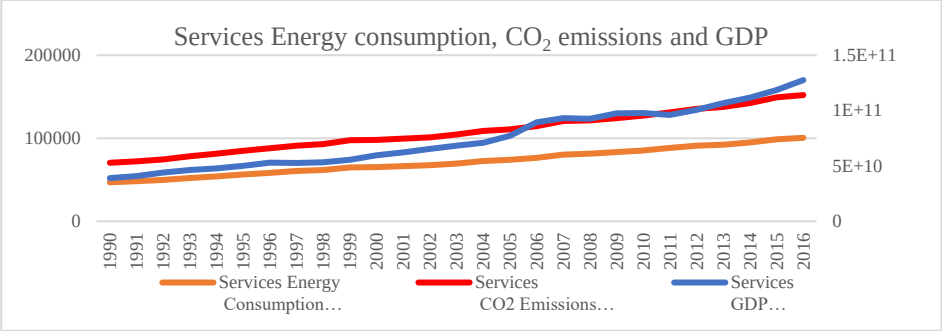

Fig 2. Energy, CO_2 and economic relationship in Services sector.

In Fig 2. we see that the CO_2 emissions of services sector of Pakistan is continuously increases from 1990 to 2016, same as in industrial sector it depends upon the energy consumption because the energy consumption also increases, this energy consumption depends upon the economy. Above graph make the relation between GDP, energy and CO_2 emissions of services sector as; GDP is directly proportional to energy and the energy consumption is directly proportional to CO_2 emissions (GDP α Eα CO_2), if the GDP of a services sector increases, the energy and the CO_2 emissions also increases

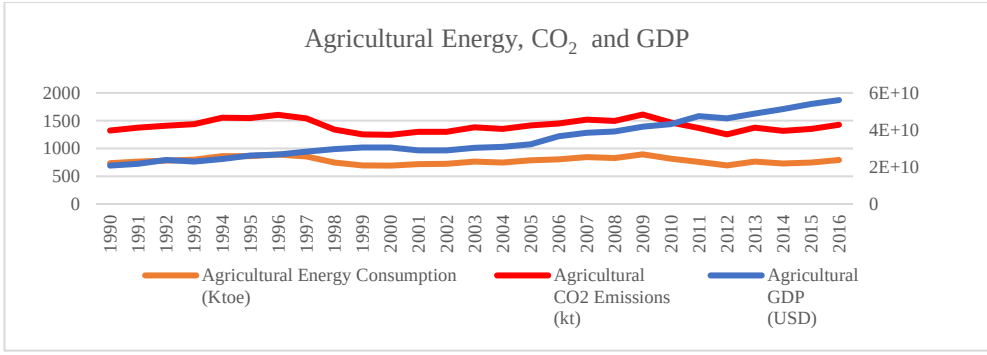

Fig 3. Energy, CO_2 and economic relationship in Agriculture sector

As compare to industrial and services sector of Pakistan the agriculture sector of Pakistan produces less CO_2 emissions but in contrast with their GDP it also increases the CO_2 emission. In above graph Fig 3. we see that the CO_2 emission of agriculture sector is zigzagging (increase or decreases) from 1990 to 2016 of Pakistan, because it depends upon the energy consumption. If the GDP of a agriculture sector increases, it means the energy and the CO_2 emissions also increases.

5.2 Decomposition Technique

According to Paul and Bhattachary the CO_2 emissions difference of time period (ΔT) can be repositioned in a direct combination as the sum of effecting factors, found as CO_2Ieffect, ECI effect, Es effect and Geffect.

CO_2I_{effect} = is the ratio of carbon dioxide and energy utilization.

ECI_{effect} = is the ratio of energy and GDP.

ES_{effect} = is the ratio of GDP of a specific sector and the total GDP.

G_{effect} = is the economic activity growth effect, this evaluate the theoretical CO_2 emissions originated by economic activity.

The computation of each effect shown in Eq (2), used to decompose the carbon dioxide emissions change are indicated by equations which is given below:

$$\mathbf{CO_2I_{effect}} = \sum_i \Delta CO2I_i \times ECI_i^0 \times ES_i^0 \times G^0 + \frac{1}{4}\sum_i \Delta CO2I_i \times \Delta ECI_i \times \Delta ES_i \times \Delta G + \frac{1}{2}\sum_i \Delta CO2I_i \left(\Delta ECI_i \times ES_i^0 \times G^0 + ECI_i^0 \times \Delta ES_i \times G^0 + ECI_i^0 \times ES_i^0 \times\right.$$

$$\Delta G) + \frac{1}{3}\sum_i \Delta CO2I_i\,(\Delta ECI_i \times \Delta ES_i \times G^0 + \Delta ECI_i \times ES_i^0 \times \Delta G + ECI_i^0 \times \Delta ES_i \times \Delta G). \quad \textbf{(3)}$$

$$\textbf{ECI}_{\textbf{effect}} = \sum_i CO2I_i^0 \times \Delta ECI_i \times ES_i^0 \times G^0 + \frac{1}{4}\sum_i \Delta CO2I_i \times \Delta ECI_i \times \Delta ES_i \times \Delta G + \frac{1}{2}\sum_i \Delta ECI_i\,(\Delta CO2I_i \times ES_i^0 \times G^0 + CO2I_i^0 \times \Delta ES_i \times G^0 + CO2I_i^0 \times ES_i^0 \times \Delta G) + \frac{1}{3}\sum_i \Delta ECI_i\,(\Delta CO2I_i \times \Delta ES_i \times G^0 + \Delta CO2I_i \times ES_i^0 \times \Delta G + CO2I_i^0 \times \Delta ES_i \times \Delta G). \quad \textbf{(4)}$$

$$\textbf{ES}_{\textbf{effect}} = \sum_i CO2I_i^0 \times ECI_i^0 \times \Delta ES_i \times G^0 + \frac{1}{4}\sum_i \Delta CO2I_i \times \Delta ECI_i \times \Delta ES_i \times \Delta G + \frac{1}{2}\sum_i \Delta ES_i\,(\Delta CO2I_i \times ECI_i^0 \times G^0 + CO2I_i^0 \times \Delta ECI_i \times G^0 + CO2I_i^0 \times ECI_i^0 \times \Delta G) + \frac{1}{3}\sum_i \Delta ES_i\,(\Delta CO2I_i \times \Delta ECI_i \times G^0 + \Delta CO2I_i \times ECI_i^0 \times \Delta G + CO2I_i^0 \times \Delta ECI_i \times \Delta G). \quad \textbf{(5)}$$

$$\textbf{G}_{\textbf{effect}} = \sum_i CO2I_i^0 \times ECI_i^0 \times ES_i^0 \times \Delta G + \frac{1}{4}\sum_i \Delta CO2I_i \times \Delta ECI_i \times \Delta ES_i \times \Delta G + \frac{1}{2}\sum_i \Delta G\,(\Delta CO2I_i \times ECI_i^0 \times ES_i^0 + CO2I_i^0 \times \Delta ECI_i \times ES_i^0 + CO2I_i^0 \times ECI_i^0 \times \Delta ES_i) + \frac{1}{3}\sum_i \Delta G\,(\Delta CO2I_i \times \Delta ECI_i \times ES_i^0 + \Delta CO2I_i \times ECI_i^0 \times \Delta ES_i + CO2I_i^0 \times \Delta ECI_i \times \Delta ES_i). \quad \textbf{(6)}.$$

Table 1. CO_2 emission factors of different energy type

Sr. No.	Energy type	CO_2 emission factor
1	Coal	90900
2	Crude Oil	71100
3	Oil Products	75500
4	Natural Gas	54300
5	Biofuels	59800
6	Electricity	75500

The main variables that need data in this study are the final energy of each economic sector and its production level. Energy data for each economic sector in Pakistan is collected by the International Energy Agency (IEA). In this research work the main sectors in Pakistan's economy are industrial, services and agriculture sector. Above given Table 1. these are the different types of fuels in kilo tone of oil equivalent which is used in energy consumption data for each economic sector, the amount of energy consumption and energy coupled CO_2 are considered to each fuel, because the nature of fuels have different emission factor. If any data is missing, the decomposition analysis cannot be accurate. Therefore, it is important to collect the data of different fuels for each sector and converted into carbon dioxide emissions according to the standard procedures and methods planned by the Intergovernmental Panel on Climate Change[33].

5.3 Analysis of data used in Pakistan.

Fig: 4. shows the total Gross Domestic Product, total energy and the emissions of all three main economic sectors of Pakistan from 1990-2016. The services sector is the fastest and the major growing sector of the world's economy and accounts for the largest share of total production and employment in the most established countries. It provides the main contribution to GDP production is 54% of Pakistan, the industrial and agriculture sectors provides 25% and 23.5% respectively in GDP of Pakistan.

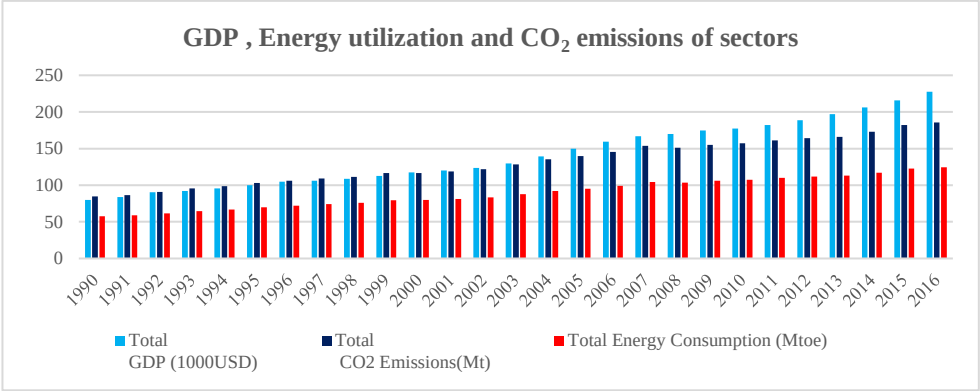

Fig:4 Total GDP, Energy Utilization and CO_2 Emissions of Various chosen Sectors

The energy utilization increases from 57.792 Mtoe to 124.553 Mtoe which accounts for almost double increased in the energy consumption from 1990 to 2016. This means Pakistan's economy will not be decoupled in terms of energy. The energy consumption progress of Industrial, Services and Agriculture sectors are +5.11%; +5.18% and +3.76% respectively.

Table 2. Energy intensity and percent changes (Mtoe/Dollars)

Sectors	1990	2016	Δ%
Industrial	9.41125E-09	1.0506E-08	11.631985
Services	2.87196E-08	1.88062E-08	-34.51802
Agriculture	8.44202E-10	3.36803E-10	-60.10399
Total	3.89751E-08	2.9649E-08	-82.99002491

Same as energy consumption, Pakistan's economy has not eliminated CO_2 emissions. In 1990 CO_2 emissions are 84.75 million tons while they are increased to 185.75 million tons in 2016. According to the data in Figure 5, the service sector is mainly responsible for increasing CO_2 emissions from 70.46 million tons to 15.198 million tons, CO_2 emissions in industry from 12.96 to 32.33. Millions of tons and the CO_2 emissions from agriculture were reduced from 1.32 tons to 1.43 million tons.

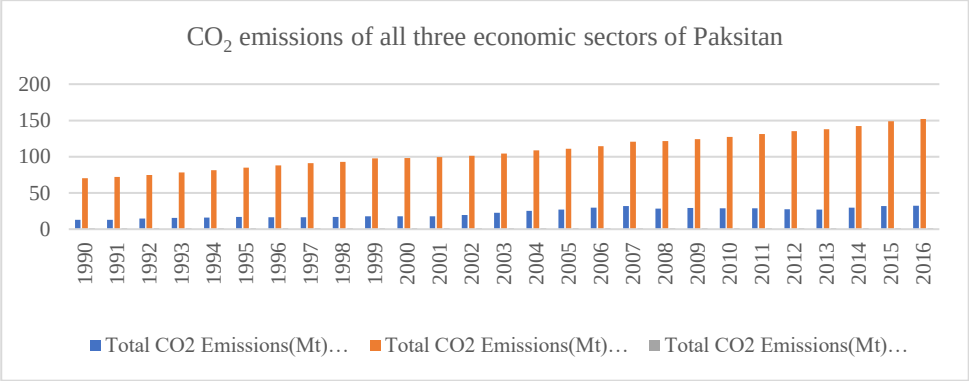

Fig: 5 Total CO_2 Emissions of all three economic sectors

6. Result

After analyzing data it is seen that CO_2 emissions increase with the increasing energy. Among these four explanatory factors, the impact of economic activity is the main factor contributing to global change. During the period 1990-2016, the G_{effect} is the most contributor to CO_2 emissions, followed by energy intensity effect. The unit of CO_2 emission is in Million tone (Mt). The negative ECI_{effect} indicates that during this period, CO_2 emissions decreased.

The result of Decomposition of carbon dioxide emissions Table 4-6 associated with energy consumption in the Pakistan's economic sectors during the period 1990-2016. The columns 2, 4, 6, and 8 report that the decomposition into four explanatory variables are CO_2I_{effect}, ECI_{effect}, ES_{effect} and G_{effect}. The total cumulative changes are the sum of four explanatory variables (CO_2I, ECI, ES, G) of various sectors are shown in the last column of respective tables. The values in columns 3, 5, 7 and 9 represent the percentage of total change for each variable, with a cumulative change of 100%. Modifications made by various explanatory variables are determined as a percentage of the total change for cumulative change. Overall analysis show that economic activity (G) has contributed significantly in CO_2 emissions. Energy intensity (ECI) is the second most common source of CO_2 emissions, and negative values of CO_2 intensity (CO_2I) can improve fuel quality and technologies to reduce CO_2 emissions. The structural changes effect (ES effect) decrease the overall CO_2 emissions due to improvement in industrial sector during the period. The results show that the economic development is the main contributor towards increasing the CO_2 emissions in all three sectors of economy in Pakistan. Whereas as per trend analysis of decoupling, it indicated the different values of decoupling index for most of the years and shows the different types of coupling and decoupling in all the three economic sectors of Pakistan.

Table 3. Carbon Dioxide intensity and percent changes (Mtoe/Dollars)

Sectors	1990	2016	Δ%
Industrial	0.068461028	0.069791871	1.943942
Services	0.062901555	0.063372259	0.7483176
Agriculture	0.0755	0.0755	-2.75718E-13
Total	0.206862584	0.20866413	0.870890167

6.1 Industrial Sector

The cumulative change shown in Table 4 shows that industrial CO_2 emissions increased to 24.756 million tons from 1990 to 2016. According to Table 2, the increase in energy intensity of industrial tasks is one of the fundamental drivers for the increase in CO_2 emissions.

Other research reports such as from 1990 to 2019, Pakistan's industrial production averaged 5.03%. In April 1991, the highest percentage of industrial production was 35.15%, and the lowest was -21.82% in April 2000 [43]. However, replacing primary energy sources with increasing use of alternative energy sources have improved mitigation technologies and reduced the intensity of CO_2 emissions from industrial production. As shown in Tables 3 and 4, most CO_2 intensity values are positive. This means that CO_2 emissions were increased from 1990 to 2016. The results shown in Table 4 highlights the major contribution in G effect in increasing emissions. The GDP growth produces the most of the carbon dioxide by industry. However, the decline share of the industrial sector in GDP and the -ve value of ES effect have helped to a certain extent reduce CO_2 emissions from industrial activities.

6.2 Services Sector

In services sector most of the values are positive in all four effects listed below in table 5, it means no decoupling achieved in this sector and the cumulated change indicated in table 5 show that CO_2 emissions of services sector increases by 833.961 Mt from 1990

to 2016. Decomposition analysis show that structural changes (ES_{effect}) and economic activity (G_{effect}) have subsidized significantly increase in CO_2 emissions from the services sector. it is the fastest and the largest growing sector of the world's economy and accounts for the largest part of total output and employment in the developed countries. The GDP contribution of this sector in Pakistan is 54%.

The results in Table 5 are consistent to the energy intensity and CO_2 intensity data listed in Tables 2 and 3. The +ve values of CO_2 emissions intensity (CO_2I_{effect}) and the -ve values of energy intensity (ECI_{effect}) clarify the latest trend affecting the use and the efficiency of devices. On the one hand, if the spreading of machines such as air-conditions significantly contributes to upgrade energy utilization and CO_2 emissions, on the other hand, significant enhancing in efficiency, especially in heating and cooling systems, provided the reduction in energy consumption.

6.3 Agriculture Sector

The cumulated change of agriculture sector indicated in Table 6, that the CO_2 emissions produced by the agriculture sector increased by 0.104 Mt from 1990-2016. Decomposition analysis show that ECI_{effect} and G_{effect} have significantly increase the CO_2 emissions from the agriculture sector. The negative values of carbon dioxide emission intensity effect (CO_2I effect) explain upgrading fuel quality and emission control techniques. In particular, the increase in biomass energy has greatly reduced the carbon dioxide emissions from agriculture. By upgrading energy and global policies as a alternative energy sources, because fossil fuels have greater carbon content than biomass and is often considered a non-net contributor to carbon dioxide emissions because it emits carbon from its carbon storage.

However, it should be noted that the +ve values of the G_{effect} and the ECI_{effect} given in Table 6 indicate that these two factors are responsible in increase in CO_2 emissions. According to the Table 2 ECI_{effect} is not dependable and show that the ECI_{effect} in this sector decreases during the reported stage (-60.10399%). As indicated in table 3. the value of CO_2 emissions intensity also negative it means CO_2 emissions are decreased.

6.4 All three Sectors

The decomposition of CO_2 emissions of all Pakistan economic sectors are listed in table 7. The cumulated change of all three economic sectors reported in the last column that the CO_2 emissions produced by the all sector increased by 3574.843 Million tone (Mt) from 1990-2016. Based on the sectoral decomposition analysis listed in Table 4 to 6, the overall analysis in table 7 shows that G_{effect} is a main factor behind CO_2 emissions. However, energy intensity (ECI) also contributor to increasing CO_2 emissions, while the -ve values of CO_2I reflects to improve the fuel quality and technologies and helps to reduce the CO_2 emissions.

Table 4. Decomposition of Industrial sector

Period	CO_2I_{effect}	Cumulated Change	ECI_{effect}	Cumulated Change	ES_{effect}	Cumulated Change	G_{effect}	Cumulated Change	$Total_{Effect}$	Cumulated Change
1990-1998	-0.342	-7.790	0.632	14.39196656	-0.777	-17.693	4.880	111.092	4.39326	100
1999-2007	0.448	3.253	4.742	34.370	-2.0404	-14.787	10.647	77.163	13.798	100
2008-2016	0.253	3.855	-3.675	-55.920	-1.045	-15.904	11.041	167.970	6.573	100

Table 5. Decomposition of Services sector

Period	CO_2I_{effect}	Cumulated Change	ECI_{effect}	Cumulated Change	ES_{effect}	Cumulated Change	G_{effect}	Cumulated Change	$Total_{effect}$	Cumulated Change
1990-1998	21.040	48.195	-2.067	-4.735	-0.041	-0.094	24.724	56.634	43.656	100
1999-2007	110.230	88.417	-31.448	-25.224	-0.442	-0.355	46.331	37.162	124.670	100
2008-2016	636.765	95.663	-13.934	-2.093	-0.231	-0.035	43.034	6.465	665.634	100

Table 6. Decomposition of Agriculture sector

Period	CO_2I_{effect}	Cumulated Change	ECI_{effect}	Cumulated Change	ES_{effect}	Cumulated Change	G_{effect}	Cumulated Change	$Total_{effect}$	Cumulated Change
1990-1998	1.85239E-10	9.3453E-07	-0.510	-2576.638	0.079	398.746	0.451	2277.891	0.020	100
1999-2007	4.03379E-11	2.2843E-08	-0.195	-110.448	-0.212	-120.191	0.583	330.640	0.176	100
2008-2016	1.38885E-10	-1.51131E-07	-0.628	683.833	0.105	-115.326	0.4305	-468.507	-0.091	100

Table7. Decomposition of Overall sectors

Period	CO_2I_{effect}	Cumulated Change	ECI_{effect}	Cumulated Change	ES_{effect}	Cumulated Change	G_{effect}	Cumulated Change	Overall $Sector_{effect}$	Cumulated Change
1990-1998	-0.426	-0.051	-3.585	-0.433	787.921	95.111	44.513	5.373	828.421	100
1999-2007	1.239	0.102	-21.457	-1.760	1155.222	94.756	84.142	6.901	1219.146	100
2008-2016	2.337	0.153	-32.812	-2.147	1480.528	96.880	78.144	5.113	1528.198	100

7. Decoupling Method

The concept of decoupling refers to separating the relationship between the two variables referred as driving forces. The driving forces are economic growth in GDP and environmental pressure (such as energy, land, materials, etc.). The consumption of fossil fuels (natural resources) creates pollutants and wastes into the atmosphere (water or air). Therefore, decoupling indicates a relationship between the economic goods and the environmental deficiencies. Decoupling obtained when the economic growth rate is greater than the environmental pressure of a given period. [44]

There are two types of decoupling are generally considered relative and absolute decoupling. Relative decoupling defined as the ratio of reduction in the emission intensity and economic output and the absolute decoupling defined as when the GDP increases, emissions generally decreases[42].

7.1 The decomposition- based decoupling model

The ideal state of a low-carbon economy is to attain negative CO2 emissions as the economy continues to grow, but this is an ideal state. The transition to a low-carbon

economy is a process of decoupling economic growth from CO2 emissions. In other words, the carbon emission growth rate is lower than the economic growth rate.

The relationship between carbon dioxide (CO2) and economic growth (GDP) can be analysed by decoupling index

The difference of growth rate are investigated by decoupling index between the environmental factors (CO2 emissions) and driving force (GDP) of a investigated period.

The decoupling index is defined as:

$$\text{Decoupling Index (Di)} = \frac{\%\Delta CO2}{\%\Delta GDP}$$

$$= \frac{\%\Delta CI + \%\Delta EI + \%\Delta ES + \%\Delta G}{\%\Delta GDP} \quad \ldots\ldots\ldots \textbf{(7)}$$

$$= Di^{CI} + Di^{EI} + Di^{ES} + Di^{G}$$

In equation (7), Di is the total decoupling index, $\%\Delta CI, \%\Delta EI, \%\Delta ES, \%\Delta G$ are the four factors carbon dioxide emission intensity, energy intensity, structural changes and economic activity $Di^{CI}, Di^{EI}, Di^{ES}, Di^{G}$ indicate the decoupling index of four factors, $\%\Delta GDP$ is the growth rate of GDP.

The decoupling indices in different sectors or different periods are compared to show how carbon dioxide emissions have evolved according to trend in economic development both in terms of aggregated levels. We have chosen the change of CO2 emissions (ΔCO2) to indicate the efforts to improve the environment at different time scales in specific sectors however, it doesn't mean the actual efforts they have made. Because change of CO2 emissions includes not only actual reduction efforts, such as reducing the energy intensity and optimizing the energy structure, but also increasing the CO2 emissions due to the development of new economic sectors. Based on the above decomposition, the real efforts to reduce the carbon dioxide emissions can be divided into carbon dioxide emissions intensity (CO2I), energy intensity (ECI) and structural changes (ES) and economic activity (G)[17].

Tapio (2005) classify the Vehmas decoupling into eight decoupling conditions because the concept of relative and absolute decoupling cannot meet all the descriptions of the relationship between the environmental pressures (CO2 emissions) and economic growth (GDP) as shown in figure below. Over the past decades, Pakistan's GDP growing rapidly. Therefore, we discuss the Conditions where ΔGDP > 0. The GDP growth rate and Carbon dioxide emissions can be coupled, weak decoupled, negatively decoupled or strong decoupled. Coupling obtained when 0.8 < Di < 1.2, means that the growth rate of Carbon dioxide emissions is equal to the growth rate of the economy. Weak decoupling obtained when 0 < Di < 0.8, means that the Carbon dioxide emissions increase with economic growth, but the growth rate is less than that of the economy. Negative decoupling obtained when Di > 1.2, means that the Carbon dioxide emissions increase with economic growth, and the growth rate is higher than that of the economy. Strong decoupling obtained when Di < 0, and Carbon dioxide emissions decrease with economic growth.[36]

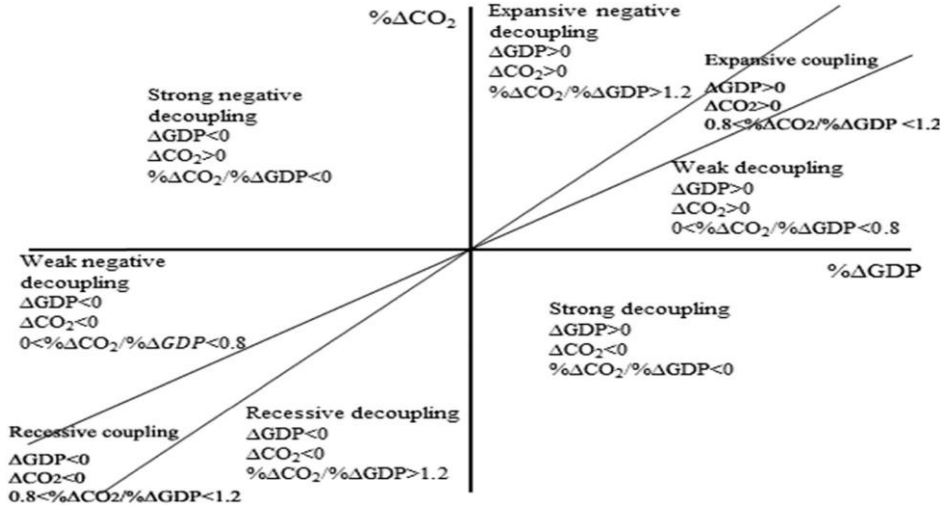

Fig.6 The Coupling and Decoupling degrees.

7.2 Overall Decoupling index between GDP and energy coupled carbon dioxide emissions of Pakistan

The overall decoupling analysis between GDP and CO2 emissions of Pakistan is listed in table 12. Which is based on the above fig 6. In table 12 we find the three conditions according to given in above fig 6 difference of carbon dioxide emissions (ΔCO2), difference of GDP (ΔGDP) but we are taking the percentage of both because the difference of GDP has greater value and the third condition is the overall decoupling of Pakistan which is the ratio of percentage difference of carbon dioxide emissions (%ΔCO2) and percentage difference of GDP (%ΔGDP) separately. In table 12 we get the different values of conditions in different periods and analyze the different types of decoupling from 1990 to 2016.

According to data given in table 12 reported in fig 7 shows the percentage difference of carbon dioxide emissions (%ΔCo2), percentage difference of Gross Domestic Product (%ΔGDP) and the decoupling index. The values of %ΔCo2 and %ΔGDP are different in different periods from 1990 to 2016 so which are in secondary axis shows in fig 7. and the values of decoupling index shows the different type of coupling and decoupling types which are on primary axis.

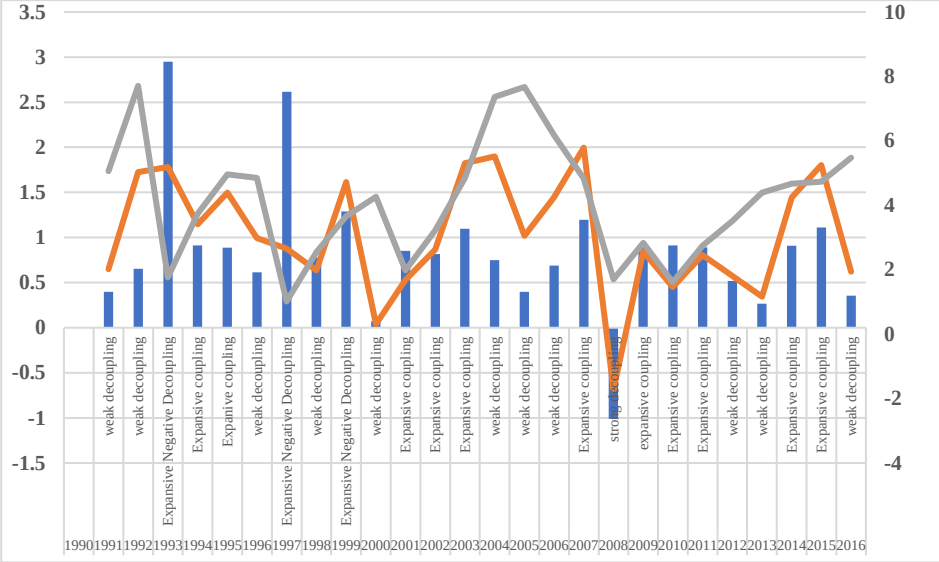

Fig.7 The degree of different types of Coupling and Decoupling of CO_2 emissions reduction from economic growth of Pakistan.

8. CONCLUSION

This study analyse the carbon dioxide emission from the energy consumption of Pakistan due to energy crises. The LMDI method is used to analyse the changes in carbon dioxide emission of Pakistan's energy consumption and investigate the effecting factors during 1990-2016. The result shows that the economic activity (G) and Energy intensity (ECI) are the major contributor to CO2 emissions while the carbon dioxide emissions intensity (CO2I) reflects to improve the fuel quality and technologies and helps to reduce the carbon dioxide emissions of Pakistan. The structural changes effect (ES effect) decrease the overall CO2 emissions due to improvement in the sectors. The economic growth, continuous use of fossil fuels, biomass, boost in transport and industries are the most contributor towards increasing the CO2 emissions in Pakistan. Furthermore, to fulfill the growing energy needs, government need to develop the renewable and efficient energy technologies (clean energy, solar, hydropower, wave, wind, geothermal and tidal) in appropriate regions. It can be expected that carbon dioxide emissions can be reduced by improving the renewable energy rather than fossil fuels (oil, coal and natural gas). Whereas as per trend analysis of decoupling, it indicates the different values of decoupling index and shows the different type of coupling and decoupling types yearly (strong, weak, expensive negative decoupling and expensive coupling) in all economic sectors of Pakistan.

8.1 Policy recommendation and Suggestions

Global climate change intensifies, carbon dioxide emissions are increasingly becoming an obstacle to economic growth. How does Pakistan develop its energy sectors while reducing carbon dioxide emissions? After completing this survey, the following steps must be performed. First step is the empirical results suggest that the population, economic growth and social revolution are the main causes of energy consumption[45]. Carbon dioxide emissions have occurred due to lack of energy and the maximum use of fossil fuels. Therefore, Vision (2025) (2014)[46] and Vision (2035) (2014)[47] will make an important contribution to reducing CO2 emissions in Pakistan.

Second step, using new technologies for sources of energy, renewable energy, energy for domestic and greenhouse gases in Pakistan are the important ways to achieve this objective. The carbon dioxide emission intensity (CIeffect) and energy intensity effect (EIeffect) policies affect the atmospheric emissions levels[48].

Third step is to analyze the carbon dioxide emission tax policy of the Pakistan's energy sectors and set a deadline for reducing emissions. Better results can be achieved by using cleaner energy in transportation and urban areas in Pakistan. The plunge in energy consumption for each fuel category (coal, kerosene, crude oil, diesel fuel, gasoline, natural gas and fuel oil) can reduce the carbon dioxide emission[3], [49].

In developing countries such as Pakistan, these renewable technologies can promote sustainable energy development, which is useful for Pakistan's local and global industries. The results analysis shows that it can reduce CO2 emissions by (i) promoting technological innovation and improving energy efficiency (ii) by improving energy consumption structure (iii) reduction in carbon life (iv) and raising awareness of energy conservation and emission reduction[50].

Finally, population growth will stimulate carbon dioxide emissions, which can be controlled through sustained contributions, for example through lifestyle changes (using less electricity consuming bulbs, switching off extra electric appliances, small distance driving instead of walking, leakage of mines, wastage of water), commercial and residential buildings, old transport surplus, agricultural production.

Reference

[1] D. Adhikari and Y. Chen, “Review of Economics & Finance Energy Consumption and Economic Growth : A Panel Cointegration Analysis for Developing Countries,” no. 1978, pp. 68–80, 2013.

[2] E. Summary, “World Energy Outlook,” 2017.

[3] B. Lin and I. Ahmad, “Analysis of energy related carbon dioxide emission and reduction potential in Pakistan,” J. Clean. Prod., vol. 143, pp. 278–287, 2017.

[4] A. Baig and A. Baig, “Impact of CO2 Emissions : Evidence from Pakistan Impact of CO 2 Emissions : Evidence from Pakistan,” pp. 0–13, 2014.

[5] T. Parties et al., “Paris Agreement, done at Paris, 12.12.2015,” pp. 1–16, 2015.

[6] “pakistan climate change with paris agreemnt.” .

[7] A. Rehman and Z. Deyuan, “Pakistan ’ s energy scenario : a forecast of commercial energy consumption and supply from different sources through 2030,” pp. 0–4, 2018.

[8] “Pakistan visioin 2014.” .

[9] “Pak INDC 2015,” pp. 1–31.

[10] M. J. C. C. R. R. Collado**, “LMDI DECOMPOSITION ANALYSIS OF ENERGY EFFICIENCY IN,” pp. 1–34, 2011.

[11] G. A. Marrero and F. J. Ramos-real, “and Policy Implications for European Countries (1991 – 2005),” Energy, vol. 6, pp. 2521–2540, 2013.

[12] X. Y. Xu and B. W. Ang, “Analysing residential energy consumption using index decomposition analysis,” vol. 113, pp. 342–351, 2014.

[13] P. Boonkham and N. Leeprechanon, “Decomposition Analysis of Changes in Energy Intensity of the Thai Manufacturing Sector during 1991-2013,” vol. 3, no. 3, 2015.

[14] D. Li and D. Wang, “Decomposition analysis of energy consumption for an freeway during its operation period : A case study for Guangdong , China,” Energy, vol. 97, pp. 296–305, 2016.

[15] F. Wang, C. Wang, Y. Su, L. Jin, Y. Wang, and X. Zhang, “Decomposition Analysis of Carbon Emission Factors from Energy Consumption in Guangdong Province from 1990 to 2014,” sustainability, vol. 9, pp. 1–15, 2017.

[16] I. Muangthai, C. Lewis, and S. J. Lin, “Decoupling effects and decomposition analysis of CO2 emissions from Thailand’s thermal power sector,” Aerosol Air Qual. Res., vol. 14, no. 7, pp. 1929–1938, 2014.

[17] H. Li and Q. Qin, “Challenges for China ’ s carbon emissions peaking in 2030 : A decomposition and decoupling analysis,” J. Clean. Prod., vol. 207, no. 2019, pp. 857–865, 2019.

[18] T. G. Cassarino, E. Sharp, and M. Barrett, “The impact of social and weather drivers on the historical electricity demand in Europe,” Appl. Energy, vol. 229, no. April, pp. 176–185, 2018.

[19] M. Zhao, S. Huang, Q. Huang, H. Wang, and G. Leng, “Copula-Based Research on the Multi-Objective Competition Mechanism in Cascade Reservoirs Optimal Operation,” pp. 1–19, 2019.

[20] T. Callan, S. Lyons, S. Scott, and R. S. J. Tol, “Working Paper No . 250 The Distributional Implications of a Carbon Tax in Ireland The Distributional Implications of a Carbon Tax in Ireland,” no. 250, pp. 1–24, 2008.

[21] J. Uribe-toril, J. L. Ruiz-real, J. Mil, and J. D. P. Valenciano, “Energy, Economy, and Environment: A Worldwide Research Update,” 2019.

[22] I. Guidelines, F. O. R. National, and G. Gas, “IPCC 2006.”

[23] B. W. Ang and F. L. Liu, “A new energy decomposition method : perfect in decomposition and consistent in aggregation . Download A new energy decomposition method : perfect in decomposition and consistent in aggregation,” 2001.

[24] B. W. Ang, “Decomposition analysis for policymaking in energy : which is the preferred method ?,” vol. 32, pp. 1131–1139, 2004.

[25] L. Liu, Y. Fan, G. Wu, and Y. Wei, “Using LMDI method to analyze the change of China ’ s industrial CO 2 emissions from final fuel use : An empirical analysis,” vol. 35, pp. 5892–5900, 2007.

[26] B. W. Ang, F. Q. Zhang, and K. Choi, “FACTORIZING CHANGES IN ENERGY AND ENVIRONMENTAL INDICATORS THROUGH DECOMPOSITION,” vol. 23, no. 6, pp. 489–495, 1998.

[27] B. W. Ang, F. L. Liu, and E. P. Chew, “Perfect decomposition techniques in energy and environmental analysis,” vol. 31, pp. 1561–1566, 2003.

[28] J. H. Cho and S. Y. Sohn, “A novel decomposition analysis of green patent applications for the evaluation of R & D efforts to reduce CO 2 emissions from fossil fuel energy consumption,” J. Clean. Prod., vol. 193, pp. 290–299, 2018.

[29] X. Xie, S. Shao, and B. Lin, “Exploring the driving forces and mitigation pathways of CO 2 emissions in China ’ s petroleum refining and coking industry : 1995 – 2031,” Appl. Energy, vol. 184, no. 2016, pp. 1004–1015, 2020.

[30] E. Akbostancı, G. Ipek, and S. Türüt-as, “CO 2 emissions of Turkish manufacturing industry : A decomposition analysis,” vol. 88, pp. 2273–2278, 2011.

[31] B. Lin and X. Ouyang, “Electricity demand and conservation potential in the Chinese nonmetallic mineral products industry,” Energy Policy, vol. 68, pp. 243–253, 2014.

[32] K. Choi and B. W. Ang, “Attribution of changes in Divisia real energy intensity index — An extension to index decomposition analysis,” Energy Econ., vol. 34, no. 1, pp. 171–176, 2012.

[33] A. Khan, F. Jamil, and N. Huma, “Decomposition analysis of carbon dioxide emissions in Pakistan,” SN Appl. Sci., no. December 2018, 2019.

[34] B. Lin and M. Y. Raza, “Analysis of energy related CO 2 emissions in Pakistan,” J. Clean. Prod., vol. 219, pp. 981–993, 2019.

[35] D. Zhou, X. Liu, P. Zhou, and Q. Wang, “Decomposition Analysis of Aggregate Energy Consumption in China : An Exploration Using a New Generalized PDA Method,” 2017.

[36] S. J. Lin, M. Beidari, and C. Lewis, “Energy consumption trends and decoupling effects between carbon dioxide and gross domestic product in South Africa,” Aerosol Air Qual. Res., vol. 15, no. 7, pp. 2676–2687, 2015.

[37] S. De and A. Hasanbeigi, “Analysis and Decomposition of the Energy Intensity of Industries in California,” vol. 46, no. June, pp. 234–245, 2012.

[38] Z. Wang, B. Zhang, and B. Wang, “Renewable energy consumption, economic growth and human development index in Pakistan: Evidence form simultaneous equation mode,” 2018.

[39] S. Rabab, K. Zaman, M. Mushtaq, and M. Ahmad, “Energy for economic growth , industrialization , environment and natural resources : Living with just enough,” Renew. Sustain. Energy Rev., vol. 25, pp. 580–595, 2013.

[40] M. Irfan, M. P. Cameron, and G. Hassan, “Household energy elasticities and policy implications for Pakistan,” Energy Policy, vol. 113, no. November 2017, pp. 633–642, 2018.

[41] X. Ma et al., “Science of the Total Environment Carbon emissions from energy consumption in China : Its measurement and driving factors,” Sci. Total Environ., vol. 648, no. 27, pp. 1411–1420, 2019.

[42] V. Andreoni and S. Galmarini, “Decoupling economic growth from carbon dioxide emissions : A decomposition analysis of Italian energy consumption,” Energy, vol. 44, no. 1, pp. 682–691, 2012.

[43] “Pakistan industrail production.” .

[44] F. Economics, “Decomposition Analysis of the Greenhouse Gas Emissions in the European Union Analiza rozkładu emisji gazów cieplarnianych w krajach Unii Europejskiej Magdal é na Drastichov á,” vol. 12, no. 2, pp. 27–35, 2017.

[45] L. Yu, Y. P. Li, G. H. Huang, Y. R. Fan, and S. Nie, “A copula-based fl exible-stochastic programming method for planning regional energy system under multiple uncertainties : A case study of the urban agglomeration of Beijing and Tianjin,” vol. 210, no. June 2017, pp. 60–74, 2018.

[46] “www.pc.gov.pk PA K I S TA N V I S I O N 2 0 2 5 i.”

[47] F. Mahmood, M. Kamal, and A. Baig, “Pakistan Energy Vision 2035.”

[48] B. Lin and I. Ahmad, “Technical change , inter-factor and inter-fuel substitution possibilities in Pakistan : a trans-log production function approach,” J. Clean. Prod., vol. 126, pp. 537–549, 2016.

[49] M. M. Saleem, “THE IMPACT OF CARBON TAX POLICIES ON FUTURE CARBON EMISSIONS FROM PAKISTAN ’ S ENERGY SECTOR USING THE TIMES MODELING FRAMEWORK,” no. 6, pp. 193–198.

[50] M. Shahbaz, “Mp r a,” no. 40959, 2012.

2020 5th International Electrical Engineering Conference (IEEC 2020)
Feb, 2020 at IEP Centre, Karachi, Pakistan

Harmonic Reduction Technique in Presence of Large Number of Non-Linear Lighting Loads by Different Manufacturers in Pakistan

Alina Naz, Muhammad Mohsin Aman, Hira Yamin, Nimra Mustafa

Department of Electrical Engineering, NED University of Engineering and Technology, Karachi, 75290, Pakistan

Abstract: This paper presents an effective method to reduce harmonic distortions in the system due to large number of non-linear lighting loads. They consume less energy with higher efficacy as compared to incandescent lamps but consume large amount of harmonic currents due to the presence of non-linear electronic ballast, producing distortion in current and voltage waves of the system and resulting in lower power factor. Therefore, the widespread use of non-linear lighting lamps is a disaster for power companies as poor power quality adversely affects the consumer appliances, making it necessary to reduce the harmonics produced for better performance. Several experiments were conducted by using various combinations of CFLs and LEDs, available by different manufacturers in the local market. Through harmonic analysis, the total $\%THD_i$ and k-factor were noted for each case. This paper shows through experimental results that filter circuits present in one lamp, filter the harmonics due to other nonlinear loads, decreasing the $\%THD_i$ of the system.

Keywords: harmonics, compact fluorescent lamps, light emitting diode, filters, non-linear loads, THD_i

I. INTRODUCTION

The objective of a utility system is to provide quality power to the consumer. Modern day technology has introduced a wide range of nonlinear devices which inject current harmonics into the system. Out of these, non-linear lighting loads such as, Compact Fluorescent Lamp (CFL) and Light Emitting Diode (LED), are being widely used in replacement of incandescent lamps, drastically increasing the system's current harmonics, resulting in voltage harmonics and power losses.

A load is considered non-linear if its impedance changes with the applied voltage. The current drawn by a non-linear load is not sinusoidal even when it is connected to a sinusoidal voltage. These non-sinusoidal currents contain harmonic currents that create voltage distortion, affecting both, the distribution system equipment and the loads connected to it [4]. Due to the presence of harmonics in the system, power efficiency and insulation lifetime decreases, also the temperature, heating loss and insulation stress increases [1].

System harmonics increase with the increase in nonlinear loads at the consumer end.

To calculate the amount of harmonic distortions, present in the system, THD_i (total harmonic distortion) is used. It is a ratio of RMS value of harmonic currents to the RMS value of fundamental component of current, and given by the following formula: [6]

$$\text{THDi} = \left(\sqrt{\sum_{n=2}^{40}\left(\frac{I_n}{I_1}\right)^2}\right)(100)\%. \quad (1)$$

Here, I_n=Harmonic component of current

I_1=Fundamental component of current

K-factor is a weighting of the harmonic load currents according to their effects on transformer heating, as derived from ANSI/IEEE C57.110. The higher the K-factor, the more significant the harmonic current content. A K-factor of 1.0 indicates a linear load (no harmonics) [8]. IEC 60076 Power Transformers limits the harmonic factor of load currents of Power Transformers to 5% of rating [10]. According to IEC standard EN 61000-3-2, lighting equipment fall in class C. It states that for lighting equipment with output power less than or equal to 25W, the third and fifth harmonic current shall not exceed 86% and 61% respectively, of the fundamental current. [5]. ANSI (American National Standard Institute) C82 states that $\%THD_i$ for electronic ballast system should be less than or equal to 32% and higher order harmonics should not exceed 7% of the fundamental [10]. The major concern in this paper is the effect of large number of non-linear lighting loads used on the system and the harmonics produced by it. CFLs and LEDs are widely used in the commercial areas as well as in the residential areas, and due to its nonlinear nature, it injects harmonics in the system.

II. LIGHT EMITTING DIODES (LED) LAMPS AND COMPACT FLORESCENT LAMPS (CFL)

A CFL has two major components i.e. electronic ballast in the base of the lamp which consists of bridge rectifier, half bridge inverter, LC resonant tank; and Gas-filled florescent tube. As shown in Fig. 1 a full wave rectifier is used to convert AC current at 50 Hz to a pulsating DC current with a fundamental frequency twice the input frequency. Capacitor **"C"** is used in parallel with bridge rectifier to minimize the voltage ripples. The DC ripples enter the Half Bridge Inverter circuit which converts the DC input into high frequency square wave (30kHz-80kHz) [3]. This circuit uses a saturable transformer which produces oscillation through the transistors connected to the secondary windings of transformer with opposite polarities [2]. The square wave enters the LC resonant tank, which converts it into a

sinusoidal wave at resonance. Initially, 3-4 times greater current is required than the normal operating current. The voltage across the tube is 500-800 in the start which reduces to 100V in normal operation.

LED lamp (Light Emitting Diode) consists of semiconductor diodes, which emit photon when power is applied. These lamps operate on low-DC voltage; hence a step-down transformer with single-phase diode rectifier is used to convert the input AC line voltage into a low DC-voltage. The DC-voltage obtained is sent to a boost converter which provides the required voltage and current. The brightness of LED depends on its current hence it must be controlled by the driver. Different converters to drive the LED can be used such as buck, boost, buck-boost, SEPIC, flyback and half bridge converter depending upon the requirement [9].

A simpler approach to improve power factor and reduce $\%THD_i$ is by using passive filters (LC filters). Valley fill filter is a type of passive filter in which two capacitors are charged in series but discharged in parallel. The rectified line voltage is applied across the capacitors, which are charged until they reach half of the peak line voltage. When line voltage falls below the peak, output voltage begins to fall towards half of peak line voltage, hence the charged capacitors start discharging into the load. A resistor is present to prevent a large in-rush current and electromagnetic interference.

Another filter called Valley fill filter with voltage doubler is designed to contribute a very small amount of power to the main circuit, just enough to improve the current waveform at current cross-over. An improved version of valley fill filter is with charge pumping capacitors which positively compensate changes between current drain from the line and charging current of the Valley fill bridge, and consequently improves the input current and DC bus voltage waveforms.

Although passive filters are cheap and simple, but greater in size and weight hence a more complex solution is the use of active filters [7].

According to B. Poorali et al., single-stage single-switch soft-switching power factor correction LED driver can be used to limit input current harmonics. It reduces switching losses and recycles the leakage energy [12].

Parallel Active Power Filter as proposed by S. Moulahoum et al. can also be used in electrical networks, to reduce harmonics generated by non-linear lighting loads. It produces an equal but opposite harmonic current to compensate the harmonic contents in line current. It is controlled by p-q theory and a hysteresis band current controller is used to control the switching of active power filter [11].

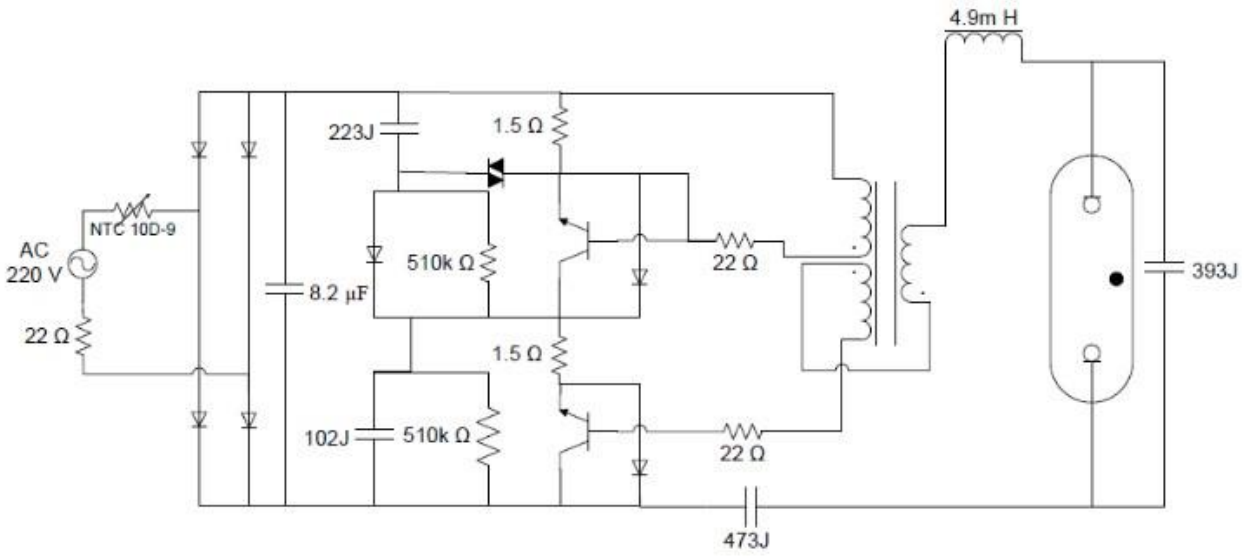

Fig. 1 Basic schematic of compact flourescent lamp

III. EXPERIMENTAL SETUP

Different methods and instruments can be used to calculate total harmonic distortion ($\%THD_i$). The instrument used for $\%THD_i$ calculation in this experiment is Fluke Power Logger 1735.

A. Case I: Individual loads

$\%THD_i$, Current (A) and K-factor of individual loads were measured at 220V and 50 Hz fundamental frequency of individual loads (CFLs and LEDs). Table 1 shows the experiment results.

Table 1 Loads label and wattage.

Load	Given Label	Manufac-turer	Watt (W)	Without Earth		
				THD_i	AMP	K
CFL 1	A	Dai-chi	25	99.8	0.16	49.64
CFL 2	B	Green light	25	99.9	0.11	28.78
CFL 3	C	Philips	27	99.9	0.17	33.85
CFL 4	D	Techno	25	99.9	0.18	46.19
CFL 5	E	Osaka	24	76.1	0.18	6.18
LED 1	F	Osaka	3	99.9	0.03	2.48
LED 2	G	Daishida	3	25.6	0.08	2.33
LED 3	H	Philips	3.5	99.9	0.03	13.34
LED 4	I	Tuff	13	99.9	0.1	64.49
CFL lamp	J	Osaka	45	29.2	0.17	4.61

B. Case II: Same loads connected in parallel

$\%THD_i$, Current (A) and k-factor of individual loads were measured at 220V and 50 Hz fundamental frequency of individual loads. For this, same CFLs of OSAKA 24W (E) were used. Table 2 shows the experiment results.

Table 2 Same loads connected in parallel.

Sequence of load connected	Without Earth		
	THD_i	AMP	K
E1 on	76.1	0.18	6.18
E1, E2 on	82.3	0.36	6.32
E1, E2, E3 on	86	0.52	6.76
E1, E2, E3, E4 on	88.8	0.7	7.66
E1, E2, E4, E5 on	91.5	0.88	7.56
E1, E2, E3, E4, E5, E6 on	92.6	1.05	8.19
E1, E2, E3, E4, E5, E6, E7 on	96.5	1.23	9.52
E1, E2, E3, E4, E5, E6, E7, E8 on	99.3	1.41	10.57

C. Case III: Different loads connected in parallel (combination 1)

In this case, 7 LEDs are taken and turned on one by one. $\%THD_i$, current (Amp) and k-factors are measured. Table 3 shows the experiment results.

Table 3 Different loads connected in parallel (Combination 1).

Sequence of load connected	*Without Earth*		
	THD_i	AMP	K
H on	99.9	0.03	2.15
F, H on	99.9	0.04	29.73
F, H, I on	99.9	0.15	38.44
F, H, I1, I2 on	99.8	0.24	58.63
F, H, I1, I2, I3 on	99.8	0.33	61.34
F, H, I1, I2, I3, G on	84.9	0.37	20.42
G on	19.7	0.07	1.47

D. Case IV: Different loads connected in parallel (combination 2)

In this case, a combination of CFLs and LEDs is turned on one by one. $\%THD_i$, current (Amp) and k-factors are measured. Table 4 shows the experiment results.

Table 4 Different loads connected in parallel (Combination 2).

Sequence of load connected	Without Earth		
	THD_i	AMP	K
C on	86.4	0.19	7.96
B, C on	90.2	0.31	10.75
B, C, I on	93.1	0.38	13.05
B, C, D, I on	99.9	0.56	22.16
A, B, C, D on	99.7	0.66	34.1
B, C, D, I1, I2 on	99.8	0.61	37.3
B, C, D, J, I on	77.6	0.68	18.5
B, C, D, J, I1, I2 on	83.1	0.75	24.22
J on	27	0.18	3.13

E. Case V: Different loads connected in parallel (combination 3)

In this case, different combinations of LEDs and CFLs are used and turned on one by one. $\%THD_i$, current (Amp) and k-factors are measured. Table 5 shows the experiment results.

Table 5 Different loads connected in parallel (Combination 3).

Sequence of load connected	Without Earth		
	THD_i	AMP	K

C on	71.2	0.21	7.39
B, C on	77.7	0.34	8.04
A, B, C on	89.7	0.53	12.02
A, B, C, D on	94.3	0.69	13.25
A, B, C, D, J on	75.2	0.82	13.11
A, B, C, D, G, J on	74.2	0.84	16.12

IV. FINDINGS AND DISCUSSION

A. Observations

1. It is observed through experiments, that total $\%THD_i$ increases as the number of lamps in the system increase
2. LED Daishida (G) and CFL Osaka Lamp (J) have very low $\%THD_i$ as compared to other lamps
3. $\%THD_i$ decreases significantly as CFL Osaka or LED Daishida is turned on with other lamps
4. As harmonics increase k-factor also increases

B. Results

The reason behind low $\%THD_i$ and hence, lower number of current harmonics in two lamps i.e. CFL Osaka 45W lamp and LED Daishida 3W is the presence of filter circuits in their electronic ballasts. As clear from the experiments conducted, these lamps when used in parallel with other CFLs and LEDs also filter out the current harmonics produced by them, resulting in lower system harmonics. This improves the system efficiency.

V. CONCLUSION

Using large number of non-linear lighting loads cause poor power quality and have a deteriorating effect on consumer appliances. In order to reduce the impact of harmonics caused by widely used non-linear lighting loads, many different combinations of CFLs and LEDs were used and examined. The experiment displayed an increase in $\%THD_i$ with increase in number of non-linear lighting loads in the system but decrease in $\%THD_i$ when higher wattage CFL (Osaka) and LED (Daishida) were turned on in parallel with other CFLs and LEDs. Harmonic analysis showed that the presence of filter circuit in one lamp removes harmonics (due to other non-linear loads) and thus decreases the overall $\%THD_i$ of the system. Further analysis of presence of harmonics can be made by using all high wattage CFLs in parallel in the system.

REFERENCES

[1] H. Nasiraghdam and M. Nasiraghdam, "Total harmonic distortion and power loss reduction in dpf mode operation of harmonic passive filters under presence of nonlinear loads in electrical power system", *Esjournals.org*, 2014.

[2] Teodosescu, M. Bojan, I. Vese, R. Marschalko. "Study of the improvement of a cfl's power factor by using a valley fill filter", *ACTA Electronica*, vol. 53, pp. 670-674, issue 1, 2012.

[3] A. Nashandi, G. Atkinson-Hope, "Impact of large number of cfls on distribution systems", *Lighting Design and Application*, pp. 26, October 2007.

[4] M. Hassenzadeh, A. Sheikholeslami, M. Nazari, "A novel method for current harmonic reduction of cfls in large number usage" in *The 6th International Power Electronics Drive Systems and Technologies Conference* (PEDSTC20 15), February 2015, Shahid Beheshti University, Tehran, Iran IranFebruary 2015, Shahid Beheshti University, Tehran, Iran.

[5] *PFC Harmonic Current Emissions*, IEC standard EN61000-3-2:2014, July 2018. [Online]. Available: http://www.epsma.org/PFC%20Guide_03032018%20(3)%20final%207-7.pdf

[6] S. Das, P. Sudhakar, "Power Factor Correction & Harmonic Distortion Control for AC-DC Fault Tolerant Power Distribution System & Power Quality Qualification Test Results as per IEC 61000-3-2", *BARC Newslett.*, pp. 5-13, March-April, 2017.

[7] M. S. Witherden, "The influence of non-linear loads on the power quality of the New Zealand low voltage electrical residential power distribution network", M. S. thesis, Energy Manage., Massey Univ., Manawatu, 2012.

[8] O. E. Gouda, G. M. Amer, W. A. A. Salem, *"*A Study of K-Factor Power Transformer Characteristics by Modeling Simulation*", ETASR - Engineering, Technology & Applied Science Research*, vol. 1, no. 5, pp. 114-120, 2011.

[9] H. Acikgoz, R. Coteli, F. Ucar, B. Dandil. (Dec 2016). Power factor correction control of led lamp driver based on robust controller. Presented at INESEC 2016. [Online]. Available: https://www.researchgate.net/publication/311708381

[10] "Installation of compact fluorescent lamps assessment of benefits", Parsons Brinckerhoff Assoc. Ltd., Wellington, New Zealand, April 2006.

[11] S. Moulahoum, H. Houassine, N. Kabache, "Parallel active filter to eliminate harmonics generated by compact fluorescent lamps", presented at the 21st Mediterranean Conf. on Control and Automat. (MED), Platanias-Chania, Crete, Greece, June 25-28, 2013.

[12] B. Poorali, H. Farzanehfard, "A single-stage single-switch soft switching power factor correction LED driver", *IEEE Transactions on power Electronics*, Dec. 2016, doi: 10.1109/TPEL.2016.2634086.

2020 5th International Electrical Engineering Conference (IEEC 2020)
Feb, 2020 at IEP Centre, Karachi, Pakistan

Fine-Grained Vehicle Classification by using Inception-V3

[1]Danish Ul Khairi, [2]Yumnah Hasan, [3]Zahida Perveen, [4]Marium Ata and [5]Mohammd Umair Arif
[1,5]Department of Electrical Engineering, Bahria University
Karachi, 75260, Pakistan
[1]danishulkhairi@gmail.com, [2]yumnahhasan.bukc, [3]zahidaparveen.bukc, [4]mariumatta.bukc, [5]umairarif.bukc@bahria.edu.pk

Abstract: Traffic surveillance plays a significant role in reducing congestion, road planning and identification of suspicious vehicles. For this purpose, different detection and classification techniques are studied by researcher to improve the accuracy in real time and different climatic scenarios. In this paper, inception V3 model based on Deep Neural Networks (DNN) is used for the two standard datasets which include Stanford cars and BMW-10. Total 16,185 and 564 images are assessed during the process for Stanford cars and BMW-10 respectively. The preprocessed images (zoom, cropped and grey scale) are utilized. The learning, training, validation parameters are changed to increase the accuracy. The highest true classification is obtained with zoom images at learning rate 0.5, validation 10% and testing 20% is 62.2% for Stanford dataset. Whereas, for BMW-10 dataset 82.7% accuracy is obtained from at learning rate 0.1, validation 10% and testing 20% with cropped at zoomed images.

Keywords: Inception V3, Deep Neural Networks, Traffic surveillance, Tensorflow.

I. INTRODUCTION

Nowadays, vehicle detection and tracking plays a vital role in the area of traffic surveillance system and developing societies where intelligent and efficient traffic management and security is main concern[1]. Being the importance of vehicles in our daily life many researchers has been working on intelligent transportation system to providing the facility to human being. The researches worked on the transportation system that are intelligent, road and infrastructure planning based on the useful information regarding vehicles [2]. They have done traffic image analysis to extract particular traffic information regarding vehicle tracking, identification of number plate, congestion rate, vehicle trajectory and classification. For developing of high quality automatic transportation system, researches used different techniques in which Artificial Neural Network (ANN) and Convolution Neural Network (CNN) is the more efficient. Prof. Suvarna Nandyal & Mrs. Pushpalata Patil used NN classifier and image processing technique to develop an efficient and intelligent transportation system (ITS) [3].

In this paper, inception V3 model is used for the classification of same type models of vehicles. Two different datasets are used for the implementation of selected technique. DNN is getting more attention in the modern era and it consumes less time as compared to NN, having larger number of layers, which contributes towards its efficient performance.

II. PREVIOUS WORK

Dehghan et al [4] proposed a system which is fully automated and performs model and color recognition task. They implemented their proposed system on ImageNet. This finegrained visual classification and identification is always a difficult task in terms of accuracy and performance[5], [6], [7], [8]. The system basically works on three steps which includes collection of dataset, pre-processing the images and then performs deep learning.The proposed system is tested on publicly available dataset of Stanford that is consist of (196 classes and total of 16,185 images) [9] and CompCars to get high performance. Due to The combination of Sighthounds unique concept to implement deep neural network on a large dataset to acquire high accuracy.

Jonatahn et al [10] present a 3D objects representation object model. They shows 3D object representations outperform and its state-of-the-art 2D counterparts for fine-grained categorization and demonstrate its efficiency. For testing purpose Stanford dataset [9] for cars and BMW-10 is used. The system results showed that converting 2D objection representations to 3D increases the efficiency for both SPM and BB. The huge difference in true classification is observed over standard and modified datasets including ultra-fine-grained datasets.

Kun et al [11] proposed a different iterative multiple learning method to model local features and various viewpoint angles combine in the similar layout and work to enhance the standard MI-SVM formulation for vehicle classification and viewpoints labels for more accuracy. They used Stanford and INRIA vehicle dataset and finally compare their results classification accuracy is detected with several attribute selection methods , different degrees of viewpoint supervision. Finally achieved better results by combining the attribute features with low-level Fisher vector features [12] and use simple blending scheme on the normalized scores of each test image.

In this paper [13], authors worked on the comparative analysis of several vehicle detection methods in which includes symmetrical features, vehicle detection based on license plate,

SVM (support vector machine), vehicle detection based on Gabor features, Haar like features ADA boost classifier. The symmetrical features has results better as compare to others three. The detection accuracy is 91.2%.

In this paper [14], authors worked on the LiDAR based vehicle detection approach is used. LiDAR is known as light detection and Ranging and it is also derived from Radar. In this platform, large number of point clouding is providing by LiDAR, objects are detected by using this point clouding. In this paper, there are two phase of LiDAR first is hypothesis generation and second is hypothesis verification. In first phase, the Difference of Normal (DoN) operator is applied to segment the 3D points cloud into the potential clusters, e.g. vehicle, pedestrian, bicycle and lamp. In second phase, the Random Hypersurface Models (RHM) is used to estimate the clusters shape parameter. Moreover,for classification of object vehicles and non-vehicles SVM classifier is used.

In this paper[15], authors worked on real time road segmentation. The LiDAR data processing technique is used for road segmentation on FPGA. For deriving a vehicle, the road segmentation and obstacles identification is so important. For this purpose convolution neural network (CNN) is used and trained this network on LiDAR sensor data. Furthermore, the efficient hardware is designed using FPGA. It can be processed on LiDAR scan data. This method is must faster.

In this paper [16], authors worked on the robust vehicle detection using LiDAR. By using 3D LiDAR authors detect greater distance of vehicle, angle view and as well as occlusions. For segmentation, RGLOS (Ring Gradient Based Local Optimal Segmentation) algorithm is used. For feature extraction, three types of features extracted in this paper, which are position-related shape, object height along length and reflective intensity histogram. In the end SVM classifier is used for classification.

In this paper [17], authors worked on the detection of vehicle using point cloud in Urban areas. In this paper, Vehicle detection methods is based on two stages one is segmentation and other is classification. Segmentation is applied, including the baseline technique using ground removal and clustering and three incremental methods (curb removal, adaptive segmentation and gap detection) and for classification Convolution Neural Network (CNN) which is based on orthogonal view projection. After while this CNN is compared with SVM and better results are achieved from CNN.

In this paper [18], authors detected vehicles using morphological features. In this image processing techniques used. Firstly pre-processing the image using convert the image into binary images using im2bw technique then apply median filter to remove the noise on the images. Then designed vehicle detection algorithm. After pre-processing then apply the sobel edge detector to detects the edges. Then apply first level binary dilation with vertical, horizontal and 45 degrees and remove boundary lines. The successful rate of this method is 85%.

In this paper[19], authors worked on the speed detection. In this most important methods are used for object detection namely Gaussian mixture model, DBSCAN (Density - based spatial clustering of applications with noise), Kalman filter and optical flow.

III. SYSTEM SETUP

The system used for the implementation of selected algorithm is core i5 processor with 2GB graphics card and 4GB RAM. The platform used for DNN technique is TensorFlow. For augmentation and modification in the dataset like crop, zoom and flip code on MATLAB is used.

IV. METHODOLOGY

A. Inception-V3

Inception V3 implemented in this paper is a widely used model for image classification or recognition that shows high accuracy result. The inception v3 model is made up of symmetric and asymmetric blocks, this model have different layer like convolution, average pool, max pool, concat, dropout, full connected and softmax these layers have used to work for complex dataset. The direction of layers shows clearly that the information flow is feed forward layer by layer to avoid complexity it will reduce the number of convolutions to maximum 3x3.Inception-v3 was trained on ImageNet ,complete architecture of Inception-v3 as shown in Fig1.

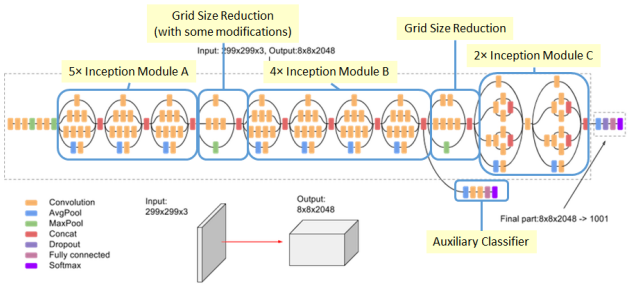

(a)

Fig.1. Inception-V3 complete architecture.

Convolution network allow width increase technique to improve features combination to make the network fast and accurate. The high-level diagram of inception v3. The outline of the proposed Inception V3 network architecture. The gained output of every module is work as an input for other module. 0 padding convolution is marked, which utilized to maintain the grid size. The grid size used inside the inception model is not reduce by 0-padding. No padding is used by other layers. The layers are factorized from 7 convolution into three 3 convolutions.

There are three traditional inception models available including 35x35 with 288 filters each is further reduced to a 17x17 grid with 768 filters by applying the grid reduction method. However, it has been observed that the quality of the network model is relatively stable. In this model, images from the both datasets are further modified by the changing the parameters which include crop, grey scale and zoom as shown in Fig.2.

The operation are executed automatically by using a MATLAB code. The model accuracy in this paper is optimized by

Table 1: Results of Vehicle Classification with Learning Rates

Dataset	Processing on Images	Testing Percenage	Validation Percentage	Learning Rate	Batch Size	Training Steps	Accuracy
Stanford	Zoom, Flip and Grayscale	20	10	0.5	100	4000	62.2%
Stanford	None	10	30	0.5	100	4000	53.7%
Stanford	None	10	30	0.01(Default)	100	4000	32.9%
BMW-10	Crop and Zoom	10	10	0.01(Default)	100	4000	61.1%
BMW-10	Crop and Zoom	10	10	0.1	100	4000	68.5%
BMW-10	Crop and Zoom	20	10	0.1	100	4000	82.7%

Fig. 2. (a) Stanford DataSet.(b) BMW-10 DataSet.

changing the factors like learning rate, training steps, batch size, testing percentage, validation percentage, duplication of images in dataset, by using preprocessed images (flip images, grey scale images, cropped images and zoomed images).

Three different settings of parameters for both datasets are used to achieve maximum accuracy of classification as shown in Table1. Dataset of BMW-10 has shown the maximum accuracy for the given parameters. The processing done is crop and zoom with testing percentage of 20 and learning rate of 0.1. The least accuracy of 32.9 is achieved for Standford when no processing is done with testing percentage of 10 and default learning rate of 0.01.

V. RESULTS AND DISCUSSIONS

The datasets of Stanford and BMW-10 are utilized to implement the inception V3 model on Tensorflow. The rate of accuracy is increased by changing the parameters from default to certain specific values. The images are preprocessed by using crop, zoom and grey scale commands. As shown in Table 1, the Stanford dataset contains zoomed images at learning rate 0.5, testing percentage 20 and validation percentage 10 has the highest accuracy of 62.2% among the other two types which have similar testing percentage and validation percentage but learning rates are different. The lowest accuracy is obtained from the default parameters which is 32.9%.

The accuracy curves are shown in Fig. 2 (a), (b), and (c). The BMW-10 dataset achieves highest accuracy of 82.7% with the settings with testing percentage 20, validation percentage 10 and learning rate 0.1 having cropped and zoom images. The lowest accuracy is observed with the default settings which is 61.1%. Obtained accuracy curves from Tensor board are shown in Fig. 2 (d), (e), and (f).

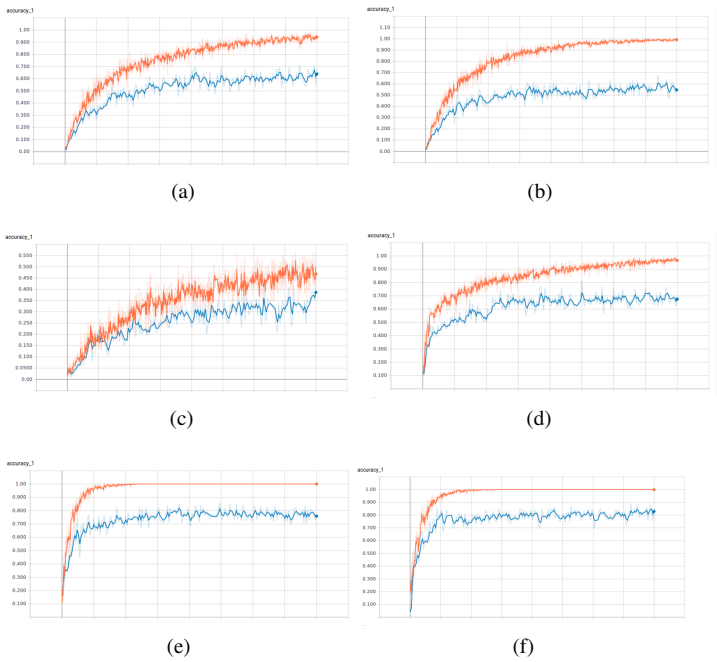

Fig. 3. (a) Accuracy of Stanford modified.(b) Accuracy of Stanford 0.5 learning rate.(c) Accuracy of Stanford default. (d) Accuracy of BMW-10 all default. (e) Accuracy of BMW- 10 changing learning rate.(f) Accuracy of BMW-10 modified

VI. CONCLUSION

The results obtained from the implemented model by using different scaling values provides a significant difference in the accuracy. The preprocessed images has an impact on the correct classification rate. In Stanford the highest accuracy is 62.2% having images with zoom feature. Whereas, the BMW-10 dataset has 82.7% accuracy of classifications with the cropped and zoomed images. However, the learning rate, testing percentage and validation percentage effects on the true classification rate. Therefore, by changing the default parameters further accuracy can be enhanced. In future, more features can be extracted to increase the efficiency like rotation, side views, color and number plate. The other models available on Tensorflow can further be used to compare the level of true classification.

REFERENCES

[1] P. K. Bhaskar and S.-P. Yong, "Image processing based vehicle detection and tracking method," in *2014 International Conference on Computer and Information Sciences (ICCOINS)*. IEEE, jun 2014.

[2] R. A. Hadi, G. Sulong, and L. E. George, "Vehicle detection and tracking techniques : A concise review," *Signal & Image Processing : An International Journal*, vol. 5, no. 1, pp. 1–12, feb 2014.

[3] P. S. Nandyal and M. P. Patil, "Vehicle detection and traffic assessment using images," *International Journal of Computer Science and Mobile Computing (IJCSMC)*, vol. 2, p. 8, Sep. 2013.

[4] A. Dehghan, S. Z. Masood, G. Shu, and E. G. Ortiz, "View independent vehicle make, model and color recognition using convolutional neural network," vol. arXiv preprint arXiv:1702.01721, 2017.

[5] L. Yang, P. Luo, C. C. Loy, and X. Tang, "A large-scale car dataset for fine-grained categorization and verification," in *2015 IEEE Conference on Computer Vision and Pattern Recognition (CVPR)*. IEEE, jun 2015.

[6] T.-Y. Lin, A. RoyChowdhury, and S. Maji, "Bilinear CNN models for fine-grained visual recognition," in *2015 IEEE International Conference on Computer Vision (ICCV)*. IEEE, dec 2015.

[7] S. Xie, T. Yang, X. Wang, and Y. Lin, "Hyper-class augmented and regularized deep learning for fine-grained image classification," in *2015 IEEE Conference on Computer Vision and Pattern Recognition (CVPR)*. IEEE, jun 2015.

[8] J. Krause, T. Gebru, J. Deng, L.-J. Li, and L. Fei-Fei, "Learning features and parts for fine-grained recognition," in *2014 22nd International Conference on Pattern Recognition*. IEEE, aug 2014.

[9] J. Krause, J. Deng, M. Stark, and L. Fei-fei, "Collecting a large-scale dataset of fine-grained cars. the second workshop on fine-grained visual categorization," 2013.

[10] J. Krause, M. Stark, J. Deng, and L. Fei-Fei, "3d object representations for fine-grained categorization," in *2013 IEEE International Conference on Computer Vision Workshops*. IEEE, dec 2013.

[11] K. Duan, L. Marchesotti, and D. J. Crandall, "Attribute-based vehicle recognition using viewpoint-aware multiple instance SVMs," in *IEEE Winter Conference on Applications of Computer Vision*. IEEE, mar 2014.

[12] M. Douze, A. Ramisa, and C. Schmid, "Combining attributes and fisher vectors for efficient image retrieval," in *CVPR 2011*. IEEE, jun 2011.

[13] M. Zhao, C. Zhao, and X. Qi, "Comparative analysis of several vehicle detection methods in urban traffic scenes," in *2016 10th International Conference on Sensing Technology (ICST)*. IEEE, nov 2016.

[14] F. Zhang, D. Clarke, and A. Knoll, "LiDAR based vehicle detection in urban environment," in *2014 International Conference on Multisensor Fusion and Information Integration for Intelligent Systems (MFI)*. IEEE, sep 2014.

[15] Y. Lyu, L. Bai, and X. Huang, "Real-time road segmentation using lidar data processing on an fpga," in *International Symposium on Circuits and Systems*, 2018, pp. 1–5. [Online]. Available: https://doi.org/10.1109/ISCAS.2018.8351244

[16] J. Cheng, Z. Xiang, T. Cao, and J. Liu, "Robust vehicle detection using 3d lidar under complex urban environment," in *2014 IEEE International Conference on Robotics and Automation (ICRA)*. IEEE, may 2014.

[17] J. Huang and S. You, "Vehicle detection in urban point clouds with orthogonal-view convolutional neural network," in *2016 IEEE International Conference on Image Processing (ICIP)*. IEEE, sep 2016.

[18] A. Ajmal and I. M. Hussain, "Vehicle detection using morphological image processing technique," in *2010 International Conference on Multimedia Computing and Information Technology (MCIT)*. IEEE, mar 2010.

[19] M. O. Jozef Ger Dominik Sopiak and Jarmila, "Pavlovificov vehicle speed detection from camera stream using image processing methods," *IEEE International Symposium ELMAR*, pp. 201–204, Sep. 2017.

2020 5th International Electrical Engineering Conference (IEEC 2020)
Feb, 2020 at IEP Centre, Karachi, Pakistan

Device-to-Device Communication Prototyping using Software Defined Radios

Sundus Ali[1*], Muhammad Imran Aslam[1], Irfan Ahmed[1] and Hira Mariam[1]

[1] Department of Electronic Engineering, NED University of Engineering and Technology, Karachi, 75290, Pakistan (sundus@neduet.edu.pk)* Corresponding author

Abstract: This paper summarizes our efforts in developing a testbed for device-to-device (D2D) communication. In this paper, we have discussed the need and importance of establishing D2D communication based prototyping testbeds. We have also provided a review of various testbeds developed globally targeting experimentation in D2D communication in LTE-Advanced and 5G networks. We have also discussed the set up and working of the D2D prototyping testbed established in our lab using software defined radios (SDRs), the first of its kind in Pakistan. Lastly, we demonstrate the preliminary functioning of SDR-based testbed using LabVIEW Communications and the Universal Software Radio Peripheral (USRP) hardware platform.

Keywords: Device-to-Device, Software Defined Radio, LTE, USRP, Testbed, prototyping

I. INTRODUCTION

By 2022, there will be 12.3 billion mobile connected devices, including around 8 billion mobile-to-mobile (M2M) modules—exceeding the world's projected population at that time [1]. Also, by 2024, of the projected 22.3 billion IoT devices, 17.3 billion of those devices have been categorized as short-range IoT [2]. All of these mobile-connecting modules require different levels of quality of service from the network serving them, like low latency, high reliability, high data rate etc.

Keeping in mind, these trends, it was imperative that the future generation of mobile technology may cater to this volume of mobile devices and machines. A solution in the form of device-to-device (D2D) communication was proposed in [3], where it was presented as an enabler of local services with tight integration into the LTE-Advanced (LTE-A) network, on the expense of limited interference impact on the primary cellular network. The authors have discussed various possible methods of D2D communication session setup and management. They have established that D2D communication can increase the total throughput observed in the cell area allowing many low-powered devices to communicate with each other without the need for cellular infrastructure, hence relieving the Base Stations (BSs) of routing traffic from thousands of such devices through its network.

The D2D communication technique was standardized in 2015 in Release 12 [4] as LTE technology for emergency and security services. In [5] , the authors have provided an insight into the vital technology components that have become a part of 3GPP for Release 12. One of these features include enabling local area access, signaling solutions for WLAN integration, MIMO enhancements, improved support for massive MTC, and D2D communications. In [6], an overview of D2D standardization activities in 3GPP have been discussed while characterizing technical challenges and deducing from initial analytical studies, and identifying best possible practices in the designing D2D-capable air interface for LTE-A networks. It includes solutions for facilitating interoperability between public safety and corporate networks. D2D has fundamentally changed the cellular architecture, reducing the prime role of eNodeBs and allowing User Equipment (UE) devices to communicate with UE devices in proximity directly. The paper emphasizes on the need for revisiting many assumptions and models used to analyze cellular networks.

In [7], the author has highlighted that with the rise of context-aware applications and accelerating growth of M2M applications, D2D communication is expected to play a key role. This is so because it can facilitate the discovery of geographically close devices, and enable direct communications between these devices, which in turn will improve communication capability and reduce latency and overall power consumption, unlike in legacy cellular networks where direct over-the-air communications between users and devices was not supported. D2D communication have been identified among the five disruptive technology directions in 5th generation cellular network in [8], where it has been discussed that massive M2M communication will require low latency, ultra-reliable proximity services, enabled by D2D communication. They have also identified challenges like quantification of the opportunities for D2D, fast local exchanges for low-latency applications, integrating D2D mode with the uplink/downlink duplexing, design of D2D-enabled devices, by flexibility at both the physical and medium access control layers, analyzing net gains associated with incorporating D2D mode, assessing extra overheads for control signaling and channel estimation.

Talking about design aspects of D2D, in [9], the authors have presented simulations that identify mode selection and power control algorithms for realizing proximity and reuse gains in mixed D2D/cellular set up. They have identified ways to integrate various forms of D2D network (pico-nets and multi-hop) in cellular

networks. They have also explored possibilities of dynamic spectrum allocations, and solutions for inter-operator D2D methods as interesting directions for future research.

The authors in [10-11] have presented a detailed survey on all the research work done in the domain of D2D communication, elaborated a taxonomy based on the D2D communicating and have reviewed the available literature. They have identified new directions into the under-explored research domains that can pose research problems for D2D communications in future cellular networks.

In order to design, develop, prototype and test D2D communication-enabled devices; various testbeds have been set up over the last few years across the globe. Prototyping such devices in real environment and constraints provide validation to the analytical solutions and simulations presented by many researchers over the years and provide insight into the practical challenges and considerations in implementing D2D communication. Considering the need to prototype and test D2D enabled networks, we have set up a D2D based prototyping testbed using Software Defined Radios (SDRs). In this paper, we have discussed the significance of developing such testbeds for rapid prototyping and presented the working set up, possible configurations and preliminary real environment results obtained through experimentation on the testbed.

The paper structure is as follows: in section II we have discussed various D2D based prototyping testbeds deployed globally highlighting their working. In section-III we have provided details of the SDR based D2D testbed established in our lab and the experiments conducted using the equipment. In section-IV, the results obtained using this testbed have been presented and discussed. Section-V concludes the paper.

II. D2D TESTBEDS FOR PROTOTYPING

In this section, we have discussed various testbeds developed for prototyping and testing D2D communication systems and its applications. Notable work done in this domain in the few years is summarized in the subsequent sub-sections.

A. Link Oppurtunistic D2D communication

The work done on the first D2D equipment set up, developed at UWICORE Laboratory, Miguel Hernandez University of Elche was presented in [12]. The testbed is hardware-independent, built by modifying the Linux kernel. Using link-aware opportunistic D2D communications, reduction in energy, improvement of rate and QoS, have been experimentally validated.

B. Direct and single-hop D2D communication

The authors in [13] have presented experimental results obtained on a testbed implemented using ZigBee standard. The results present D2D communication protocol, showing the experimental range doubling in the relay mode of D2D communication due to single hop technique. Spectral efficiency has been presented as a function of distance and used to define cell parameters. Network coding and cognition can be implemented as an extension to this testbed to analyze sophisticate D2D networks.

C. MIMO system testbed for D2D communication

In [14], authors have presented the deployment and possible services of co-existence of D2D communication in full-duplex MIMO architecture, operating on the same spectrum. They have deployed a two-UE pair, one pair directly communicating with the eNodeB, the other pair directly communicating with each other using D2D. They have used FPGA base software defined radios (SDR) platform with 20MHz bandwidth in 2x2 MIMO mode. One of the key milestone achieved through this tested is the full duplex operation of a UE is while incorporating self-interference capability with guaranteed performance.

D. V2V transmission using D2D communication

In [15], the authors have presented potential practical issues in the vehicle-to-vehicle (V2V) transmission using D2D communication. They have developed a SDR based platform for V2V communication using USRP. By modifying the LTE framework they have emulated the LTE-V standard and producedl results based on the real measured signals.

E. Cryptographic security for D2D communication

Security vulnerabilities are a consequence of introducing D2D communication due to the ad-hoc nature of network. Separate signaling protocols and implementation are required to handle key management, access and privacy control, secure routing, and transmission. The authors in [16] have proposed a key generation and management technique for securing D2D communication as well as a stream cypher encryption mechanism, to ensure confidentiality of the message being communicated. The techniques have been validated by testing on a SDR testbed.

F. LTE-standard compliant D2D communication

In [17], the authors have presented the design and implementation of the first LTE Release 12 standard complaint D2D communication functionality for LTE. They have implemented the system on SDR-based testbed, expanding the open-source LTE eNodeB and UE implementation provided by the srsLTE software suite. The results presented in the paper suggest cell extension capabilities of D2D in the form of Signal-to-Noise Ratio (SNR) and throughput computed by a UE (cell-edge) when directly connected with eNodeB and when provided connectivity through the relay UE.

G. D2D communication for Clustered UEs

In [18], the authors have analyzed opportunistic D2D clustering from a theoretical and practical aspect. Their experimental evaluation supports their hypothesis of the impact of UE cluster size on various network performance parameters like throughput and latency. The experiments have been performed using a controller and eight SDRs. They have also tested and compared mmWave WiFi results with WiFi Direct, finding that because of wider bandwidth, the mm-Wave results perform better compared to WiFi Direct.

H. In & out-band D2D Communication Framework

In [19], the authors have presented the first experimental testbed, developed at Technische Universität Darmstad, Denmark, capable of carrying out in-band D2D communications in 5G. They have worked on LabVIEW Communications LTE Application Framework, making necessary changes and extending the framework to support multiple UEs. Recently in [20], the same authors, along with their team from the Secure Mobile Networking Lab (SEEMOO) at Technische Universität Darmstadt have prototyped the first testbed based on SDRs, capable of in-band and out-band D2D communication. The results shown in the paper indicate a two times increase in aggregate system throughput which confirms and validates the simulation evaluation.

With the testbeds for D2D prototyping being developed and used worldwide, we have also developed a D2D prototyping testbed in NED University of Engineering and Technology as the first D2D communication testbed in Pakistan.

III. TESTBED STRUCTURE

Our testbed comprises of an eNodeB and two UEs. As our hardware platform, we have used two NI USRP RIO SDRs. These SDRs comprise of two TX and RX ports and an FPGA for computationally extensive operations. For our software, we have used LabVIEW Communications LTE Application Framework, which has an implementation of the Physical Downlink Control and Shared Channels (PDCCH and PDSCH) and the Physical Uplink Shared Channel (PUSCH) for the eNodeB and the UE. The changes made to the LTE Application Framework to incorporate D2D at the eNodeB and UE side are highlighted in figs 1 and 2. The system model of the eNodeB is shown in Fig 1. Apart from the eNodeB functions already defined in the LTE framework, some changes have to be made in order to allow UE data to transmit via the uplink channel, and to deploy a scheduler which measures link quality in cellular and D2D mode to schedule uplink/D2D resources. Moreover, the system should include signaling protocols to control which mode of communication (cellular/D2D) the UEs should opt for data transfers, through the PDSCH.

Fig 2 shows the system model of the UE. Again, certain modifications are required to be made in the UE system model defined in the LTE Application Framework. This includes integrating an additional D2D receiver chain, an improved MAC layer implementation and D2D signaling protocols to allow addressing between UEs and D2D link control.

The SDRs we have used are USRP 2953R and USRP 2943R. The difference between the two is that USRP 2953R comprises of a GPS-disciplined oscillator, which allows locking the internal clocks to a GPS reference signal, synchronize using GPS timing information, and query GPS location information.

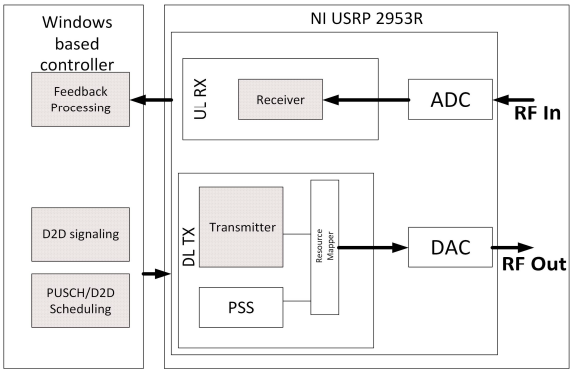

Fig 1. eNodeB system architecture for D2D communication

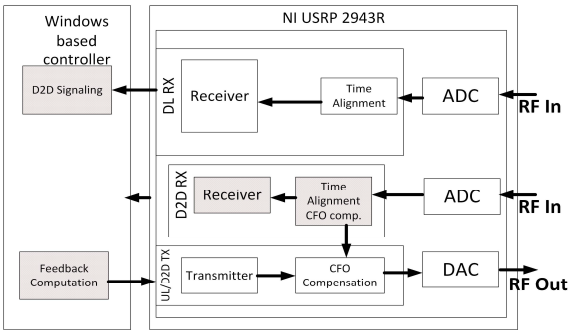

Fig 2. UE system architecture for D2D communication

For the network topology and structure, we are considering two possible scenarios for D2D communication to take place between two UEs. Their details are discussed below:

A. Partial Coverage Scenario:

In this scenario, two UEs are positioned in proximity to each other. One of them is in full coverage of the eNodeB and the other UE is positioned at such a distance where the downlink signal quality from the eNodeB is degraded (cell-edge). Hence the connectivity of the cell-edge UE with the eNodeB is weak. In such a situation, the UE with strong downlink/uplink connectivity with the eNodeB can function as a “Relay” in parallel and forward the downlink/uplink signal from/to the eNodeB to/from the cell-edge UE in D2D mode. This technique will allow the cell-edge UE to communicate with the eNodeB through the Relay UE at a higher data rate as compared to when it communicates

directly with the eNodeB. In fig 4, we have shown the network diagram where the solid black line shows the D2D relay connection between the UEs and dashed black line represent direct connectivity of UEs with the eNodeB (infrastructure mode).

B. In-coverage Scenario:

In this scenario, two UEs are positioned in proximity to each other, in coverage of an eNodeB. The data exchange between the UEs can be done either through the eNodeB in infrastructure mode or directly through a D2D connection. Fig 5 shows the network set up where the red line denotes the D2D connection and black solide lines show connectivity of UEs through the network infrastructure (eNodeB).

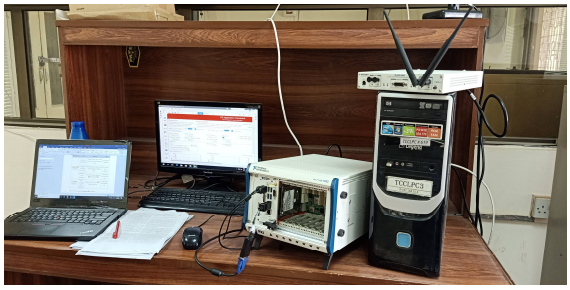

Fig 3. System set up

A screenshot of the Graphical User Interface can be seen in Fig 6, which shows the eNodeB functions along with an active power spectrum of transmitted and received signal. Power spectrums of the passband of the signal is shown in the fig 6. As can be seen in the figure, received power spectrum, the signal's strength is weak, and pose a research problem of recovering useful signal. The authors consider this as their next immediate task. Similarly, in fig 7, we have presented the UE GUI showing received signal power spectrum. and in fig 8, we have shown the power spectrums of a basic Downlink connection between eNodeB and UE.

IV. CONCLUSION

In this paper, we have discussed the need for establishing reliable testbeds for validating the efficacy of D2D communication in 5th generation cellular networks. We have presented the first experimental testbed for D2D communications in Pakistan established at NED UET, Karachi. Moreover, we have implemented D2D mechanism in eNodeB SDR using LTE application framework and obtained some preliminary results. Our next step will be to implement D2D set up at UEs end to test the two scenarios mentioned in section-IV. This demonstration is the first step to further investigate D2D communication using SDR testbed in real-world environment with practical channel characteristics, specifically in Pakistan and comparing them with the results obtained globally in different environments.

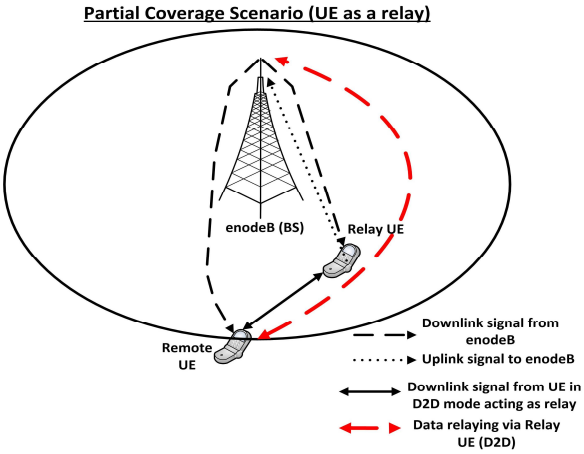

Fig 4. Partial coverage scenario with UE working as a relay

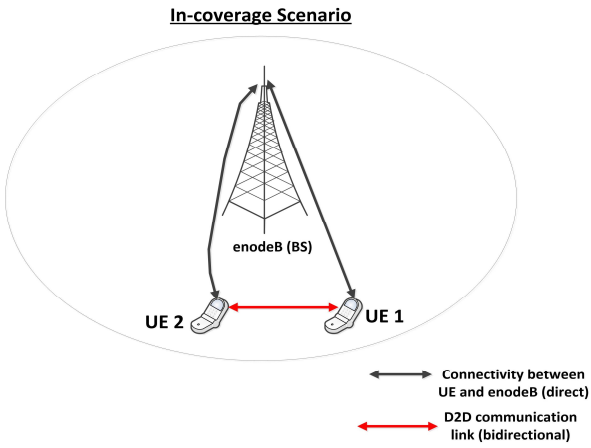

Fig 5. In-coverage scenario with two UEs in proximity to each other can connect directly via D2D connectivity

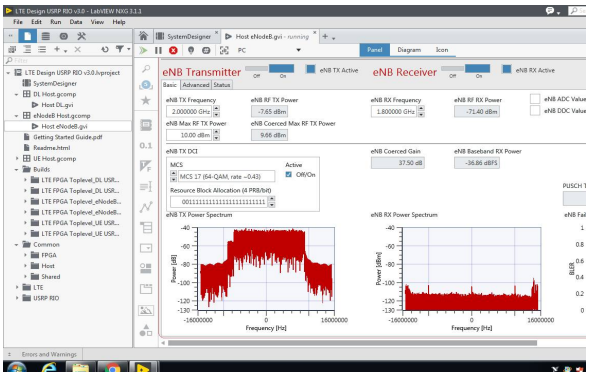

Fig 6. eNodeB GUI showing signal transmission and reception power spectrum

ACKNOWLEDGMENT

The work has been carried out as part of the project 'Flexible Testbed for Device-to-Device Communication in 5G Cellular Network', funded by Higher Education Commission, Pakistan under Grant No. 6054, National Research Program for Universities (NRPU), 2016.

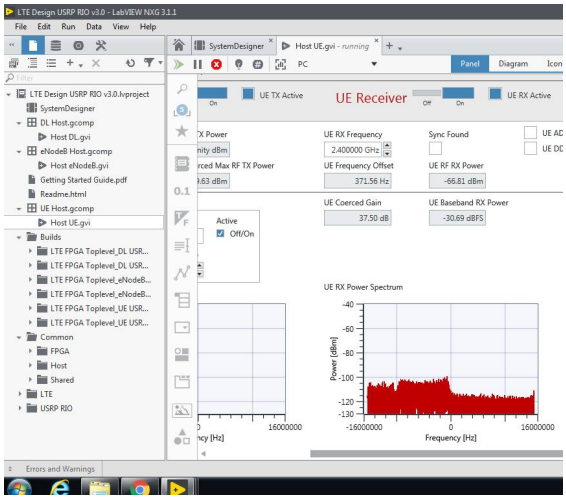

Fig 7. UE GUI showing received signal power spectrum

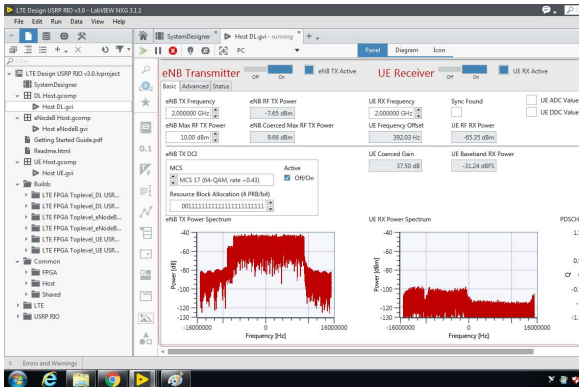

Fig 8. GUI showing a basic Downlink connection of eNodeB and UE

REFERENCES

[1] "Cisco Visual Networking Index 2017-2022," February 2019.

[2] Ericsson, "Ericsson Mobility Report," June 2019.

[3] K. Doppler, M. Rinne, C. Wijting, C. Ribeiro, and K. Hugl, "Device-to-device communication as an underlay to LTE-advanced networks," Comm. Mag., vol. 47, pp. 42-49, 2009.

[4] 3GPP, "3GPP Release 12," 2015.

[5] D. Astely, E. Dahlman, G. Fodor, et al, "LTE release 12 and beyond", IEEE Communications Magazine, vol. 51, pp. 154-160, 2013.

[6] X. Lin, J. G. Andrews, A. Ghosh, et al, "An overview of 3GPP device-to-device proximity services," IEEE Communications Magazine, vol. 52, pp. 40-48, 2014.

[7] X. Shen, "Device-to-device communication in 5G cellular networks," IEEE Network, vol. 29, pp. 2-3, 2015.

[8] F. Boccardi, R. W. Heath, A. Lozano, et al, "Five disruptive technology directions for 5G," IEEE Communications Magazine, vol. 52, pp. 74-80, 2014.

[9] G. Fodor, E. Dahlman, G. Mildh, et al., "Design aspects of network assisted device-to-device communications," IEEE Communications Magazine, vol. 50, pp. 170-177, 2012.

[10] A. Asadi, Q. Wang and V. Mancuso, "A Survey on Device-to-Device Communication in Cellular Networks," in IEEE Communications Surveys & Tutorials, vol. 16, no. 4, pp. 1801-1819, Fourth quarter 2014.doi: 10.1109/COMST.2014.2319555.

[11] H. Mariam, M. I. Aslam, I. Ahmed, "Device-to-Device Communication in Cellular Networks: A Survey", International Conference on Emerging trends in Telecommunication and Electronics Engineering, Karachi, Pakistan, February 27 - 28, 2018.

[12] A. Moraleda-Soler, B. Coll-Perales, and J. Gozalvez, "Link-aware opportunistic D2D communications: Open source test-bed and experimental insights into their energy, capacity and QoS benefits," in 2014 11th International Symposium on Wireless Communications Systems (ISWCS), 2014, pp. 606-610.

[13] V. K. Singh, H. Chawla, and V. A. Bohara, "Measurement results for direct and single hop device-to-device communication protocol," in 2016 International Conference on Advances in Computing, Communications and Informatics (ICACCI), 2016, pp. 2515-2520.

[14] M. Chung, M. S. Sim, D. K. Kim, et al, "Compact Full Duplex MIMO Radios in D2D Underlaid Cellular Networks: From System Design to Prototype Results," IEEE Access, vol. 5, pp. 16601-16617, 2017.

[15] F. Peng, S. Zhang, S. Cao, and S. Xu, "A Prototype Performance Analysis for V2V Communications using USRP-based Software Defined Radio Platform," in 2018 IEEE Global Conference on Signal and Information Processing (GlobalSIP), 2018, pp. 1218-1222.

[16] T. Balan, A. Balan, and F. Sandu, "SDR Implementation of a D2D Security Cryptographic Mechanism," IEEE Access, vol. 7, pp. 38847-38855, 2019.

[17] S. Jain, Y. Zhang, and L. A. J. a. p. a. DaSilva, "LTE Standard-Compliant D2D Communication: Software-defined Radio Implementation and Evaluation," 2019.

[18] A. Asadi and V. Mancuso, "Network-Assisted Outband D2D-Clustering in 5G Cellular Networks: Theory and Practice," IEEE Transactions on Mobile Computing, vol. 16, pp. 2246-2259, 2017.

[19] M. Engelhardt and A. Asadi, "The first experimental SDR platform for inband D2D communications in 5G," in 2017 IEEE 25th International Conference on Network Protocols (ICNP), 2017, pp. 1-2.

[20] A. Ortiz, A. Asadi, M. Engelhardt, et al, "CBMoS: Combinatorial Bandit Learning for Mode Selection and Resource Allocation in D2D Systems," IEEE Journal on Selected Areas in Communications, vol. 37, pp. 2225-2238, 2019.

2020 5th International Electrical Engineering Conference (IEEC 2020)
Feb, 2020 at IEP Centre, Karachi, Pakistan

Case Study for Solar Cooling System using Hybrid Multijunction PV and CST Technology

Muhammad Shahram[1] and Tariq Javid[2]

[1] Graduate School of Engineering Sciences & Technology
[2] Faculty of Engineering Sciences & Technology
Karachi, 74600, Pakistan
muhammadshahram67@gmail.com, tariq.javid@ hamdard.edu.pk

Abstract: Presently, the solar energy is a promising solution among existing renewable energy resources. The energy still needs an adequate amount of change by improve the efficiency of either photo voltaic (PV) or concentrated solar thermal side (CST). This paper proposes a management enhancement for both PV and CST for the solar cooling system. The study is based on the existing infrastructure on which data monitoring and analysis is performed. The PV system provide 35kw of power to drive electrical chiller during day time while the concentrated solar provide 35kw energy to drive absorption chiller during the night time. The multijunction solar cell concept is used to improve the efficiency of the solar panel. The GaInP/GaAs/Ge material is used in multijunction solar cell for better utilization of solar spectrum as these material have wider band gap. Sand is use as a heat storage material in concentrated solar side to raise the temperature up to 1000 degree centigrade. The purposed solution working day and night during the day time PV drive the electrical chiller to fulfill the requirement while CST storage heat in a large storage tank use in night to drive the cooling system. The simulation managing both sources showed a significant energy fit to the cooling load reaching a peak during the summer days. The output result shows that the proposed solution Environment Friendly, Economical and Working day and Night.

Keywords: Hybrid solar, concentrated solar technology, multijunction PV cell, heat storage material, solar cooling, absorption chiller.

I. INTRODUCTION

Developing countries like Pakistan are most concerned about energy crises, global warming, climate change and heat up of the environment. The country energy policies encourage using renewable energy technologies to overcome related crises and reduce use of fossil fuels; and subsequent results for pollution minimization and clean green environment. Most of studies in the research literature rate the climate change as having the major impact on the energy demand. As in hot days, lot of energy is consumed in the cooling purpose. Therefore, cooling have a lot of impact due exhaust of harmful gases severely affecting the environment.

As technology advances in thermal solar generation, it couples with the need for more renewable sources of energy, thereby increasing the interest in concentrating solar thermal power. Concentrating solar thermal power concentrates the sunlight onto a heat transfer fluid (HTF) which is then used to drive the steam turbine [1]. The concentrating solar power (CSP) can both generate and store renewable energy, all in one plant. For store solar energy use the molten salt power tower; and use the heat exchanger to store the energy in a molten salt tank [2]. As the technology of thermal solar power increase CSP use for cooling purpose and drive cooling chiller by using thermal heat of sun for this purpose ammonia-water compression-absorption cooling system have been used [3].

A solar heat storage tank have been added with the adsorption cooling system to enhance the efficiency and working time of the system. In this system lithium bromide solution have been used because ammonia is toxic. The chiller is started with silica gel-water single stage adsorption chiller is used [4]. The performance assessment comparison of solar thermal cooling system with the conventional plants. This provide more comprehensive investigation through a comparison of these two families of solar cooling system (with solar thermal and PV) thus the technology of electricity generation is better because it have less effect on environment and its efficiency is also good as compared to the conventional plant. This system have natural gas burner that feed the absorption chiller generator and improve the system assessment [5].

In this study performance, energy efficiency, cost competitive and global warming assessment of solar thermal and off-grid PV driven DC air conditioning and convention air conditioning system in a hot area. The first system is integrated solar thermal cooling system with the thermal heat of solar and drive chiller. This system consist of evacuated solar collector array which increase the efficiency of the air conditioning system, whereas the market available AC consume a lot of

energy [6]. Flat plate collector is used as it has good efficiency as compare to evacuate and other available concentrating sources.

Evaluation of solar thermal cooling system is performed in office building by selecting the six different cities of Saudi Arabia its most efficient, economical and reduce the peak load using flat plate collector [7], [8]. Low cost solid material is used to store and transport the energy and it raised the temperature up to 1000 degree Celsius; for the purpose of heat recovery, the particles can be discharge applying a moving bed heat exchanger to run a rankine cycle and store the heat in a system [9].

Photovoltaic (PV) technology has a number of distinct advantages over the conventional method of electricity. The high efficiency multijunction PV played a very significant rule in reducing the cost through concentrating PV system. The single junction solar cell is used and performed a comparison of solar energy absorption indium gallium arsenide indium phosphide and indium gallium antimonide base high efficiency solar cell have been produced[10], [11]. Recently the multijunction solar cell is produced with efficiency greater than 60 percent. The highest efficiency of solar cell have been obtain by using lattice match junction to harness as much of the sun energy [13].

A study is focused to find the less costly and most effective element to store the heat in a sand. Sand is a unique and eco-friendly alternative to store the heat. The oil is used to store the heat and collect the heat from the collector plate to the heat storage tank. In this system the concentrated solar thermal technique is used and flat plate collector is used to capture the solar thermal heat [14]. The hybrid design of solar collector is designed to purify the water and heating purpose by using solar thermal and electrical energy from the sun. This collector of electricity work during day time about 12 hours and during night time the storage heat of flat plate collector is used to fulfill the requirement [15].

A recent research on solar cooling system is to develop an appropriate solution for Dubai energy crises overcome. In this system the adsorption and absorption chiller is used which run with the thermal energy of the sun and evacuated tube collector is used to collect the energy. In the adsorption chiller water and silica gel solution is used; while in the absorption chiller lithium bromide and water solution are used to produce the cooling effect for a building. This system is useful for building cooling purpose as it reduces the water temperature through 22 degree Celsius [17]. By using this technique, a system is proposed (Fig. 1) to overcome the energy crises of Pakistan with environment friendly due lesser amount of toxic gases. In concentrated solar thermal side, flat plate collector is used; whereas multijunction solar cell is used in PV side to improve the efficiency.

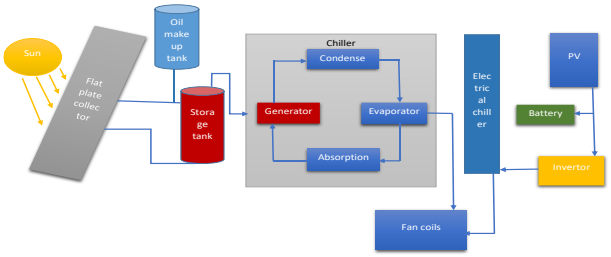

Fig. 1 The hybrid cooling system with PV and CST technology.

II. PROPOSED DESIGN

The objective of study of the proposed system is to create a cooling system which is environment friendly and yet provides acceptable cooling effect. An operational hybrid solution for 24x7 not producing too much toxic gases. The future works will compare the cooling effect of both the technology and improve the efficiency of both side PV and CST technology.

A. Novelty

The design proposed in this work is the addition of an electrical chiller that drives the solar panel and the multijunction solar cell to further improve the efficiency of existing technology. The use of sand as heat storage medium enable temperature of storage heat up to 1000 degree Celsius.

B. Benefits

During the summer days, a lot of energy is consumed toward building cooling. These energy generated by using expensive fuel and technology which put a burden on economy of any country. When these resources have a short fall or costly then energy crises is started; while on the other hand solar cooling system is cheap reliable and environment friendly, especially during summer days. Solar cooling system has many global benefits and impacts as ac air conditioned and other cooling devices generate radiations which have impact on life. These devices also increase in thermal temperature of the environment. Therefore, a solar cooling system is a good solution, especially for a developing country like Pakistan.

III. METHODOLOGY

A. Solar Thermal Cooling System

The solar cooling system is main research topic in this research work that uses 42 flat plate collector which drive 19kw double effect absorption chiller associated with a cooling tower. A storage tank is used to store the energy, drain and make up oil tank is also used. A sand-bed is used to store energy, pump used to circulate the oil from sand bed to the flat plate collector. There are two phase of sand; one is charging phase and another is discharging at first sand reached to its desire temperature after that it start discharged. At day time cold oil is passed from flat plate collector and heat is stored in sand by passing it from heat exchanger and during the night time the storage energy of sand is consumed by circulating the cold oil from the oil tank and hot water through this storage of heat [14] (Fig. 2). By using this process absorption chiller is drove to consume (water and lithium bromide) solution and produce cooling effect for the building.

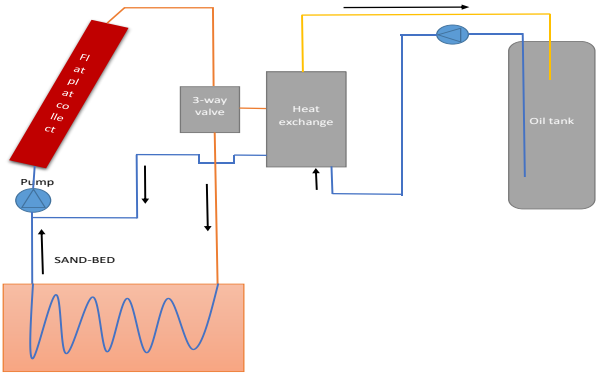

Fig. 2 The Solar Thermal Cooling System.

B. Photovoltaic Side

In photovoltaic side, multijunction solar cells are used to improve the efficiency of photovoltaic module [13]. Multijunction solar cells direct sunlight towards matched spectral sensitivity by splitting the spectrum into small slices. In [10], multijunction solar cells are used in which first layer have high band gape energy and blue in colour and second have less then first and yellow in colour and last have red in colour and absorb less radiation (Fig. 3).

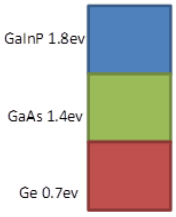

Fig. 3 j-v characteristics: V = Vtop + Vmid + Vbot, J = min(Jtop, Jmid, Jbot).

IV. CONCLUSION

This study has primary focus on power generation from solar thermal technology and integrating both the PV technology and concentrated solar thermal toward building a cooling system. The existing design is extended by introduction of electrical chiller to drive solar panel multijunction solar cells and sand to store heat. The proposed design has been developed by adding the electrical cooling system working parallel with the thermal solar cooling system powered by the PV plant to take advantage of both technologies. The PV plant work in day time and CST system work with absorption chiller and store thermal power in storage system which work day and night. In future, the proposed design is converted into a computer simulation as an intermediate step toward prototype development.

REFERENCES

[1] R. Sioshansi and P. Denholm, “The value of concentrating solar power and thermal energy storage,” IEEE Transactions on Sustainable Energy, vol. 1, no. 3, pp. 173-83, 2010.

[2] RI. Dunn, PJ. Hearps, and MN. Wright, “Molten-salt power towers: newly commercial concentrating solar storage,” Proceedings of the IEEE, vol. 100, no. 2, p.504-15, 2011.

[3] Z. Qiu, Y. Gong, H. Li, and W. Ma, “Studies on an Ammonia-Water Compression-Absorption Cooling System (CACS) Drived by Solar Energy,” *IEEE International Conference on Computer Distributed Control and Intelligent Environmental Monitoring*, pp. 1319-1322, 2011.

[4] RA Rouf, KA. Alam, MH. Khan, BB. Saha, and II. El-Sharkawy, “Performance Analysis of Solar Adsorption Cooling System-Effect of Position of Heat Storage Tank,” Appl. Appl. Math., special issue no. 2, pp. 52-68, 2016.

[5] M. Beccali, M. Cellura, P. Finocchiaro, F. Guarino, S. Longo, and B. Nocke, “Life Cycle Assessment performance comparison of small solar thermal cooling systems with conventional plants assisted with photovoltaics”, Energy Procedia, vol. 30, pp. 893-903, 2012.

[6] AH. Ali and AN. Alzaed, “Residential scale solar driven cooling systems versus conventional air-conditioning in hot arid areas: a comparative study,” Materials Physics and Mechanics, vol. 32, no. 1, p. 21-30, 2017.

[7] BL. Gupta, N. Jha, D. Vyas, and A. Daiya, "Performance analysis of solar thermal cooling system for an office building in Indian climates using flat plate collector," International Journal of Engineering and Techniques, vol. 3, no. 4, pp. 36-40, 2017.

[8] MT Linjawi, Q. Talal, and FA. Al-Sulaiman, "Evaluation of solar thermal driven cooling system in office buildings in Saudi Arabia," *E3S Web of Conferences, World Renewable Energy Congress*, vol. 23, p. 05001, 2017.

[9] L. Qoaider, Q. Thabit, and S. Kiwan, "Performance assessment of a Moving-Bed Heat Exchanger with a sensible heat transfer medium for solar central receiver power plants," *The 8th IEEE International Renewable Energy Congress*, pp. 1-5, 2017.

[10] I. Bhattacharya and SY. Foo, "Indium phosphide, indium-gallium-arsenide and indium-gallium-antimonide based high efficiency multijunction photovoltaics for solar energy harvesting," *The 1st Asia Symposium on Quality Electronic Design*, pp. 237-241, 2009.

[11] S. Kibaara, S. Chowdhury, and SP. Chowdhury, "Analysis of cooling methods of parabolic trough concentrating solar thermal power plant," *IEEE International Conference on Power System Technology (POWERCON)*, pp. 1-6, 2012.

[12] K. Hinzer, MN. Beattie, MM. Wilkins, and CE. Valdivia, "Modeling techniques for multijunction solar cells," *IEEE International Conference on Numerical Simulation of Optoelectronic Devices (NUSOD)*, pp. 133-134, 2018.

[13] R. Núñez, M. Victoria, S. Askins, I. Antón, C. Domínguez, R. Herrero, and G. Sala, "Spectral impact on multijunction solar cells obtained by means of component cells of a different technology," IEEE Journal of Photovoltaics, vol. 8, no. 2, pp. 646-53, 2018.

[14] S. Haggag, G. Ibrahim, A. Katsikogiannis, A. Tesh, H. Kamal, N. Menezes, and R. Al-Nuaimi, "Experimental study of solar thermal energy storage in sand system," The 4th IEEE International Conference on Engineering Technologies and Applied Sciences (ICETAS), pp. 1-6, 2017.

[15] J. Grandidier, BJ. Nesmith, TJ. Hendricks, MB. Petach, E. Tward, SA. Whitney, J. Cepeda-Rizo, JP. Garcia, ME. Devost, H. Hayden, and N. Fette, "Full spectrum hybrid photovoltaics and thermal engine utilizing high concentration solar energy," *IEEE 43rd Photovoltaic Specialists Conference (PVSC)*, pp. 0563-0565, 2016.

[16] RD. Salim, "Manufacturing Procedure of a Hybrid Design of Solar Collector (Sterilization and Water Heating) By Solar and Electrical Energy, IEEE International Conference on Advanced Science and Engineering (ICOASE), pp. 353-356, 2018.

[17] M. Almahmood and A. Odeh, "Modeling of solar thermal cooling system in Hatta-Dubai," IEEE 5th International Conference on Renewable Energy: Generation and Applications (ICREGA), pp. 250-255, 2018.

2020 5th International Electrical Engineering Conference (IEEC 2020)
Feb, 2020 at IEP Centre, Karachi, Pakistan

An Empirical Study of Face Recognition for Occluded and Low-Resolution Images

Muhammad Ibrahim Syed[1], Mehreen Mubashar[1], Muhammad Waqas Zeb[2], Aiman Tahir[1], Nazeer Muhammad[3], and Zahid Mahmood[1*]

[1]Department of Electrical and Computer Engineering, COMSATS University Islamabad, Abbottabad, Pakistan.
[1]{muhammadisyed, mehreenmubashar, aimantahir19}@gmail.com, [1*](zahid0987@cuiatd.edu.pk)

[2]Department of Computer Science, Barani Institute of Management Sciences, Rawalpindi, Pakistan.
[2](zebwaqas892@gmail.com)
[3]Department of Mathematics, COMSATS University Islamabad, Wah Campus, Pakistan.
(nazeermuhammad@ciitwah.edu.pk)
* Corresponding author

Abstract: Human faces that appear in multimedia applications, for instance digital entertainments are exposed to substantial variations in pose, face image resolutions, and occlusions. Recent research also targets to achieve reliable and robust face recognition under aforementioned issues. This paper presents an experiential study of three recently developed face recognition methods on challenging LFW dataset. Our simulations indicate that for 15×15 pixels and up to 256×256 pixels face image, the local binary pattern histogram based face recognition algorithm, which is integrated with haar-cascade classifiers yields the highest recognition accuracy across frontal (0°), ±35°, and +45° of pose variations. In addition, for three different occlusions, the aforementioned algorithm also surpasses the compared algorithms in terms of recognition accuracy. The weighted kernel sparse representation based recognition algorithm was observed to be near real-time. The context aware local binary feature learning based algorithm was found to be most computational expensive among the compared algorithms.

Keywords: Face Recognition, Face Pose, Recognition Rate.

I. INTRODUCTION

One of the active areas used in face technology is to recognize the face, which is achieved through facial features, for instance nose, mouth, eye structure, and cheeks. Two well-known categories in face recognition are identification and recognition [1]. A person's facial appearance gradually changes over time, which leads to age-related inclusions, for instance wrinkles that constitutes crucial challenges. Existing Face Recognition (FR) systems report good accuracy in controlled situations. However, their performance lowers in conditions, such as occlusion or image resolution variation [2]. Similarly, recognizing facial expressions is also a challenging task in applications, such as identifying applications and security [3]. Many FR algorithms published recently, for example, [1],[2], and [3] aim to solve a specific problem, for instance occlusion or expression [4]. This paper aims to present a study of recently developed three FR methods on challenging LFW database. Particularly, the paper focuses to present a comparative study on face pose, low-resolution, and execution time. Main contributions in this study are highlighted below.

- We present a comparative study of three recently developed FR algorithms on two challenging issues, which are face pose and occlusion. In our experiments, we investigate four different face poses, which are 0^0, $\pm35^0$, and $+45^0$. Moreover, we also consider face image resolution for each pose, which are 256×256, 125×125, 50×50, 30×30, 20×20, and 15×15 pixels.
- We investigate complex and challenging occlusions present in facial images provided in the LFW dataset along with huge variety of image resolution and pose to authenticate the strength of the developed FR algorithm.
- We are optimistic that this study will be beneficial for future face recognition algorithms to be deployed in specific scenarios.

The paper is organized as follows. Section II presents recent advances in face recognition. While, Section III briefly describes the compared FR algorithms in this study. Simulation results are discussed in Section IV along with critical discussion. Finally, conclusions are drawn in Section V with hints for possible future research directions.

II. RELATED WORK

This section briefly reviews new developments in face recognition. In [5], researchers present robust techniques for facial recognition in complex backgrounds. The proposed technique mainly consists

of algorithms based on Adaboost, PCA, and cascade classifier. In [6], proposed Multimodal Deep Face Representation (MM-DFR), involves two main steps, which are multimodal feature extraction using 8 CNNs and the features merging using sparse autoencoder. In [7], a technique based on Local Binary Pattern (LBP) had been proposed for reliable face recognition. Whereas in [8], researchers introduce a modified LBP method, which is inspired from local texture descriptors and ternary patterns that yield high discrimination. Appearance based approaches are categorized as either non-linear or linear methods. In [9], the researchers implement face recognition by integrating the LDA and the PCA. In particular, the researchers implemented kernel principle component analysis (KPCA), which creates a model of the human face that robustly captures facial variations. In [10], a novel pose aware model is developed to analyze a face by employing several pose specific, Deep Neural Networks (DNN). In [11], the researchers attempted to introduce an algorithm for Pose-Invariant (PI) by creating a dense network of 3D facial benchmarks that are projected on every 2D face pattern. Also, the algorithm involved the homography to rectify texture deformation due to pose changes.

In [12], the researchers propose a technique to create a composite feature vectConor for face recognition using discriminant analysis. In [13], panoramic image-based algorithm is implemented, which results in less complexity and low computational cost. In [14], a DCNN based on Independent Component Analysis (ICA) filters is implemented for the purpose of facial recognition. In [15], the authors present the theoretical analysis of feature pooling and how feature pooling is efficient in the cases of image transformations and noise. In [16], a technique based on sparse representation is introduced that helps in solving the two problems, **(a)** feature extraction and **(b)** robustness against occlusion. In [17], the researchers enhance the performance of the technique based on sparse representation by employing the L0-normalization, that helps in high classification performance. In [18], the researchers introduced kernel sparse representation (KSR), that helps in reducing the quantization error and enhances the sparse coding performance. In [19], a new technique for restoring the occluded images to increase the performance of the face recognition algorithms is presented by using inpainting based methods. In [20], a modified form of sparse representation is developed that helps in occluded face recognition by partitioning the face image into four blocks and then applying representation on it. This results in significant increase in the performance of face recognition algorithm.

III. FACE RECOGNITION ALGORITHMS

This section briefly describes the compared face segmentation algorithms.

A. Context Aware Local Binary Feature Learning (CA-LBFL) Based FR Algorithm

This method focuses to make efficient use of contextual information of neighboring bits to make face representation more robust. The FR is achieved by making the adjacent bits nearly alike by restraining the shift in the summation of bits. This limitation enables the descriptor to be stable even if there exist a small change in original code. The aforementioned criteria aids in learning of binary codes, which are capable of suppressing noise without hurting the uniqueness of binary code. In the CA-LBFL methodology the first step was the extraction of Pixel Difference Vectors (PDVs) locally. These PDVs were then mapped into binary vector by applying a learned *k*-hash mapping functions in an unsupervised approach on each pixel. Formation of this projection matrix is an optimization problem with the objective function as described in Eq. (1).

$$min_W\ J = J_1 + \lambda_1 J_2 + \lambda_2 J_3 + \lambda_3 J_4$$
$$min_W\ J = tr(((AB)^T(AB) - I_N)^2 + \lambda_1 \left|\left|(B - 0.5) - W^T X\right|\right|_F^2 + \lambda_2 \left|\left|(B - 0.5) I^{NX1}\right|\right|_F^2 - \lambda_3\, tr(B - U)^T (B - U)$$
$$B = 0.5 \times (sgn W^T X + 1) \quad (1)$$

where N shows PDVs that are obtained from the original images, μk represents mean of the k[th] bit of N Pixel Difference Vector (PDV)s, λ1, λ2, λ3 are three parameters to balance the weight of parameters, and B and W are optimized by iterative approach.

After that, they generated a codebook by using *k* mea n clustering method on the extracted context aware bina ry codes. Finally, the entire image was represented by a histogram feature. The final recognition was done using nearest neighbor classifier. Complete details of this algo rithm can be seen in [21].

B. Weighted Kernel Sparse Representation (WKSRC) Based FR Algorithm

In the WKSRC, each input face image is plotted into kernel feature space followed by dimension reduction. Later a matrix that contains the similarity between the probe and gallery samples is produced by Multi-Scale Retinex (MSR). The MSR is the weighted sum of different Single Scale Retinex (SSR) as shown in Eq. (2).

$$R_i(x, y) = \log[I_i(x, y)] - \log[F(x, y) * I_i(x, y)] \quad (2)$$

Where $F(x, y)$ represents the surround function, $I_i(x, y)$ represents the image spreading in the i^{th} spectral band, and * represents the convolution procedure. The final output of the MSR is shown in Eq. (3).

$$R_{MSR_i} = \sum_{k=1}^{k} w_k R_{ki} \quad (3)$$

where *k* is the number of scales, R_{ki} is the i^{th} factor of the k^{th} scale, and w_k is the associated weight in a scale. To obtain an effective vector, the WKSRC converts I_1-minimization problem into the weighted

I_1-minimization problem in kernel feature space. Complete details of this algorithm can be seen in [22].

C. Haar-Cascade Classifiers and Local Binary Pattern Histogram (LBPH) Based Face Recognition Algorithm

The LBPH algorithm consists of face detection and recognition steps. Initially, Haar-cascade classifier is used to locate the face. The Haar-cascade classifier works with very high efficiency and accuracy. Haar features are equivalent to convolution kernels to detect existence of the of the relevent features. Once a face is located in the input image, the LBPH is used to find and identify the characteristics feature of the image. The LBPH extracts faces by comparing pre-processed data with training dataset. Facial feature extraction is carried out by the image generator. For that purpose, an intermediate image is generated from the input image to describe the original image in an intangible way by emphasizing the facial features of the image.

To implement this, a sliding window is used which represents the image in the matrix form, that helps in generating an intermediate image. The intermediate image is then used for extracting the histogram of the image in terms of extracted face features. The extracted histogram is equated with histograms of all images deposited in the gallery database to return the face with the contiguous histograms match. Complete details of the algorithm can be seen in [23]. For readers' easy understandings, we denote the CA-LBFL as *Algorithm A*, the WKSRC as *Algorithm B*, and LBPH as *Algorithm C* in rest of the paper.

IV. SIMULATION RESULTS

To run simulations, we select intel core-i7 workstation with 16 GB of RAM. The MATLAB 2018 is used to execute simulations on publicly available LFW face dataset.

LFW Database [28, 29]: This database contains over 13000 images of 5749 different people. This dataset contains images with diverse poses and illuminations as depicted in Fig.1. In the experiments, from each set frontal images are used for training and the four different pose images and occluded images as shown in Fig.1(a)-(b) are selected for testing. The CMU-Multi-PIE database [24] contains face images with systematic pose variations. Therefore, in our work to analyze the pose accurately, we aligned the LFW database images with Multi-PIE database to achieve the correct face pose.

A. Pose Analysis

We perform detailed experiments for the four different poses to observe the recognition accuracy of each algorithm as shown in Table 1. From Table 1, important observations are listed below.

- On the LFW database, highest recognition accuracy of 35.06% is observed for frontal images (0^0) followed by $+35^0$ and -35^0, respectively. The accuracy for $+45^0$ is found to be least due to its large face deviation from frontal.
- For high face image resolution, such as 50×50 pixels and above and for $+45^0$ of face pose, the *Algorithm C* yields the highest recognition rate of 64.30%.
- For low face image resolution, such as 30×30 pixels and below, the *Algorithm A* is unable to identify any pose across entire range of face image resolution.
- An interesting observation is that for same and opposite face pose, such as $+35^0$ and -35^0, the face recognition accuracy of each algorithm is not same.

B. Occlusion Analysis

In our work, we investigate three different occlusions, which are black eye glasses, mic in front of face, and hand in front as shown in Fig. 1(b). Since occlusion decreases face features that are later used by recognition algorithms to recognize a face. Therefore, in our work to analyze the effects of occlusions on the performance of face recognition algorithms, we use a standard 256×256 pixels face image. Table 2 summarizes the occlusion results. From Table 2, important observations are highlighted below.

- For all the occlusions shown in Fig. 1(b), the *Algorithm C* comprehensively outperforms the compared algorithms on the LFW database. For eye glasses category of occlusion, the *Algorithm A* yields 34.2801% recognition accuracy followed by *Algorithm B* that yields 29.80% recognition accuracy.
- For hand occlusion category of occlusion, the *Algorithm B* yields the least recognition accuracy of 26.3416% followed by *Algorithm A* that yields 30.1210% recognition accuracy.
- For mic in front of face occlusion category, again the *Algorithm C* beats the compared algorithms by yielding 74.6600% recognition accuracy followed by *Algorithm A*, which yields 36.36% recognition accuracy. The performance of the *Algorithm B* is found to be least on mic occlusion category with 33.45% recognition accuracy.
- For minor occlusion, such as transparent eye glasses shown in 2nd image in top row of Fig. 1(b), all the three compared algorithms yield over 78% recognition accuracy. However, for major occlusions, such as dark eye-glasses, the recognition accuracy is below 70% for the three compared schemes. For such situations, *Algorithm B* has very low recognition accuracy of below 30%.

Among the three investigated occlusions, the mic occlusion category has the highest recognition accuracy of 48.1566% recognition accuracy, followed by eye glasses occlusion category, which has 44.2152% accuracy. The hand in front of the face category yielded the lowest recognition rate in our experiments. This might be due to the loss of key face features, such as chin region.

C. Discussion

Although the aforementioned section highlighted important observations during the execution of complex face recognition task. However, discussion below sheds

(+45°) (+35°) (0°) (-35°)

(a) Pose Description

(non-occluded face image) (occlusion with glasses) (occlusion with mic) (Occlusion with hand)

(b) Occluded Images

Fig. 1 Sample images from LFW database, **(a)** Pose image, **(b)** Occluded Images

Table 1 Performance analysis of pose variation

Face Image Resolution Category	Algorithm	Image Resolution (in pixels)	Recognition Accuracy (%) And Execution Time on LFW database (sec)				
			$+45^0$	$+35^0$	0^0(Frontal)	-35^0	Average Recognition Rate
High Face Image Resolution	A	256×256	30.4300	39.4715	51.2914	29.6014	37.6985
	B		42.8372	37.5000	57.5064	32.8504	42.6735
	C		64.3083	75.6010	83.4011	73.8063	74.2791
	A	125×125	8.6914	21.0147	31.7031	20.7023	20.5278
	B		13.5426	26.6439	37.8714	26.2014	26.0648
	C		56.7548	67.4047	81.6786	66.8500	68.1720
	A	50×50	8.2323	5.2604	14.8765	6.4040	8.6933
	B		10.5650	12.4970	22.8514	11.5124	14.3564
	C		51.4501	61.6700	78.6545	60.6144	63.0972
Low Face Image Resolution	A	30×30	0.0000	0.0000	0.0000	0.0000	0.0000
	B		9.1895	10.5214	14.1109	10.2122	11.0085
	C		39.6707	45.5547	61.5509	44.66	47.8590
	A	20×20	0.0000	0.0000	0.0000	0.0000	0.0000
	B		6.1205	6.4500	8.6114	6.3210	6.8757
	C		28.5690	36.5711	48.6701	36.1201	37.4825
	A	15×15	0.0000	0.0000	0.0000	0.0000	0.0000
	B		3.2400	5.2152	7.7714	5.9900	5.5541
	C		15.6773	21.6904	30.5312	20.5015	22.1000
Whole Average			**21.6265**	**26.2814**	**35.0600**	**25.1304**	–

Table 2 Occlusion analysis

Face Image Resolution Category	Algorithm	Image Resolution (in pixels)	Recognition Accuracy (%) on LFW database to handle occlusion		
			Glasses	Hand	Mic
High Face Image Resolution	A	256×256	34.2801	30.1210	36.3600
	B		29.8240	26.3416	33.4500
	C		68.5417	61.5792	74.6600
Whole Average			**44.2152**	**39.3472**	**48.1566**

For low face image resolution of 50×50 pixels and above, the *Algorithm C* yields the highest recognition rate of 74.275% for 256×256 pixels input face image for entire range of face pose from frontal to 45^0.

- For all the three occlusions compared above, the mean recognition accuracy was found to be 43.9063%, which is far below than 50%. Therefore, future work could also investigate to handle the aforementioned occlusions on the LFW database.
- Authors of *Algorithm A* originally tested their algorithm on You Tube Face (YTF) database. In their work, they report nearly 80% recognition accuracy. However, the recognition accuracy of *Algorithm A* on dropped below 40% on the LFW database for variation in pose, image resolution, and occlusions.
- Authors of *Algorithm B* originally tested their algorithm on Yale and AR databases. In their work, they report nearly 90% recognition accuracy. However, the recognition accuracy of *Algorithm B* on dropped below 45% on the LFW.
- Authors of *Algorithm C* originally tested their algorithm on their own developed small database to identify human faces and genders. Our study finds this algorithm to achieve the highest recognition accuracy of 74.2791% on whole LFW database.

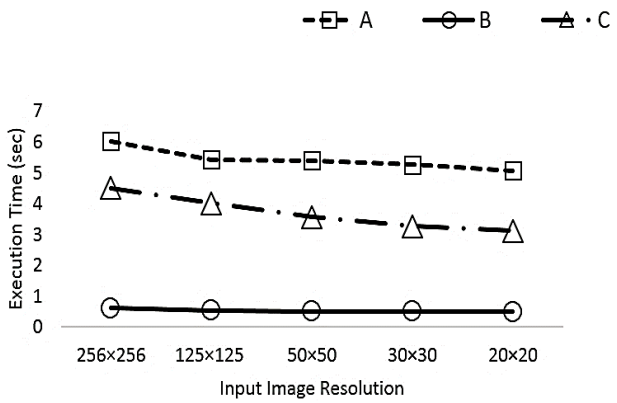

Fig. 2 Execution time comparison

- For all the compared face recognition algorithms, we observe the significant drop in accuracy of compared algorithms face recognition on the LFW database. We observe that substantial drop is due to the fact that the LFW database contains huge variations, such as inter-class, intra-class, illumination, and background variations.

D. Execution Time Comparison

We report the execution time as the time consumed to yield the recognition result for any test image. Fig. 2 shows the detailed comparison for the compared algorithms. Fig. 2 indicates that *Algorithm A* is most computationally expensive. For a standard 256×256 pixels face image, the *Algorithm A* consumes slightly over 6 seconds to yield the recognition result. Execution time of *Algorithm C* is also found to be higher for real-time applications as for 256×256 pixels face image, it consumes nearly 5 seconds. Therefore, in current study, the *Algorithm B* is found to be near real-time as it consumes less than 1 second across entire range of face resolutions from 256×256 pixels and down to 20×20 pixels to yield the output.

V. CONCLUSION

This paper presented an empirical study of three recently developed face recognition algorithms on challenging LFW dataset. The algorithms compared in this study are **(a)** context aware local binary feature learning, formally expressed as *Algorithm A*, **(b)** weighted kernel sparse representation, expressed as *Algorithm B*, and **(c)** local binary pattern histogram integrated with haar-cascade classifiers, expressed as *Algorithm C* in this paper. Our simulations revealed that for six different face image resolutions of 15×15, 20×20, 30×30, 50×50, 125×125, and 256×256 pixels face images, the *Algorithm C* yields the highest recognition accuracy across frontal (0^0), $\pm35^0$, and $+45^0$ of pose variations. In addition, for three different occlusions, which are glasses on face, hand in front, and mic in front of face, the aforementioned algorithm also surpasses the compared algorithms in terms of recognition accuracy. The *Algorithm B* was observed to be near real-time among the compared algorithms. Finally, the *Algorithm A* was found to be most computational expensive.

In the future, a real-time pose-invariant recognition algorithm could be developed with the ability to reliably recognize human faces with arbitrary pose variations [25]. To achieve this issue, pose normalization could be an effective tactic to preserve texture fidelity. Similarly, a cloud computing based [26] robust face recognition algorithm can be proposed to shift the burden of complex machine learning algorithms to cloud platform. To use a face recognition algorithm in outdoor environments for security situations, a robust image enhancement scheme [27, 30 31] can be induced to achieve high recognition rate in outdoor environments.

REFERENCES

[1] Z. Mahmood, N. Muhammad, N. Bibi, and T. Ali, "A review on state-of-the-art face recognition approaches," *Fractals*, Vol. 25, No. 2, 2017, pp. 1750025-1−1750025-19.

[2] M. Haq, A. Shahzad, Z. Mahmood, A. Shah, N. Muhammad, and T. Akram, "Boosting the Face Recognition Performance of Ensemble Based LDA for Pose, Non-uniform Illuminations, and Low-Resolution Images," *KSII Transactions on Internet and Information Systems*, 2019, Vol. 13, No. 6, pp. 3144−3164.

[3] Z. Mahmood, T. Ali, N. Muhammad, N. Bibi, I. Shahzad, and S. Azmat, "EAR: Enhanced augmented reality system for sports entertainment applications," *KSII Transactions on Internet and Information Systems*, Vol. 11, No. 12, 2017, pp. 6069−6091.

[4] Z. Mahmood, O. Haneef, N. Muhammad, and S. Khattak, "Towards a fully automated car parking system," *IET Intelligent Transport Systems*, 2018. DOI: 10.1049/iet-its.2018.5021.

[5] X. Zhang, T. Gonnot, and J. Saniie, "Real-Time Face Detection and Recognition in Complex Background,"*Journal of Signal and Information Processing*, 8, 2017, 99-112. https://doi.org/10.4236/jsip.2017.82007

[6] C. Ding and D. Tao, **"**Robust Face Recognition via Multimodal Deep Face Representation**",** *IEE Transaction on Multimedia*, vol.17, pp. 2049 – 2058, 2015.

[7] T. Ahonen, A. Hadid, and M. Pietikainen, "Face escription with local binary patterns: application to face recognition," *IEEE Trans. Pattern Anal. Mach. Intell.*, vol. 28, no. 12, pp. 2037-2041, 2006

[8] X. Tan, and B. Triggs, "Enhanced local texture feature sets for facerecognition under difficult lighting conditions," *IEEE Trans. Image Process.*, vol. 19, no. 6, pp. 1635-1650, 2010.

[9] S. Gayathri, R. priya and S. Valarmathy, "Face Recognition by Using Distance Classifier Based on PCA and LDA," *International Journal of Innovative Research in Science, Engineering and Technology*, 3(3), pp.1121-1126, 2014.

[10] I. Masi, F. Chan, J. Choi *et al*, "Learning Pose-Aware Models for Pose-Invariant Face Recognition in the Wild," *IEEE Transactions on Pattern Analysis and Machine Intelligence*, vol.41, pp. 379 – 393, 2018

[11] C. Ding and D. Tao**,** "Pose-invariant face recognition with homography-based normalization**",** *Elsevier pattern recognition*, vol.66, pp. 144-152, 2017

[12] S. Choi, S. Lee, and S. T. Choi, "Face Recognition Using Composite Features Based on Discriminant Analysis," *IEEE Access*, 6, 13663 – 13670, 2018. https://doi.org/doi: 10.1109/ACCESS.2018.2812725

[13] F. Liu, J. Guo, P. Liu, J. Lee and, C. Yao, "Panaromic Face Recognition," *IEEE Transactions on Circuits and Systems for Video Technology*, 8, 1864 –1874, 2018 https://doi.org/10.1109/TCSVT.2017.2693682.

[14] Y. Zhang, T. Geng, X. Wu, J. Zhou. and, J. Gao, "ICANet: A Simple Cascaded Linear Convolutional Network for Face Recognition," *Journal on Image and Video Processing*, 7, 119-211. ,2018

[15] Y. L. Boureau, J. Ponce, Y. L. Cun, "A theoretical analysis of feature pooling in visual recognition," *ICML*, 2010.

[16] J. Wright, A. Y. Yang, A. Ganesh, S. S. Sastry, *et al.*, "Robust face recognition via sparse representation," *IEEE transactions on pattern analysis and machine intelligence*, vol. 31, no. 2, pp. 210-227, 2009.

[17] Z. Fan, M. Ni, Q. Zhu, C. Sun, *et al.*, "L0-norm Sparse Representation Based on Modified Genetic Algorithm for Face Recognition," *Journal of Visual Communication and Image Representation*, vol. 28, 2015, pp. 15-20.

[18] S. Gao, I. W. H. Tsang, and L. T. Chia, "Kernel sparse representation for image classification and face recognition," in *European Conference on Computer Vision Computer Vision (ECCV 2010)*, ed: Springer, 2010, pp. 1-14.

[19] S. V. Khamele, S. G. Mundada "An approach for restoring occluded images for face-recognition," *Int J Adv Res Comput Commun Eng* 4(17):571–575, 2015

[20] S. Zhao, Z. P. Hu, "Double layers sparse representation for occluded face recognition," *Opt Int J Light Electron Opt* 126(21):3016–3019, 2015

[21] Duan, J. Lu, J.Feng, and J. Zhou, "Context-Aware Local Binary Feature Learning for Face Recognition", *IEEE Transactions on Pattern Analysis and Machine Intelligence*, Vol. 40, 2018, pp. 1139 – 1153.

[22] X. Liu, L. Lu, Z. Shen, K. Lu, "A novel face recognition algorithm via weighted kernel sparse representation", *Future Generation Comput. Syst.*, 2016

[23] K. Shrivastava, S. Manda, P. S. Chavan, T. B. Patil, S. T. Sawant-Patil. "Conceptual model for proficient automated attendance system based on face recognition and gender classification using Haar-Cascade, LBPH algorithm along with LDA model. International," *Journal of Applied Engineering Research. 2018;10:8075-8080.*

[24] Z. Mahmood, T. Ali, and S. U. Khan, "Effects of pose and image resolution on automatic face recognition," *IET Biometrics*, 2016, Vol. 5, No. 2, pp. 111−119.

[25] S. N. Khan, N. Muhammad, S. Farwa, T. Saba, S. Khattak, and Z. Mahmood, "Early CU Depth Decision and Reference Picture Selection for Low Complexity MV-HEVC," *MDPI Symmetry*, 2019, Vol. 11, No. 454, pp. 1−24.

[26] Z. Mahmood, N. Bibi, M. Usman, U. Khan, and N. Muhammad, "Mobile cloud based framework for sports applications," *Multidimensional Systems and Signal Processing*, 2019, doi.org/10.1007/s11045-019-00639-6.

[27] Z. Mahmood, N. Muhammad, N. Bibi, Y. Malik, and N. Ahmed, "Visual enhancement of human observatory system using multi-scale retinex," *Elsevier Informatics in Medicine Unlocked*, 2018, doi: 10.1016/j.imu.2018.09.001.

[28] F. Munawar, U. Khan, A. Shahzad, M. Haq, Z. Mahmood, S. Khattak, and G. Z. Khan, "An Empirical Study of Image Resolution and Pose on Automatic Face Recognition," *16th International Bhurban Conference on Applied Sciences & Technology* (*IBCAST*), 2019, pp. 558−563.

[29] O. Haneef, S. Maqbool, F. Siddique, Z. Mahmood, S. Khattak, and G. Z. Khan, "Effects of Image Resolution on Automatic Face Detection," 2nd *International Conference on Communication, Computing and Digital Systems (C-CODE)*, 2019, pp. 231−236.

[30] N. Muhammad, N. Bibi, A. Wahab**,** Z. Mahmood, T. Akram, S. Naqvi, H. Sook, and D. Kim, "Image de-noising with subband replacement and fusion process using bayes estimators," *Computers and Electrical Engineering*, 2018, Vol. 70, pp. 413-427.

[31] N. Muhammad, N. Bibi, A. Jahangir, and Z. Mahmood, "Image denoising with norm weighted fusion estimators," *Pattern Analysis and Applications*, 2018, Vol. 21, N0. 4, pp. 1013−1022.

2020 5th International Electrical Engineering Conference (IEEC 2020)
Feb, 2020 at IEP Centre, Karachi, Pakistan

A Comparative Study of CNN Based Vehicle License Plate Recognition Algorithms

[1]Waqar Ahmad, [1]Zaineb Shah, [2]Nazeer Muhammad, [3]Muhammad Waqas Zeb, [1]Syed Muhammad Ijlal Hussain, and [1*]Zahid Mahmood

[1]Department of Electrical and Computer Engineering, COMSATS University Islamabad Abbottabad, Pakistan.
[1]{waqarahmad3411, xainabshah, ijlalh}@gmail.com. [1*](zahid0987@cuiatd.edu.pk).
[2]Department of Mathematics, COMSATS University Islamabad, Wah Cantt, Abbottabad, Pakistan.
[2](nazeermuhammad@ciitwah.edu.pk)
[3]Department of Computer Science, Barani Institute of Management Sciences, Rawalpindi, Pakistan.
[3](zebwaqas892@gmail.com)

[1*] Corresponding author

Abstract: License Plate Recognition (LPR) is attracting huge interest in recent years for its active role in smart traffic management systems. Owing to its authenticity, several LPR algorithms have been developed, which consist of license plate location, character segmentation, and character recognition. In most cases the afore described three-step scheme yields satisfactory recognition performance in controlled environment. To address the uncontrolled challenge, we present a comparative study of two recently developed LPR algorithms, which are (a) CNN-RNN and (b) CNN-GRU based license plate recognition algorithms. Extensive simulations on the PKU dataset indicate that for high license plate image resolution of 80×40 pixels and above and low license plate resolution of 50×30 pixels and below, the CNN-RNN based LPR algorithms outperforms its companion algorithm in terms of recognition accuracy on all five categories of PKU dataset. While, CNN-GRU license plate recognition algorithm is computationally efficient. In addition, none of the algorithms achieve recognition on low license plate resolution of 15×15 pixels.

Keywords: Character Recognition, License Plate Recognition, Recognition Rate.

I. INTRODUCTION

Automatic License Plate Recognition (ALPR) has become an essential part of smart city development in developing countries. This is due to the fact that an ALPR plays an energetic role in several real-time applications, such as toll collection or parking lot access [1]. In literature, many sophisticated methods have published that address the challenges of license plates with blur, erased, broken, or rotated alphabets [2]. These challenges are common throughout the world in which people observe diverse vehicles and license plates around them. With the recent developments in transportation systems, the ALPR has attracted research community interest. Most of the developed algorithms work well under pre-set license plate image capture systems in controlled conditions. However, an ALPR is still a challenging task in open environments. This difficulty appears due to the diversity in character patterns, for instance different fonts, occlusion, or distortions along with complex backgrounds, such as general text in boards and non-uniform illuminations.

To address such limitations, we present a comparative study of license plate recognition on a PKU dataset, which has diverse variations, such as illumination variations at different day times along with multiple license plates that appear in the input images. Our contributions in this paper are listed below.

- We compare two recently developed license plate recognition algorithms [10], [23] on challenging PKU dataset. The PKU dataset has five distinct categories G1, G2, G3, G4, and G5 (PKU−G1~G5). Each category has diverse road conditions that significantly change the appearance of the license plates.
- We consider large number of license plates variations in our study. We investigate high license plate resolution and low license plate resolutions. In our work, high license plate resolution category contains 80×40, 100×40, 200×50 pixels license plates. While low license plate resolution category contains 50×30, 35×25, and 15×15 pixels license plates on PKU−G1 to G5 categories. To the best of our knowledge, none of the paper compares aforementioned resolutions.
- We believe that this study will be beneficial for the researchers to improve these algorithms in their specified license plate recognition applications.

The paper is organized as follows. Section II presents recent advances in license plate recognition. While, Section III briefly describes the ALPR algorithm presented in this paper. Simulation results are discussed in Section IV along with critical discussion. Finally, conclusions are drawn in Section V with directions for possible future research.

II. RELATED WORK

This Section briefly describes recent advances in the ALPR domain. In [3], authors proposed a novel 37-class CNN to detect the text in an image, and a plate/non plate binary class CNN is used to eliminate false positives. To recognise the characters in the detected licence plate RNN with LSTM is used. In [4], proposed ALPR-Net consists of multiple nets that extracts basic features through a multiscale network using a regression

2020 5th International Electrical Engineering Conference (IEEC 2020)
Feb, 2020 at IEP Centre, Karachi, Pakistan

model to locate and recognise license plates. In [5], authors introduced a scale invariant CNN and hierarchical based ALPR technique. The proposed method achieves slightly higher recognition accuracy than few compared works. In [6], proposed ALPR method is based on deep neural networks, which aims to solve the LAPR problem in real life images. In [7], proposed method uses LPR Convolution Neural Network (LPRCNN) to achieve robust recognition of blurred and obscured license plates. In [8], researchers tackle the problem of ALPR under different environment and weather conditions for high speed applications. This works uses Connected Component Analysis (CCA) to segment characters and four novel scale invariant features for character recognition. In [9], proposed ALPR method is based on Riesz fractional model that initially enhances image quality and to improve character recognition. In [10], an intelligent combination of CNN and GRU is introduced to boost the license plate recognition in outdoor conditions. In [11], a joint trained method aims to achieve simultaneous car license plate recognition. The proposed method extracts discriminative features of license plates through different layers used therein. In addition, the proposed method also enquires about area proposal network, an RoI pooling layer, perceptron's layers, and Recurrent Neural Networks (RNNs) for plate recognition. In [12], the ALPR algorithm is based on YOLO object detectors. This work trains a distinct CNN network for each ALPR stage. Finally, in character recognition phase, alphabets/digits are separately identified. In [13], authors combine CNN and RNNs to achieve robust license plate recognition. In [14], a YOLO object detector is used to recognize the license plates. A CNN is trained under different condition of license plate like changes in lightening conditions low resolution camera images etc. The author also uses data augmentation like flipping the characters inverted license plates, which achieve state-of-the-art accuracy.

In [15], the ALPR method is based on CNN and kernel-based ELM (KELM) classifier. This method uses CNN without fully connected layers and learns deep features of license plate characters in Chinese. In [16], proposed ALPR technique is based on multiple features extraction and their fusion that extracts Histogram of oriented gradients (HOG) and eight geometric features. In [17] propose ALPR achieves recognition mainly through segmentation. The localization of number plate, vehicle and determination of the vehicle type is performed by a fully Convolutional Network. In [18], proposed a three-step mechanism to detect and recognize license plates. i.e. detection by using a binary class CNN, character segmentation of upper-case alphabets (A-Z) and digits (0-9) and a 37 class CNN to recognize the characters. In [19], an ALPR algorithm is developed using Deep-CNN, which simultaneously extracts and classifies features. In [20], the proposed method consists of a CNN to locate license plates, which are then passed to Optical Character Recognition (OCR) system to achieve the final results. In [21], a two-stage ALPR scheme is presented. In the first stage, a weak Sparse Network of Winnows (SNoW) classifier extracts a set of candidate regions. In the second stage, these regions are filtered using a CNN. The license plates images that fail the primary test for license plate localization are further classified in order to understand the reasons for failure. In [22], the developed approach uses single CNN for character localization and recognition. This approach also processes the license plate image through the CNN. The last convolutional layer of CNN is connected to 8 branches of fully connected layers, which predict the 8 characters of the license plate.

Above described are the nice efforts to solve the license plate recognition problem. In next Section, we describe the ALPR algorithms that we implemented.

III. LICENCE PLATE RECOGNITION ALGORITHMS

This section briefly describes the compared license plate recognition algorithms.

A. CNN-RNN Based License Plate Recognition Algorithms

This algorithm uses a variant of 16-layers VGGNet. Every convolutional layer in this architecture is followed by the Batch Normalization Layer (BNL). The purpose of this normalization layer to boost the learning process the input provide to this architecture is not preprocessed. The image is resized to 240× 120 pixels. The output of this architecture is not used as the final output but this model is followed by RNN model, which has 36 hidden units for further sequencing. The sequences generated by the RNN model are shown in Eq. (1) ~ (2).

$$r(t) = h[r(t-1), w_k(t)], \quad (1)$$

$$o(t) = h[r(t-1), w_k(t)], \quad (2)$$

where $h(.)$ is sigmoid function, $r(t)$ and $o(t)$ are the hidden state and at time t the output of the recurrent layer and $w_k(t)$ is the embedding k^{th} predicted label. The training phase of CNN-RNN model is done using cross-entropy loss on the softmax of CNN. For parameter optimization gradient descent algorithm is used and a decreasing learning rate on each layer, which is $(\frac{0.1}{(10\times \text{epoch})})$ is used. The evaluation purpose of sequence labeling is to evaluate perfectly predicted labels. For this purpose, average edit distance and average ratio between two sequences is calculated. The ratio of two sequences are given as:

$$\frac{(M+N)-distance}{(M+N)}, \quad (3)$$

Where M and N are the length of sequences and distance is the edit distance. This criterion is to take in account to measure the difference between predicted and target sequence. Complete details of this algorithm can be seen in [23].

Fig. 1 Sample images from the PKU database with top row as G1, second row as G2, and subsequently bottom row as G5

B. CNN-GRU Based License Plate Recognition Algorithm

Character segmentation followed by recognition are two key steps in any license plate recognition process. Segmentation process segments the whole license plate characters into individual characters. Currently, segmentation methods use character matching along with template library. These methods lack in robustness and has poor segmentation. The CNN-GRU technique uses both the CNN and the GRU. The CNN is used to extract features, which are helpful to describe the high-level semantics in the input image.

The GRU neural network is used as the sequence learning device to model the internal relations of the sequence. Since the first step is feature extraction. Therefore, the CNN-GRU model initially takes source image and extracts license plate image features through CNN. The CNN produces tensors with shape 32*16*16 in which, two convolutional layers and two max pooling layers are used. The feature map's height, width, and depth equals to 32, 8, and 16, respectively. These features are matched with FC layers. Meanwhile, a reshaping operation is performed. After FC layers, softmax layer is used to get the vector of 32 elements. In the CNN-GRU method, the GRU is used as encoding algorithm with input feature vector of 32*32. Each vector of 32 elements is given as input to the GRU, which has output vector of 512 elements. The final shape of the early stage of GRU is 32,512. Two more GRU are used to give the concatenated output, which is 32,1024. During the decoding phase, at each LSTM time step there are eight vectors of probabilities. The more probable symbol is to be taken at each step and a string of eight character is to be obtained at each step. Complete details of this algorithm can be seen in [10]. There are 4 max pooling layers in the CNN-GRU algorithm of size 2×2. In the CNN-GRU methods, the ReLU activations are used throughout the entire network. The detection block contains two convolutional layers in parallel one to infer the probability and second to regress the affine parameters. The character segmentation and recognition of rectified license plates is done using a modified YOLO network.

For the three networks in the proposed method followin g thresholds are used, 0.5 for vehicle (YOLOv2) and LP (WPOD-NET) detection and 0.4 for character detection and recognition (OCR-NET). Complete details of this al gorithm can be seen in [20].

In Section IV, we present the comparison of these two algorithms. For readers' easy flow, we write the CNN-RNN based license plate recognition algorithm as *Algorithm A* and CNN-GRU based method as *Algorithm B* in rest of the paper.

IV. SIMULATION RESULTS

For simulations, we choose intel core-i3 machine with 4GB of RAM along with Matlab 2018 as a simulation tool.

The PKU Database [1, 25]: this database contains a total of 3,977 vehicle images out of which 4,263 license plates are visible. The administrators of the PKU database have created different types of vehicles in categories, which they name as G1, G2, G3, G4, and G5.

2020 5th International Electrical Engineering Conference (IEEC 2020)
Feb, 2020 at IEP Centre, Karachi, Pakistan

Table 1 Performance analysis

License Plate Resolution	Algorithm	Image Resolution (in pixels)	Recognition Accuracy (%) on PKU Database					
			G1	G2	G3	G4	G5	Average on Database
High License Plate Resolution	*A*	200×50	46.0000	46.0000	45.0000	43.0000	38.0000	**43.6000**
	B		40.0000	40.0000	38.0000	38.0000	30.0000	**37.2000**
	A	100×40	43.0000	42.0000	42.0000	42.0000	35.0000	**40.8000**
	B		41.0000	41.0000	41.0000	40.0000	33.0000	**39.2000**
	A	80×40	39.0000	39.0000	39.0000	38.0000	30.0000	**37.0000**
	B		37.0000	37.0000	37.0000	36.0000	30.0000	**35.4000**
Low License plate Resolution	*A*	50×30	34.0000	34.0000	33.0000	33.0000	30.0000	**32.8000**
	B		34.0000	33.0000	33.0000	33.0000	28.0000	**32.2000**
	A	35×25	30.0000	30.0000	30.0000	28.0000	25.0000	**28.6000**
	B		25.0000	25.0000	25.0000	–	–	**25.0000**
	A	15×15	–	–	–	–	–	–
	B		–	–	–	–	–	–
Average on each Category			**36.9000**	**36.7000**	**36.3000**	**33.1000**	**27.9000**	

In each of the category, there are at least 550 license plate images. From G1~G3, the input images have 1082×728 pixels resolution, while G4~G5 have 1600×1236 and 1600×1200 pixels resolution, respectively. We choose this database for our experiment because it introduces license plates variations at different day times on diverse road situations. Few of the images from the PKU database are shown in Fig. 1 in which top to bottom row show images from G1~G5 category. In Fig. 1, green bounding box indicates the license plate area, which have been manually cropped to observe the license plates recognition accuracy**.**

A. Performance Analysis

We perform detailed experiments on each of the PKU database category. We perform experiments on high and low license plate resolutions. In our work, from license plate resolution of 80×40 pixels and above, we treat them as High License Plate Resolution, whereas for 50×30 pixels and below, we analyze as Low License Plate Resolution. Results are summarized in Table 1. Below we shed light on important observations as shown in Table 1

- On PKU−G1 and G2 categories and for high image resolution, the highest license plate recognition accuracy of 46.0000% is achieved for 200×50 pixels license plate by *Algorithm A*. whereas for license plate image resolution, the lowest license plate recognition accuracy of 25% is achieved for 35×25 pixels license plate by *Algorithm B* on PKU−G1, G2, and G3 categories.
- On PKU−G4 category and for high image resolution, the highest license plate recognition accuracy of 43% is achieved for 200×50 pixels license plate by *Algorithm A*. whereas for license plate image resolution, the lowest license plate recognition accuracy of 28% is achieved for 35×25 pixels license plate by *Algorithm A* on PKU−G4 category.
- PKU−G5 is the most challenging category in the dataset due to multiple license plates per image along with illumination variations and partial occlusions. Therefore, the highest recognition accuracy of 38% is achieved by *Algorithm A* on 200×50 pixels license plate resolution.
- For both high and low license plate image resolutions, the highest accuracy of 36.9000% is achieved on the PKU−G1 category.
  While, the lowest accuracy of 27.9000% is achieved on the PKU−G5 category. In addition, both the PKU−G2 and G3 are observed to be almost similar recognition accuracy of 36.7000 and 36.3000, respectively.
- An important observation during our simulations is that none of the algorithm is able to process the license plate resolution of 15×15 pixels. Moreover, none of the algorithms process license plate resolution of 35×25 pixels and below on PKU−G4, G5 categories.
- For high license plate image resolution of 80×40 pixels and above, *Algorithm A* is the clear winner in terms of recognition accuracy, followed by

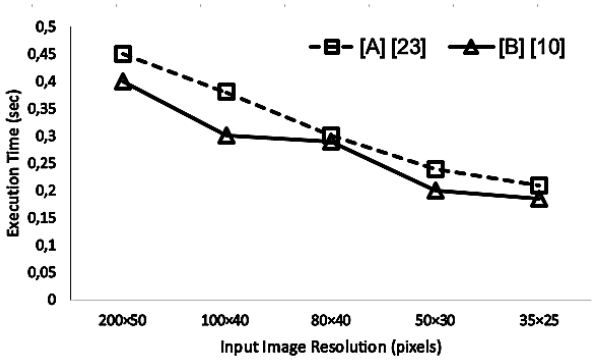

Fig. 2 Computational complexity comparison

Algorithm B. Similarly, for low license plate image resolution of 50×30 pixels, both the compared algorithms yield nearly equal recognition accuracy of over 32%.

B. Discussion

Although afore described discussion sheds detailed light on the performance of the compared algorithm. Points below, give more and detailed insight about the license plate recognition algorithms.

- *Algorithm A* [23] was originally tested on 2,713 license plate images on the VLP dataset. In their experiments, author report 94% license plate recognition accuracy. when tested on real-life images of the PKU dataset, the recognition accuracy of the *Algorithm A* dropped to 43.6000% for a standard 200×50 pixels license plate image. We observe that this significant accuracy change is due to the high variations present in the PKU−G1 to G5 set. In particular, and also shown in Table 1 that PKU−G5 category is the most challenging among all its companion categories. The performance of the *Algorithm A* was much low on PKU−G5 category as compared to the other categories.

- While *Algorithm B* [10] was tested on few hundreds license plate images of authors' own developed dataset. In their work, authors report 99% license plate recognition accuracy. However, when tested on all categories of the PKU dataset, the *Algorithm B* yielded maximum accuracy of 39.2000% for 100×40 input license plate image. We observe that the *Algorithm B* was more prone to the illumination variations induced by the PKU−G5 category that resulted in much lower recognition accuracy performance than the original dataset.

C. Computational Complexity

We evaluate the computational complexity as the time consumed to yield the final license plate recognition result, after the input image is fed to the algorithm. From Fig.2, it is obvious that *Algorithm B* is more computationally efficient than the *Algorithm A*. For a standard 200×50 pixels input license plate image, both the compared algorithms consume less than a half second. Therefore, we find that both the compared algorithms are near real-time.

V. CONCLUSIONS AND FUTURE WORK

In this paper, we presented a comparative study of two recently developed LPR algorithms, which are **(a)** CNN-RNN, which we referred as *Algorithm A* and **(b)** CNN-GRU, which we referred as *Algorithm B* in this paper. Extensive simulations on the PKU dataset indicate that for high license plate image resolution of 80×40 pixels and above and low license plate resolution of 50×30 pixel and below, the CNN-RNN based LPR algorithms outperforms its companion algorithm in terms of recognition accuracy on all five categories of PKU dataset. We also observed that CNN-GRU license plate recognition algorithm is computationally efficient. In the future, we propose the following possible research
orientation.

- The compared algorithms in this study have a great capacity to be improved on the low-resolution license plate images. As shown in Table 1 that for license plate resolution of 35×25 pixels, both the algorithms yielded very low recognition rate of less than 30%. Many times, images captures have very low resolution, such as CCTV cameras and other image capturing devices that are installed on highways. Therefore, in such situations, these algorithms can be investigated in future to yield more reliable with high accuracy results.
- Illuminations variations is another factor that significantly changes the recognition accuracy of recently developed algorithms. Since the PKU dataset introduces real life and huge non-uniform illuminations. As shown in Table 1 that PKU−G5 category contains substantial illuminations variations and both the compared algorithms yielded less than 40% recognition accuracy. Therefore, in future, these algorithms can be modified to compensate illumination variations [27].
- Real-time application [26] is another key factor for license plate recognition algorithms. In future, these algorithms can be shifted to cloud computing domain [27] to achieve real-time execution that can be ultimately deployed in several applications and systems [28]−[35].

REFERENCES

[1].A. M. Khan, S. M. Awan, M. Arif, Z. Mahmood, and G. Z. Khan, "A robust segmentation free license plate recognition method," *1st International Conference on Electrical, Communication and Computer Engineering (ICECCE)*, 2019. (Accepted and to appear).

[2].Z. Mahmood, O. Haneef, N. Muhammad, and S. Khattak, "Towards a fully automated car parking system," *IET Intelligent Transport Systems*, 2018. DOI: 10.1049/iet-its.2018.5021.

[3].H. Li, P. Wang, M. You, and C. Shen, "Reading car license plates using deep neural networks," *Image and Vision Computing*, vol. 72, 2018, pp. 14-23.

[4].D. Wang, Y. Tian, W. Geng, L. Zhao, and C. Gong, "LPR-Net: Recognizing Chinese license plate in complex environments," *Pattern Recognition Letters*, 2018

[5].L. Qiang, L. Yu, H. Jing, Y. Xiaohui and H. Qingxin, "License plate detection and recognition using hierarchical feature layers from CNN," *Multimedia Tools and Applications*, vol. 78, no.11, 2019, pp. 15665—15680.

[6].S. Zherzdev and A. Gruzdev, "LPRNet: License Plate Recognition via Deep Neural Networks," *ArXiv*, vol. abs/1806.10447, 2018.

[7].C. H. Lin, Y. S. Lin, and W. C. Liu, "An Efficient License Plate Recognition System Using Convolution Neural Networks," *International Conference on Applied System Invention (ICASI)*, 2018, pp. 224-227.

[8].R. Panahi and I. Gholampour, "Accurate Detection and Recognition of Dirty Vehicle Plate Numbers for High-Speed Applications," *IEEE Transactions on Intelligent Transportation Systems*, vol. 18, no. 4, 2017, pp. 767-779.

[9].K. S. Raghunandan, P. Shivakumara, A. Hamid, R. W. Ibrahim, G. H. Kumar, U. Pal, and T. Lu, "Riesz Fractional Based Model for Enhancing License Plate Detection and Recognition", *IEEE Transactions on Circuits and Systems for Video Technology*, vol. 28, no. 9, 2018 pp. 2276-2288.

[10]. F. You, Y. Zhao, X. Wang, "Combination of CNN with GRU for Plate Recognition", *journal of physics: conference series*, vol. 1187, 2019

[11]. H. Li, P. Wang and C. Shen, "Toward End-to-End Car License Plate Detection and Recognition with Deep Neural Networks," IEEE Transactions on Intelligent Transportation Systems, vol. 20, no. 3, 2019, pp. 1126-1136.

[12]. R. Laroca *et al.*, "A Robust Real-Time Automatic License Plate Recognition Based on the YOLO Detector," *International Joint Conference on Neural Networks (IJCNN)*, 2018, pp. 1-10.

[13]. P. Shivakumara, D. Tang, M. Asad zadeh kaljahi, T. Lu, U. Pal and M. Hossein Anisi, "CNN-RNN based method for license plate recognition," in *CAAI Transactions on Intelligence Technology*, vol. 3, no. 3, 2018, pp. 169-175.

[14]. R. Laroca *et al.*, "A Robust Real-Time Automatic License Plate Recognition Based on the YOLO Detector," *2018 International Joint Conference on Neural Networks (IJCNN)*, 2018, pp. 1-10.

[15]. Y. Yang and D. Li, Z. Duan , "Chinese vehicle license plate recognition using extreme learning machine with deep convolutional features," *IET Intelligent Transport Systems*, vol. 12, pp. 213-219, 2018.

[16]. M. A. Khan, M. Sharif, M.Y. Javed, T. Akram, Y. T. Saba, "License number plate recognition system using entropy-based features selection approach with SVM," *IET Image Processing*, vol. 12, pp. 200-209, 2018

[17]. N. Dorbe, A. Jaundalders, R. Kadikis, and K. Nesenbergs, "FCN and LSTM Based Computer Vision System for Recognition of Vehicle Type, License Plate Number, and Registration Country," *Automatic Control and Computer Sciences*, vol. 52, pp. 146-154, 2018.

[18]. Z. Selmi, M. Ben Halima and A. M. Alimi, "Deep Learning System for Automatic License Plate Detection and Recognition,"*14th IAPR International Conference on Document Analysis and Recognition (ICDAR)*, Kyoto, 2017, pp. 1132-1138.

[19]. Hong-Hyun Kim, Je-Kang Park, Joo-Hee Oh, and Dong-Joong Kang, "Multi-task Convolutional Neural Network System for License Plate Recognition," *International Journal of Control, Automation and systems*, Vol. 15, no. 6, 2017, pp 2942–2949.

[20]. S. M. Silva and C. R. Jung, "License Plate Detection and Recognition in Unconstrained Scenarios," *European Conference on Computer Vision*, 2018, pp 593-609.

[21]. O. Bullan, V. Kozitsky, P. Ramesh, and M. Shreve, "Segmentation- and Annotation-Free License Plate Recognition with Deep Localization and Failure Identification," *IEEE Transactions on Intelligent Transportation Systems*, vol. 18, no.9, 2017, pp.2351-2363.

[22]. J. Spanhel, J. Sochor , R. Juránek , A. Herout , L. Maršík , and P. Zemčík, "Holistic Recognition of Low Quality License Plates by CNN using Track Annotated Data," *14th International Conference on Advanced Video and Signal Based Surveillance (AVSS)*, 2017, pp. 1-6.

[23]. T. K. Cheang, Y. S. Chong, and Y. H. Tay, "Segmentation-free Vehicle License Plate Recognition using ConvNet-RNN," *International Workshop on Advanced Image Technology (IWAIT)*, 2016, pp. 1−5.

[24]. S. M. Awan, S. Khattak, G. Z. Khan, and Z. Mahmood, "A Robust Method to Locate License Plates under Diverse Conditions," 2nd *International Conference on Applied and Engineering Mathematics (ICAEM), 2019*

[25]. S. N. Khan, N. Muhammad, S. Farwa, T. Saba, S. Khattak, and Z. Mahmood, "Early CU Depth Decision and Reference Picture Selection for Low Complexity MV-HEVC," *MDPI Symmetry*, Vol. 11, No. 454, 2019, pp. 1−24.

[26]. Z. Mahmood, N. Bibi, M. Usman, U. Khan, and N. Muhammad, "Mobile cloud based framework for sports applications," *Multidimensional Systems and*

Signal Processing, 2019, doi.org/10.1007/s11045-019-00639-6.

[27]. Z. Mahmood, N. Muhammad, N. Bibi, Y. Malik, and N. Ahmed, "Visual enhancement of human observatory system using multi-scale retinex," *Elsevier Informatics in Medicine Unlocked*, 2018, doi: 10.1016/j.imu.2018.09.001.

[28]. Z. Mahmood, T. Ali, N. Muhammad, N. Bibi, I. Shahzad, and S. Azmat, **"**EAR: Enhanced augmented reality system for sports entertainment applications," *KSII Transactions on Internet and Information Systems*, Vol. 11, No. 12, 2017, pp. 6069−6091.

[29]. N. Muhammad, N. Bibi, A. Jahangir, and Z. Mahmood, "Image denoising with norm weighted fusion estimators," *Pattern Analysis and Applications*, 2018, Vol. 21, N0. 4, pp. 1013−1022.

[30]. N. Muhammad, N. Bibi, Z. Mahmood, and I. Qasim, "Digital watermarking using hall property image decomposition method," *Pattern Analysis and Applications*, 2018, Vol. 21, No. 4, pp. 997−1012.

[31]. N. Muhammad, N. Bibi, Z. Mahmood, T. Akram, and R. Naqvi, "Reversible integer wavelet transform for blind image hiding method," *PLOS ONE*, 2017, Vol. 12, No. 5, pp. 1−17.

[32]. M. I. Shahzad, Y. Shah, Z. Mahmood, A. W. Malik, and S. Azmat, "K-means based multiple objects tracking with long-term occlusion handling," *IET Computer Vision*, 2017, Vol. 11, No. 1, pp. 68−77.

[33]. N. Muhammad, N. Bibi, A. Wahab, Z. Mahmood, T. Akram, S. Naqvi, H. Sook, and D. Kim, "Image de-noising with subband replacement and fusion process using bayes estimators," *Computers and Electrical Engineering*, 2018, Vol. 70, pp. 413-427.

[34]. Z. Mahmood, T. Ali, S. Khattak, L. Hassan, and S. U. Khan "Automatic player detection and identification for sports entertainment applications," *Pattern Analysis and Applications*, 2015, Vol. 18, No. 4, pp. 971−982.

[35]. Z. Mahmood, T. Ali, and S. Khattak, "Automatic player detection and recognition in images using AdaBoost," *9th International Bhurban Conference on Applied Sciences & Technology* (*IBCAST*), 2012, pp. 64-69.

2020 5th International Electrical Engineering Conference (IEEC 2020)
Feb, 2020 at IEP Centre, Karachi, Pakistan

Heliostat Field Layout: An Overview of Modern Trends in Generation, Optimization and Control Strategies

Muhammad Haris[1*] and Syed Owais Athar[2]

[1] Electrical Engineering Department, Balochistan University of Information Technology, Engineering & Management Sciences, Quetta, Pakistan. (mohammad.haris1@yahoo.com) *Corresponding Author

[2] Electronic Engineering Department, Balochistan University of Information Technology, Engineering & Management Sciences, Quetta, Pakistan. (syedowaisathar@gmail.com)

Abstract: As the configuration of the current energy mix of Pakistan hangs in the balance for not being more responsive to power fluctuations and peak demand; the government and researchers continue to find out ways that define sustainability, cost-effectiveness, and efficiency. Recent developments in concentrating solar thermal power, especially, solar power tower technologies are being made at a faster pace. Two of the most important aspects that define the performance of such plants are Heliostat field layout and the control strategies deployed for solar tracking. A comprehensive review of various strategies active to generate and optimize the field layout is presented. Along with that, the methods used to track the sun for increased power input to the receiver are also reflected in the paper. Finally, the best available solution in methods for generation, optimization, and control are presented in comparison to their counterparts.

Keywords: Heliostat Field, Optimization, Algorithms, Concentrated Solar Thermal, Power Tower.

I. INTRODUCTION

As an emerging technology to generate electricity at a large scale, an enormous amount of research work has been presented to improve and optimize the behavior of central receiver based solar thermal power plants or more concisely, solar power towers. The idea of harvesting heat energy from the sun however is not quite recent as the Native Americans hailing from the canyons of Arizona used to place their adobe buildings in caves ingeniously to enable the sunlight to soak them at the right angle. [1]

The basic working of any concentrating solar thermal plant (CSP) is based on the concentration of sunlight on concentrators which involve reflective or refractive surfaces. In the case of solar power towers, the reflectors or mirrors are used as concentrators. This is not very much different from the work of Archimedes who, according to a legend, in 212 B.C., used mirrors to destroy an invading Roman fleet at Syracuse. He did so by focusing sunlight on the invaders [2]. These mirrors, called “heliostats”, are specially designed to track the sun throughout the day and year. Electrical motors and sensors that process and feed data from and to an electronic control system respectively enable the mirrors to accomplish this task. The heat energy is reflected onto a receiver placed inside a tower where a heat storage medium is present. Significant research work is also present which is focused on improving the heat storage capacity, reduction in the cost of heat density storage which includes phase change materials (PCM) development etc. [3]. Molten salts, according to Ref. [3], are one of the most mature technologies that are deployed usually in power towers. The salts are placed in a heat exchanger where their high temperatures convert water into steam. This steam is then used to run a steam turbine coupled to a generator which generates electricity [4].

Evidently, from its working principle (see Fig. 1), the CSP technology provides a zero-carbon emission-based power generation block. The radiant flux remains as high as 1.75 x 105 TW outside the atmosphere which is equivalent to 5.9 x 106 tons of coal making the resource richer than any other fuel [5]. Some of the notable CSP based plants around the world are summarized in Table 1.

Table 1 Notable Concentrated Solar Thermal Plants

Facility Name	Ivanpah	Planta Solar 10	Themis (Experimental)
Owned By	United States of America	Spain	France
Generation Capacity	392 MW	11 MW	2 MW
No. of Heliostats	173,500	624	201
First Operation	2013	2007	2004
Energy Storage Technology	-	Superheated and Pressurized water at 50 bar and 285° C	Molten Salts (KNO_3 and Sodium Nitrate)

The capacity of a CSP plant is directly proportional to the size of the heliostat field layout. This layout dictates literally 50% of the total cost and 40% of the total losses of a CSP [6]. As more and more power towers get connected to the grid, the need for increased capacity of such a system increases. This increase in heliostat field size is also in direct relation with the size of the tower, where the receiver is placed. The height of the tower is limited by its cost [7]. For some locations, seismic factors also come into play. Therefore,

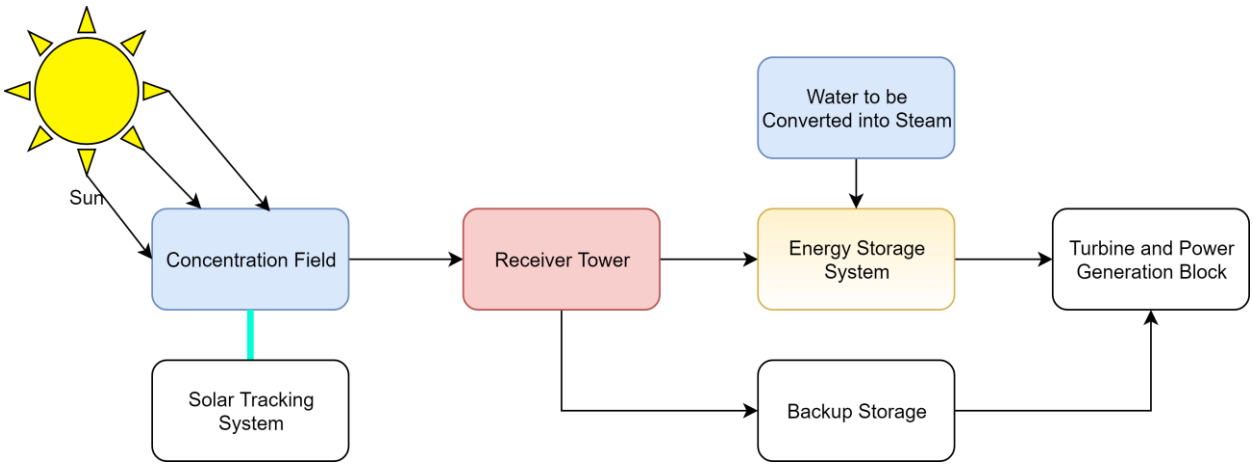

Fig. 1 Block Diagram of a Typical Solar Thermal Power Plant

improvement of the heliostat field layout has always remained a major area of research for academicians around the world.

Fig. 2 Example of a Heliostat Field

The heliostats are arranged around the receiver in different configurations including radial stagger [8], cornfield [9] etc. (Fig. 2) Each of the configurations has its own pros and cons that influence the overall concentration efficiency of plant. These are discussed in detail in the following section.

II. HELIOSTAT FIELD GENERATION AND OPTIMIZATION STRATEGIES

As summarized in Table 2 and explained in this paragraph, a wide number of methods to improve the performance of a heliostat field have been studied.

The overall efficiency of a field is a function of different variables like attenuation efficiency [10], cosine efficiency [8] , intercept efficiency, spillage factor, blocking factor , site slant range etc. [11]. The optical efficiency of a heliostat field was calculated in [12].

Table 2 Different Optimization Strategies as Proposed and Their Impact on Overall Efficiency

Study	[6]	[20]	[21]	[23]	[25]	[22]	[36]	[37]
Optimization Strategy	Genetic Algorithm	Analytical Flux Density Function [38]	Analytical Geometry Methods	Nonrestricted Refinement	Differential Evolution Algorithm	Genetic Algorithm	Combination of Sobol and Simulated Annealing Algorithm	Particle Swarm Optimization
Location	Almeria, Spain	Almeria, Spain	Gemasolar, Spain	PS10, Spain	Dhahran, Saudi Arabia	Gemasolar, Spain	Gemasolar, Spain	Gemasolar, Spain
No. of Heliostats	467	303	2650	624	2940	2650	2650	2636
Increase in Overall Efficiency (%)	0.5	-	0.57	0.8	1.8	5.71	Levelized Cost of Electricity was Reduced by 3.49 ¢/ kWhe	0.49

Paper [6] optimized a heliostat field layout using an objective function involving the factors mentioned in previous paragraph. The authors optimized field layout with the help of a genetic algorithm [13] and proposed a better field layout than existing one.

Spillage loss is also a function of heliostat field, the distance of heliostats from receiver and beam focus. The size of the receiver also affects this efficiency. Based on the HFLCAL model [14], the spillage factor was estimated and its contribution to overall incident heat power on receiver was evaluated using a new analytical flux density model [15]. This was then compared with a previous work [16]. A new model was developed with less computational costs.

One of the widely used field layout model was developed by [17]. The authors presented a mathematical model for mitigation of blocking factor. The heliostats are arranged based on mathematical equations which take the mirror's width to length ratio and a new group of heliostats is introduced when the density of mirrors reaches a certain value. This algorithm theoretically and practically provided a no-blocking layout throughout the year.

Graphic Processing Unit was used to simulate the Monte Carlo Ray tracing algorithm for calculation of annual optical efficiency by [18]. The results were verified by optimization of field layout based on two different configurations namely radial and cornfield.

Rosen projection method and simulated annealing smart algorithm was used for improvement of heliostat field parameters [19]. The findings of the research work that the spiral field layout performed more efficiently in the north field, but a decreased efficiency was seen in the south and circular field because of bad cosine efficiency. In the end, a hybrid field layout was presented which combined characteristics of both fields and an improvement in efficiency was observed.

A preliminary design for surrounding field was proposed by [20]. The study discussed a simplified procedure for generation of field layout. Different design points based on solar positions were considered and compared with a previous study.

Analytical Geometry methods to improve field efficiency of Gemasolar Power plant, Spain were proposed by [21]. The results were compared and an overall increase in efficiency of 0.57% annually was observed. A Genetic algorithm toolbox [22] improved the efficiency of the same layout by 5.71%.

Non-Restricted refinement based field layout improvement for achieving 0.8% more annual energy while keeping the operation & maintenance cost unchanged was proposed by [23]. The study amalgamated different previously presented tools like HFLCAL [14], DELSOL [24], UHC etc. In this study, the heliostat field layout is first developed using a tool and then efficiency of field is improved using the said strategy.

A differential evolution algorithm for the local coordinates for Dhahran, Saudi Arabia saw a 1.8% increase in annual averaged field efficiency [25]. A reduced computational time along with different approaches involving insolation weighted efficiency was characterized by the algorithm.

As a result of improvement in artificial intelligence techniques to solve complex engineering problems, the execution of a field layout has enhanced to a great extent. Field efficiency can be greatly improved if the mirrors are aligned to concentrate sunlight throughout the day and year automatically. This area also has driven attention of control engineers and scientists. A review on work done is presented in following article.

III. HELIOSTAT FIELD CONTROL AND TRACKING METHODS

A typical heliostat assembly is shown in Fig. 3. The elevation and azimuthal axis of heliostats can be controlled by using actuators like stepper motors etc. [26]. Solar position for a location is theoretically and mathematically predictable. Mechanisms installed in a heliostat can easily change the angle of heliostat to point at the receiver spot after a certain amount of time has passed. However, such open-loop systems are prone to error accumulation overtime. Closing the loop can help in mitigating the error as much as possible. Significant research material to support either systems is presented in the literature.

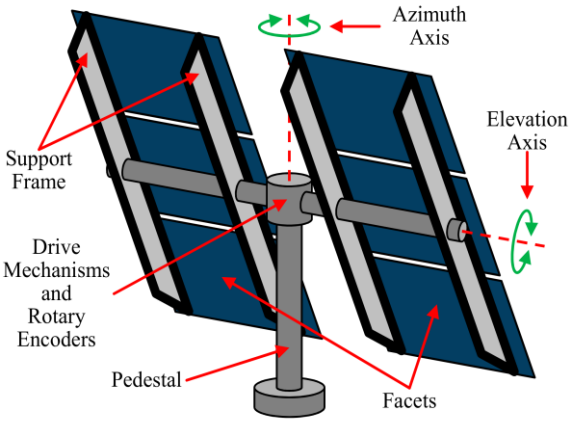

Fig 3 Typical Heliostat Assembly

Generalized sun tracking formula based on mathematical coordinate system was presented to point a sunray at an arbitrary location on earth [27]. Mechanical oscillations during changing the angle of heliostat make the sun tracking susceptible to errors as well. This problem was addressed by [28] in which a velocity controlled system was presented and different scenarios were considered to test the system.

Heuristic knowledge based on previous experience of controlling the heliostats was used to propose an automatic control strategy for solar tracking [29]. The system eliminated the need for continuous human intervention for positioning of mirrors.

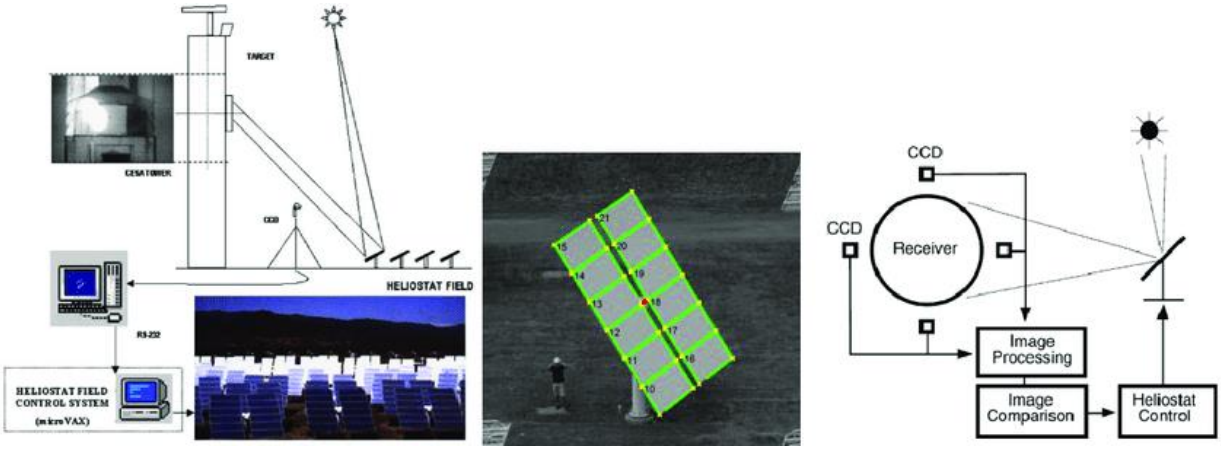

Fig. 4 Camera Based Heliostat Control Assembly

Open loop offset correction based on images taken by cameras has also been proposed [30] however, image processing coupled with machine learning approaches are also quite efficient strategies as presented. Microelectromechanical Systems (MEMS) based actuators and sensors are also employed [31], [32].

Using raytracing and PID-control algorithms, a control system was designed to aim heliostats at multiple receivers based on required power generation output [33].

Supervisory Control and Data Acquisition (SCADA) and fuzzy logic based system was designed to determine the solar position at any time of the day and then point the heliostat at a focal point by [26].

Based on receiver spillage taken up by four different cameras (apart from their other function of fault diagnosis [34]) placed around cylindrical tower, an image processing algorithm was designed by [35] (see Fig. 4). The method reduced aiming and tracking errors significantly.

IV. CONCLUSION

In terms of cost effectiveness and efficiency, algorithms designed to generate and optimize a typical field of heliostats are focused on machine learning and artificial intelligence approaches. These methods are less computationally expensive and provide more significant solutions as compared to hit and trial methods.

Image processing algorithms have dominated the control systems designed to align heliostats for achieving maximum flux profile at the receiver however, open loop systems are also proved to be working at a substantial level. With an introduction of closed loop in the control algorithm, the overall performance of field in particular and complete power generation system in general improved markedly.

REFERENCES

[1] G. Hailu, “Seasonal Solar Thermal Energy Storage,” *Therm. Energy Batter. with Nano-enhanced PCM*, pp. 1–22, 2019.

[2] C. J. Chen, *Physics of Solar Energy*. 2011.

[3] International Energy Agency, “Technology Roadmap,” 2011.

[4] M. G. William B. Stine, *Power from the Sun*. 2001.

[5] Y. Xiao, Q. Xie, and Z. Deng, “A Review on Heliostat Field Layout and Control Strategy of Solar Tower Thermal Power Plants,” *Proc. 2018 Chinese Autom. Congr. CAC 2018*, pp. 1909–1912, 2019.

[6] P. Talebizadeh, M. A. Mehrabian, and H. Rahimzadeh, “Optimization of Heliostat Layout in Central Receiver Solar Power Plants,” *J. Energy Eng.*, vol. 140, no. 4, p. 04014005, 2014.

[7] K. W. Battleson, Solar power tower design guide: Solar thermal central receiver power systems. A source of electricity and/or process heat. 1981.

[8] M. Sánchez and M. Romero, “Methodology for generation of heliostat field layout in central receiver systems based on yearly normalized energy surfaces,” *Sol. Energy*, vol. 80, no. 7, pp. 861–874, 2006.

[9] F. W. Lipps, “A Cellwise Method for The Optimization of Heliostat Field Layout,” no. d, pp. 505–516, 1978.

[10] N. Hanrieder, S. Wilbert, D. Mancera-Guevara, R. Buck, S. Giuliano, and R. Pitz-Paal, “Atmospheric extinction in solar tower plants – A review,” *Solar Energy*. 2017.

[11] J. a. Duffie, W. a. Beckman, and W. M. Worek, *Solar Engineering of Thermal Processes, 4nd ed.*, vol. 116. 2003.

[12] H. Lee, J. Kim, S. Lee, H. Yoon, Y. Kang, and M. Park, “Calculation of optical efficiency for the first central-receiver solar concentrator system in Korea,” *Energy Procedia*, vol. 69, pp. 126–131, 2015.

[13] R. L. Haupt, and S. E. Haupt, *Practical Genetic Algorithms Second Edition*. 2004.

[14] P. Schwarzbözl, M. Schmitz, and R. Pitz-paal, “Visual HFLCAL – A Software Tool For Layout

And Optimisation Of Heliostat Fields."
[15] L. García, M. Burisch, and M. Sanchez, "Spillage estimation in a heliostats field for solar field optimization," *Energy Procedia*, vol. 69, pp. 1269–1276, 2015.
[16] A. M. Manuel J. Blanco, Juana M. Amieva, "The Tonatiuh Software Development Project: An Open Source Approach To The Simulation Of Solar Concentrating Systems," 2015, pp. 1–8.
[17] F. M. F. Siala and M. E. Elayeb, "Mathematical formulation of a graphical method for a no-blocking heliostat field layout," *Renew. energy*, vol. 23, no. 1, pp. 77–92, 2001.
[18] Y. Zhou and Y. Zhao, *Heliostat Field Layout Design for Solar Tower Power Plant Based on GPU ⋆*, vol. 47, no. 3. IFAC, 2014.
[19] M. Zhang, L. Yang, C. Xu, and X. Du, "An efficient code to optimize the heliostat field and comparisons between the biomimetic spiral and staggered layout," *Renew. Energy*, vol. 87, pp. 720–730, 2016.
[20] F. J. Collado, "Preliminary design of surrounding heliostat fields," *Renew. Energy*, vol. 34, no. 5, pp. 1359–1363, 2009.
[21] J. Wang, L. Duan, Y. Yang, and L. Yang, "Rapid design of a heliostat field by analytic geometry methods and evaluation of maximum optical efficiency map," *Sol. Energy*, vol. 180, no. August 2018, pp. 456–467, 2019.
[22] R. Buck, "Heliostat Field Layout Improvement by Nonrestricted Refinement," *J. Sol. Energy Eng.*, vol. 136, no. 2, p. 021014, 2013.
[23] A. Mutuberria, J. Pascual, M. V Guisado, and F. Mallor, "Comparison of heliostat field layout design methodologies and impact on power plant efficiency," *Energy Procedia*, vol. 69, pp. 1360–1370, 2015.
[24] M. Atif and F. A. Al-Sulaiman, "Optimization of heliostat field layout in solar central receiver systems on annual basis using differential evolution algorithm," *Energy Convers. Manag.*, 2015.
[25] E. Salgado-plasencia, R. V Carrillo-serrano, E. A. Rivas-araiza, and M. Toledano-ayala, "applied sciences SCADA-Based Heliostat Control System with a Fuzzy Logic Controller for the Heliostat Orientation," 2019.
[26] Y. T. Chen and C. S. Lim, "General Sun Tracking Formula for Heliostats With Arbitrarily Oriented Axes," vol. 128, no. May 2006, pp. 245–250, 2016.
[27] I. For, "Velocity-controlled tracking of the sun," vol. 21, pp. 207–212, 1990.
[28] M. Berenguel, A. Valverde, and E. F. Camacho, "Heuristic Knowledge-Based Heliostat Field Control For The Optimization Of The Temperature Distribution In A Volumetric Receiver," vol. 66, no. 5, pp. 355–369, 1999.
[29] M. Berenguel, "An artificial vision-based control system for automatic heliostat positioning offset correction in a central receiver solar power plant," vol. 76, pp. 563–575, 2004.
[30] N. Goldberg and A. Zisken, "Heliostat surface estimation by image processing," *Energy Procedia*, vol. 69, pp. 1885–1894, 2015.
[31] P. J. Harper *et al.*, "Use of Mems and Optical Sensors for Closed Loop Heliostat Control," vol. 070015, no. 2016, 2017.
[32] F. Gross, M. Geiger, R. Buck, F. Gross, M. Geiger, and R. Buck, "A Universal Heliostat Control System," vol. 030022, 2017.
[33] Y. Song and W. Huang, "A Vision-based Fault Diagnosis System for Heliostats in A Central Receiver Solar Power Plant," pp. 3417–3421, 2012.
[34] A. Kribus, I. Vishnevetsky, A. Yogev, and T. Rubinov, "Closed loop control of heliostats," vol. 29, pp. 905–913, 2004.
[35] F. J. Collado, A. Gómez, and J. A. Turégano, "An analytic function for the flux density due to sunlight reflected from a heliostat," *Sol. Energy*, vol. 37, no. 3, pp. 215–234, 1986.
[36] Y. Luo, T. Lu, and X. Du, "Novel optimization design strategy for solar power tower plants," *Energy Convers. Manag.*, vol. 177, no. September, pp. 682–692, 2018.
[37] M. Izygon, K. McMurtrie, and N. Vu, "Particle swarm optimization of the layout of a heliostat field," *AIP Conf. Proc.*, vol. 2033, no. November, pp. 1–10, 2018.
[38] F. J. Collado, A. Gómez, and J. A. Turégano, "An analytic function for the flux density due to sunlight reflected from a heliostat," *Sol. Energy*, vol. 37, no. 3, pp. 215–234, 1986.

2020 5th International Electrical Engineering Conference (IEEC 2020)
Feb, 2020 at IEP Centre, Karachi, Pakistan

Evaluating the role of motion planning and steering control modules of autonomous vehicles in the perspective of single and mix traffic scenarios: A survey

Marya Rasib[1], Saba Malik[2], Faisal Raiz[3*], Iram Javed[4], Iftikhar Ahmed[5], Abdul Ghafoor[6], Yasir Mehmood[7], Mobeen Rafaqat[8]

[3] Control, Automotive and Robotics Lab affiliated lab of National Center of Robotics and Automation (NCRA HEC Pakistan), and with the Department of Computer Science and Information Technology, Mirpur University of Science and Technology (MUST), Mirpur-10250, AJK Pakistan

[1,4,5,6,7,8, 9]Department of Computer Science and Information Technology, Mirpur University of Science and Technology (MUST), Mirpur-10250, AJK Pakistan

([1]marya.rasib@yahoo.com, [2]saba10706@gmail.com, [3*]faisal.raiz@must.edu.pk, [4]iram.javed95@gmail.com, [5]ify_ia@yahoo.com, [6]ghoridar@gmail.com, [7]yasir.mehmood@must.edu.pk, [8]mobeen.rafaqat2@gmail.com)

Abstract: Motion planning is the process of finding a collision-free path from source state to destination position. Path planning and path tracking are two important modules of autonomous vehicles and a variety of techniques have been mentioned broadly inside the literature for both fundaments. In this paper, we present a review of crucial strategies of path planning techniques and steering control path tracking techniques of autonomous vehicles (AVs). Our contribution leads to discuss different aspects of motion planning in an efficient manner. The review includes main algorithms in motion planning and path tracking controllers presented in the form of taxonomy, their features, and their applications to driving, along with key challenges. This study shows that while advanced control methods improve tracking performance, in most cases the results are valid only within well-regulated conditions. In the end, some open problems related to the possible role of motion planning and steering control have been presented as well.

Keywords: Autonomous Vehicle (AVs), Motion Planning, Path Planning, Steering Control

I. INTRODUCTION

Motion planning and control are considered as the most fundamental components of the AVs, which are responsible for route selection, safe maneuvering and vehicle control in the dynamic road environment. According to Rowduru et al. [1], the architecture of AVs is based on SPPA (Sense, Perceive, Plan, Act) cycle, through which autopilot of an AV collects the data from the different sensors to perceive the environment, plan the motion and control the actuators accordingly. In another research work, Huang and Kumar [2] discussed that the researchers have presented the state-of-the-art techniques to address the issues in motion planning, however, the proposed systems have been either evaluated through performing simulations or tested in controlled road environment only. These limitations are an indication towards the need for robust motion planning and steering control algorithms to overcome these issues [3].

In the existing research work, motion planning has been divided into two major categories i.e. (i) path planning and (ii) path tracking (steering control) [4]. Path planning helps an AV to plan the possible routes to reach the destination from the source location. Whereas, the path tracking steering control module helps in lateral wheel control of the AV to follow the planned route generated by the planning algorithm [5].

Driving path generation in AVs is a complex task because of the dynamic and unpredictable nature of real-world traffic scenarios [6]. Path planning is a process to regulate the appropriate motion actions that lead from simple spatial route planning to reach a certain target, by using different decision and planning algorithms. The motion planning method has been described as map-based [7] and sampling-based [8] motion planning algorithms. While, steering control is responsible for actuating the instructions directed by the path planning algorithms to laterally control the AV [23, 43]. In literature, the steering control techniques has been categorized into (i) geometric based controller and (ii) feedback based controller such as pure pursuit [22-27], Stanley [28], vector pursuit [30-32], MPC [33-34], SMC [39], proportional integral derivate [21], Neural Networks [35, 49], Fuzzy logic controller [38] and many more in different perspectives.

Contribution: The major contributions of this paper are as follows:

1. Most recent state-of-the-art motion planning and control algorithms for AVs have been evaluated.
2. Presented a novel taxonomy structuring the evaluated path planning and steering control algorithms.
3. Presented a tabulated comprising of contributions and limitations of the discussed path planning and steering control algorithms.
4. Open research problems have been discussed to indicate future research directions for motion planning and steering control path tracking in this domain.

The rest of the paper is organized as follows: In section II, Path planning algorithms for AVs have been discussed. Deterministic steering control techniques and open research problems have been presented in section III and IV respectively, and Lastly, the discussion is concluded in section IV.

II. PATH PLANNING IN SELF-DRIVING VEHICLES

Path planning for AVs in unique situations is a testing issue, due to the requirements of vehicle dynamics and the presence of encompassing vehicles. According to Raiz et al. [53] Computational intelligence (CI) has been explored for better Collision free path planning. Commonplace trajectories of vehicles include extraordinary methods of moves [17]. The path planning

2020 5th International Electrical Engineering Conference (IEEC 2020)
Feb, 2020 at IEP Centre, Karachi, Pakistan

problem is concerned with locating a terrific-first-class route from start to destination that does not result in a

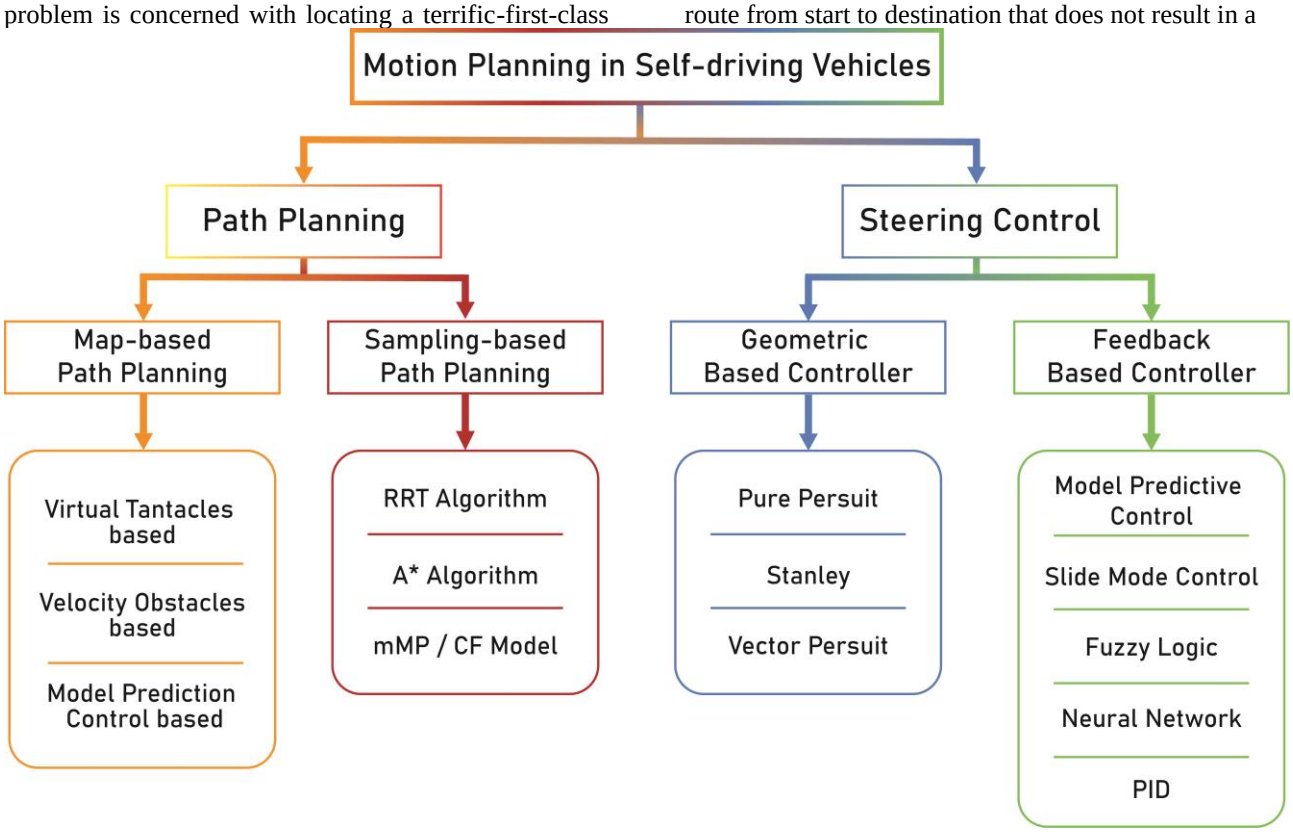

Fig. 1. Taxonomy of Motion Planning in Self-Driving Vehicles

collision with any obstacles. The definition of a path normally relies upon the type of cellular device (a robotic) and the environment (area). This has fostered -the improvement of a wealthy type of path-planning algorithms, catering to a particular needs [9].

A. Map-based planning

In robots, finding a collision free path to reach from source to destination is a key challenge for the real world. Applying programmable architecture for motion planning accelerates the collision detection and solves a robotic problem. Road map-based planning task rapidly works in a dynamic environment without accelerate reprogramming. Bellman-Ford algorithm approach handles data-flow for path searching having a low-cost interconnection network [7].

i. Velocity obstacle

The collision-free path planning is crucial for an AV. It saves life and helps to complete the task in time [55]. The velocity obstacle algorithms are acquainted with getting the collision-free velocity of vehicles. This method has a wide practical application on AVs to improve traffic safety [11]. Chen et al. [12] provide an algorithm based on a barrier function named obstacle avoidance algorithm. This technique is applied to explain the navigation and pedestrian evasion issue of a low-speed autonomous vehicle. Few studies based on clustering of vehicle are conducted for driving assistant, flow control and route planning [43-44].

ii. Virtual tentacles

A novel motion planning algorithm utilizing circular-arc virtual appendages is proposed, which depends on the insect's obstacle evasion by tentacles. An obstacle evasion track that is smooth and can meet the kinematic requirements of the vehicle is given by the virtual tentacles algorithm [13]. In an AV's Urban challenge, researchers mix the methods with a GPS-based absolutely way devotee. As the fundamental strategy is a lot of Virtual tentacles that comprise pre-calculated directions which are characterized inside the inner self-focused organize space of the AV. Like an insect's radio wires or antennas, they fan out with exceptional arches discretizing the basic driving choices of the vehicle [14].

iii. Model predictive control (MPC) algorithm

The model predictive control (MPC) algorithm for motion planning is used to avoid obstacles, collision avoidance and crash mitigation. Field testing of the motion planning method is in process and more urban situations should be analyzed in the future, such as emergency situations at the traffic lights [15]. The MPC utilizes a framework model to anticipate the future conditions of the framework and produces a control vector that limits a specific expense work over the forecast horizon within the sight of disturbing influences and limitations [16].

B. Sampling-based planning

Sampling-based motion planning (SBMP) has emerged as a highly effective algorithmic paradigm for solving complex motion planning problems. SBMP avoids the explicit construction of the state space [8]. Many planning algorithms for dynamic conditions produce planning solutions in a real-time environment and avoid moving objects. The SBMP algorithms often struggle to find collision-free paths and avoid moving

2020 5th International Electrical Engineering Conference (IEEC 2020)
Feb, 2020 at IEP Centre, Karachi, Pakistan

obstacles. This method also works in the complex road environment and search path in high dimensional space efficiently.

i. RRT Algorithm

The RRT algorithms usually require significant time to plan a path to one target. This algorithm is generally utilized in versatile mobile robotics and exhibit its better performance over past approaches [18].

There are a large number of evolution's for RRT algorithms in AVs, but currently few applications for driving which finds more efficient nearest-neighbor techniques with probabilistic optimality in RRT* [19].

ii. A* Algorithm

Hybrid A* extended the A* algorithm by searching in continuous coordinate space, which allows the modeling of vehicle motion models. This method was successful in path planning tasks for driving in a semi-structured road environment [7].

An exact cost-to-go map, obtained by solving a relaxed problem, is then used by the A*-based algorithm with model predictive flavor in order to compute the optimal motion trajectory. In a multi-lane scenario with a traffic signal motion planning framework proved to be an efficient solution for planning automated driving and demonstrated the capability to provide slow and fast trajectory. The improved approach should include a more elaborated model of interaction with other traffic participants [20].

iii. mMP and CFmodel

Machine learning methods for the motion planning of AVs, focus on the longitudinal behaviors and their impact on traffic congestion. Focus in connections between mMP and traditional car-following (CF) models [21].

Table. I. Motion Planning in Self-Driving Vehicles

Technique (s)	Author(s)	Types	Simulation / Practical	Contribution	Early work
Velocity Obstacles	Lewis et al. [1] Lee et al. [3]	Map-based	Simulation	Presented Single Vehicle path planning and Multi-Vehicle Path Planning, clumsy path planning has been composed, improve traffic safety and solved multi-lane vehicle path planning problems.	Proposed collision avoidance trajectories by focusing on single obstacles, proposed a tracking method that developed a velocity profile based on optimal trajectory and obstacle size and position.[2]
Virtual tentacles	Keke et al.[4]		Both	A novel motion planning algorithm using circular-arc virtual appendages is proposed. Best smooth path meets kinematics requirements of vehicle, build obstacle evasion track	a similar method in the path planning for ALV and proposed very efficient and fast to implement navigation system intended for use with multi-beam LIDARs.[5]
Model Predictive Control	Wang et al.[54]		Simulations	Potential crash severity and Artificial potential fields are filled into the controller objective to achieve general obstacle avoidance and the lowest crash severity,	Graph Search and A* algorithm
RRT + A*	Zhou et al.5	Sampling-based		Path prediction with FCN (Fully conventional neural network)	N/A
A* Algorithm	Ajanovic et al.[8]			Lane decision making and velocity trajectory planning.	Long horizon, behavioral layers were applied, spatiotemporal state lattice with dynamic programming was used.
Virtual Tentacles	Von et al. [7]		Simulations/ Practical	Proposed very efficient reactive navigation system, the geometric connection between the tentacles and the network is static, permitting pre-computation of grid addresses. This static relationship is the principal purpose of the proficiency of the technique.	Shakey Robot in 1984 used “cat-whiskers” to sense the presence of a solid object within the braking distance of the vehicle when traveling at top speed.[10]
Mmp Model +CF	Zhou et al.[9]		Sim	Reduce Traffic Congestion	N/A

III. DETERMINISTIC PATH TRACKING TECHNIQUES FOR STEERING CONTROL

Motion planning and control of autonomous vehicles are the most trending subjects nowadays. The steering control improvement has been flued via the latest advances in path tracking strategies as their essential goal is to minimize the difference between planned and actual path with respect to the lateral distance and vehicle heading [24].

Various path tracking methods have been presented in the literature for steering control, which is divided into geomantic-based path tracking and feedback based path tracking methods [22-25].

A. Geometric-based Controller

The geometric controllers are popular method in practical AVs due to its simplicity and real-time calculation. Geometric-based path tracking strategies are based on geometric relationships between the actual position of the vehicle, and the reference path to

calculate the steering angle [24-25]. Geometric based methods including pure pursuit, Stanley and vector pursuit have been widely used for solving path tracking problems.

i. Pure Pursuit Algorithm

The pure pursuit method is relatively easy to implement and robust to large errors [23]. Its performance depends upon the look-ahead distance L_{ad} which is the main tuning property, well selecting the L_{ad} needs intention because too shorter L_{ad} may fluctuate the control and too long L_{ad} leads to cut corners, and a steady-state error occurs at high speed. Therefore, to overcome the dependencies of L_{ad} and tune the performance of the pure pursuit Chen et al.[24] Proposed PP-PI controller based on a combination of pure pursuit PP and proportional-integral, they also add low pass filters to increase the stability of the control. Moreover, authors have used the CARLA to assess the performance of the proposed solution PP_PI. Hence, results show that the PP_PI has smaller tracking error and could effectively reduce the dependence on the L_{ad} and obtain better tracking accuracy. Andersen et al. [25] proposed an alternative formulation to the pure pursuit by considering not only the relative position of the pursued point but also the orientation of the path at that point. To validate the effectiveness of the algorithm the authors tested the algorithm by implementing it on an autonomous golf cart, in a pedestrian environment. Experiment results show that the cross-track error magnitude significantly improves at the larger curvature by reduces the root mean square (RMS) cross-track error up to 46%. Serna et al.[27] have Presented curve safety subsystem for path tracking based on pure pursuit and L_{ad} definition, an algorithm analyze the GPS information offline classifies high curvature segments and estimate the convenient speed for each one, furthermore, authors proposed a method to estimate dynamically L_{ad} based on the vehicle speed and lateral error. While pure pursuit proved to be a good path tracker, but researchers have neglected the throttle brake effect in controller.

ii. Stanley

Stanley is another geometric path tracking method that provides better performance as compared to the pure pursuit and does not cut corners. The Stanley was the name of autonomous that was first introduced by Stanford University in the second DARPA Urban Challenge 2005 [27,30]. According to Bacha et al. [24], Stanley is the nonlinear function which depends on heading error and lateral error. Existing methods suffer from a lack of global stability, tracking accuracy, or dependence on smooth road surfaces, any one of them could lead to the loss of vehicle control in autonomous off-road terrain. To address these issues, Hoffmann at el. [28] presented non-linear control law based on Stanley algorithm to track trajectory in an efficient manner, by considering the parameters location, orientation, curvature and speed of the front wheels with respect to the desired trajectory. The control law was implemented on Volkswagen Touareg “Stanley”, hence the experimental results demonstrated the ability of the controller to accurately track trajectories in a variety of off-road settings, between dangers, and over rough and curvy terrain. Snider [29] and Andresen et al. [27] have presented the comparison of the Stanley and other geometric and kinematics controllers where Stanley does not robust to external disturbance, steady-state error and overshoot occurs at high speed.

iii. Vector Pursuit Algorithm

Wit et al.[30] presented another geometry technique Vector pursuit based on a screw technique that was introduced by Sir Robert S. Ball in 1900 [31] to control the non-holonomic ground vehicle. Vector pursuit technique used position and orientation to determine the desired motion of the vehicle. The researcher performed experiments and simulations in real-time with Navigation Test Vehicle (NTV) to validate the proposed solution. Furthermore, Yeul et al. [32] Proposed vector pursuit method to track vehicles in order to generate vehicle motion following a specified path, and a control method based on the relation between traction force and track slip. The performance of the proposed solution has been evaluated by Matlab and tested by Draw Bar Pull but this proposed solution used only for tracked vehicles it would be interesting if the proposed solution and relation equations applied on the manufactured vehicle models and performance should be evaluated by performing the number of practical tests. The weakness and strengths of the geometric based path tracking techniques cited in literature have been highlighted in Table II.

B. Feedback-Based Controller

Feedback controller has been accounted as a steering controller, makes the vehicle track a given trajectory with the minimum of tracking error. The feedback controller comes with an advantage is that it’s quickly responded to the tracking error [23]. In Literature, feedback-based path tracking techniques are classified into (i) Model-based and (ii) Non-model based. Model-based path tracking methods use either kinematic or dynamic models or use both [27]. In model-based techniques, model predictive controller (MPC) and neural networks controller techniques are most frequently used for tracking purposes. In non-model-based techniques, Proportional Integral Derivative PID, Fuzzy logic and Slide mode controller [40-42] have been considered for path tracking in the literature.

i. MPC

MPC is the popular model-based controller among steering controllers of autonomous vehicles because it handles system constraints and nonlinearities systematically by using simple vehicle dynamics for the reference model. However, simple vehicle dynamics are not enough for evasive steering maneuvers which require very fast steering actions. To address this issue, Nam et al. [33] Proposed an MPC layout based on them combination of steering system model and vehicle model that works for such maneuvers, proposed model provides information about the disturbances, bandwidth

of the actuator, and the motor voltage at the same time as maintaining an easy structure to keep the computational load low. The proposed solution has been experimentally validated and compared with regular MPC which demonstrated that proposed MPC handled the system constraints effectively than a regular MPC. In another research, WANG et al. [34] proposed the MPC controller based on Fuzzy logic which ensures the tracking accuracy and vehicle dynamic stability by improving the weight of the cost function of classical MPC by using the kinematic and dynamic models. The researchers validated the proposed solution by CarSim-Matlab and performed the comparison with classic MPC, hence researchers claimed that the result is 82% better than classic ones. However, slip spectacles, aerodynamic effects and interruption moments are neglected.

ii. Neural Networks

In literature, neural networks have been accounted as a model-based steering controller. Sharma et al. [49] have proposed an end-to-end learning model-based controller for motion control in AVs. The authors have divided the motion control into (i) lateral control and (ii) longitudinal control; and proposed two models i.e. steering model and speed model dealing with the input parameters such as steering angle and speed respectively. The presented models have been tested in the simulation environment designed in "TORCS" and achieved 100% autonomy in the e-road track. In another research work, Simmons et al. [50] have proposed an end-to-end learning approach for road lane-following in self-driving vehicles. The authors have trained two models: a deep neural network model and the convolutional neural network model for lateral motion control (steering control) and longitudinal motion control (speed control) of the self-driving vehicle. The experiment results have been compared with the state-of-the-art networks i.e. DenseNet and VGG16 and show that the CNN model achieved a higher degree of accuracy during validation than the DNN model. Moreover, Chen and Huang [51] have proposed an end-to-end learning architecture for autonomous steering angle generation and road lane-keeping in self-driving vehicles. The authors have presented a self-optimized convolutional neural network model to take visual input and produce the steering angle from lane marking autonomously. The proposed model has been evaluated on the road videos and results show that the presented CNN model performed well throughout the provided road scenarios.

iii. Proportional Integral Derivate (PID)

Undeniably, there is a lot of researches on the control theory, among which the extensively applied strategy is the PID controller. As a mature control method, the PID controller has a simple principle and strong applicability. However, PID does not deal with parameter optimization and take long computational time for controlling the immediate path error. To address these issues, Zhao et al. [36] have presented a lateral dynamic model of the vehicle based on a bicycle model to design the PID controller to solve the AGV trajectory control problem, genetic algorithm has been utilized for the sake of optimizing the parameter's used by the controller. Though, the proposed controller performed well even in the presence of external disturbance in simulations however, any practical experiment is not performed. Zhao et al. [37] designed the Adaptive PID controller named "intelligent pioneer" which focused on path tracking and stability of motion to efficiently navigate in an unfamiliar environment. In this regard, the researcher developed a degree of freedom dynamic model to formulate the path tracking problem in a state-space format which increased flexibility of the vehicle control system. The proposed solution has been validated using Matlab, however, the researchers do not consider factors such as disturbances by GPS signal attenuation, changing road conditions, changing vehicle parameter's with time, and other factors. It would be interesting if these issues also consider during lateral motion control of the vehicle.

iv. Fuzzy logic controller

The fuzzy logic controller is another feedback path tracking controller has greater importance in steering control maneuver due to its capability to incorporate human knowledge and experience, through language. According to Riaz and Niazi [52], human driver features has been modeled to elude rear end collision using fuzzy logic. Moreover, Rastelli and Penas [45] has proposed a fuzzy-logic inference engine based steering controller for autonomous vehicles to predict and execute the safe maneuver in roundabout complex scenarios. The authors have divided the roundabout into three stages, (i)entrance, (ii)inside, and (iii)exit, and presented the cascade architecture to generate the predicted trajectory and execute the maneuver accordingly. Additionally, Van et al. [46] have presented a human driver behavior that inspired the fuzzy logic-based steering controller for AVs. The proposed system extracts the road lane information using a visual sensor, processes it into the designed inference engine and executes the driving rule to control the steering angle and velocity accordingly. The authors have tested the presented system on the straight road having slight curvature, and the results show that the system performed well comparatively. Furthermore, according to Riaz and Niazi [56] the excessive number of fuzzy rules directly prejudices their efficiency.

v. Slide Mode Control

Motion control involves a steering system that is badly influenced by external disturbance, parameter perturbation, and real-time ability of control algorithm and tracking good accuracy and stability has become a challenge. To address the steering accuracy, He et al. [48] have proposed a sliding model control-based emergency steering controller for AVs to predict the collision scenario and execute the safe maneuver to ensure the collision avoidance along with the stability of the vehicle. The authors have presented two-layer control architecture, (i) decision making layer, and (ii) motion control layer to predict the collision condition,

designed the elicitation mechanism to control the actuator using the kinematical model and developed the back-stepping SMC based tire controller for lateral control in emergency situation accordingly. In another research work, Dai et al. [47] have proposed a kinematic model and slide mode control-based hybrid approach to estimate the steering angle and control the four independent wheel of the vehicle. Furthermore, the authors have utilized a PSO algorithm for the velocity and acceleration control respectively. The proposed system has been tested in the simulation and results have been compared with state-of-the-art solutions.

Table. II. Motion Planning in Self-Driving Vehicles

Technique(s)	Author(s)	Type	Simulation / Practical	Contribution	Strengths	Weakness
Pure Pursuit	Park et al. [26]	Geometric-Based	Both	Adaptive Pure Pursuit Algorithm using PI control theory in a lateral offset to reduce cutting corners	Easy to implement, Robust to disturbances and large lateral error	Cutting corners problem, the steady-state error occurs at high speed
	Chen et al. [24]		Simulation	PP-PI based on a combination of pure pursuit and proportional-integral to overcome the dependence of look-ahead distance	It could effectively reduce the dependence on look-ahead distance L_{ad} and obtain better tracking performance.	Tracking performance highly dependent on L_{ad} When L_{ad} is too short then Oscillation occurs, when Lad is long then cut corners occur.
Stanley	Ander sen et al.[25]		Practical	The Stanley method based on a nonlinear control law that considers the cross-track error	Batter tracking performance doesn't occur the cutting corners	Not as robust to disturbances, Has a higher tendency for oscillation,
	Park et al. [26]			Reduce cross tracking error, yaw heading error information	Better tracking performance than the pure pursuit doesn't occur the cutting corners	Occurs the overshoot turns.
Vector pursuit	Wet et al. [28]		Practical/ Simulation	Vector pursuit based on screw theory to describe the instantaneous motion of the vehicle from its current location to a target position and orientation	Robust and Less sensitive to look ahead distance	Complex calculation
SMC	Wang et al. [39]			Proposed Backstepping Slide mode controller based on kinematic & dynamic model, and to describe the tacking accuracy derived the deviation of direction-angle and lateral position.	Fast response, Strong robust to parameter perturbation and external disturbance	As the chattering is inevitable
MPC	WANG et al. [34]	Feedback Based Controller	Simulation	Improved MPC strategy to deal with the path tracking problem, which adaptively controls the weight of the cost function by using a fuzzy adaptive control algorithm	Based on tire and vehicle dynamics	Less tracking accuracy, instability, and uncomforted ride
	Nam et al. [33]		Both	Proposed an MPC design based on the combination of the steering system model and vehicle model that works for evasive steering maneuvers	Ability to explicitly handle, consider constraints, traffic uncertainties sub-optimal performance verified	For evasive steering maneuvers, simple vehicle dynamics is not sufficient
Fuzzy Logic	Van et al.[46]		Practical	Presented a human driver behavior inspired fuzzy logic-based steering controller for self-driving vehicles	Easy implementation, well dynamic model of the plant is not required, Handle vagueness in information efficiently	Rules can become unmanageable if the number of variables is larger
	Hodge et al. [38]		Sim-lations	Proposed fuzzy logic Controller based on humans thinking while driving, for steering the self-driving cars towards a target.	Ability to incorporate human knowledge and experience, via language, into the relationships.	Required more prior knowledge, Controller tuning is not systematic with no formal stability analysis.
Proportion Integration Differentiation (PID)	Zhao et al. [36]		Practical	A two-degree-of-freedom dynamic model is developed to formulate the path-tracking problem in the state-space forma	Simple structure, strong robustness, applicability, Requires less prior knowledge	Long computing time, Doesn't deal with parameter optimization, external environment disturbances, several control objectives.
	Zhao et al. [37]		Simulation	PID controller is designed to achieve AGV trajectory tracking, a genetic algorithm is utilized to determine the optimal parameters, which is good to get the optimal control performance.	Simple principle and strong applicability and robustness, easy to be used.	Parameter tuning of the PID controller is the time consuming, needs experience
Neural Network	Kehtarnavz et al. [35]			A neural network training models based on Backpropagation BP and functional-link FL networks have been utilized to a perceived heading angle and range.	Sufficient training can emulate human driving to make the automated car feel natural	Larger amounts of real-world training data required by the controller, No failure explanation possible

2020 5th International Electrical Engineering Conference (IEEC 2020)
Feb, 2020 at IEP Centre, Karachi, Pakistan

IV. OPEN RESEARCH CHALLENGES

During the review of path planning and path tracking techniques following open research questions have been found related to the motion of AVs.

A. Lack of hybrid system for steering control

In literature, steering control techniques along with their strengths and limitations have been discussed comprehensively. Geometric-based path tracking technique is highly robust to lateral error and external disturbance but has look-ahead distance dependence which ends up with cut corners or oscillators [22-27], while model-based path tracking techniques have reliable tacking performance at low speed, but at high speed, they have fidelity issues, complex computation and not robust at discontinues path [23], and non-model based can response to tracking rapidly but has dependence on optimal parameters tuning which is highly computational and time-consuming [22-24]. Thus, there is a need to propose such hybrid steering controllers that should incorporate the strong capabilities of three different methods (i) model-based (ii) non-model based and (iii) geometric based instead of the same method in such a manner that controller should be able to make up the weaknesses of them and improves for better path tracking. Moreover, to eliminating all negative factors, it would be interesting to apply the optimization techniques on existing hybrid systems which should be based on a combination of different methods of path tracking techniques.

B. Autonomous vehicle Overshoot

During the comprehensive survey of existing state-of-the-art path tracking techniques, it has been observed that overshoot happened at high speed in self-driving vehicles. In Stanley, overshot occur at sharp turns [27-29], while in kinematic and dynamic models' overshoot has increased when vehicle speed and curvature rate increased and changed rapidly [26]. Moreover, the PID feedback controller always suffers from the optimization of parameters and overshoots in tracking [42]. Hence, there is a need to propose the solution to resolve overshoot issues of the autonomous vehicle at a higher speed through a model-based, non-model based and geometric-based algorithm.

C. Dynamic limitations in Motion Planning

Despite the way that few productive techniques have been discussed in [5] [12-14] [16-17]. Many motion planning issues have been relentlessly developing. These issues include assurance of collision-free route, limited path, and low run time, demonstrating of evolving environment, multiple ideal functions, and dynamic limitations, to give some examples. These limitations create motion planning issues to be all the more testing, what's more, require increasingly solid and effective algorithms.

V. CONCLUSION

In this paper, we have reviewed different techniques towards path planning and steering control for self-driving Vehicles. We present the comprehensive review of the sampling-based, map-based path planning techniques and path tracking techniques include geometric and feedback-based. The deterministic tables are also given for both the above-discussed fundamentals of AVs. In the end, it is concluded from the above study that all the techniques discussed in the paper for path planning are for single vehicle control. Multi-Vehicle control algorithms need to be proposed for better coordination on Road. Furthermore, integration of path tracking strategies of different methods needs to be proposed to overcome the flaws of the existing path tracking techniques. While, in this survey, we try to highlight the keys elements of AVs, path planning and path tracking techniques within the area they belong to.

REFERENCES

[1] Rowduru, S., N. Kumar, and A. Kumar, A critical review on automation of steering mechanism of load haul dump machine. Proceedings of the Institution of Mechanical Engineers, Part I: Journal of Systems and Control Engineering, 2019: p. 0959651819847813.

[2] Huang, J. and A. Vijayakumar, Asurvey FOR MULTI-SENSOR FUSION ON AVS. 2019.

[3] Wang, W.-J., et al. Optimal Trajectory Planning with Dynamic Constraints for Autonomous Vehicle. in 2019 58th Annual Conference of the Society of Instrument and Control Engi[neers of Japan (SICE). 2019. IEEE.

[4] Paden, B., et al., A survey of motion planning and control techniques for self-driving urban vehicles. IEEE Transactions on intelligent vehicles, 2016. 1(1): p. 33-55

[5] Murray, S., et al. A Programmable Architecture for Robot Motion Planning Acceleration. in 2019 IEEE 30th International Conference on Application-specific Systems, Architectures and Processors (ASAP). 2019. IEEE.

[6] Saleem, H., et al., Evaluating the role of neural networks and cyber security for the development of next generation autonomous vehicles: A Survey

[7] Jahanshahi, H., et al., Robot motion planning in an unknown environment with danger space. Electronics, 2019. 8(2): p. 201.

[8] Ichter, B. and M. Pavone, Robot motion planning in learned latent spaces. IEEE Robotics and Automation Letters, 2019. 4(3): p. 2407-2414.

[9] Bhattacharya, P. and M.L. Gavrilova, Roadmap-based path planning-using the voronoi diagram for a clearance-based shortest path. IEEE Robotics & Automation Magazine, 2008. 15(2): p. 58-66.

[10] Zhou, H., et al., Real-time Multi-target Path Prediction and Planning for Autonomous Driving aided by FCN. arXiv preprint arXiv:1909.07592, 2019

[11] Lee, K. and D. Kum, Collision Avoidance/Mitigation System: Motion Planning of Autonomous Vehicle via Predictive Occupancy Map. IEEE Access, 2019. 7: p. 52846-52857.

[12] Chen, Y., H. Peng, and J. Grizzle, Obstacle avoidance for low-speed autonomous vehicles with barrier function. IEEE Transactions on Control Systems Technology, 2017. 26(1): p. 194-206.

[13] Ke-ke, W., et al. A motion planning algorithm for autonomous land vehicle based on virtual tentacles. in 2011 Chinese Control and Decision Conference (CCDC). 2011. IEEE.

[14] Von Hundelshausen, F., et al., Driving with tentacles: Integral structures for sensing and motion. Journal of Field Robotics, 2008. 25(9): p. 640-673.

[15] Wang, H., et al., Crash mitigation in motion planning for autonomous vehicles. IEEE Transactions on Intelligent Transportation Systems, 2019. 20(9): p. 3313-3323.

[16] Aram, A. and F. Janabi-Sharifi, Theory and applications of HVAC control systems–A review of model predictive control (MPC). Building and Environment, 2014. 72: p. 343-355.

[17] Liu, C., et al. Path planning for autonomous vehicles using model predictive control. in 2017 IEEE Intelligent Vehicles Symposium (IV). 2017. IEEE..

[18] Ma, L., et al., Efficient sampling-based motion planning for on-road autonomous driving. IEEE Transactions on Intelligent

Transportation Systems, 2015. 16(4): p. 1961-1976.
[19] Claussmann, L., et al., A review of motion planning for highway autonomous driving. IEEE Transactions on Intelligent Transportation Systems, 2019.
[20] Ajanovic, Z., et al. Search-based optimal motion planning for automated driving. in 2018 IEEE/RSJ International Conference on Intelligent Robots and Systems (IROS). 2018. IEEE.
[21] Zhou, H. and J. Laval, Longitudinal Motion Planning for Autonomous Vehicles and Its Impact on Congestion: A Survey. arXiv preprint arXiv:1910.06070, 2019.
[22] M. Cibooglu and M. Turan, "Mertcan Cibooglu, $4;: (8(7H5(8 (5+ Mehmet Turan Söylemez," vol. 8, pp. 583–588, 2017.
[23] M. Park and W. Han, "Corresponding author 2," no. Iccas, 2014.
[24] Y. Chen, Y. Shan, L. Chen, K. Huang, and D. Cao, "Optimization of Pure Pursuit Controller based on PID Controller and Low-pass Filter," pp. 3294–3299, 2018.
[25] H. Andersen, Z. J. Chong, Y. H. Eng, S. Pendleton, and M. H. A. Jr, "Geometric Path Tracking Algorithm for Autonomous Driving in Pedestrian Environment θ L," pp. 1669–1674, 2016.
[26] M. Park, S. Lee, and W. Han, "Development of steering control system for autonomous vehicle using geometry-based path tracking algorithm," *ETRI J.*, vol. 37, no. 3, pp. 617–625, 2015, doi: 10.4218/etrij.15.0114.0123.
[27] G. Citlalli, "GPS-Based Curve Estimation for an Adaptive," pp. 497–511, 2017, doi: 10.1007/978-3-319-62434-1.
[28] G. M. Hoffmann, C. J. Tomlin, M. Montemerlo, and S. Thrun, "Autonomous Automobile Trajectory Tracking for Off-Road Driving : Controller Design , Experimental Validation and Racing †."
[29] J. M. Snider, "Automatic Steering Methods for Autonomous Automobile Path Tracking," *Work*, no. February, pp. 1–78, 2009, doi: CMU-RI-TR-09-08.
[30] J. Wit, C. D. Crane, and D. Armstrong, "Autonomous ground vehicle path tracking," *J. Robot. Syst.*, vol. 21, no. 8, pp. 439–449, 2004, doi: 10.1002/rob.20031.
[31] "Review Reviewed Work (s): A Treatise on the Theory of Screws by Robert Stawell Ball Review by : Carl Barus Published by : American Association for the Advancement of Science Stable URL : https://www.jstor.org/stable/1628817," vol. 12, no. 313, pp. 1001–1003, 2020.
[32] T. Yeul, S. Park, S. Hong, H. Kim, and J. Choi, "jschoe}gmoeri.re.kr," pp. 2781–2786, 2006.
[33] H. Nam, W. Choi, and C. Ahn, "MODEL PREDICTIVE CONTROL FOR EVASIVE STEERING OF," vol. 20, no. 5, pp. 1033–1042, 2019, doi: 10.1007/s12239.
[34] H. Wang, B. Liu, X. Ping, and Q. An, "Path Tracking Control for Autonomous Vehicles Based on an Improved MPC," *IEEE Access*, vol. PP, p. 1, 2019, doi: 10.1109/ACCESS.2019.2944894.
[35] N. Kehtarnavaz and W. Sohn, "Steering control of autonomous vehicles by neural networks," *Proc. Am. Control Conf.*, vol. 3, pp. 3096–3101, 1991, doi: 10.23919/acc.1991.4791978.
[36] B. Zhao, H. Wang, Q. Li, J. Li, and Y. Zhao, "PID Trajectory Tracking Control of Autonomous Ground Vehicle Based on Genetic Algorithm," *Proc. 31st Chinese Control Decis. Conf. CCDC 2019*, pp. 3677–3682, 2019, doi: 10.1109/CCDC.2019.8832531.
[37] R. Paper *et al.*, "Design of a Control System for an Autonomous Vehicle Based on Adaptive-PID," pp. 1–11, 2012, doi: 10.5772/51314.
[38] N. E. Hodge and M. B. Trabia, "Fuzzy an," *Mech. Eng.*, no. May, pp. 2482–2488, 1999.
[39] P. Wang, S. Gao, L. Li, S. Cheng, and L. Zhao, "Automatic steering control strategy for unmanned vehicles based on robust backstepping sliding mode control theory," *IEEE Access*, vol. 7, pp. 64984–64992, 2019, doi: 10.1109/ACCESS.2019.2917507.
[40] M. Kabeer, F. Riaz, and M. A. Butt, "Emotion Enabled Cognitive Driver," pp. 1–5.
[41] H. Saied *et al.*, "From Non-Model-Based to Model-Based Control of PKMs : A Comparative Study To cite this version : HAL Id : hal-01631006," 2017.
[42] Y. Shan, W. Yang, C. Chen, J. Zhou, L. Zheng, and B. Li, "CF-Pursuit: A Pursuit Method with a Clothoid Fitting and a Fuzzy Controller for Autonomous Vehicles," *Int. J. Adv. Robot. Syst.*, vol. 12, no. 9, 2015, doi: 10.5772/61391.
[43] Ahmad, I., et al., *A Cooperative Heterogeneous Vehicular Clustering Mechanism for Road Traffic Management.* International Journal of Parallel Programming, 2019.
[44] Ahmad, I., R. Md Noor, and M. Reza Z'aba, *LTE efficiency when used in traffic information systems: A stable interest aware clustering.* International Journal of Communication Systems, 2019. **32**(2): p. e3853.
[45] J. Pérez and M. Santos, "Fuzzy logic steering control of autonomous vehicles inside roundabouts," vol. 35, pp. 662–669, 2015, doi: 10.1016/j.asoc.2015.06.030.
[46] E. Vans, "Vision Based Autonomous Path Tracking of a Mobile Robot using Fuzzy Logic," *Asia-Pacific World Congr. Comput. Sci. Eng.*, pp. 1–8, doi: 10.1109/APWCCSE.2014.7053862
[47] X. He, Y. Liu, C. Lv, X. Ji, and Y. Liu, "Emergency steering control of autonomous vehicle for collision avoidance and stabilisation," *Veh. Syst. Dyn.*, vol. 57, no. 8, pp. 1163–1187, 2019, doi: 10.1080/00423114.2018.1537494.
[48] P. Dai, J. Taghia, S. Lam, and J. Katupitiya, "Integration of sliding mode based steering control and PSO based drive force control for a 4WS4WD vehicle," *Auton. Robots*, vol. 42, no. 3, pp. 553–568, 2018, doi: 10.1007/s10514-017-9649-6.
[49] Sharma, S., Tewolde, G. and Kwon, J., May. Lateral and Longitudinal Motion Control of Autonomous Vehicles using Deep Learning. In *2019 IEEE International Conference on Electro Information Technology (EIT)* (pp. 1-5). IEEE
[50] B. Simmons, P. Adwani, H. Pham, Y. Alhuthaifi, and A. Wolek, "Training a Remote-Control Car to Autonomously Lane-Follow using End-to-End Neural Networks," *2019 53rd Annu. Conf. Inf. Sci. Syst.*, pp. 1–6, 2019.
[51] Z. Chen, X. Huang, and S. Member, "End-to-End Learning for Lane Keeping of Self-Driving Cars," no. Iv, pp. 1856–1860, 2017.
[52] Riaz, F. and M.A. Niazi, "Towards social autonomous vehicles Efficient collision avoidance scheme using Richardson's arms race model". PloS one, 2017. 12(10)
[53] Riaz, F., et al., *An efficient collision avoidance scheme for autonomous vehicles using genetic algorithm.* J Appl Environ Biol Sci, 2015. **5**(8): p. 70-76**.**
[54] Qureshi, A.H., et al. Motion planning networks. in 2019 International Conference on Robotics and Automation (ICRA). 2019. IEEE**..**
[55] Rauf, R., et al., *An Exploratory Goal-Based Modeling of Optimized Collision Avoidance Action Selection in Autonomous Vehicles.* BRAIN. Broad Research in Artificial Intelligence and Neuroscience, 2019. **10**(3): p. 74-88.
[56] F. Riaz and M. A. Niazi, "Enhanced emotion enabled cognitive agent-based rear-end collision avoidance controller for autonomous vehicles," *Simulation*, vol. 94, no. 11, pp. 957–977, 2018, doi: 10.1177/0037549717742203.

2020 5th International Electrical Engineering Conference (IEEC 2020)
Feb, 2020 at IEP Centre, Karachi, Pakistan

Design and Simulation of Energy Efficient Campus

Anam Shah[1*], Nayyar Hussain Mirjat[2], Faheem Khuhawar[1], Suhail Ahmed Shaikh[2]

[1] Department of Telecommunication Engineering, Mehran University of Engineering and Technology, [2]
[2]Department of Electrical Engineering, Mehran University of Engineering and Technology,
Jamshoro, 76062, Pakistan (anam@edu.pk)
Corresponding author: nayyar.hussain@faculty.muet.edu.pk

Abstract: Pakistan as a third world country has failed to cope with energy shortage and as a result country is facing huge economic crisis. Energy shortage has affected all the fields of life due to increase in Electricity demand and consumption. Moreover, rapid growth in population and increased use of electronic appliances has contributed to increase in cost of electricity and CO2 emissions. To solve the rising environmental and economic problems, it is crucial to optimize energy consumption by putting into place energy efficient measures. Our idea is to investigate the current wastage and propose simulation-based energy consumption model. In our work, we studied the currently deployed power consumption model based on real time power measurement data. The electric load data was fed to Homer simulation tool to create a fine load curve. Homer based simulation model was built to obtain the optimized energy consumption behavior. The simulation model used the off-grid PV. Further, we obtained cost of electricity and net present cost of system. As a result of this study off-grid PV based hybrid system was obtained as the optimal configuration to meet peak demand of 195.14 kW. The Cost of Electricity (COE) and Net Present Cost (NPC) from PV hybrid system are estimated to be 8.24 Rs/kWh and 114,540 Rs respectively. The COE obtained from off-grid PV system is cheaper as compared to grid, i.e. 17 Rs/kWh with reduced carbon emissions.
Keywords: Energy Efficient, Green, Campus, Simulation, Model, Cost of Electricity, Net Present Cost.

I. INTRODUCTION

Electricity has become essential part of our lives and its usage in houses, buildings, campuses contribute to one third of the energy consumption as well as CO2 emission worldwide [1]. Hence, the increase in generation of Electricity produced by thermal power plants or other energy sources to meet the rising trend in energy consumption add to environmental pollution [2]. Thus, there is a severe need to develop means and methods to save energy and eventually solve the rising environmental and economic problems[3]. User behavior towards utilization of appliances in buildings is considered to have huge impact on energy consumption [4]. For example, occupant's or resident's negligent behavior in buildings can result in increase in energy consumption [5]. To solve this, developing a simulation model could be helpful to test and predict performance of a building in terms of energy efficiency [6]. Simulation model enables designers to implement energy efficient policies and reduce energy cost as well as create energy efficient environment [7].

In our work we optimized energy consumption model to estimate the alternative requirement of our system using simulation. Hence, the focus of this work is to develop and simulate Energy Efficient model to help and optimize energy consumption of the building.

II. LITERATURE REVIEW

In recent years several different approaches and tools have been introduced to make system energy efficient. For example [8], use MATLAB simulations as well as multi-objective genetic algorithms to save energy consumption by avoiding simultaneous usage of devices at the same time. Similarly [9], also use genetic algorithm to decrease energy cost through MATLAB simulations. Whereas the authors in [10] develop agent-based simulation model (ABM) that integrates human behavior, energy management policies as well as technology to optimize energy consumption by electrical devices. The overall energy utilized by different buildings across the campus was proposed in [11] using macro scale energy management setup. In [12] used different models based on Diesel generator and solar-wind for electricity generation using HOMER simulation tool in different areas of Nigeria. They obtained the result cost effective with reduced carbon footprint.

From the literature review it was perceived that the previous works used complex approach and focused only on residential appliances and did not provide productive usage of electricity. In our work, we have presented simple simulation model made using HOMER (Hybrid Optimization of Multiple Energy Resources) tool. To develop the Model, we have used the real power consumption data acquired through efergy Wireless Energy Monitor device. The measured data

was used in HOMER software to create the load profile and simulation model.

III. METHODOLOGY

A. Architecture

As a case study, we have considered the building of Educational Institution, namely, The Department of Telecommunication Engineering, Mehran UET, Jamshoro (TL-MUET). The load of TL-MUET uses 3-phase system, each phase carries evenly distributed load which supply electricity to whole building. The architecture of Department of Telecommunication has two floors namely Ground and 1st floor. It has a total of 12 laboratories with 6 laboratories on each floor. Similarly, there are 22 offices, 16 offices on ground floor, and 6 offices on 1st floor. Distribution of power consumption devices is shown in Figure 1.

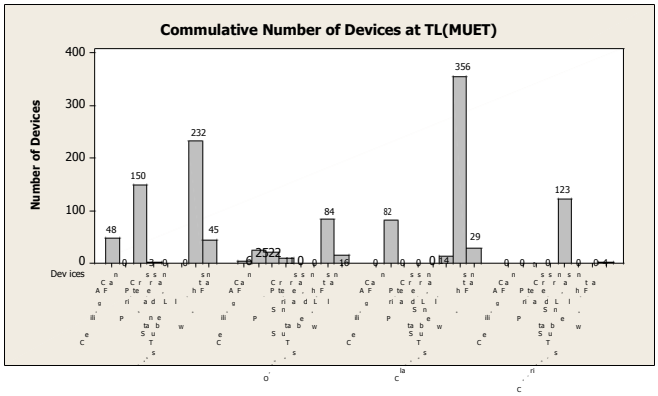

Figure 1 : Total Number of Devices at TL-MUET

Each laboratory has around 10 to a maximum of 32 PCs. To ensure proper illumination, each laboratory has 10 to 32 tube-lights. Whereas to maintain temperature, each laboratory has 4 air conditioners. Similarly, each office has at least one wall fan, roof fan, and a PC along with 8 to 12 tube lights. There are six offices that have 1.5-ton air conditioner installed in it.

Furthermore, the TL-MUET building has 12 classrooms with each having 32 tube-lights and 12 roof fans to regulate temperature and ensure proper illumination. Some classes also have 4 to 5 wall fans. To add, the corridors luminance is maintained via 123 energy saving bulbs.

The estimated power consumption behavior of the mentioned electrical appliances is shown in Table 1

Table 1 : Estimation of Power Consumption Load at TL-MUET

Appliances	Power rating (W)	Devices in use	Duration (Hrs)	Total load (kWh/day)
Air conditioner	1980	54	5	534.6
PC	100	172	7	120.4
Tube lights	80	672	7	376.32
Wall fans	55	90	7	34.65
Ceiling fans	75	107	7	56.175
Printers	300	14	7	29.4
Pedestal fans	50	14	6	4.2
Energy saver bulbs	25	123	12	36.9
TOTAL LOAD OF BUILDING				**1192.64**

B. Power Consumption Model

To design and simulate power consumption model, we utilized HOMER (Hybrid Optimization of Multiple Energy Resources) software. This software is used to find optimal design parameters for off grid photovoltaic (PV) system or solar power system in order to achieve economically feasible system. Electric loads are taken as input to carryout simulations based on different system's behavior. As a result, optimized simulation model is obtained in terms of NPC and COE.

The framework adopted for our system is shown in Figure 2

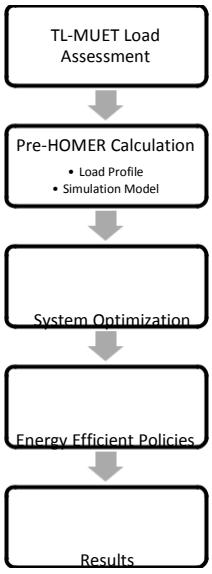

Figure 2 : Schematic diagram showing methodology used for analysis

To obtain electric load of TL-MUET, we used Efergy Energy Monitor to obtain real-time power consumption behavior. Efergy Energy monitor records the power consumption values every 3 seconds and sends it to central hub. These values can be visualized remotely. The results suggest that the power consumption load various during working hours from 8:00 AM to 3:00 PM as shown in Figure 3. Whereas, the load is reduced almost during postgraduate classes starting from 3:00 PM to 7:00 PM. The power consumption load is minimum during off hours.

Figure 4 visualizes the load profile for whole year. We can observe that the power consumption is high during summer season due to the continuous use of air conditioners. The peak load came about to be 322.83

kW in the month of August. This data is useful in estimating the upper limits of power consumption to be used to design off-grid PV solar system.

- Y-axis represent power consumption in Watts and X-axis represent time in Hours

Figure 3 : Load profile for 24 hours at TL-MUET

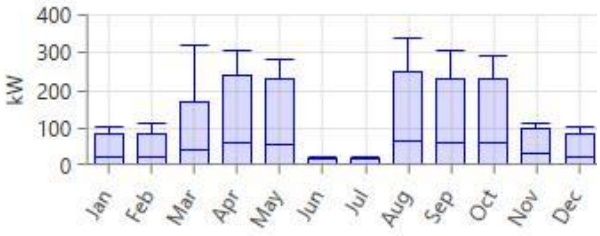

- The box plot shows mean and range of variation in power consumption

Figure 4 : Monthly load profile at TL-MUET

C. Solar Irradiance Profile

In our scenario, the solar radiations data was acquired from National Renewable Energy Laboratory (NREL) database for TL-MUET location. The results shown in Figure 5 suggest that the average and maximum solar radiations are 5.54 kWh/m2/day and 6.73 KWh/m2/day. The blue line in Figure 5 shows clearness index data. The data suggest that the solar irradiance data is sufficient to generate required power load for TL-MUET via PV system. Solar irradiance is the power per unit area received from Sun.

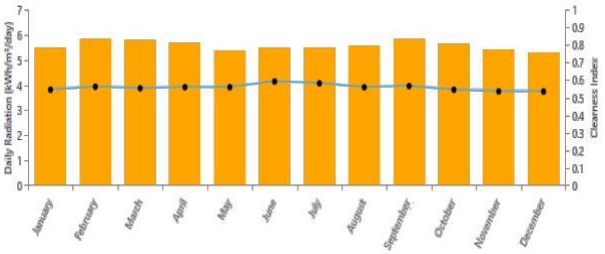

Figure 5 : Monthly solar radiation profile

C. HOMER Simulation Model

To design optimal off-grid PV system to generate electricity that is cost efficient. We used HOMER software tool to design the model.The components consist of PV solar plates, DC-AC convertor, and batteries. In order to meet the required load of 322.83 kW peak demand along with minimum CAPEX, the design specifications are as follows.

1. In Pakistan, solar energy is best available source for generating electricity. To achieve this, different types of PV modules are present, however, we have considered poly crystalline PV module to create an economically feasible system.
2. As solar energy is present during daytime to generate electricity, however during the night when solar energy is absent, hence electricity cannot be generated. In this case, the system needs to calculate and include extra batteries to store excess PV output power / electricity generated during day time.
3. According to load requirements, the system needs to include convertor to convert DC output power to AC output.

D. Energy Efficient Policies

We utilize energy saving policies. To ensure proper luminance, a significant portion of electricity is utilized during working hours between 7 AM to 3 PM. However, we can reduce the consumption of power with proper planning such as use of sunlight as well as reduce the number of electrical sources of luminance. We measured luminance using lux meter at offices and labs for two different scenarios.

1. Scenario-1: The usual electric power consumption at offices and labs
2. Scenario-2: To reduce 50% of electric sources used for luminance during working hours

The results suggest that a lot of energy saving can be achieved with slight compromise in luminance intensity.

We can further reduce power consumption if we can avoid power consumption wastage in office and labs when they are not in use. To reduce the wastage, we propose three schemes.

1. Scheme-1: To reduce 50% of electric sources during inactive/idle hours between 7:00 AM to 3:00 PM. For instance, laboratories should use 50% of total number of air conditioners.
2. Scheme-2: To reduce more than 90% of electric sources during inactive/idle hours.
3. Scheme-3: To reduce power wastage during non-working hours. We assume negligible power consumption.

   In this way power wastage can be avoided energy saving can be achieved

IV. RESULTS AND DISCUSSION

A. Optimization Results

In this Process, HOMER performs several simulations and different optimal configurations are obtained but the most feasible is selected from all configurations.Net Present Cost, capital cost and Cost of Electricity of the optimal PV-battery system are Rs114,540 Rs 94760 and 8.24 Rs/kWh. With 81.6kW of PV, 1kW of battery and 0.204kWof Converter. The NPC and COE of this system is much less as compared to other configurations.

V. CONCLUSION

In our work, we have developed simulation model via real-time measurements to estimate cost saving if we deploy off-grid solar power system at TL-MUET. Moreover, with the use of energy saving polices one can avoid energy wastage and reduce the power consumption load. The simulation model based on real-time measurements also helps to estimate the trend of power over the span of 24 hours as well as during a year-old recurrent duration. The COE and NPC obtained from the system are Rs114,540 and 8.24 Rs/kWh a a result optimization configuration. The COE is more economical as compared to conventional grid system i-e 17 Rs/kWh. The initial investment for this system is higher but they are cheaper once it is installed. The prosed system can over come the power environmental pollution and economic problems.

REFERENCES

[1] V. Oikonomou, F. Becchis, L. Steg, and D. Russolillo, "Energy saving and energy efficiency concepts for policy making," *Energy Policy*, vol. 37, no. 11, pp. 4787–4796, Nov. 2009.

[2] M. E. BASOGLU and B. CAKIR, "Design Principles of and Modelling Self-Sufficient Green Houses," in *International Conference on Renewable Energy Research and Applications (ICRERA)*, 2012, pp. 1–5.

[3] H. Honglian, T. Yan, P. Yujun, and Z. Qianduo, "Carbon Footprint of Energy Consumption and Environmental Impact in Autonomous Regions of China," *2012 Int. Conf. Comput. Distrib. Control Intell. Environ. Monit.*, Mar. 2012, doi: 10.1109/cdciem.2012.51.

[4] T. A. Nguyen and M. Aiello, "Energy intelligent buildings based on user activity: A survey," *Energy Build.*, vol. 56, pp. 244–257, Jan. 2013, doi: 10.1016/j.enbuild.2012.09.005.

[5] C. P. Au-Yong, A. S. Ali, and F. Ahmad, "Improving occupants' satisfaction with effective maintenance management of HVAC system in office buildings," *Autom. Constr.*, vol. 43, pp. 31–37, Jul. 2014, doi: 10.1016/j.autcon.2014.03.013.

[6] M. Pollock, Y. Roderick, D. McEwan, and C. Wheatley, "Building Simulation as an Assisting Tool in Designing An Energy Efficient Building: A Case Study," in *11th International IBPSA Conference*, 2009, pp. 1191–1198.

[7] J. Sousa, "Energy Simulation Software for Buildings: Review and Comparison," in *In Proceedings of the international workshop on information technology for energy applications (IT4ENERGY 2012)*, 2012.

[8] P. E., M. F., F. M., and D. V. P., "GA strategies for optimal planning of daily energy consumptions and user satisfaction in buildings," in *IEEE-12th International Conference on Environment and Electrical Engineering (EEEIC)*, 2013, pp. 440–444.

[9] O. Oladeji and O. O. Olakanmi, "A genetic algorithm approach to energy consumption scheduling under demand response," *2014 IEEE 6th Int. Conf. Adapt. Sci. Technol.*, pp. 1–6, 2014.

[10] T. Zhang, P.-O. Siebers, and U. Aickelin, "Modelling electricity consumption in office buildings: An agent based approach," *Energy Build.*, vol. 43, no. 10, pp. 2882–2892, 2011, doi: http://dx.doi.org/10.1016/j.enbuild.2011.07.007.

[11] Y. Agarwal, T. Weng, and R. K. Gupta, "The energy dashboard: improving the visibility of energy consumption at a campus-wide scale," *Proc. First ACM Work. Embed. Sens. Syst. Energy-Efficiency Build. - BuildSys '09*, pp. 55–60, Nov. 2009, doi: 10.1145/1810279.1810292.

[12] L. Olatomiwa, S. Mekhilef, A. S. N. Huda, and O. S. Ohunakin, "Economic evaluation of hybrid energy systems for rural electrification in six geo-political zones of Nigeria," *Renew. Energy*, vol. 83, no. C, pp. 435–446, 2015, doi: 10.1016/j.renene.2015.04.

2020 5th International Electrical Engineering Conference (IEEC 2020)
``

Impacts of Coal investments under CPEC on National Economy of Pakistan: An Input-Output Analysis

Sumia Khatyan,[1] Faheemullah Sheikh[2], Nayyar Hussain Mirjat[2], Suhail Ahmed Shaikh[2]

[1] Department of Energy system Engineering, Mehran University of Engineering and Technology, Jamshoro, 76090, Pakistan (12el06@quest.edu.pk)

[2] Department of Electrical Engineering, Mehran University of Engineering and Technology, Jamshoro, 76090, Pakista

(engrfaheemshaikh@gmail.com),(nayyar.hussain@faculty.muet.edu.pk),(suhailshaikh393@gmail.com)

Abstract: Coal is the most important energy resource. Coal is important to Pakistan's economy, providing cheap electricity throughout our economy to households, enterprises, manufacturing facilities, transportation and communications systems, and utilities. It is crucial to promote the microeconomic growth of Pakistan's national economy. The INPUT-OUTPUT framework is used in this analysis to calculate the overall effect of CPEC coal investment in the economy of Pakistan.

The overall economic impact coefficients are 2.437 on production, considering in which every component of total FD changes in the investment of coal

The overall economic impact coefficients of Gross Domestic Product (GDP) were 3.0979, despite every component of FD change in the water sector for electricity gas. The direct and indirect effects on the overall CPEC coal project production is 2.44 and the sector's induced impact is 6.803E-07. Higher direct impacts were reported on some of those industries which consume electrical and mechanical energy directly, indirectly. In the future, the effects of coal investment on Pakistan's national economy may increase as the energy crisis decreases.

Keywords: Coal investment, CPEC, Input-Output, Economic impacts ,GDP

I. INTRODUCTION

Utilization of energy promotes economic development of Pakistan. Financial resources of Pakistan are consistently increasing, so for correct execution of states development a large amount of energy is required to satisfy the demand. Financial development and energy are two coordinated diminishing sources of energy, elevating effect of loss in national funds or economy by importing oil. Requirement of energy is rising day by day and is having many effects on the states economy. So, the officials are advising to explore new resources instead ofpetroleumproducts.Transferring through non-renewab le energy to clean energy in less duration seems to be di fficult, because it needs an extensive fundamental invest ment [1].

Pakistan plays Pivotal role for china's (BRI) Grand Belt and Road Initiative, where they are investing about 46 Billion US Dollars as (CPEC) China Pakistan EconomicCorridor.A complete mean project aims at dev eloping infrastructure for energy and connectivity and in creasing commercial buildings. For this an amount of 34 Billion is administered for energy sector project like coal, hydro, wind, and solar. Anticipating CPEC energy projects as obsolete for energy strategy to beat the powercrisis.facedfurther imperious attribute of develop ment projects under the CPEC is to change the energy m ix with a larger share of nuclear, hydropower and renewable energy. Relating to policy records, the state contains "a vast quantity of untapped coal stock around 186 billion tons approximately" and the authorities focuses to improve domestic coal production from 4.5 to 60 million tons yearly

Global beholders and analysts declare that CPEC will help Pakistan to get away of its power shortage. Relating to kugelman (217,p.16) "CPEC can formulate the energy deficit of the country to nil", That varies between 5k and 7k mega watts[2].

The pen pusher notes that "imported petrochemicals pric e a colossal 90% of states oil usage" although the game changer (CPEC) will increase a country's sustainable en ergy mix by more than two hundred million inhabitants. As referred earlier, sponsoring native energy resources can empower Pakistan to minimize overall reliance on imported oil from the Middle East which charge heavily to nation.

Total number of nineteen energy projects involving th e manufacture of new installations and the customisatio n of power lines evaluating upcoming energy needs. Experiencing energy projects comprehensive list, there is mixed of coal, hydel, solar and wind projects. The bulk are coal-based. Present projects of hydel power are comprised of three with total capability of 2700MW.Accordingly, there are numerous sustainable e nergy ventures, most of which, except for Quaid-e-Aza m Solar Park in Bahawalpur, are not exceptional. Punja b with a capacity of 1000 MW with Ten coal-based pow er projects with a total of about 8880MW(CPEC Secretariat 2018)[3].

No doubt coal-based energy plants are cheap source of energy production but on the other hand it has severe environmental effects.

The experts from Pakistan and China can form a joint team, accurately targeting on ''Managing the Hazardous

risk and multifariousness of Natural habitat issues'' to reduce ecological effects of CPEC – related urbanization [4].
Likewise, protection of natural habitat in areas of buildingplants,
geological survey must be carried out and various partne rships with civil society will contribute their positions at different stages of the project to ensure that all partners are involved in the results and consequences. [5]

In this research, effect of coal investment on multiple sectors of economy, sum of output and effects on Gross Domestic Products is estimated and correlate by Wassily Leontief input output model research guide us specified modesty of every single sector on coal investment.

II. METHODOLOGY AND DATA COLLECTION

World Multi - Regional Input Output table (World M RIO) discloses and retains information collected for IO t able.The abstract recommended for country's IO table is , however, disclosed by association and information mai ntained with advanced-country, standardized data which officially announces IO data annually.Model informatio n is already in tabular format separated by columns and rows as outputChristianetat[18].Leontief suggests some assumptions as necessary return to scale, linearity, secto r similarity and no capability constraints, these assumpti ons can terminate table accuracy as Davis et al points ou t[19].IO framework do not display proper data so it is used for short term analysis.

$$xi1 + xi2 + \dots xij \dots xin + yi = Xi \quad (1)$$

Where: xij= Sector development i purchased by sector j, yi is the sector's final demand ,and
Xi = Sector i total output. Where to

$$\alpha ij = xij\,Xj \quad (2)$$

If Xj has complete sector production j Eq. (2) Can be laid down as follows:

$$xij = \alpha ijX \quad (3)$$

Eq. (1) will be,

$$Xi = \alpha i1X1 + \alpha i2X2 \dots + \alpha ijXj \dots + \alpha inXn + yi \quad (4)$$

Matrix notation is given below

$$\mathbf{A} = \begin{bmatrix} a_{11} & a_{12} & \dots & a_{1j} & \dots & a_{1n} \\ a_{21} & a_{22} & \dots & a_{2j} & \dots & a_{2n} \\ \dots & \dots & \dots & \dots & \dots & \dots \\ a_{i1} & a_{i2} & \dots & a_{ij} & \dots & a_{in} \\ \dots & \dots & \dots & \dots & \dots & \dots \\ a_{n1} & a_{n2} & \dots & a_{nj} & \dots & a_{nn} \end{bmatrix} \mathbf{X} \begin{bmatrix} Y1 \\ Y2 \\ \dots \\ Yi \\ \dots \\ Yn \end{bmatrix} = \begin{bmatrix} X1 \\ X2 \\ \dots \\ Xi \\ \dots \\ Xn \end{bmatrix} \quad (5)$$

At Eq. (5) Y(nx1) is the total demand matrix, and X(nx1 1) is the output vector, and A(nxn) is the mathematical c oefficient matrix.:

$$AX + Y = X \quad (6)$$

Eq6 defined as:

$$(I - A)\,X = Y \quad (7)$$

In Equation 7 (I−A) is wassely IO and I matrix is identity matrix simultaneously, Eq. (7) further expressed as:

$$Y = (I - A)^{-1}\,X \quad (8)$$

$(I-A)^{-1}$ is an inverse matrix determination, Eq. (8) the fi nal solution of the IO model is to split the final demand into net export and expenditure final consumption. Now for the Eq. (6) Takes

$$AX + CX + TX + FD = X \quad (9)$$

Eq .nine CX is consumption vectors and TX is net export vectors accordingly, FD, final demand vector and somet imes called main consumption and AX is intermediate o r secondary consumption and primary consumption is th at consumed directly by the end-user.

$$C = \begin{bmatrix} c11 & & & & \\ & c22 & & & \\ & & \dots & & \\ & & & cii & \\ & & & \dots & \\ & & & & cnn \end{bmatrix} \quad (10)$$

$$T = \begin{bmatrix} t11 & & & & \\ & t22 & & & \\ & & \dots & & \\ & & & tii & \\ & & & \dots & \\ & & & & tnn \end{bmatrix} \quad (11)$$

In the above Eq. (10) termcii Measure the industry ratio I end demand in the producti on market. Where in the Eq. (11) tii is the ratio of indust ry i's net export to industry i's results.Eq 9 introduced as

$$(I - A - C - T)\,X = FD \quad (12)$$

The Equations (12): (I − A – C − T) is a matrix of nonsingular and can be written as Eq. (13)

$$(I - A - C - T)\text{-}1 \times FD = X \quad (13)$$

Where the overall FD change is made, the progress will be made in X (production) as seen in eq14.

$$\Delta X = (I - A - C - T)\text{-}1\,\Delta FD \quad (14)$$

Use Eq.14 To evaluate the overall influence, by placing

0 at C matrx, then Eq. (14) only evaluate direct and indi rect impacts, since CX final consumption does not acco unt for in this scenario. Now for the Eq. (14) shall be as follows:

$$\Delta X = (I - A - T)^{-1} \Delta FD \qquad (15)$$

Eq's Difference. (14) and Eq. (15) quantify impacts to c ause.

$$\Delta X \, Inducing = ((I - A - C - T)^{-1} - (I - A - T)^{-1}) \, \Delta FD \qquad (16)$$

III.RESULTS AND DISCUSSION

3.1. Calculation of economic impacts coefficients. Impacts above product are determined by applying Eq. $(I-A-T)^{-1}$ taking column of Electricity, Gas and Water (column thirteen) out of table. All aspects of the sector 13 measure direct and indirect effects on parallel sector. Overall effects are aggregate of direct, indirect and induced effects, by applying Eq.15 direct and indirect effects aredetermined and Eq (16) is applied for calculatinginducedimpacts.When each component shift i n just the Final Demand vector is assumed the same cha nge will occur in the overall results,Final Demand is Tot al Output contributor which is shown in Eq.(6),The mea n that sector 13 has a direct and indirect impact of 2.437 291 and 6.803E-07 in the 2015 Table.Use Eq. (16) the i nduced impacts of the sector are estimated, provided tha t each unit of the final increase or decrease in demand i s 2.513E-10 in the power, gas and water sector;

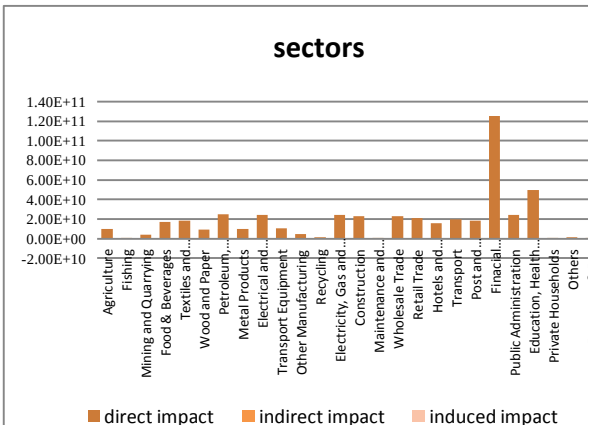

Figure 1. Total Output Impacts of the Coal investment on different sectors (year 2015)

Figure 4.2 shows the total impact of the 2015 input output table on different sectors.Petroleum, transportation, mining and financial intermediation were indirectly effected by the electricity gas and water sector (13),The energy-using field was directly impacted whic h is shown in fig.

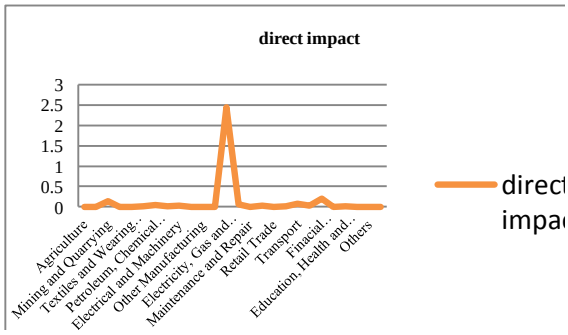

Figure 2. Direct impacts of coal investments in various industries (2015 fy)

From the findings, it can be observed that the direct i mpact of coal production on the electricity gas water ma rket was higher than all other sectors of the 2015 IO tabl e shown in Figure 2. Power Gas Water industry directly used a great quantity of Coal products in the form of ele ctricity and transportation.Consumer of the Coal produc ts directly in transportation and electric power station. F or the above statistics, it is inferred that effects have vari ed according to varyingconsumer preferences. The effec ts of direct impact appear unique and in comparision wit h indirect impact.Total effect on Sector13 were higher i n selected table (2015), similarly second greater effects on mining quarrying were recorded. Total impacts in th ose industries that are explicitly indirectly linked to ener gy usage have been observed.

IV. CONCLUSION

Every developed nation needs bulk energy, the economy of Pakistan needs a sufficient supply of energy.Discove red coal in Pakistan have the potential to play a key role incountry'seconomy.ResultsIn view of each component of final demand change in the electricity gas and water f ield, the overall economic impact coefficients of product ion are 2.437, and the total impact on GDP is 3.0979 , pr ovided
every component of total demand variation in the econo mic impact coefficients of the coal industry. The finding showsthatCPEC coal investments result in an annua l increase in output ranging from ($4679270 billion) to ($4819370 billion) over the entire period under consideration, which corresponds to 3-5% of the c ountry's GDP.Overall impacts on output were high er for those fields that generate and absorb electric al energy or mechanical power.The same as Electri city
sector, Drilling, fabrication, servicing, and repair. Quarry, Building, Servicing.Coal is used in the electri city sector
13, similarly its implications in sector 13 have been reco rded greater.

REFERENCES

[1] Bhayo, F., Shaikh, F., Harijan, K., & Abbas, Z. Impacts of Petroleum Products on National Economy of Pakistan: An Input-Output Analysis.

[2] Kugelman M (2017) The China-Pakistan economic corridor: what it is, how it is perceived, and implications for energy geopolitics. In: Downs E, Herberg ME, Kugelman M, Len C, Yu K (eds) Asia's energy security and China's Belt and Road Initiative. The National Bureau of Asian Research, Washington, DC, pp 15–28Google Scholar

[3] CPEC Secretariat (2018) Energy projects. Retrieved January 08, 2018, from http://cpec.gov.pk/energy

[4] Nabi G, Ullah S, Khan S, Ahmad S, Kumar S (2018) China-Pakistan Economic Corridor (CPEC): melting glaciers- a potential threat to ecosystem and biodiversity. Environ Sci Pollut Res 25(4):3209–3210CrossRefGoogle Scholar

[5] Ali, M. (2018). Pakistan's quest for coal-based energy under the China-Pakistan Economic Corridor (CPEC): implications for the environment. Environmental Science and Pollution Research, 25(32), 31935-31937.

[6] Christian. K.; and Klaus, H.; (2009) "Assessing the Suitability of Input-Output Analysis for Enhancing Our Understanding of Potential Economic Effects of Peak Oil. Journal of Energy V.34, pp. 284-90. [19] Davis H . (1990) "Regional Economic Impact Analysis and Project Evaluation". Vancouver, BC: University of British Columbia Press.

Fault current analysis and its effects comparison on HVDC and HVAC of 660kV Matiari to Lahore project (Pakistan)

Muhammad Usman Javed **Muhammad Ali** **Safdar Raza**

NFC,IET,MULTAN,PAKISTAN **NFC,IET,MULTAN,PAKISTAN** **NFC,IET,MULTAN,PAKISTAN**

Usmanjaved992@gmail.com muhammadali1003@gmail.com Safdar.raza@nfciet.edu.pk

Abstract

Fault current is the flow of abnormal current in transmission system. It occurs in three states i) Sub-transient state ii) Transient state iii) Steady-state. They have an impact on power loss and power system physical parameters. This paper describes a special case of HVDC transmission simulated in ETAP installed at 660kV and performs fault current analysis of HVDC and HVAC. The results show that HVDC gives less value of fault current in case of longer transmission lines

Keywords: *Fault current analysis, HVAC system, HVDC system, longer transmission lines*

I-INTRODUCTION

The whole power system is based on HVAC currently. HVAC reliability and economics need to be analyzed for very long distances [1][2]. This article explores how HVDC is more favorable in comparison of HVAC at very long distances. In this case study analysis a real time National Transmission Dispatch Company, Pakistan project 660KV 4000MW Bipole HVDC Matiari-Lahore which is in under construction phase [3]. This project has 878KM length of project which will connect the power generation in north of Pakistan with the generation of south Pakistan [4][5]. It has power converter stations at both end of HVDC transmission to convert HVDC in to HVAC for the usage [6]. It will connect the Thar coal power generation block at 500 KV high voltage AC with 500 KV grid station after it further it will connect at Matiari HVDC converter station which will convert the HVAC into HVDC through rectifiers and it will transmit to Bi-pole transmission line at 660 KV, it will cross the 878 KM distance at 660KV to Lahore converter station and it will again convert into HVAC through Inverters and it will connect with 500KV grid and transmission system in Lahore. This article simulates the fault current for both HVAC and HVDC for comparison [7][8]. The simulation will be performed in ETAP 16.0 software which is powerful tool to for the simulations of power system [9]. In this simulation all the conductors, transformers and generators are used with the real time and actual data as per Water and Power Development Authority rule and regulations.

Sub transient reactance:

The flux crossing the air gap is massive all along a primary no of cycle .so the reactance through 2 to 3 cycles is least and short circuit current is high. The reactance is named sub transient reactance.

Transient reactance:

After a primary few cycles, the decrement within the r.m.s. value of short current is a smaller amount accelerate than the decrements during the primary few cycles.

Steady state reactance

Finally the transient dies out and also the current reaches a gradual curving state referred to as the Steady State.

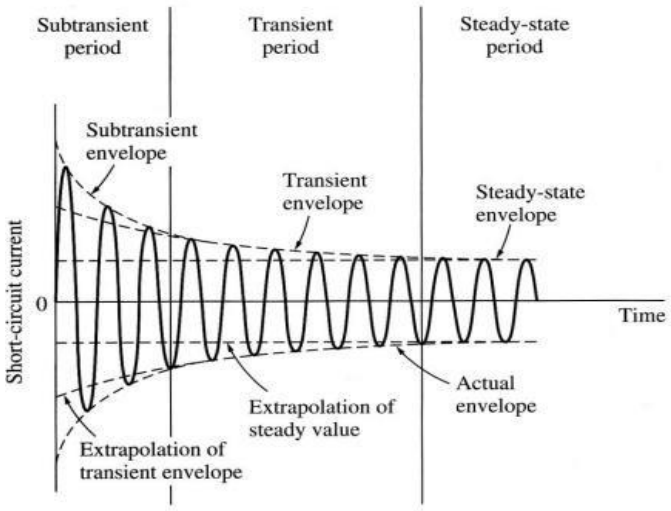

Figure.1 Transient /sub transient and steady state condition

Simulation in ETAP:

The simulation will be performed in ETAP 16.0 which considers in new versions of ETAP which can easilydetermine losses by load flow analysis and fault current through fault current analysis in HVDC and HVAC transmission lines. In the proposed project the conductor used in this project is rail conductor which is heavy duty low resistance conductor. For generation purpose synchronous generators are used which are built in feature of ETAP. For the flow of power transmission line module is used and for the consumption of electric power lumped load is

used.

Single Line Diagram in ETAP:

The proposed HVDC and HVAC system is designed in ETAP. The HVDC transmission system is simulated from Matiari to Lahore with same length and parameters. From Matiari side it's is connected with Thar coal block power generation plants at 500 KV HVAC transmission system. Bus4, Bus6, Bus8, Bus10, Bus12, Bus15 feeding the electric power from power plants to national grid at Bus2 which is connected with DC_LINK1 HVDC transmission system. The HV DC transmission system which has 878 km has rail conductor and it's dc resistance is 0.0180 and has AC resistance of 0.0188 ohm connected with Bus-17 at 500 KV voltage level HVAC.

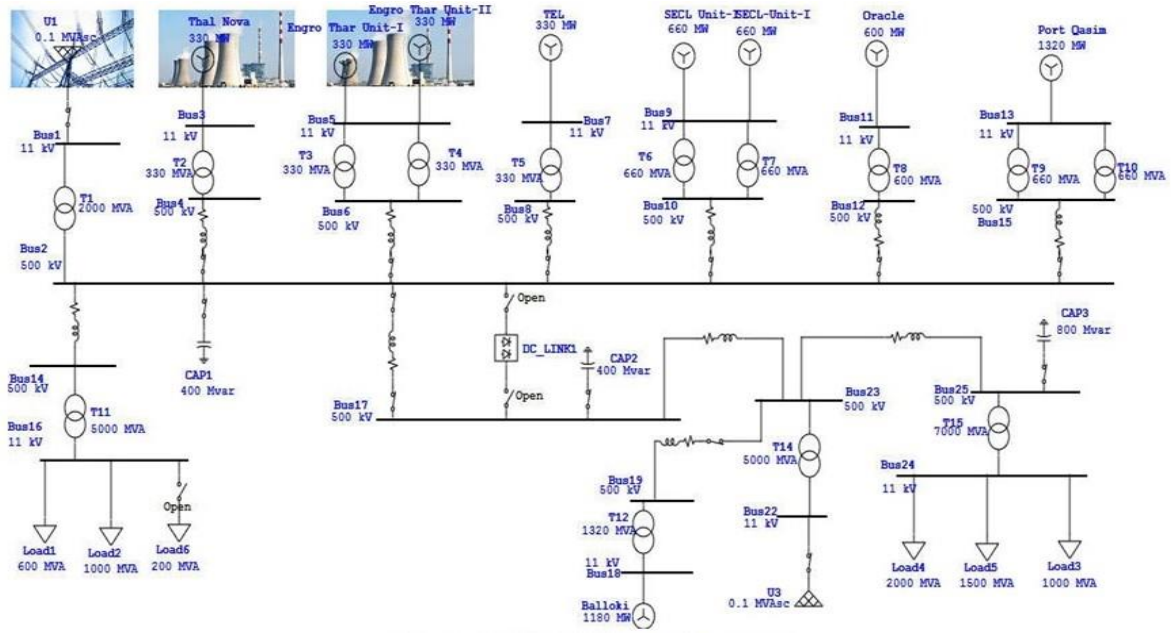

Figure 2. (ETAP Simulation of HVAC &HVDC)

HVDC block has two sections

- Rectifier Section
- Inverter Section

Rectifier Section

Rectifier section has rectifier transformer which step up the voltage from 500 kV to 660 kV HVAC and then feed to rectifier's for the conversion from HVAC to HVDC through silicon control rectifier's (SCR) or power diodes and then feed to transmission line.

Inverter Section

Inverter section firstly comprise with DC to AC inverters which convert the 660KV DC voltages into AC voltages and then Inverter transformer to meet the voltage level of HVAC side which is 500 KV. The Matiari to Lahore line is simulated with the both side power plants for desired power generation and loads connected for power consumption. For voltage step-up unit transformers are also installed at power generation generators.

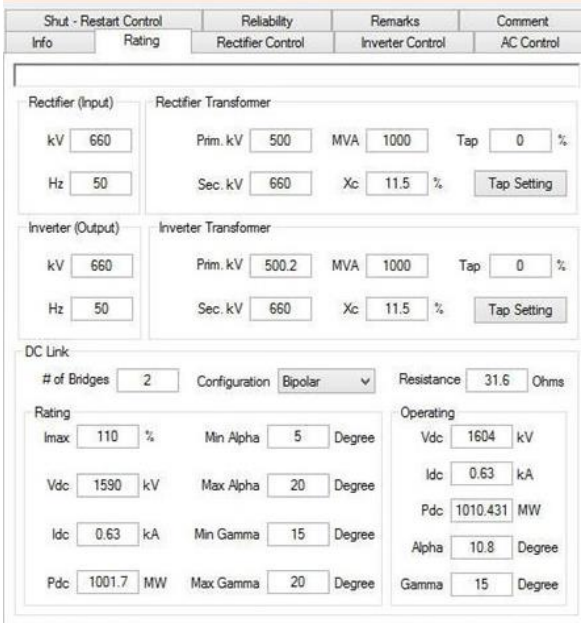

Figure 3. Values for HVDC Block

Case 1: Analysis of fault current at 878 Km HVDC

In this case study fault current analysis is made on 878 Km high voltage dc transmission line with the power flow of 1010 MW from Bus-2 to Bus-17.In this simulation it is depicted that HVDC can be applicable for the flow of bulk power from one side of power network to other side of network. The put up values in the DC block has shown in figure 3.

After putting the values in DC-Link of ETAP for HVDC. The load flow analysis have to be performed for the confirmation of simulation and to check the normal parameters of transmission line and other power system components. In load flow analysis all the power system components, bus voltages, rated power generations on rated voltages, power flow in transmission lines, transformers transformation ratio and their losses, consumption of electrical energy across the loads and other power system parameters should be in nominal ranges. Here in this simulation lumped loads are used for the flow of electrical power from transmission line to electric loads. In this simulation lumped load are used to consume large amount of power. Lumped load is the built in block in the ETAP. Which is the static load and can be used for large power consumption. Just like the load 4 which has power rating of 2000 MVA.

Fault Current Analysis of Case-1.

Fault current analysis of HVDC transmission line at 878 km is further divided in three types

- **Fault Current in Sub-Transient state (1/2 cycle)**
- **Fault Current in Transient (1.5- 4 cycle)**
- **Fault Current in Steady State (30 Cycle)**

Fault Current in Sub-Transient state (1/2 cycle):
When there is short circuited in any element of power system. There is three-phase current rise up with the value of 10 to 18 times of full load current during first half cycle. The impedance reactance during this half cycle is very least and that's why short circuit is very high. This reactance is called sub-transient reactance denoted by X". This state is denoted by sub-transient state. The fault current analysis has made on case-1 at sub-transient state at bus- 2 and bus-17 the busses which are connected with high voltage DC transmission. In fault condition the every source feed the fault current at fault location. In this case fault current has to be determine on HVDC DC_Link which is connected with Bus2 and Bus17.

Fault Current in Transient (1.5-4cycle):
In this state reactance of the fault increased and during this state fault current decreases but in this state the decrement in fault current is not fast as in sub-transient state. This is called transient state and denoted as X'. The fault current analysis has made on case-1 at transient state at bus-2 and bus-17 the busses which are connected with high voltage DC transmission.

Fault Current in Steady State (30 Cycle):
After transient state the fault current reaches to steady state. In this state the current is very less then sub-transient state and reactance is high in this state. But the decrease in current is slow from all previous states. This reactance is known as steady state reactance which is denoted as X. The fault current analysis has made on case-1 at steady state at bus-2 and bus-17 the busses which are connected with high voltage DC transmission.

Comparison of fault current analysis in Case-1 HVDC at 878 km.
The comparison of fault currents in all three states has been made on Bus-2 and Bus-17. The fault current in transient state is very high on Bus-2 and Bus-17 while in steady state the fault on Bus-2 and Bus-17 is quite less than transient state. So these are the current values in HVDC transmission line.

Table 1:(Fault current analysis in HVDC in three transient states)

Fault states	**Case 1 HVDC 1010 MW At 878 km**
Fault current in Sub-Transient state	Bus2: 20.924 KA Bus17:12 KA
Fault current in Transient state	Bus2: 20.924KA Bus17: 10.1KA
Fault current in Steady state	Bus2: 18.988KA Bus17:8.498 KA

Losses in HVDC transmission line in case-1.

The load flow analysis shows the following results of losses in HVDC transmission line in following table.

Table 2: (Power Losses in Case-1)

Transmission Length	**Case 1 HVDC 1010 MW Power flow losses**
878 km	12.542 MW

Case 2: Analysis of fault current at 878 Km HVAC

In this case study fault current analysis is made on 878 Km high voltage ac transmission line with the power flow of 1010 MW from Bus-2 to Bus-

17. In this simulation it is depicted that HVAC can also use for the transfer of bulk power from one side of power network to other side of network. In this case same three types of faults will be analyzed at 878 km

Fault Current in Sub-Transient state (1/2 cycle)
The fault current analysis has made on case-2 at sub-transient state at bus-2 and bus-17 the busses which are connected with high voltage AC transmission line. The results shows that there is 25.109 kA at Bus-2 and 17.329 kA at Bus-17 which is in very large value than in case-1 in sub-transient state.

Fault Current in Transient (1.5- 4 cycle):
The fault current analysis has made on case-1 at transient state at bus-2 and bus-17 the busses which are connected with high voltage DC transmission. Here in this result we can see that the fault current is same as in sub-transient state on bus-2 and bus-17 which is 25.109 kA and 17.329 kA respectively.

Fault Current in Steady State envelop (30 Cycle):
The fault current analysis has made on case-1 at steady state at bus-2 and bus-17 the busses which are connected with high voltage AC transmission line.

In this case the fault current in more than sub-transient state of case-1. So it can be easily determine that the fault current in steady state of HVAC is more than the fault current in sub-transient state of HVDC. So in HVAC the fault current is very high and for interrupting this fault current large capacity circuit breakers have to be need and strong quenching media is required.

Comparison of fault current analysis in Case-2 HVAC at 878 km.
The comparison of fault currents in all three states has been made on Bus-2 and Bus-17. The fault current in transient state is very high on Bus-2 and Bus-17 while in steady state the fault on Bus-2 and Bus-17 is quite less than transient state. So these are the current values in HVAC transmission line.

Table 3: (Fault current analysis in HVAC in three transient states)

Fault states	**Case 2 HVAC 1010 MW At 878 km**
Fault current in Sub-Transient state	Bus2: 25.109 KA Bus17: 17.329 KA
Fault current in Transient state	Bus2: 25.109 KA Bus17: 17.3 KA
Fault current in Steady state	Bus2: 22.884 KA Bus17:15.56.498 KA

Losses in HVAC transmission line in case-2
The load flow analysis shows the following results of losses in HVAC transmission line in following table. Table 4 clearly show that power loss in HVAC system is very high making it in-efficient for very long distance.

Table 4: (Power Losses in Case-2)

Transmission Length	**Case 2 HVAC 1010 MW Power flow losses**
878 km	43.2 MW

Case 3: Analysis of fault current at 500 Km HVDC:
In this case study fault current analysis is made on 500 Km high voltage dc transmission line with the power flow same as in previous case from Bus-2 to Bus-17. In this simulation the fault current analysis will be analyzed on the basis of distance. In this case same three types of faults will be analyzed at 500 km.

Fault Current in Sub-Transient state (1/2 cycle):
The fault current analysis has made on case-3 at sub-transient state at bus-2 and bus-17 the busses which are connected with high voltage DC transmission line. The results shows that there is 20.924 kA at Bus-2 and 12 kA at Bus-17 in sub- transient state.

Fault Current in Transient (1.5- 4 cycle):
The fault current analysis has made on case-3 at transient state at bus-2 and bus-17 the busses which are connected with high voltage DC transmission. In transient state the fault current is less than sub-transient state which is 10.1 kA at Bus-17.

Fault Current in Steady State envelop (30 Cycle):
The fault current analysis has made on case-3 at steady state at bus-2 and bus-17 the busses which are connected with high voltage DC transmission line. In steady state it's depicted that in all cases the peak fault current has reduced to some extent than other states.

Comparison of fault current analysis in Case-3 HVDC at 500 km.
The comparison of fault currents in all three states has been made on Bus-2 and Bus-17. The fault current in transient state is very high on Bus-2 and Bus-17 while in steady state the fault on Bus-2 and Bus-17 is quite less than transient state. So these are the current values in HVDC transmission line.

Table 5: (Fault current analysis in HVDC in three transient states)

Fault states	**Case 3 HVDC 1010 MW At 500 km**
Fault current in Sub-Transient state	Bus2: 20.924 KA Bus17: 12 KA
Fault current in Transient state	Bus2: 20.924 KA Bus17: 10.1 KA

Fault current in Steady state	Bus2: 18.988 KA Bus17: 8.498 KA

Losses in HVDC transmission line in case-3:
The load flow analysis shows the following results of losses in HVDC transmission line at 500 km in following table.

Table 6: (Power Losses in Case-3)

Transmission Length	**Case 3 HVDC 1010 MW Power flow losses**
500km	7.14 MW

Case 4: Analysis of fault current at 500 Km HVAC
In this case study fault current analysis is made on 500 Km high voltage ac transmission line with the power flow same as in previous case from Bus-2 to Bus-17. In this simulation the fault current analysis will be analyzed on the basis of distance. In this case same three types of fault states will be analyzed at 500 km.

Fault Current in Sub-Transient state (1/2 cycle):
The fault current analysis has made on case-4 at sub-transient state at bus-2 and bus-17 the busses which are connected with high voltage AC transmission line. The results shows that there is 25.698 kA at Bus-2 and 18.555 kA at Bus-17 in sub- transient state .

Fault Current in Transient (1.5- 4 cycle):
The fault current analysis has made on case-4 at transient state at bus-2 and bus-17 the busses which are connected with high voltage AC transmission. In transient state the fault current is 18.55 kA at Bus-17.

Fault Current in Steady State envelop (30 Cycle):
The fault current analysis at steady state on bus-2 and bus-17 has performed. These are the busses which are connected with high voltage AC transmission line. In steady state it's depicted that in all above cases the peak fault current has reduced to some extent than other states.

Comparison of fault current analysis in Case-4 HVAC at 500 km.
The comparison of fault currents in all three states has been made on Bus-2 and Bus-17. The fault current in sub-transient state is very high on Bus-2 and Bus-17 while in steady state the fault on Bus-2 and Bus-17 is quite less than sub-transient state. So these are the current values in HVAC transmission line.

Table 7: (Fault current analysis in HVAC in three transient states)

Fault states	**Case 4 HVAC 1010 MW At 500 km**
Fault current in Sub-Transient state	Bus2: 25.698 KA Bus17: 18.555 KA
Fault current in Transient state	Bus2: 25.698 KA Bus17: 18.555 KA
Fault current in Steady state	Bus2: 23.371 KA Bus17: 16.541 KA

Losses in HVAC transmission line in case-4:
The load flow analysis shows the following results of losses in HVDC transmission line at 500 km in following table. Table 8 shows that even at 500 km HVDC system is more efficient than HVAC system.

Table 8: (Power Losses in Case-4)

Transmission Length	**Case 4 HVAC 1010 MW Power flow losses**
500 km	24.7 MW

Conclusion
This paper shows a fault current analysis and comparison between HVAC and HVDC at 660kV transmission system. For better analysis and comparison, both simulation environments are kept same and distance is changed to 878km and 500km.
Fault current in HVAC transmission system is much higher than HVDC system. Also the effects of fault current in HVAC transmission system are highly destructive. But in HVDC, these effects are comparatively negligible and less harmful for longer transmission system.

REFERENCES:

[1] Rahman, Md Mizanur, Md Fazle Rabbi, Md Khurshedul Islam, and FM Mahafugur Rahman; 2014; "HVDC over HVAC power transmission system: Fault current analysis and effect comparison; IEEE *2014 International Conference on Electrical Engineering and Information & Communication Technology*;pp. 1-6.

[2] Meah, Kala, and Sadrul Ula; 2007; "Comparative evaluation of HVDC and HVAC transmission systems; In *2007 IEEE Power Engineering Society General Meeting* ; pp. 1-5.

[3] Siyal, Mohsin Ali, Viwak Kella Maheshwari, Ahmed Mustafa Memon, Lala Rukh Memon, Arsalan Hussain, and Nayyar Hussain Mirjat; 2018; "Techno-Economic Analysis of HVDC Transmission Line Project of China-Pakistan Economic Corridor (CPEC); IEEE *2018 International Conference on Power Generation Systems and Renewable Energy Technologies (PGSRET)*; pp. 1-6.

[4] Khan, Fida Muhammad, Ayesha Abbasi, Muhammad Azam Khan, and Muhammad Imran Khan ;2015; General overview of using High

Voltage Direct Current (HVDC) transmission in Pakistan for maximum efficiency and performance; IEEE *2015 Power Generation System and Renewable Energy Technologies (pgsret)*; pp. 1-5.

[5] Hafeez, Kamran, and Shahid A. Khan; (2019); "High voltage direct current (HVDC) transmission: Future expectations for Pakistan; *CSEE Journal of Power and Energy Systems* 99 ;1-5.

[6] Naeem, Rehan, M. Asad Sarfraz Khan, Zeshan Ali, Wajahat Sultan, and Farhan Naeem ; 2016; Impact of DC grid topology on transient stability of HVDC-segmented power system; IEEE *2016 International Conference on Intelligent Systems Engineering (ICISE);* pp. 51-54

[7] Shair, Jan, Muhammad Abdul Basit, and Rabiah Badar; 2018; Damping low frequency oscillations in an HVDC system using Neuro-Fuzzy SMC; IEEE *2018 1st International Conference on Power, Energy and Smart Grid (ICPESG)*; pp. 1-6.

[8] Lei, Bing, Peng Zhang, Man Zhang, Yuguang Lai, and Lin Guan; 2013; "An operation availability index for the evaluation of HVDC transmission reliability and its influence on the power system; In *2013 IEEE PES Asia-Pacific Power and Energy Engineering Conference (APPEEC)*; pp. 1-5.

[9] Okba, Mohamed H., Mohamed H. Saied, M. Z. Mostafa, and T. M. Abdel-Moneim. ;2012; IEEE High voltage direct current transmission-A review, part I." In *2012 IEEE Energytech* ; pp. 1-7.

2020 5th International Electrical Engineering Conference (IEEC 2020)
Feb, 2020 at IEP Centre, Karachi, Pakistan

Design and Control of Automatic Elevator Using Arduino

M.Faizan Khan-A[1] , Shafique Ahmed Soomro-A[1] , Syed Abid Ali Shah-A[2] , Muhammad Faisal-A[1] , Munam Khalil-A[1] and Mahesh kumar –A[1]

[1]*Faculty of Engineering science & Technology (FEST) Indus University Karachi, Pakistan*
(faizan.khan@indus.edu.pk),(shafiq.soomro@indus.edu.pk), (muhammad.faisal@indus.edu.pk)
(munam.khalil@indus.edu.pk), (Mahesh.kumar@indus.edu.pk)
[2]*Electrical engineering ,Department QUEST Campus Larkana*
(abidshah@quest.edu.pk)

Abstract: The sudden transportation from rural to urban sites has created immense growth in population. This situation has created the congestion issue in residence and there is an essential need for vertical high buildings. As the development in building construction is getting fast with more story level which creates the need for a machine that operates with the latest power controller scheme to save time. This paper proposes the developed model for monitoring and controlling of elevator system to maintain autonomy. The design parameters of the elevator are calculated with an Arduino controller. The system connected with a designed Ethernet card that is assembled with hypertext machine language. This card is designed to solve client problems further more clients easily monitor and control the system in order to monitor the elevator, card is installed in the design system. The card connection also comprises of the sensor module. Secondly, the control of the elevator is attained by a designed graphical user interface system that acknowledges the proper maintenance of the prototype. To validate the effectiveness of the proposed method, the system is analyzed with simulation and hardware assembly. The overall results verify that the Arduino is suitable to monitor the prototype with the help of the webpage through the Ethernet shield.

Keywords*:* Arduino, Elevator, Floors, Liquid Crystal Display Monitor Motor, sensor

I. INTRODUCTION & RESEARCH BACKGROUND

The main necessity of today's world is to save the time that is required to travel. The elevator system is the one that was introduced for high rise buildings to save time and to give people some relaxation. Elevators need a control system for controlling all the components which are connected to the panel. It provides guidance to the elevator cabin from where the call was made and then carries the passengers to different floors. They control all the sensors i.e. opening and closing of doors and many more safety switches. The system is based on relay and contactors logic [1]. The card installed in this system sends the information of the lift through Ethernet to the authority and through this, the authority can be monitored with the parameters of the elevator. Hence all the parameters which are being monitored can be easily controlled. The page is a hypertext machine page whose coding is at the end. The following contributions have been made which are listed as below:

- Status alert capability
- Easy maintenance
- Low cost
- Safety and reliability
- Updated status on the internet after every second

Lifts are utilized around the world as a moving gadget in workplaces, schools, healing facilities and so forth. They ordinarily take the colossal measure of individuals and things on routine premise. In a lift, there is the number of showcase gadgets and all presentations are relegated a particular undertaking. There are diverse insurances that are made, for control disappointment, fire caution; earth tremor and so forth there are distinctive kinds of light that characterizes different positions of lift. Sound data is additionally introduced in the enclosure so the travelers can without much of a stretch be educated about the lift. In addition to this, now day's video gadgets are also introduced to keep away from savagery. A couple of individual's fights that lifts began as clear rope or chain. A lift is essentially a phase that is either pulled or pushed up by a mechanical means. A front-line lift involves a pen mounted on a phase inside an encased space called a shaft. Previously, lift drive parts were filled by steam and water weight drove barrels or by hand. In a "balance" lift, cars are pulled up by techniques for moving steel ropes over a significantly scored pulley, consistently called a sheave in the business [2]. The largeness of the auto is balanced by a stabilizer. On occasion, two lifts are produced with the objective that their automobiles constantly move synchronously in opposite ways, and are each other's stabilizer. The disintegration between the ropes and the pulley furnishes the balance which gives its name.

II. PROPOSED TECHNOLOGY

The need for elevators with developed technology enforces the system operators to apply an optimal monitoring scheme. The currently monitoring and scheduling of elevators in high/ low stories, commercial, residential sectors are not satisfied with existing elevators operations. So the client needs simple monitoring and control systems. The proposed project consists of different types of equipment i.e. Arduino (MEGA- 2560), liquid crystal display (16x2), Relay, Power-supply, Breakers, contactors, Opto-couplers, Transistors (BC-547), overload relay, Phase Failure, Limit switches, Magnetic switches and LM-35 [3]. For the monitoring of the elevator using Arduino

mega along with an ethernet shield is utilized, including the sensors such as IR sensor, oxygen sensor, and load cell. The Mega is compatible with most shields designed for the Arduino Duemilanove [4]. The IR sensor is used to protect humans or any object that comes in between the door. [6-9] If the sensor senses anything between the transmitters to the receiver, the door will not get closed. The load sensor is used to detect the load, if the load is above the maximum pre-set value then the sensor will send a signal to the motor and the motor will not operate until the load comes below with the pre-set value. The load sensor also provides the facility of an occupancy sensor that is, if the weight is at or less than the set value for enough time than it will turn off the fan and lights. The oxygen sensor is used to detect the level of oxygen in the cabin. If oxygen is less as per requirement, the elevator cabin will automatically move to the nearest floor.This paper proposed the elevator which have sending the ststus command to the concerned person or client, who is responsible for the maintenance of elevator. This technology the company can easily maintain the status by just accesing the web page. The technology is feasible for remote location.

III. WORKING

The microcontroller receives the signal from relay after pressing the call button by lift user. The microcontroller rechecks the status of the lift and signals of the optocoupler. The optocoupler drives the relay which drives the contactor and sends a signal to operates the motor until the desired floor is reached. The Ethernet shield is connected to the RJ-45 connector. If any safety or sensor switch is shutdown the cabin also stops, and it generates a warning to the user in the office via Ethernet. The motion of the cabin will not start until the safety or sensor motion starts working properly.

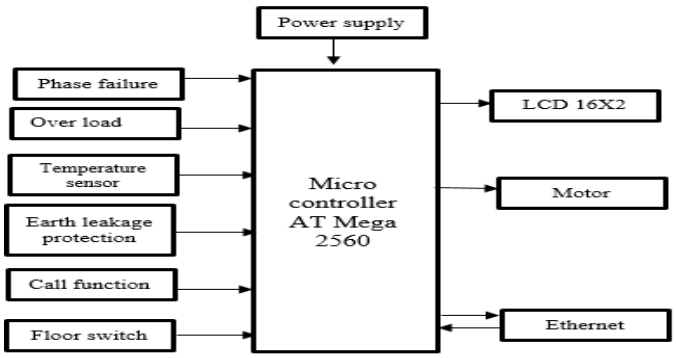

Fig. 1 Working Block Diagram for Elevetor Alert and Control

A. Block diagram for lift alert and control

The block diagram for Arduino based elevator control system is shown in Fig. 1,

1) Arduino controller

An Arduino microcontroller is a user-friendly controlling card that controls different functions and variable levels of complexity. [6].The Arduino Mega 2560 is a microcontroller board based on the ATmega2560 show in Fig. 2. It has 54 digital input/output pins (of which 14 can be used as PWM outputs), 16 analog inputs, 4 UARTs (hardware serial ports), a 16 MHz crystal oscillator, a USB connection, a power jack, an ICSP header, and a reset button. It contains everything needed to support the microcontroller; simply connect it to a computer with a USB cable or power supply to the AC-to-DC adapter . In this elevator system, the Arduino controller is the main element that controls the main parameter of the elevator. Arduino receives the input signal from different sensors that are used on various floors for performing many functions. The Arduino controller senses all the signals that are being given by the sensors. The controller controls the motion of the motor and the result is displayed on the Liquid Crystal Display. The Signals are sent and received by the Ethernet shield.

Table 1 specification of parameters using in Arduino

Micro controller	ATmega2560	DC Current for 3.3V Pin	50 mA
Operating voltage	5V	Flash Memory	256 KB of which 8 KB used by the boot loader
Input voltage	7-12V	SRAM	8 KB
Input voltage limit	6-20v	EEPROM	4 KB
Digital I/O Pins	54 (of which 14 provide PWM output)	Clock Speed	16 MHz
Analog input pins	16	Length and width	101.52 mm And 53.3 mm
Dc current per I/O pins	20 mA	Weight	37 g

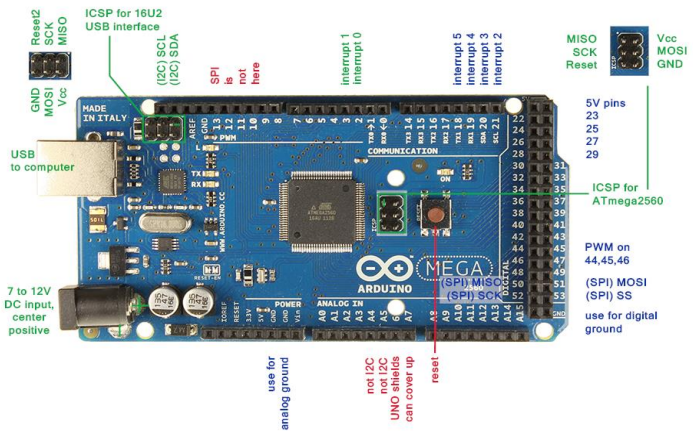

Fig. 2 Microcontroller of arduino mega 2560

2) Elevator Cabin

Elevator cabin has connected with all switches and sensors. It is the one that carries the passengers to their

desired floor. As per the requirement of the building, different sizes of cabins are used

1)Power supply

The 230V AC is step downed. A similar power supply is utilized in the model which is used in the computer system. The dc motor operates at +12V and the controller is operated at +5V.

2) Motor

A motor is an electrical machine which changes over an electrical imperativeness in mechanical energy. The elevator system uses a confined instrument. The lift engine is related to a pulley and ropes are hovered around. The motor that is used to move the cabin is a DC motor that is operated at +12V dc. The bidirection motor is used in this research work. When the polarity changes the motor rotates in the opposite direction. The motor that is attached to the cabin is a DC motor shown in Fig. 3, It can move bi-directionally. Dc motor is used to move the cabin from ground to top floor or vice versa. We have used relays and contractors to make the motor move in the reverse and forward direction. Operating voltages of dc motor are 12V.

Fig.3 Show Dc motor coupling with the panel

3) Sensors

The proximity sensor is used to protect the consumer from damage. If accidentally the consumer comes in between the doors the bpanel will automatically open the door of lift. The oxygen sensor is used to protect human life. If oxygen level falls below the human need thebelevator will automatically reach the nearest floor and doors will get open. The limiy switches are used to identify floor's to the cabin. The load cell is used to detect the load on the cabin. If the load is excessive then the door will not close and lift will generate warning to the user's. Another advantage of this sensor is that if the lift has no user then after some time the electrical parameter will turn off.

4)Load Cell

Load Cell is a transducer or sensor that changes overpower which is to be estimated into an electrical flag. Strain measure is a resistive load cell. At the point when a heap/drive/stretch is connected to the sensor, it changes its opposition. This adjustment in opposition is estimated as far as an electrical voltage when an information voltage is connected. Here it additionally serves as the capacity of inhabitance sensor. At the point when the weight is at or not exactly set at least an incentive for adequate time, then it makes the fans and additional lights off and when the weight is more than max preset esteem, the control framework will stop the engine. The engine will not begin until the point that the heap is dipped under max pre esteem.

5)Buttons

Push-buttons are used in the elevator system. There are two categories of a push button. First is known as maintained push button which is that when we push a button it activates and after pressing it one more time it will deactivate. The other one is a momentary push button that is when we push the button it is activated and when the press is released it deactivates.

6) Limit switch

A limit switch is an electromechanical tool that consists of an actuator that is mechanically joined to set of contacts. An object comes into contact of an actuator, the device operates the contacts to make or break an electrical connection.

B. Display Function:

1)Digital display function

This circuit is designed to display the output of the floors on seven segments IC shown in fig .4, When the limit switch is activated sends a signal to the output to coupler through the diode and display the current status of the specific floor for cabin

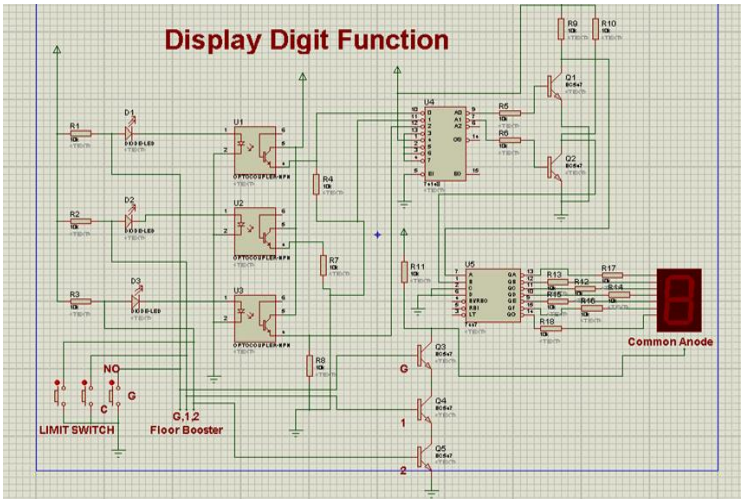

Fig. 4 Circuit Design for display floor output on seven segment

2)Graphical user and interface webpage page

This is a hypertext machine language page show in Fig.5, on which the status of the elevator is displayed. the page is connected via an Ethernet module to show all parameters of the elevator.

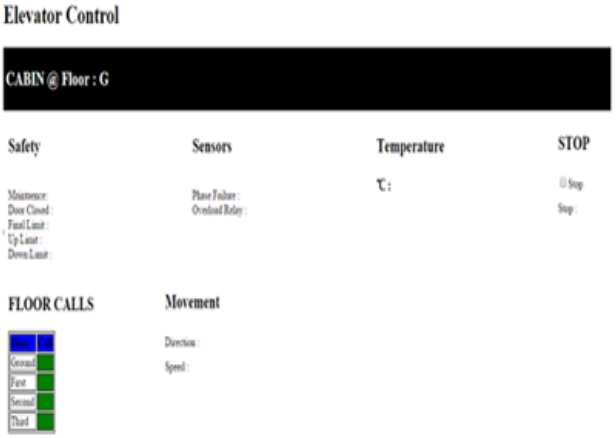

Fig. 5. Show HTML Page

3)Liquid crystal Display

Liquid Crystal Display (LCD) screen is an electronic display module used in a wide range of applications. A 16x2 LCD display shown in Fig. 6, is a very basic module, commonly used in various devices and circuits. This module is preferred over seven segments and other multi segment LEDs. The reasons being: LCDs are economical; easily programmable; have no limitation of displaying.

Fig. 6 Show LCD with different parameters .

4) Ethernet shield

It allows the circuit to send data on internet.It is used in the panel for sending the status of the elevator includes the different parameters through the sensor update. After every two second the status updated on hyper text machine language page.

C. Relay driving circuit

The circuit show in Fig. 7, displays the floor status of the lift on Lcd and the relay drives the motor which takes the cabin to the desired floor. The Arduino sends the signal to the implemented optocouplers and Lcd receives the data. Lcd displays the current floor, temperature & a warning signal if there is an overload in the cabin.

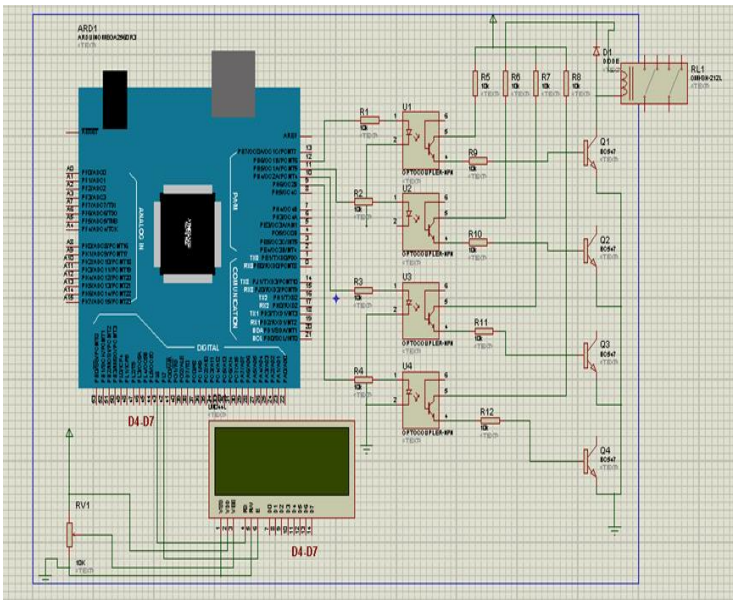

Fig. 7 Circuit Design for display floor output on seven segments and relay drive the motor

D. Input command circuit

This input command circuit is shown in Fig.8. In this experiment, the four different input commands have been used. If there is an emergency call, then the stop button is is pressed whih will suddenly stop the elevator. Additionally, by pressing any input buttons, the Arduino is capable to receives the command through the optocoupler.

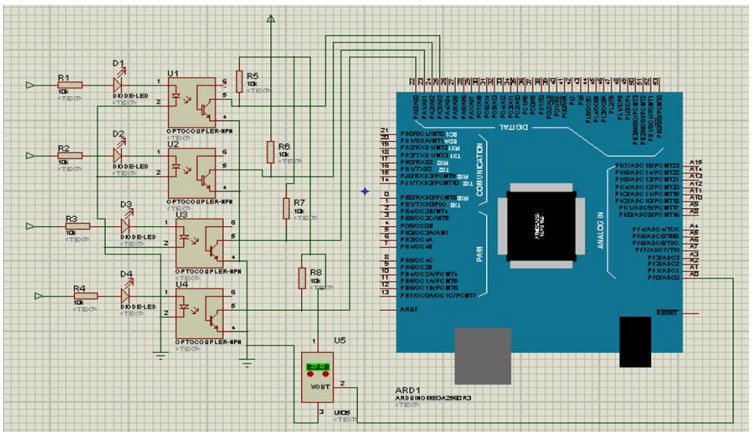

Fig. 8 The designed circuit with input command and emergency stop

E. Call /Booster function

The circuit shown in Fig.9, is used to call the cabin of the elevator at desired floor or it is also used to reach the desired floor.

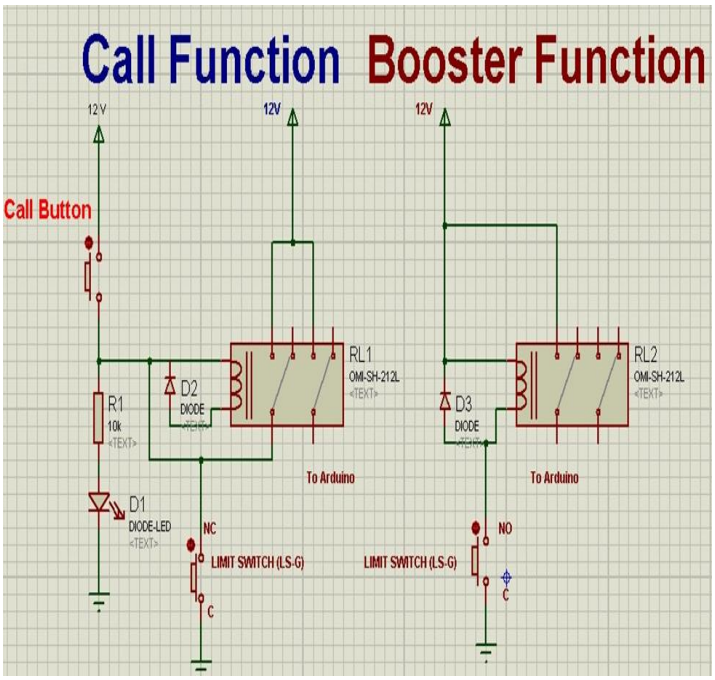

Fig. 9 The circuit design used for calling the elevator

F. Elevator Panel

The elevator panel in the metal box contains all-important protection and other equipment as shown in Fig. 10.

Fig. 10 panel of elevator

IV. MOTIVATION

In Pakistan there are many cities where elevators are a part of daily routine. There are many major companies that install elevator in different buildings. This card is necessary for such companies. In this way it can be monitor all the parameters of elevator by just accessing the web page and through that page we can also control all the parameters.

V. CONCLUSION AND FUTURE WORK

This paper has proposed the speed and the status of the elevator monitored by an authentic team. The team has the capability to control the parameters of lift via the internet. The main advantage is that a monitoring team can remotely operate and control the elevator. The experimental results confirmed the proposed prototype exhibits a promising future application using the IoT scheme and can advance the technology by adding a voice control tool in the elevator. Additionally, the installation of the RFID system can make the system more secure by utilizing sensor technologies.

REFERENCES

[1] M. King, B. Zhu, and S. Tang, "Optimal path planning," *Mobile Robots*, vol. 8, no. 2, pp. 520-531, March 2001.

[2] H. Simpson, *Dumb Robots*, 3rd ed., Springfield: UOS Press, 2004, pp.6-9

[3] M. King and B. Zhu, "Gaming strategies," in Path Planning to the West, vol. II, S. Tang and M. King, Eds. Xian: Jiaoda Press, 1998, pp. 158-176.

[4] Chae, H., & Han, K. (2005, December). Combination of RFID and vision for mobile robot localization. In 2005 International Conference on Intelligent Sensors, Sensor Networks and Information Processing (pp. 75-80). IEEE.Y. Yorozu, M. Hirano, K. Oka, and Y. Tagawa, "Electron spectroscopy studies on magneto-optical media and plastic substrate interface," IEEE Translated J. Magn. Japan, vol. 2, pp. 740-741, August 1987 [Digest 9th Annual Conf. Magnetics Japan, p. 301, 1982].

[5] M. Young, *The Technical Writer's Handbook*, Mill Valley, CA: University Science, 1989

[6] Optimization model for elevator system published in 2011 First International Workshop on Complexity and Data Mining, Nanjing, Jiangsu, China

[7] Design and implementation of the CAN based elevator control system Conference: Information, Communication and Automation Technologies, 2009. CAT 2009. XXII International Symposium

[8] Development of a distributed elevator control system based on the microcontroller PIC 18F458 computational technologies in Electrical and Electronics Engineering (SIBIRCON), 2010 IEEE region 8 international conference , Novosibirsk, Russia

[9] Tall Buildings and Elevators: A Review of Recent Technological Advances. Department of Urban Planning and Policy, College of Urban Planning and Public Affairs, University of Illinois at Chicago, Chicago, IL 60607, USA; E-Mail: profkheiralkodmanyuic@gmail.com Academic Editor: Chimay J. Anumba Received: 26 June 2015 /

Accepted: 31 August 2015 / Published: 17 September 2015

[10] Figure # 2 http://www.instructables.com/id/Arduino-Ethernet-Shield-Tutorial

[11]https://www.arduino.cc/en/Main/ArduinoBoardEthernet/

RESPONDS FOR THE REVIEWER 'S

Paper Title: "Design and Control of Automatic Elevator Using Arduino".

Dear reviewer 's

Thank you very much for your attention and the reviewers for their invaluable comments on our paper. We have considered your helpful advice and revised our paper accordingly. Please find attached the revised paper for your consideration. In addition, we also respond to the comments point to point as follows.

Detailed Reviewers Answers.

Reviewer # 1

Comment 1: Several spelling and grammar mistakes are spread throughout the paper. Kindly pass it through a spell and grammar check. For example, in the abstract 'proposes' is written 'purposes', the sentence 'The methodology used to calculate....' is incomplete and also in the abstract 'This card design to solve.....' should be 'This card is designed to solve'. There are several similar mistakes throughout the article.

Respond: Dear sir I agreed with you. I have gone through the mistakes mentioned by you and have corrected.

Comment 2: Figure 3 is incorrectly labelled '....16x2 LCD.

Respond: Dear sir I have also corrected Figure # 3.

Comment 3: There is no discussion or mention of Ethernet module in the methodology or design as stated in the Abstract.

Respond: Thank you for kind your kind suggestions here I have also added in heading of display function part #4 .

Comment 4: Figure numbers should be numbered like Fig. 3, Fig. 4, etc. They should not have alphabet subscripts like Fig. 3(b.

Respond: dear sir there is no uses of alphabet subscripts in figure # 3 and figure #4.

Comment 5:

No discussion on the Hyper Text Machine Language interface design.

Respond: Thank you for kind your kind suggestions here I have also added in heading of display function part #2 and I also show html page in figure # 5.

Reviewer # 2

Comment 1: Combine Introduction and research background headings. Please refer few more research works. Also, explain your motivation and contribution in more detail

Respond: Dear sir as per your precious instruction. I have also corrected and I added Heading of motivation.

Comment 2: System overview heading should not be in research background

Respond: Dear as per your suggestions I have done it.

Comment 3: In proposed technology section, please point out your added features or uniqueness

Respond: Dear as per your suggestions I have added it.

Comment 4: Fig. 1 and Table. I should be adjusted with column

Dear sir I done it

Comment 5: Text in Fig.2 and Fig. 3 is not readable. Also, please don't use copyright pictures, if necessary, take the permission from commented organization/website etc.

Respond: As for as figure #2 and # 3 are commented, I have made for readable. I have followed copyright law and mention the source of the picture in the reference.

Comment 6: Align Text within headings. For instance, text is misaligned in heading IV

Respond: sir thanks for your suggestion. I done it.

Comment 7: in working section, rather than explaining sensors detail focus on explaining how you have used that in your project.

Respond: Sir thanks for valuable review of my paper. I have clearly focused on my mistakes and corrected all.

Comment 8: Fig.3,4,5 and 6 are not viewable/readable either use both column or placed it in appendix

Respond: As for as figure # 3,4,5,6 and are commented, I have made for readable.

Comment 9: Correct other presentation, spelling and formatting issues

Respond: Dear sir I agreed with you and I I have gone through the issues mentioned by you and have corrected.

Data Acquisition System & Real Time Monitoring of the Parameters of Induction Motor via Wireless Communication.

Maqsood Ali[1] and Shariq Shaikh[2*]

[1] Department of Electrical Engineering, NED University of Engineering and Technology, Karachi, 75290, Pakistan (maqsoodalined@gmail.com)

[2] Department of Electrical Engineering, NED University of Engineering and Technology, Karachi, 75290, Pakistan (shariq.shaikh@hotmail.com) * Corresponding author

Abstract: The aim of this paper is to provide methods and techniques used for wireless monitoring of the parameters of a widely-used induction motor through interfacing of Arduino UNO (for wired communication) and Node Micro Controller Unit (NodeMCU) Wi-Fi module (for wireless communication) with MATLAB (Matrix Laboratory) software. The parameters which can be monitored through the techniques discussed in this paper are current waveform, voltage waveform, temperature (Celsius), rms value of voltage and current, peak to peak values of current and voltage, power factor, magnitude spectrum of induction motor. Technique of carrying out Motor Current Signature Analysis (MCSA) has also been discussed in this paper for health monitoring of the motor.

Keywords: Induction motor, motor current signature analysis, MATLAB, magnitude spectrum

I. INTRODUCTION

Recently induction motors have been employed for numerous applications due to is various advantages. Such as Induction Motors are used for pumping, drilling machine, pressing machine, linear actuators etc. Since there are many uses of Induction Motor so there is a need for data acquisition of its parameters for monitoring and analyzing the motor to ensure flexibility and safe operation. Failures and faults in the motor can lead to great losses in industrial and manufacturing sector. Therefore, it is necessary to detect the fault at its earliest to protect the motor. The health monitoring of induction motor can detect incipient faults of the motor before any major breakdown and unexpected failure. In the present paper the methods of online health monitoring have been discussed which involves monitoring of the parameters of induction motor while it is in the operating state. The methods discussed in this paper will help in reducing major failures, unplanned shutdowns and maintenance costs [1].

The method discussed in this paper involves data acquisition which will help users to perform the automation test and it provides the user to easily monitor the performance of the motor with the help of user interface [2]. The software which is used for data acquisition in this technique is MATLAB (Matrix Laboratory). Arduino UNO (for wired communication) and Node Micro Controller Unit (NodeMCU) ESP8266 Wi-Fi module (for wireless communication) are used for interfacing with the MATLAB. MySQL Database has been used along with phpMyAdmin for administrating the database [3].

In this paper Motor Current Signature Analysis (MCSA) has been discussed for the detection of fault in the motor. The parameters of Induction Motor are monitored in real time and displayed on laptop so that the production will not come to halt and the deviation from the normal operating condition will cater in the little span of time. The respective goal is achieved using microcontroller, laptop, temperature sensor, Current Transformer (CT) and Potential Transformer (PT).

II. FLOW CHART OF THE PROPOSED SYSTEM

The generalized flow diagram for health monitoring and detection of faults in induction motor with intelligent techniques is shown in Fig. 1. Sensors and microcontroller are employed at induction motor to pick up the signals that are detected from the faulty zone which are then displayed on laptop and monitored by operator to take decisions accordingly.

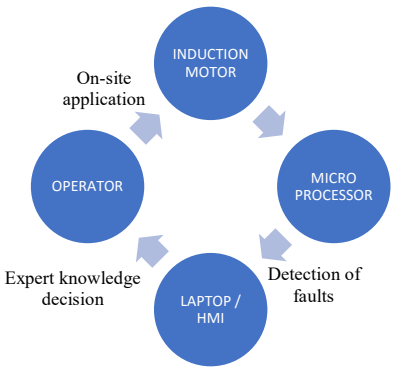

Fig.1. Flowchart of the health monitoring system of induction motor.

III. SYSTEM SETUP

A. Hardware Setup

The system which is discussed in this paper consist of a normal healthy ½ HP (373Watts) single phase induction motor, a ½ HP single phase induction motor with bearing fault, a ½ HP single phase induction motor with rotor fault, a Direct Online (DOL) starter, current transformer

for sensing current flowing through the motor, potential transformer for sensing voltage across the motor, Negative Temperature Coefficient (NTC) thermistor for sensing the temperature of motor's winding, Infrared (IR) sensor for Rotations Per Minute (RPM) measurement of motor. All the four signals (i.e. current, voltage, temperature, speed) are picked up by the analog pins of Arduino UNO and Node MCU ESP8266 for wired and wireless communication respectively. The use of WIFI module (NodeMCU ESP8266) enabled us to receive the data wirelessly on laptop screen.

B. Software Setup

The system archives all of data received through the analog pins of microcontroller in MySQL (My Structured Query Language) database at intervals of 10ms [4]. MySQL is a free and open source database management system. It uses Structured Query Language (SQL). It is used for storing and manipulating the data.

The MySQL database is administrated by phpMyAdmin. It is a free administration tool written in PHP. It is used for administrative handling of MySQL database. It is a control panel from where we can manage our database as shown in Fig. 2.

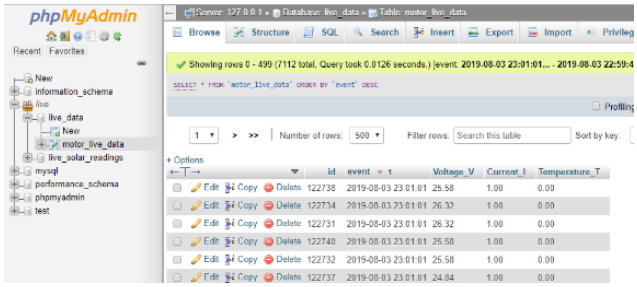

Fig. 2. Data in phpMyAdmin

The data from the MySQL is then transmitted to MATLAB with the help of XAMPP (Cross-platform Apache MariaDB PHP and Perl) for signal analysis. XAMPP is a free open source web server solution that is used by developers to create a local web server. The system processes the raw data through MATLAB code by scaling, filtering and amplifying. This whole process is generalized with help of flowchart which is shown in Fig. 3.

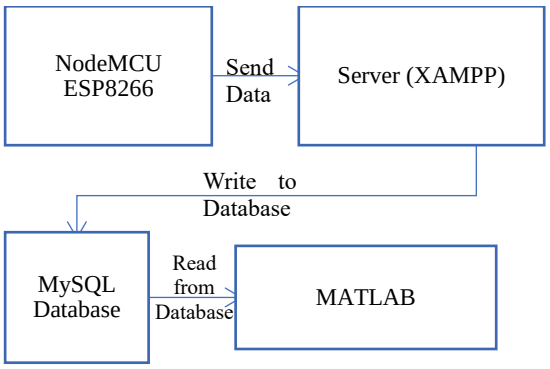

Fig. 3. Flowchart of wireless communication setup

The frequency spectrum in dB of Induction motor is displayed on laptop screen in Fig. 4. and single sided amplitude spectrum of current signal is shown in Fig. 5. whereas current waveform of induction motor is displayed on Smartphone screen in Fig. 6.

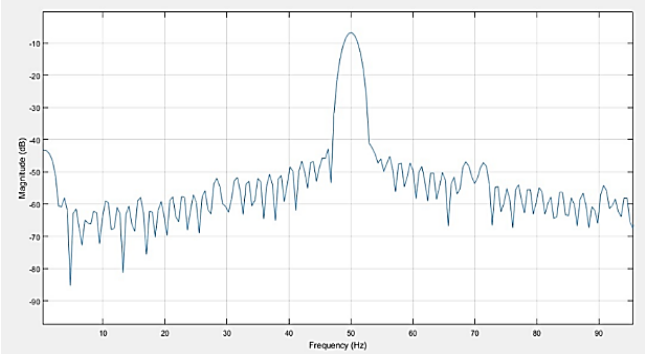

Fig. 4. Frequency Spectrum in dB displayed on laptop

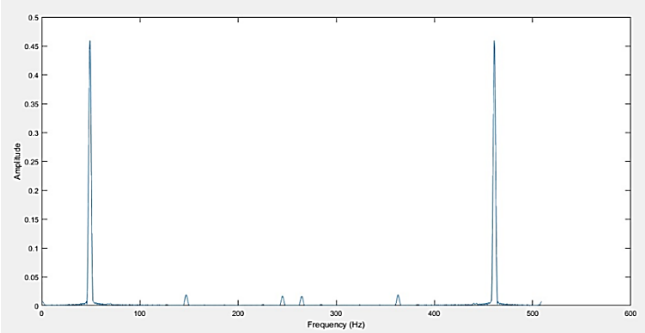

Fig. 5. Single Sided Amplitude Spectrum of current signal displayed on laptop

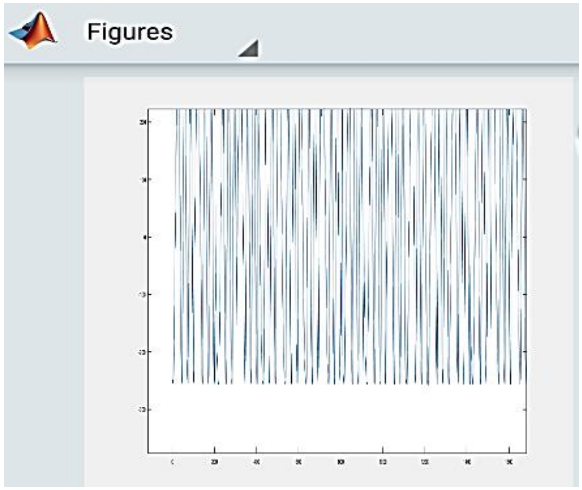

Fig. 6. Current waveform on MATLAB on smartphone screen

Through MATLAB code, the set of data is further processed to determine parameters like magnitude spectrum, power factor, power, rms value of voltage, peak to peak value of voltage and current. A GUI

(Graphical User Interface) is also developed to make the monitoring of motor user friendly which is shown in Fig. 7.

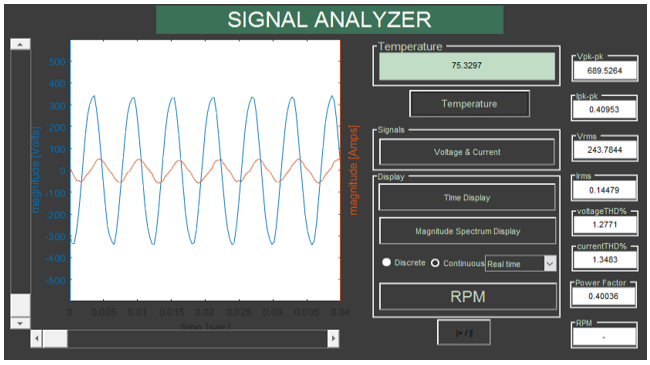

Fig. 7. GUI of Signal Analyzer

IV. MOTOR CURRENT SIGNATURE ANALYSIS (MCSA)

MCSA is a process that is deployed to record motor current values and analyzes them in frequency domain. It is a maintenance tool used for motors. It is used for analyzing induction motors, generators, transformers and other electrical equipment. MCSA monitors stator current of the motor, picks the signal from rotor and that current is sensed by a current sensor. The current signal is then transferred to spectrum analyzer. MCSA can detect faults in an induction motor by analyzing current even if the motor is in service [5].

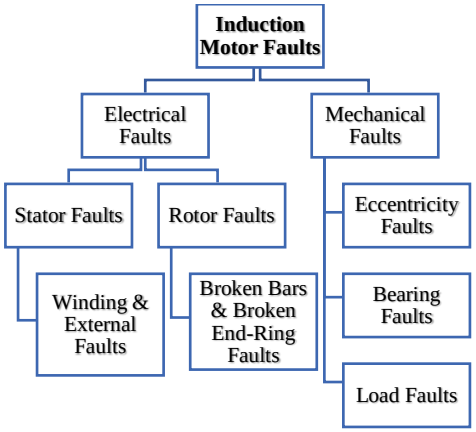

Fig. 8. Types of induction motor faults

The MCSA can detect static and dynamic airgap irregularities, broken rotor bar or cracked rotor end-rings, stator faults, abnormal connection of stator windings, bearing and gearbox failures. In this paper we have focused on two types of faults one is rotor fault and the other is bearing fault [6]. For this purpose, three single phase induction motors are used. Firstly, the healthy motor was tested. Then, tests were conducted on faulty motors.

A. Rotor Faults

In an induction motor, a rotor fault may arise due to electrical failure such as bar defects or breakage or mechanical failure such as rotor eccentricity. Electrical failure occurs due to thermal stress, hotspots, start duty cycles, pulsating mechanical loads or fatigue stress during operations like motor [7]. In this system the rotor fault was introduced by drilling into the rotor bars.

In the Fig. 9, the upper and lower side bands or supply frequency are separated by twice the slip frequency and that slip frequency can be obtained by the following formula:

$$f_b = f_1(1 \pm 2s) \quad (1)$$

where,

f_b = broken rotor bar frequency
f_1 = supply frequency
s = per unit slip

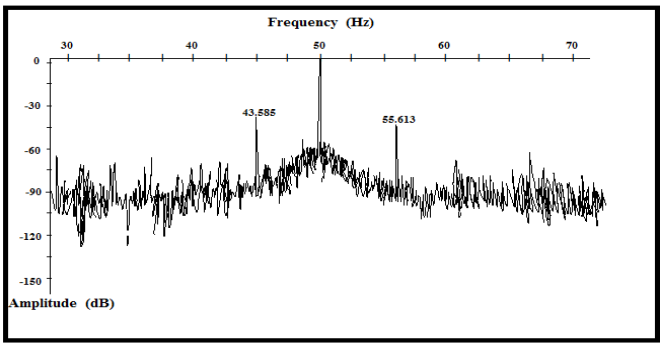

Fig. 9. Frequency spectrum of a motor with broken rotor bars

During broken rotor bar fault the current components in stator windings can be detected at frequencies given by the following formula:

$$f_b = f_1\left[k\left(\frac{1-s}{p}\right) \pm s\right] \quad (2)$$

where,

f_b = broken rotor bar frequency
f_1 = supply frequency
p = number of pole pairs
s = per unit slip
k = 1, 2, 3, …n

B. Bearing Faults

Defected bearings result in mechanical fault. Bearing is an arrangement of two concentric rings. Bearing is said to be defected when misaligned, surface roughness, off-size rolling elements, cracks on rolling surfaces, spalls and pits. Bearing faults are not easy to detect as the rotor cage faults. With the help of frequency components, MCSA can detect bearing faults in between six to twelve balls [8].

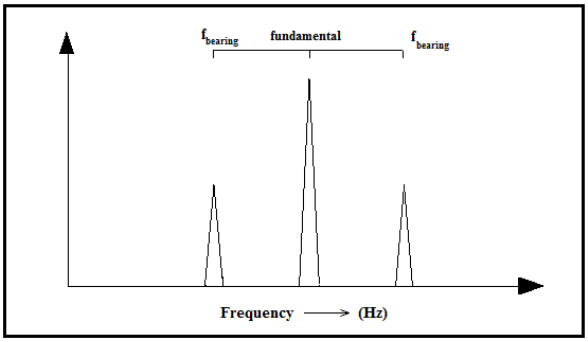

Fig. 10. Frequency spectrum of motor with damaged bearings

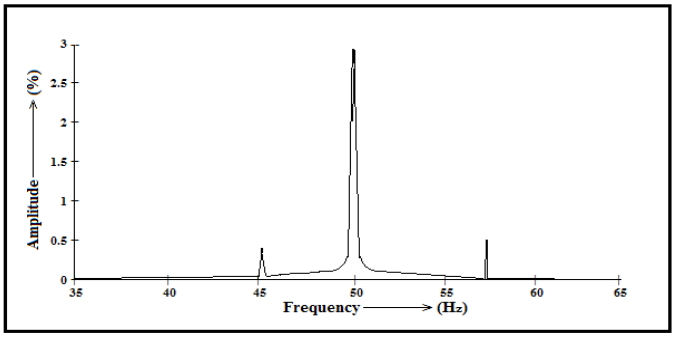

Fig. 11. FFT with initial condition for broken bars

For finding bearing fault the current components can be detected at frequencies given by the following formulae.

$$f_0 = 0.4nf_m \quad (3)$$

$$f_1 = 0.6nf_m \quad (4)$$

where,

f_0 = lower frequency
f_1 = upper frequency
n = number of balls in the bearings
f_m= rotor's mechanical frequency

C. Fault Detection

For the detection of faults, the spectrum of supply current of an induction motor and various frequencies are analyzed. When there is a fault in a motor, the harmonic part of supply current reforms and a resultant backward rotating field in the airgap occurs [9]. In this paper one fault detection technique is discussed which is given below.

D. Fast Fourier Transform (FFT)

MCSA analyzes current harmonics in the stator current that occurs due to new rotating flux components. For measuring motor current, we need a current sensor (CT) and for data acquisition FFT to be performed on stator current. The data is computed as a function of first harmonic amplitude and then analyzed. This reduces impacts of motor's load conditions. The current readings are recorded in time domain and then analog-to-digital conversion is performed. FFT is used to analyze signal in frequency domain. This technique reduces the number of computations. FFT is suitable for invariable signals and not for variable signals [10].

V. CONCLUSION

The objective of this paper has been to develop a parameter, health monitoring and analyzing system for induction motors based on IOT. The timely and precise health monitoring of induction motor can make the system reliable and prevent the motor from any catastrophic/incipient fault. MCSA is highly efficient and cost-effective fault diagnostic tool for the induction machinery. This tool can be employed to rectify and localize variable electrical and mechanical faults in induction motor. The faults in the machine can be detected by screening the magnitude spectrum of stator current. The sidebands appearing around the fundamental frequency and the harmonics give information about the nature of fault. The online health monitoring of the motor via MCSA, also helps in the assessment of wear and tear of remote motors that are inaccessible during processing of plant.

REFERENCES

[1] K. M. Siddiqui, K. Sahay and V.K.Giri, "Health Monitoring and Fault Diagnosis in Induction Motor," *International Journal of Advanced Research in Electrical, Electronics and Instrumentation Engineering,* vol. 3, no. 1, pp. 2320-3765, 2014.

[2] Cakir, H.C. and G. T., "Remote Controlling and Monitoring of Induction Motors through Internet," *TELKOMNIKA Indonseian Journal of Electrical Engineering,* vol. 12, no. 12, pp. 8051-8059, 2014.

[3] Bayindir and S. V. R., "Real-Time Monitoring and Control of the Parameters of an Induction Motor," *ELEKTRONIKA IR ELEKTROTECHNIKA,* vol. 19, no. 10, 2013.

[4] S. Liu, Z. Ji, Y. Wang and Z. Zhang, "Real time state monitoring and fault diagnosis system for motor based on LABVIEW".

[5] S. A. A. R., A. A. and G. Ibrahim, "A More Reliable Method for Monitoring the Condition of Three-Phase Induction Motors Based on Their Vibrations," vol. 9, 2012.

[6] Duan and F., "Induction Motor parameters estimation and fault diagnosis," vol. 1, 2014.

[7] T. Neelam, "Fault Diagnosis of Induction Motor using MCSA," *International Journal of Electrical and Computer Engineering,* vol. 8, no. 1, pp. 13-18, 2016.

[8] K. S. Gaeid, H. W. Ping, M. Khalid and A. L. Salih, "Fault Diagnosis of Induction Motor Using MCSA and FFT," *Electrical and Electronic Engineering,* 2012.

[9] N. Mehla and R. Dahiya, "An Approach of Condition Monitoring of Induction Motor Using MCSA," 2007.

[10] C. Marcelo, J. P. Fossatti and J. I. Terra, Fault Diagnosis of Induction Motors Based on FFT, Intech, 2012.

2020 5th International Electrical Engineering Conference (IEEC 2020)
Feb, 2020 at IEP Centre, Karachi, Pakistan

IoT Based Monitoring for Work efficiency Calculation of a Metal Fabrication Plant

Durr E Shehwar[1*], Dr. Syed Sajjad Haider Zaidi[2] and Dr. Bilal Khan[3]

[1] Department of Electrical Engineering, National University of Sciences and Technology, Karachi, 75350, Pakistan (email@nust.edu.pk)* Corresponding author

Abstract: Process improvement and optimization is the prime goal of every industry. If an enterprise is not continuously improving the way it performs, it will likely fall behind in the market. Succeeding in today's business environment means consistently adopting ways to do things better. With tools for process enhancement, companies can evaluate performance standards and optimize processes without hindering existing team procedures. Descriptive reports and analytics provide insights into delivery trends to remove obstructions, predict future issues, and take proactive decisions to adapt workflow processes for improved productivity.

This paper discusses a comprehensive solution around this problem by modeling a system which can monitor the Overall Equipment Effectiveness (OEE) in real-time using the state of the art technology of Internet of Things (IoT) and cloud computing so that any undesired operation can be diagnosed well before time. This will be achieved by the utilization of real-time data and its prognosis using OEE calculation techniques. Overall Equipment Effectiveness is the critical metric to monitor the actual performance of a tool relative to its performance capabilities under optimal manufacturing conditions. By controlling the system's expected future performance along with pinpointing the exact underlying problem and rectifying it so that abrupt shutdowns are avoided and productivity is not compromised.

Keywords: Industry 4.0, Cloud Computing, OEE, Smart factory.

I. INTRODUCTION

Survival in today's competitive environment has become a great challenge to big as well as small industries [1]. Hence, process optimization is the need of today's world. Rapid technological advancements have upgraded the way industries perform. In order to reduce or eliminate time and resource wastage, unnecessary costs, bottlenecks, and mistakes while achieving the process objective, we need to incorporate latest technologies to the existing system to gain improved efficiency. To carry out this, seamless real time monitoring of process to estimate plant's efficiency is necessary. The lack of such a system results in the unmonitored work and plant's production is affected largely. Therefore, a methodology is proposed to meet this requirement. The benefits it offers are numerous which include faster calculations, reduced cost, reduced labor, minimized error.

II. SCOPE OF WORK

A tool that can monitor work efficiency of working plant in order to maximize Return on Investment (ROI) through optimization of process and equipment usage will help to enhance the efficiency of process. The proposed solution to the fore-mentioned problem is an IoT-based cloud computing system for equipment efficiency monitoring at production line of an industry. In long term, data from the implemented system will help to identify bottlenecks and causes of efficiency losses which can then be used for process optimization to yield enhanced productivity and ensure maximum usage of the available resources [2]. This will ensure timely replacement of faulty equipment which will minimize downtime to ensure high availability which will maximize return on investment. Additionally, in short term, process monitoring can improve day-to-day operation of the system i.e. system upkeep and daily data logging. Furthermore, it can develop quantitative data on reliability offered by the OEE estimation system. This will improve consumer awareness about the significance of checking quality and quantity of delivered output and availability of equipment offered by the proposed system which will improve company's confidence in the field.

Figure 1 Process optimization cycle

III. LITERATURE REVIEW

A rigorous performance measurement system for manufacturing processes is the current demand of global competitive environment. Overall equipment effectiveness (OEE) is one such performance measurement tool that measures different types of production losses and indicates areas of process improvement [3].

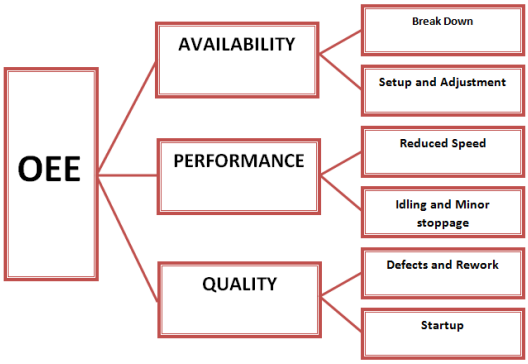

Figure 2 Factors affecting OEE with possible reasons

A. Availability

Availability of machine takes into account the time when machine is unavailable for production because of a fault induction, tooling or being idle [5].

$$\textbf{Availability} = \frac{\textit{Actual production time}}{\textit{Planned production time}}$$

B. Performance

Performance of a machine gives an insight about the speed of a process. It compares the number of units produced by a machine per hour with the ideal production rate.

$$\textbf{Performance} = \frac{\textit{Actual speed of process}}{\textit{Idealcycle time}}$$

C. Quality

Third major factor of OEE affecting plant's productivity is the material wastage and quality shortfalls. Quality of machine's production gives the insight about rejection rate.

$$\textbf{Quality} = \frac{\textit{Number of good parts produced}}{\textit{Total units produced}}$$

The mathematical model of OEE is expressed as:

OEE= Availability × Performance × Quality

The net effect of the components of this framework is seen on the overall equipment performance. A de gradation in one factor downgrades the net performance [5].

The effect of slight efficiency loss of each component can be seen in figure 3.

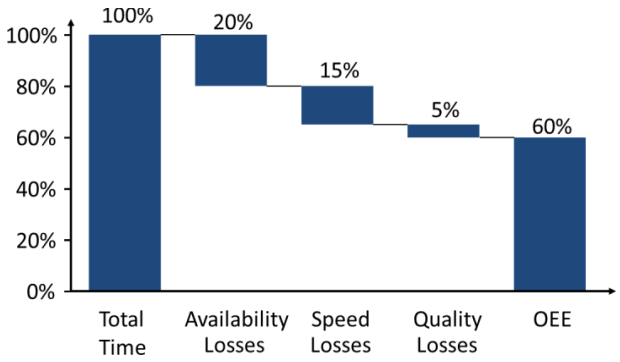

Figure 3 Effect of individual OEE factors

Conventionally, the efficiency of equipment at manufacturing plant of company is estimated monthly or other intervals. The process of data collection and data logging is manual and hence, is more prone to errors and less efficient. Manual procedures slow down the overall process and instant results cannot be observed. Hence there exists a need of a system that can carry out the tasks of data collection, data logging and analysis autonomously. Developing such a system offers greater reliability of results and much quicker insight of the system's overall performance.

IV. METHODOLOGY

The concept of industry 4.0 requires more in-depth research and study to be practically implemented. The complexity and variation of process need to be considered for developing a monitoring system for production line. Inappropriate system will result in inefficient and unreliable data which will ultimately fail to serve the purpose [6].

This is achieved by using IoT and industrial internet technologies. This provides a real time monitoring and data logger to store data for analysis and optimization.

For this purpose, smart sensors for sensing and calculating mechanism to perform analysis are developed and deployed on production line.

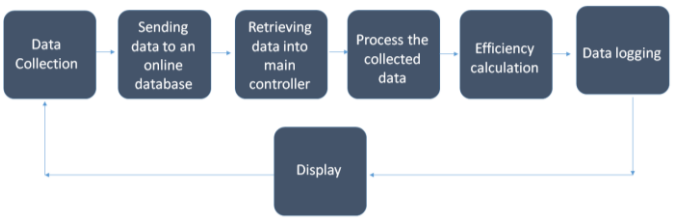

Design Goals

The product will monitor the vital parameters of equipment at plant with the following goals:

The proposed system will be autonomous, reducing both human energy and efforts. The proposed system will be cost effective. The proposed system will be designed to be rigorous and more accurate as compared to conventional methods of OEE calculation.

V. TECHNOLOGY FOR THE IMPLEMENTATION OF INDUSTRY 4.0

After the fourth industrial revolution, there has been a drastic change in the emerging trends in industrial sector. This has provided a new approach to increase productivity of plant by minimizing the operating cost and maximizing the output within the available resources. With technological advancements and researches, such methods are being developed [4].

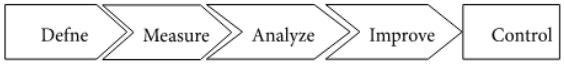

Figure 4 Steps involved in process optimization

Based on the above discussion, there are five steps to achieve the project objectives. This includes:

1. Based on the type of process, appropriate method for collecting data from production line is proposed. For a metal fabrication plant, a technique is developed to calculate OEE of a mechanical press. This is done by using a network of sensors. The next step is to log the collected data in a database. This makes the data readily available for analysis and hence process optimization.
2. After the data has been collected and logged, the next step is to process the data and convert it into useful information. OEE calculation techniques are applied and the raw data is made meaningful to give an insight about the plant's production and equipment effectiveness.
3. Compare the information formulated using techniques with peer machines and standard time for that process and determine bottlenecks and faulty procedures.
4. The most important step is the analysis based on the gained information. This will help to see the true picture of equipment effectiveness of plant and provide conclusions for future changes to increase productivity.
5. Based on the analysis results, steps to optimize the process to yield increased productivity are taken.

The database used for this purpose is FIREBASE, which is a mobile and web application development platform and online real time database. It provides ease of access and authentication to access data with the facility of remote configuration. The collected data is logged on FireBase.

The analysis and calculations involved are performed using NodeMcu which has embedded Wi-Fi module to enable data transference over internet and cloud computing.

V. RESULTS

A comparative study is made and following results are obtained.

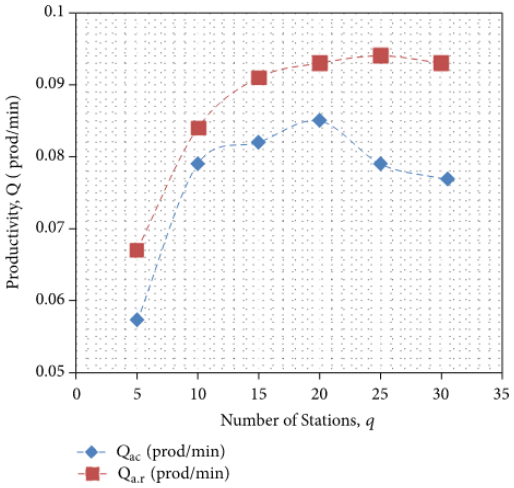

Figure 5 Graph of actual efficiency with average reliability effectively

Productivity of plant refers to the net output produced by the plant and hence is a reflection of OEE of production line equipment. In the results shown above, we see a comparison between productivity of plant with unmonitored OEE and that of monitored OEE. By close observation of both results, we conclude that the efficiency of equipment is greatly increased as we switch from conventional method to the proposed system. The proposed system offers greater productivity by proving a well in time insight of the losses so that necessary actions can be taken.

The second important result that we draw is that 100 percent OEE cannot be achieved due to several limitations. There are certain unavoidable losses that cause a decrement in Overall Equipment Effectiveness. A list of these parameters is attached below in table 1.

Table 1 Comparison of actual and modeled OEE results

	Potential Parameters	Explanation of Parameters	Frequency
(i)	Defected parts	Loss of quality	Frequently happens in all production lines
(ii)	Different reliability of working stations	Slow cycle time and results in performance loss	Frequently happens in all production lines
(iii)	Machining bottleneck time	Availability loss due to shutdowns and stoppage	Frequently happens in serial action production lines
(iv)	Time losses of managerial problems	Availability losses due to unplanned breaks	Minor happening in production line due to avoidable parameter

The Overall Equipment Effectiveness is reduced due to the loss of availability, performance and quality [9]. The reasons of loss vary with process and methodology adopted by individual industry. The net efficiency after considering all losses is much lesser than the ideal efficiency of plant. The efficiency losses are presented via Losses Efficiency Diagram.

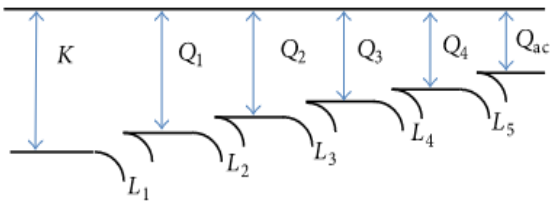

Figure 6 Losses efficiency diagram

Here K is the ideal OEE. L1 is the planned production loss, L2 is unplanned production loss, L3 is the speed loss due to slower processes and L4 is the quality loss. Q1 is the efficiency left after L1 losses. Q2 is the efficiency left after L2 losses. Q3 is the efficiency left after L3 losses. Q4 is the efficiency left after L4 losses. Qac is the net efficiency after all the losses have been considered. This is the true picture of actual OEE.

V. CONCLUSION

The proposed methodology is to be applied to develop a system which can offer real time monitoring and automated data logging equipment used at production plants. The proposed solution will enable system managers to undertake repair/ replacement activities which will in turn reduce downtime and enhance the system's availability. This will ensure timely repair/replacement of different components of the system and process. The product will also offer real-time monitoring features of various parameters of production line. The vital parameters of the system will be made available to the managers placed at remote location through use of advanced IOT and Cloud computing techniques. Moreover, the vital parameters will be processed in an automated manner to generate alarms/ warnings to the system managers. The processing of vital parameters' history can be performed later on the collected data to improve process.

REFERENCES

[1] G. Chryssolouris, Manufacturing Systems: Theory and Practice, Springer, New York, NY, USA, 2nd edition, 2010.

[2] Tan Chan Sin, Ryspek Usubamatov, Mohd Fidzwan B. Md. Amin Hamzas "*Investigation of Mathematical Model of Productivity for Automated Line with Availability by DMAIC Methodology*",2016

[3] J. Heizer and B. Render, Operations Management, Pearson Education, Upper Saddle River, NJ, USA, 2006

[4] P. Muchiri, "*Performance measurement using overall equipment effectiveness (OEE): literature review and practical application discussion"*, 15 Apr 2008.

[5] *"Developing performance measurement system for Internet of Things and smart factory environment"*, Gyusun Hwang, Taylor and Francis

[6] Gill H (2008) from vision to reality: *cyber-physical systems. Present, HCSS Natl. Work. New Res. Dir. High Confid. Transp. CPS Automotive*, Aviat. Rail, pp 1–29.

2020 5th International Electrical Engineering Conference (IEEC 2020)
Feb, 2020 at IEP Centre, Karachi, Pakistan

Image Processing Based Detecting & Tracking for Security System

Atiq Ur Rehman[1], Naqeeb Ullah [1*], Naeem Shehzad [2], Muhammad Daniyal[1],
[1] Department of Electronic Engineering BUITEMS,
Quetta, Pakistan (atiqkhantareen@gmail.com), (naqeeb.ullah@buitms.edu.pk) *Corresponding author (daniyalhaleem117@gmail.com)
[2] Department of Electrical Engineering, COMSATS
Lahore, Pakistan (naeem.shehzad@ciitlahore.edu.com)

Abstract: Security systems are getting more attention and importance. Various security systems based on sensors and wireless communication is available for human force, machinery or electronic applications. These traditional systems have some drawbacks like it has no capability to examine the suspect. And it is very difficult to expand the traditional security system by adding several sensors because of the complexity of the algorithm of the system. Hence, viewing the former points, this paper proposes the method of image processing to design a security system consisting of detection, tracking, via wireless communication and generating an alarm. The Optical Flow technique of image processing is used to detect using motion analysis of two consecutive frames from the imaging source. The block analysis determines the tracking capabilities of the system by the property of Good Features to track. The wireless link between the imaging sources is established through XAMPP. While the functionality of the alarm is performed at the commencement of the detection process. The obtained results are encouraging and increasing the efficiency of the security system.

Keywords: Detection; Embedded systems; Image processing; Tracking, Optical Flow technique

I. INTRODUCTION

The security of public gathering spaces, banks, and large events are crucial for the smooth function of public and government activities at all level. People have a profound trust in any provided areas of well-being just of keeping the core of security in their minds and of their loved ones. The traditional security system relies on a motion sensor, IR sensors, and CCTV cameras to observe a suspect, individual and ongoing activity. The technologies used in these security systems are of diverse behaviors intended for several specified jobs according to their credibility and nature [1].

Generally, the CCTV cameras for crime preventions in the factories' warehouses, and strong rooms of banks just record the situation and do not inform the host side at runtime [2][3]. This paper provides a security system based on Image Processing, which does not only inform the host side at the runtime through alarm but also detects and tracks the present situation by locating the target. Moreover, it also provides the advantage of wireless communication between the imaging sources in the case of a wide area coverage purpose.

II. RELATED WORK

These days the tracking of objects, for example, individuals or vehicles, coming all through specific spaces is constantly a significant issue in security and operation management. For example, in a shopping center, following the number of clients may help the market arranging, staff organization and tracking the number of staff individuals may help in the workforce. In addition, object tracking for spots, for example, banks, buildings, and streets may improve traffic control.

In general, the object tracking is possible by utilizing entryway counters, or infrared sensor to recognize Objects coming all through spaces. Conventionally object tracking methods require a camera above or the entrance/exit way of a place to capture the images. However, these approaches are expensive and require human operator observers who detect any suspicious individual and therefore, challenging to obtain a prior knowledge about all objects in real-time. Therefore a real-time tracking and detecting system is required to detect an unauthorized person in a prohibited area and alarming the security system at the same time

A GSM based home security system includes control panel, door and windows sensors to monitor both coming in and out from the house. These systems use wireless communication to receive the SMS from a cell phone and observe the safety and ensure the security of the home by an SMS [5]. Moreover, Zigbee based parameter monitoring and controlling system using microcontrollers are used to track and secure the environment of industries [6]. However, these systems have no capability to analyzes the suspect and generate a real-time response. Moreover, it is very difficult to expand the security system by adding several sensors because of the complexity of the algorithm of the system.

The present bank security system focuses only on the security of lockers and has a limited level of a security system. The digital cameras used only for monitoring. And require the manual approach to inform the security. Therefore image processing based tracking and detecting system is required for security purpose that alerts the security through a certain alarm in case of any uncertainty [9] [10].

III. SYSTEM CONFIGURATION

The proposed system configuration makes the system cost-effective, reliable and flexible in performance. The

block diagram of the proposed research work is illustrated in Fig.1.

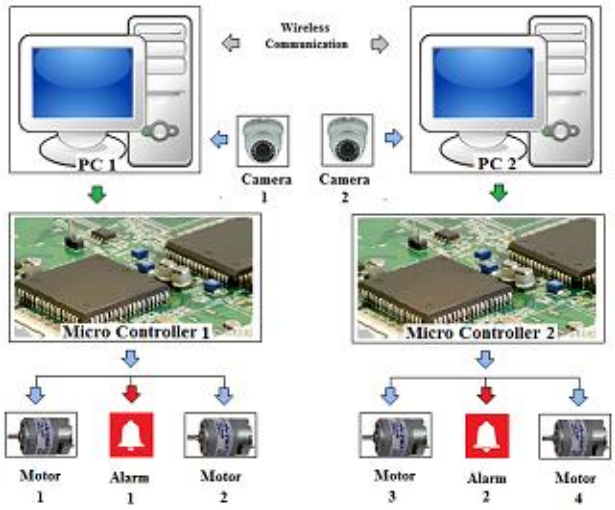

Fig 1. Block Diagram of the system consisting of two same modules with a wireless link as a source of communication between them.

A webcam is the main component, which detects a change in its field of view (FOV) connected with the PC for its working and display. While microcontroller is used to control the motors both in terms of pan and tilt. Further by using the technique of motion control, provides the capability to track the subject of motion along with sending of an alarm signal.

IV. METHODOLOGY

The methodology of the system is based on the technique of Image processing and its subclasses such as the Optical Flow method, Canny algorithm and Block analysis, which helps in the achievement of the results as detecting, tracking and motion control.

A. Optical Flow

Among the parts of the segmentation, a technique to extract information and perform the action according to the requirement is the optical flow method. In this step of the segmentation two or more consecutive frames are taken. Moreover, the pixels are tracked from frame to frame in single mode or can be tracked in the cluster form as well [12].

Firstly, the images are converted into grey scale in order to identify the change and track the object easily. The process on both of them is performed as such that the new image is compared with the background image.

However, this process is also known as the Thresholding process because of applying of the values to the produced change in the background as described through Eq. (1).

$$\begin{matrix} 1 & Di > T1 \\ 0 & Di < T \end{matrix} \quad (1)$$

Where Di - Change between two connective frames
Ti - Thresholding value.

A filter is used to make the process quick and flexible to detection of the change. Moreover, the accuracy of the detection depends upon the size of the subject, its background, connection and distance during the detecting process. A field of view (FOV) of the camera can be easily detected by comparing the two consecutive frames of video streaming to detect the change between them in terms of the change in single or cluster of pixels.

B. Motion Control

The computer or the processing unit capable enough to respond as fast as possible especially as the speed is a critical point. the following procedures are applied [13].

i. Block Analysis

This block analysis is the method that tracks the object based on the Good Features to track the subject extracted from the OpenCV. Thus, various blocks are being created during the tracking process. Now to select the block a condition is applied to select the block with the highest value.

ii. Finding intensity gradient

After smoothing the Image, it is again filtered to get the derivatives of the image both in the vertical and horizontal directions most probably first derivatives. Thus, the direction, as well as the gradient of the pixel, can be easily determined by using the Eq. (2) and Eq. (3) respectively.

$$\text{Angle} = \tan^{-1}\left(\frac{Gy}{Gx}\right) \quad (2)$$

$$\text{Edge Gradient} = ((Gx^2 + Gy^2)^{1/2} \quad (3)$$

Where G_x is the Horizontal direction is is G_y is Vertical direction. The direction of the gradient is always perpendicular to the edges and is rounded to one of four angles to represent the horizontal and vertical directions along with the two diagonal directions.

iii. Threshold values

The intensity gradient value of each edge is comparing with the maximum and minimum values of the threshold. If the value of the intensity gradient is more than the maximum threshold value it will be considered as the sure edge. While the edges having values of intensity gradient between the minimum and maximum values of the threshold will be considered as edges only if they are connected to the sure edges. Further those edges are neglected which are not connected to the sure edge or having a value less than the maximum threshold value as determined for the process [13]. After the selection of the specific block, its center point will be determined based on which the motion will be controlled as the cameras will keep the target in their center. As illustrated in Fig. 2.

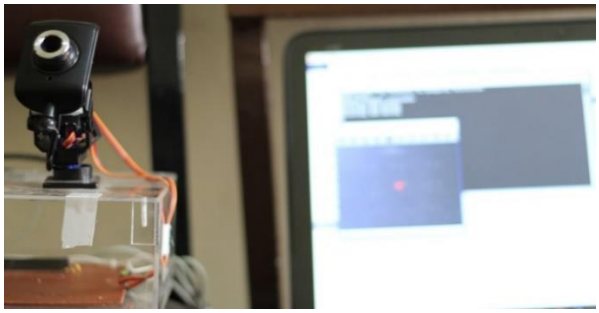

Fig. 2 Center of the block is designed, as shown by a red spot

The center of the block is identified by a red spot in the center. Hence on the basis of the motion of the object, the motion of the cameras will be controlled as when to pan and tilt.

C.Motor Delays

However, the delay in the motion of the motors does wholly depends upon the movement of the subject, the processing speed of the microcontroller, its delays and time associated with its responsively. The control structure of the motors is shown in Fig. 3.

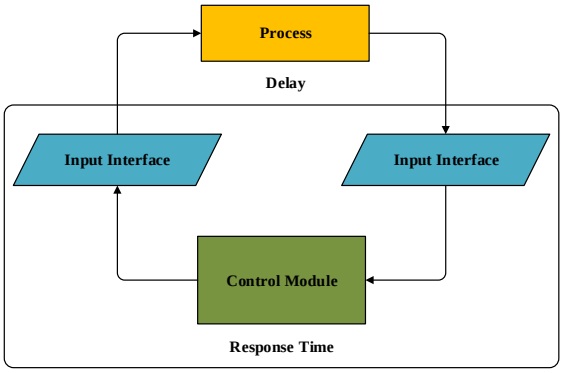

Fig. 3 Motor delay control for the purpose of the precise motion of the motors w.r.t camera

By motor delay control the process can be made more responsive and quicker by decreasing the size of the image, as a smaller number of pixels will be involved, with less memory transportation between the controllers and imaging source during the process of live surveillance.

V. RESULTS

The following results are achieved after the successful running of the system which is given below

A.Detection

To detect the face using the property of the Good Features to Track. The proposed system can detect any type of the object within the installed area up to a distance of 12 feet approximately by one module. While the time interval for the system to detect any unauthorized entry is about 1.5 seconds as illustrated in Fig. 4.

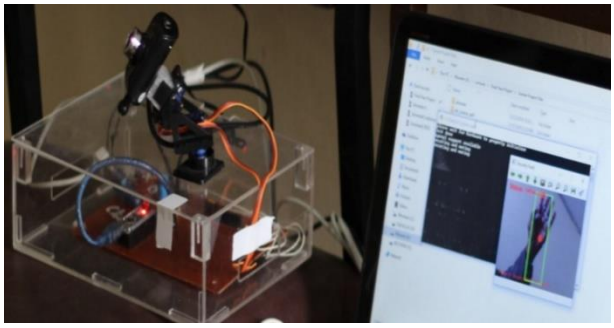

Fig. 4 Detection property of the system

B.Tracking

The tracking of the motion of the subject within the prohibited region pan and tilt the camera with the help of servo motors. This function of the project works as whenever there is any subject of motion, it will be tracked until the last range of distance value is achieved by the camera which is approximately 12 feet after onward the subject of motion is tracked by the camera of the second module after communicating through the established wireless link between them. The following observations were concluded which are mentioned with the help of graphs.

i. Distance

As shown in Fig. 4 the distance is inversely proportional to the detection and tracking properties of the system

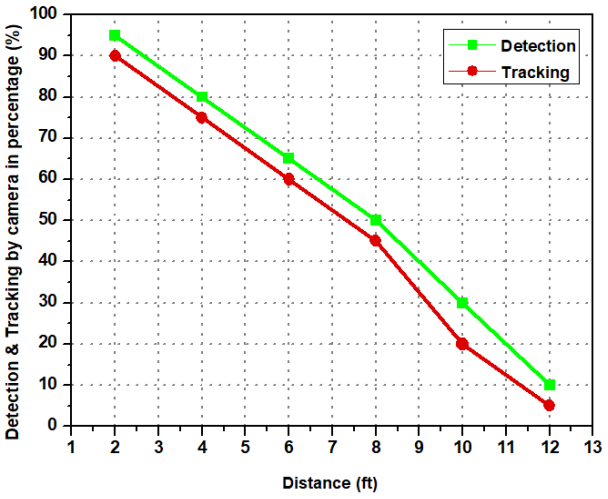

Fig. 4 Detection and tracking by camera vs. distance

ii. Light intensity

Light intensity is among main factors which will greatly affect the working of the system both in terms of detection and tracking of the object through the camera. After running the project in different light intensities, the following observations are achieved shown in Fig. 5.

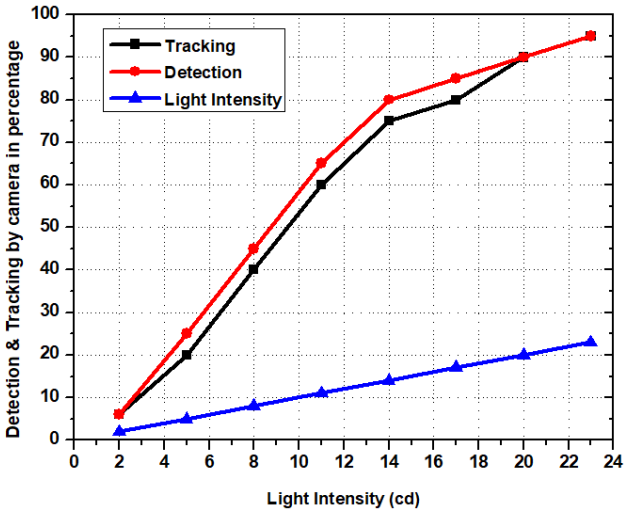

Fig. 5 Detection and tracking vs. light intensity

iii. Speed

Fig. 6 shows the results achieved with the help of the human motion and a stopwatch representing detecting and tracking accuracy in percentage on the y-axis and speed in meters per second on the x-axis respectively.

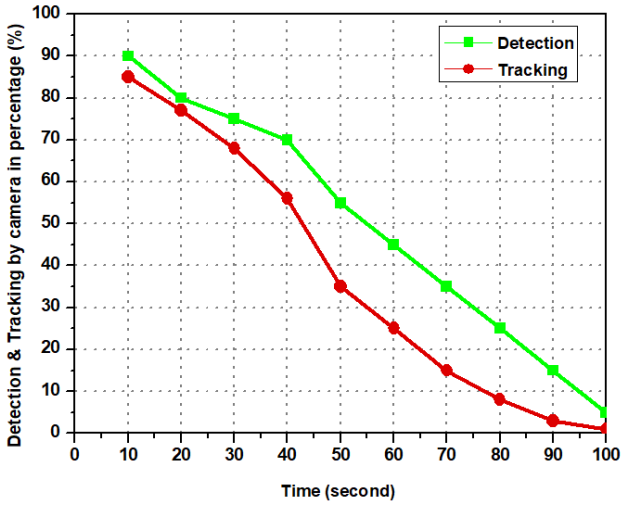

Fig. 6 Detection and tracking by camera vs. speed

VI. CONCLUSION

In this paper, image processing based detecting and tracking system is proposed for monitoring public gathering venues like railway stations, banks, airports, and stadiums. The proposed system uses the Optical flow method with the Canny algorithm along with the property of Good Features with pan and tilt of the camera to Track and detects any type of the moving object. Moreover, an alarm will be played automatically whenever there is any unauthorized entry into the entrance prohibited region. Moreover, in this paper it has observed that distance between the object and tacking system is inversely proportional to detection and tracking properties of the system .However light intensity of the light is inversely proportional to detection and tracking accuracy. Though, the speed of the moving object is also inversely proportional to the accuracy of the detecting and tracking system. In the future, the accuracy and performance can be enhanced by implementing artificial intelligence and advanced moving object detection methods.

IV. REFERENCES

[1] J. Wolfendale, “Terrorism, security, and the threat of counterterrorism,” *Stud. Confl. Terror.*, vol. 30, no. 1, pp. 75–92, 2007.

[2] E. L. Piza, B. C. Welsh, D. P. Farrington, and A. L. Thomas, “CCTV surveillance for crime prevention: A 40-year systematic review with meta-analysis,” *Criminol. Public Policy*, vol. 18, no. 1, pp. 135–159, 2019.

[3] G. Alexandrie, “Surveillance cameras and crime: a review of randomized and natural experiments,” *J. Scand. Stud. Criminol. Crime Prev.*, vol. 18, no. 2, pp. 210–222, 2017.

[4] Q. I. Sarhan, “An Integrated Real-Time Vision Based Home Security System,” *Int. J. Adv. Res. Technol.*, vol. 2, no. 5, pp. 331–336, 2013.

[5] Arijit Pal, Akanksha Singh, and Bijay Rai, “GSM Based Home Automation, Safety and Security System Using Android Mobile Phone,” *Int. J. Eng. Res.*, vol. V4, no. 05, 2015.

[6] N. Ullah, M. S. Akram, H. U. Buzdar, A. U. Rehman, M. A. Khan, and S. Khan, “ZigBee-based Parameter Monitoring and Controlling Scheme for Multiple DC Motors,” Indian J. Sci. Technol., vol. 13, no. February, pp. 725–734, 2020.

[7] Q. Zhu, “Data Acquisition Technology of Air Pollution Sources in Ecological Monitoring Database,” vol. 28, no. 107, pp. 3035–3044, 2019.

[8] N. C. C. U. Ren C. Luo, IEEE Fellow, Te Y. Hsu, Tung Y. Lin, “No Title,” in *The Development of Intelligent Home Security Robot*.

[9] R. T. Collins and T. Kanade, “A System for Video Surveillance and Monitoring Robert,” *IEEE Trans. Pattern Anal. Mach. Intell.*, vol. 22, no. 8, pp. 745–746, 2000.

[10] R. M. DA Monroe, “Portable, wireless monitoring and control station for use in connection with a multi-media surveillance system having enhanced notification functions.”

[11] C. Stauffer and W. E. L. Grimson, “Learning patterns of activity using real-time tracking,” *IEEE Trans. Pattern Anal. Mach. Intell.*, vol. 22, no. 8, pp. 747–757, 2000.

[12] S. Sutton, Richard, “Learning to Predict by the Method of Temporal Differences,” *Mach. Learn.*, vol. 3, no. 1, pp. 9–44, 1988.

[13] C. Bregler, “Learning and recognizing human dynamics in video sequences,” *Proc. IEEE Comput. Soc. Conf. Comput. Vis. Pattern Recognit.*, no. June, pp. 568–574, 1997.

[14] “XAMPP https://www.apachefriends.org/index.html (last access: 29 November-2019).”

2020 5th International Electrical Engineering Conference (IEEC 2020)
Feb, 2020 at IEP Centre, Karachi, Pakistan

Security, Privacy and Trust using Blockchain in Industrial Internet of Things (IIoT): A Review

Faizan Hussain[1], Adnan Ahmed Siddiqui[1], Iqbal Uddin Khan[1], and Fahad Rafiq[1]

[1] Department of Computing, Faculty of Engineering Science and Technology (FEST), Hamdard University Karachi, 74600, Pakistan

Faizanhussain535@outlook.com, Adnan.Siddiqui@hamdard.edu.pk, Iqbaluddin.khan@hamdard.edu.pk, and engr.fahadrafiq@gmail.com

Abstract: With time there have been significant progressions that occurred under the umbrella of information technology. Internet of Things has been considered as one of the most active cultivation that had taken place and supports people in the provision of significant ease. In addition, with time the concept of the internet of things has also been improved which is depicted in its different generations. Internet of things played an essential role in several vicinities such as schools, medical, agriculture, and other areas; however, in industries, the concept of industrial internet of thing has also been stimulated. The term industrial Internet of things has been summarized with several development and activities that have been involved in the evolution of different processes and procedures of industries such as production, automation, logistics that had an impact on productivity. In addition, the concept of industrial Internet of things could also be improved with the help of Blockchain. Therefore, with regards to security, privacy, and trust in accordance with Blockchain has been delineated in this paper comprehensively that help the readers in the development of relevant knowledge and information concerning security, privacy and trust using blockchain in the industrial internet of things.

Keywords: IoT, IIoT, Blockchain, Information Technology.

I. INTRODUCTION

As per [1] the concept of Internet of Things (IoT) is an interrelated system of computing devices, digital and mechanical machines, different objects and others that support in the provision of unique identifiers along with the capability to transfer the information or data over a network which requires H2H human-to-human or H2C human to computer interaction adequately. IoT has also been referred to as the interconnection of networks that are often fortified with the ubiquitous intelligence [2]. With time IoT increases the ubiquity of the internet through integrating every object for communication, connection, and interaction via the embedded system [3]. Moreover, this leads to the highly distributed network of devices that have been communicating with end-users as well as other devices adequately.

In [4] author highlights that IoT has also come up with remarkable opportunities aimed towards making improvements in the quality of our life. In addition, such aim of IoT has been discussed by [5] in which the author states that the aim of IoT has been accomplished and occurred under the umbrella of four different generations known as 1.0, 2.0, 3.0, and 4.0. However, the concept of IoT generations has also been cultivating towards the next generations of the Tactile IoT that brings together the hyper-connectivity under the banner of 5G and beyond, computing edge, DLT Distributed Ledger Technologies, augmented and virtual reality, Artificial Intelligence (AI) and Blockchain transformations. Moreover, IoT is playing an active role in the provision of significant aspects to the end-users; however, it can only be attained through making adequate interventions and actions by focusing on security, privacy, and trust [6]. Therefore, it can be stated that this ultimately helps in making the impact of IoT more prominent among the globe. Currently, in IoT to maintain its security, privacy, and trust there has not been any standard developed [6]. Although there have been several platforms such as big data and knowledge, EPC Global Electronic Product Code, or EPCTM, Software/Run-time Layer Security and numerous others have been proposed and studies such as in [7], [8], [5] but there has not been a proper standard defined.

In addition, the aim of this paper has been formulated with regard to the industrial internet of things. Moreover, concerning the IIoT same aspect of the standard has also been eliminated. Although IIoT in several developed and under-developed countries is making a remarkable impact there is the necessity of proper standard and framework aimed towards maintaining and managing the data. This is because with time the amount of data had increased and continuously increasing. Similarly, [9] has investigated that in industrial and in accordance with the 4.0 revolution the amount of data will be enhanced as compared to the previous generations. The rationale behind this is the technology which is making people's lives easier and therefore, technology means are enthusiastically adopting by them.

There must be an adequate approach, standard or framework developed which might be helpful in order to attain the security, privacy, and trust of data in the IIoT. Through Blockchain such standard could be achieved in the IIoT which has been further discussed in this paper comprehensively. The layout of the paper has been divided into five sections such as introduction, related work, methods, discussion, and analysis, along with conclusion and recommendation. Fig. 01 depicted such facet pictorially.

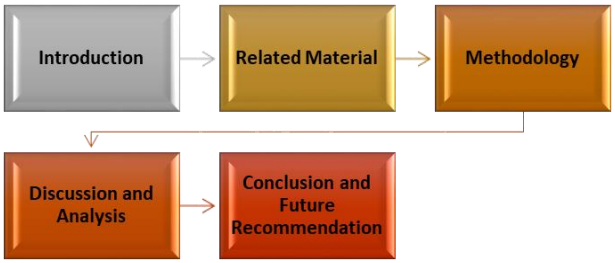

Fig. 1 Layout of Paper.

II. RELATED STUDIES

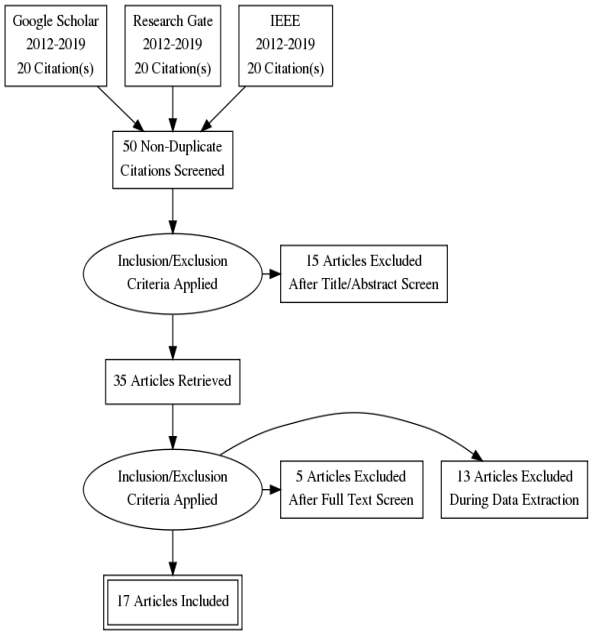

Fig. 2 Literature Search via PRISMA

According to [10], with time IoT has been evolved so as to their centralized architectures that are aimed towards device data manipulation. According to [11] Blockchain and its distributed ledger technology resolve several issues that might occur in the domain of IoT. [5] has posited that the use of Blockchain technology is the domain of IoT is facilitating the sharing of resources and services and also help in the provision of automation aspects to perform their function in a secured manner. Therefore, it can be stated that Blockchain in the domain of IoT has been playing an active role in the provision of a secured platform. The authors of [12] demonstrated that the amalgamation of IoT with Blockchain is a robust technique lead towards the novel business model that could improve the traditional aspects of industrial IoT and might help in the attainment of automaton aspects in several areas of industries.

It is a combination that has been formulated with regard to business models and distributed applications. The utilization of Blockchain in the infrastructure of IoT as a data storage management technique might play an essential role in data manipulation [13]. In addition, it has been discussed earlier that in IIoT there has been a significant amount of data that is getting increased with time. However, Blockchain might be considered as an effective approach with regards to data storage and therefore, such concept has also been supported by [14], [15], [16] in which author stated that Blockchain is the most discussed technology nowadays precisely using for the data manipulation through ledger-based technique. In addition, such a ledger-based technique accomplishes data processing aspects in the big system. Therefore, it can be stated that in IIoT there has been a vast amount of data; however, Blockchain ledger-based technique for data processing will be beneficial to eradicate the complexities that have been occurred in IoT previously. Blockchain data stored through IoT devices might exchange easily and might be stored as a unique transaction [12]. However, such a statement has also been cited in [5] where the author has stated that the unique transaction of Blockchain subsequently distributed and aimed towards the amid nodes that ensure the security and integrity of the communication between them.

The decentralized peer-to-peer discussed in [17] is fundamentally grounded on Blockchain networks for Industrial IoT. The consensus-driven and decentralized structures of Blockchain help in the attainment of the secured ecosystem of IoT [17]. Recently, [18] has proposed that token-based access control and the Fair Access model concept that might be accomplished through Blockchain in IoT that facilitates accessing the control mechanism for the transactions that come under the umbrella of Blockchain infrastructure. IoT platform under the umbrella of IBM Watson supports the private ledger through Blockchain that helps in sharing IoT through the transaction [19]. Furthermore, (Autonomous Decentralized Peer-To-Peer Telemetry) ADEPT, a research-oriented project under the umbrella of Blockchain in the domain of IoT utilizes the technology such as BitTorrent, Telehash, Ethereum and others [20].

According to [12] Blockchain technology and its implementation in IoT comes with the solution of data storage management. It also comes with the advantage of the infrastructure that facilitates integrity, autonomy, scalability, security, privacy, trust and resilience. However, Blockchain additional uses cases in accordance with future enhancement [21]; nevertheless, Blockchain help in the attainment of security, privacy, and trust particularly concerning their interaction with external entities, such as a caregiver [22]. Blockchain is tamperproof technology that is comprised of only authentic information [23]. Likewise, it is a P2P peer-to-peer technology and is not controlled by any singular centralized entity. Blockchain technology help in the provision of P2P communication based on contractual aspects among the IoT related devices and helps in the delineation of the single point of failure, scalability, trust, privacy, reliability challenges and of IoT [24]. Furthermore, [25], defined that Blockchain technology also helps in the provision of simple IoT devices infrastructure that supports the process of data

transfer among one and other devices under the umbrella of consistent, secured and time-stamped contractual manner. However, it can be stated that using Blockchain in maintaining the security, privacy, and trust in IIoT support in the attainment of quality outcomes. Therefore, Blockchain allows autonomous functionating of the smart devices as well as it also permits the IoT application to work effectively. Thus, in Table. 1 the list of 17 articles that have been included in this paper has been depicted.

Table 1 List of Articles Included via PRISMA Model in Related Study

#	Cite	Title
1	[5]	Security in Industrie 4.0-challenges and solutions for the fourth industrial revolution.
2	[10]	Industry 4.0: Developments Towards the Fourth Industrial Revolution
3	[11]	An architecture for the Internet of Things with decentralized data and centralized control
4	[12]	Blockchain technology for security issues and challenges in IoT.
5	[13]	Blockchain for Ensuring Security, Privacy, and Trust in IoT Environments: The State of the Art
6	[14]	Securing IoT in the distributed blockchain: Analysis, requirements and open issues
7	[15]	Blockchain in Data Analytics
8	[16]	Block IoT intelligence: A blockchain-enabled intelligent IoT architecture with artificial intelligence
9	[17]	Security and privacy challenges in the industrial internet of things
10	[18]	Managing IoT devices using the blockchain platform
11	[19]	IoT security: Review, blockchain solutions, and open challenges
12	[20]	Survey on blockchain for the Internet of Things
13	[21]	Blockchain regulation and governance
14	[22]	Blockchain for the Internet of Things: A systematic literature review
15	[23]	Challenges and opportunities of blockchain-based platformization of digital identities in the public sector
16	[24]	Blockchain for 5G-enabled IoT for industrial automation: A systematic review
17	[25]	Blockchain technology for record-keeping: Help or Hype?

III. METHODS AND MATERIAL

This paper has been based on comprehensive analysis which has been conducted with the help of examining and evaluating different previous published research papers. It helps in analyzing and understanding the view and perception of the people that have been modified with time. The adopted methodology of this paper is qualitative which is further supported with the strategy known as secondary search. The essentialness behind going for such a method helps the readers in profound examination regarding Blockchain along with security, privacy, trust in IIoT adequately.

IV. DISCUSSION AND ANALYSIS: BLOCKCHAIN AND IIOT

The concept of IoT is paying a vigorous role, it is rapidly increased and has attained significant prominence among the globe. With IoT, the association of medical vicinity makes the IoMT Internet of Medical Things, association with educational institutions makes IoET Internet of Educational things others. However, all these areas come under the umbrella of industry and therefore, the concept of IIoT has been developed. The prime reason behind this is the significant cultivation and progression that have occurred in the 21st Century [26]. Since, the entitled research has been formulated in such a manner that the most possible solution to maintain and manage the risk and uncertainties with regards to security, privacy, and trust in IIoT has been discussed for several industries. However, under the umbrella of the industry, there are several areas that come underneath such as healthcare units, smart homes, smart cities, access and identity management, supply chain management, insurance and educational institutions and numerous others. [27] has stated that the word industry and its association with the IoT have been playing an active role which is facilitating the people with significant ease, usability, and feasibility. However, there are some issues that have been occurred which must be improved with time. In addition, several studies have previously discussed but the issues, risk, and uncertainties with regards to IIoT have not been mitigated appropriately. In contradiction, [28] has defined that the discussed solutions and techniques in order to mitigate the issues, risk, and uncertainties such as Data content and encoding, Upgrade and Platform Management Services and others are based on the traditional methods which might be one of the reasons behind the lack of appropriate solutions in accordance with the data management particularly in IIoT as the concept of IIoT has also been further cultivating towards IR 4.0 (Industrial Revolution). On such discussion and stance, in this paper, the authors have conducted comprehensive research with regards to the use of Blockchain in IIoT to overcome the issues, risks, and uncertainties in maintaining and managing the security, privacy, and trust in IIoT. Table. 2 is addressing the risk along with the solution that might help in eliminating the risk with the help of Blockchain. Table 3 Industries and Blockchain solutions.

A. Data Manipulation

In IoT data manipulation issues have been discussed widely; however, it can be stated that the data manipulation issues in IIoT might come due to the centralized nature of IIoT and its platforms [12]. Moreover, due to its centralized nature data can be manipulated and might be used in an unappropriated manner. Traditional systems of data management in IIoT handle the retrieval, storage, and update of data items, files, and records that might not be enough capacity to prevent the data to get accessed by unauthorized users

[5]. However, with blockchain, such aspects could be mitigated that ultimately help in the attainment of the trust level. Blockchain can only be updated with the consent of the majority of system participants and allows users to remain anonymous to protect their privacy. By using blockchain, audit trails are created which make responsibility that makes automatic and accountability seamless.

B. Central Control

IoT comes with a centralized structure. The central nodes in IoT act as a point of failure that might negatively impact the entire system of IoT. Moreover, the central node is open in order to distribute the DoS Denial-of-Service attacks, remote hijacking, data theft, and hackings. Therefore, due to the centralized structure and single point failure leads towards the collapse of the entire IIoT system [12].

C. Security and Privacy

Due to the centralized structure of the IIoT system, there has been a strong chance of security risks. If the central system might get affected it ultimately impact the entire system. The system cannot be secured as there are high chances of security risk and unauthorized access. Therefore, this eventually impacts the privacy of data and thus, the trust of end-users might get affected.

Table 2 Risk, Issues, Uncertainties: Blockchain Solutions

Risk, Issues or Uncertainty	Blockchain Solution
Data Manipulation	Through blockchain immutability of data and decentralized access might be beneficial in solving such risk factor
	Devices are interlocked, malicious actives could be easily detected and prevented due to a secured framework.
Central Control	Blockchain practices resources of all nodes participating. This decreases delays, eradicates many-to-one flows of traffic and disables the problem of a single point of failure that has been present in basic IIoT infrastructure.
	Blockchain also comes with secure communication among different devices. This permits the device identity validation along with transaction verification. Therefore, Blockchain comes with decentralized architecture and thus the risk regarding the centralized system might get resolved architecture is decentralized
Security and Privacy	The blockchain inherent anonymity is well suited for most IIoT based vicinities where the users identify is obligatory to keep private
	Security and privacy of IIoT might get resolved by blockchain due to its decentralized nature. It can provide military-grade security. It grasps a protected network over untrusted parties, that is required in IIoT with heterogeneous and numerous devices.

Table 3 Industries and Blockchain

Industries	Issues	With Blockchain
Smart Homes [12] [29]	In applications of a smart home, users can perform malicious activities	Blockchain allows the smart home to turn out to be immutable
Identity and Access Management [30]	Storage of information, digital rights management, and identification of items	Through blockchain credentials of users, properties of physical assets, and other pertinent data can be stored reliably and securely
Healthcare Sector [12]	Integration of medical devices might consider as an issue	Through blockchain, medical devices access can be done effectively, open standards for data operation and sharing via blockchain help in mitigating the integration issues

V. CONCLUSION

To conclude, in this paper the main aim was to conduct compressive research with regards to security, privacy, and trust using Blockchain in IIoT. To accomplish the aim several papers have been examined; however, with the help of extracted data paper has been formulated. Inspected from the comprehensive analysis the security, privacy, and trust in IIoT has been difficult to maintain; however, there are several risks, issues, and uncertainties that negatively impact the performance of the systems based on IIoT. Among several issues, there have been discussed such as Data manipulation, Central Control, along with Security and Privacy. Moreover, through Blockchain the solution has also been discussed. In addition, among the industrial IoT, there are several areas such as healthcare units, smart homes, smart cities, access, identity management, supply chain management, insurance, and numerous others. However, precisely with regards to smart homes, healthcare sector, and Identity and Access Management the issues and solutions via Blockchain have also been discussed.

REFERENCES

[1] Abdul-Qawy, Antar Shaddad, P. J. Pramod, E. Magesh, and T. Srinivasulu. "The Internet of Things (IoT): An Overview." International Journal of engineering Research and Applications 1, no. 5 (2015): 71-82.

[2] Chen, Edward T. "The internet of things: opportunities, issues, and challenges." In The Internet of Things in the Modern Business Environment, pp. 167-187. IGI global, 2017.

[3] Elijah, Olakunle, Tharek Abdul Rahman, Igbafe Orikumhi, Chee Yen Leow, and MHD Nour Hindia. "An overview of Internet of Things (IoT)

and data analytics in agriculture: Benefits and challenges." IEEE Internet of Things Journal 5, no. 5 (2018): 3758-3773.

[4] Ahlmeyer, Matthew, and Alina M. Chircu. "Securing the Internet of Things: A review." Issues in information Systems 17, no. 4 (2016).

[5] Waidner, Michael, and Michael Kasper. "Security in industrie 4.0-challenges and solutions for the fourth industrial revolution." In 2016 Design, Automation & Test in Europe Conference & Exhibition (DATE), pp. 1303-1308. IEEE, 2016.

[6] Rong, Ke, Guangyu Hu, Yong Lin, Yongjiang Shi, and Liang Guo. "Understanding business ecosystem using a 6C framework in Internet-of-Things-based sectors." International Journal of Production Economics 159 (2015): 41-55.

[7] Stankovic, John A. "Research directions for the internet of things." IEEE Internet of Things Journal 1, no. 1 (2014): 3-9.

[8] Li, Shancang, Li Da Xu, and Shanshan Zhao. "The internet of things: a survey." Information Systems Frontiers 17, no. 2 (2015): 243-259.

[9] Yan, Zheng, Peng Zhang, and Athanasios V. Vasilakos. "A survey on trust management for Internet of Things." Journal of network and computer applications 42 (2014): 120-134.

[10] Kumar, Kaushik, Divya Zindani, and J. Paulo Davim. Industry 4.0: Developments Towards the Fourth Industrial Revolution. Springer, 2019.

[11] Salman, Ola, Imad Elhajj, Ayman Kayssi, and Ali Chehab. "An architecture for the Internet of Things with decentralized data and centralized control." In 2015 IEEE/ACS 12th International Conference of Computer Systems and Applications (AICCSA), pp. 1-8. IEEE, 2015.

[12] Kumar, Nallapaneni Manoj, and Pradeep Kumar Mallick. "Blockchain technology for security issues and challenges in IoT." Procedia Computer Science 132 (2018): 1815-1823.

[13] Erdem, Ahmet, Sevgi Özkan Yildirim, and Pelin Angin. "Blockchain for Ensuring Security, Privacy, and Trust in IoT Environments: The State of the Art." In Security, Privacy and Trust in the IoT Environment, pp. 97-122. Springer, Cham, 2019.

[14] Moin, Sana, Ahmad Karim, Zanab Safdar, Kalsoom Safdar, Ejaz Ahmed, and Muhammad Imran. "Securing IoTs in the distributed blockchain: Analysis, requirements and open issues." Future Generation Computer Systems 100 (2019): 325-343.

[15] AHMED, SABBIR. "CHAPTER THREE BLOCKCHAIN AND INDUSTRY 4.0 SABBIR AHMED AND RAZIB HAYAT KHAN." Blockchain in Data Analytics (2020): 52.

[16] Singh, Sushil Kumar, Shailendra Rathore, and Jong Hyuk Park. "Block IoT intelligence: A blockchain-enabled intelligent IoT architecture with artificial intelligence." Future Generation Computer Systems (2019).

[17] Sadeghi, Ahmad-Reza, Christian Wachsmann, and Michael Waidner. "Security and privacy challenges in industrial internet of things." In 2015 52nd ACM/EDAC/IEEE Design Automation Conference (DAC), pp. 1-6. IEEE, 2015.

[18] Huh, Seyoung, Sangrae Cho, and Soohyung Kim. "Managing IoT devices using blockchain platform." In 2017 19th international conference on advanced communication technology (ICACT), pp. 464-467. IEEE, 2017.

[19] Khan, Minhaj Ahmad, and Khaled Salah. "IoT security: Review, blockchain solutions, and open challenges." Future Generation Computer Systems 82 (2018): 395-411.

[20] Wang, Xu, Xuan Zha, Wei Ni, Ren Ping Liu, Y. Jay Guo, Xinxin Niu, and Kangfeng Zheng. "Survey on blockchain for Internet of Things." Computer Communications 136 (2019): 10-29.

[21] Finck, Michèle. Blockchain regulation and governance in Europe. Cambridge University Press, 2018.

[22] Conoscenti, Marco, Antonio Vetro, and Juan Carlos De Martin. "Blockchain for the Internet of Things: A systematic literature review." In 2016 IEEE/ACS 13th International Conference of Computer Systems and Applications (AICCSA), pp. 1-6. IEEE, 2016.

[23] Guggenmos, Florian, Jannik Lockl, Alexander Rieger, and Gilbert Fridgen. "CHALLENGES AND OPPORTUNITIES OF BLOCKCHAIN-BASED PLATFORMIZATION OF DIGITAL IDENTITIES IN THE PUBLIC SECTOR."

[24] Mistry, Ishan, Sudeep Tanwar, Sudhanshu Tyagi, and Neeraj Kumar. "Blockchain for 5G-enabled IoT for industrial automation: A systematic review, solutions, and challenges." Mechanical Systems and Signal Processing 135 (2020): 106382.

[25] Stančić, Hrvoje, Andro Babić, Nikola Bonić, Magdalena Kutleša, Ira Volarević, Vladimir Bralić, Anabela Lendić, and Ivan Slade-Šilović. "Blockchain technology for record keeping: Help or Hype?." In Blockchain technology for record keeping: Help or Hype?. Social Sciences and Humanities Research Council of Canada, 2016.

[26] Wortmann, Felix, and Kristina Flüchter. "Internet of things." Business & Information Systems Engineering 57, no. 3 (2015): 221-224.

[27] Moazed, Alex, and Nicholas L. Johnson. Modern monopolies: what it takes to dominate the 21st century economy. St. Martin's Press, 2016.

[28] Habib, Mohammad Ashfaq, Mas S. Mohktar, Shahrul Bahyah Kamaruzzaman, Kheng Seang Lim, Tan Maw Pin, and Fatimah Ibrahim. "Smartphone-based solutions for fall detection and prevention: challenges and open issues." Sensors 14, no. 4 (2014): 7181-7208.

[29] Dorri, Ali, Salil S. Kanhere, Raja Jurdak, and Praveen Gauravaram. "Blockchain for IoT security

and privacy: The case study of a smart home." In the 2017 IEEE international conference on pervasive computing and communications workshops (PerCom workshops), pp. 618-623. IEEE, 2017.

[30] Indu, I., PM Rubesh Anand, and Vidhyacharan Bhaskar. "Identity and access management in the cloud environment: Mechanisms and challenges." Engineering science and technology, an international journal 21, no. 4 (2018): 574-588.

2020 5th International Electrical Engineering Conference (IEEC 2020)
Feb, 2020 at IEP Centre, Karachi, Pakistan

A Comprehensive Study: 5G Wireless Networks and Emerging Technologies

Sadiq Ur Rehman[1], Afzal Hussain[2], Faizan Hussain[2], and Muhammad Adeel Mannan[2]
[1]Department of Electrical Engineering, Faculty of Engineering Science and Technology (FEST), Hamdard University
[2]Department of Computing, Faculty of Engineering Science and Technology (FEST), Hamdard University
Karachi, 74600, Pakistan
sadiq.rehman@hamdard.edu.pk, Afzal.hussain@hamdard.edu.pk, faizanhussain535@outlook.com, and
adeel.mannan@hamdard.edu.pk

Abstract: Fifth generation networks are the area in which a lot of researchers are spending their time to enhance its performance as per dynamic change in wireless communication. The essential utilization of such a technique (5G) is used to have higher data rates containing minimum latency. The data rate of 5G technology is usually gigabits per second (Gbps). With respect to other technologies like 3G, 4G, LTE, and other networks, 5G networks provide better capacity for the base station along with above the average Quality of Service (QoS). With the advancement in technology and rise in the usages and demand of multimedia data, 5G networks are the most suitable option to achieve the best QoS, improved capacity and overcoming the latest issue of cellular networks. Since many base stations and devices are in connection with each other in 5G,

Keywords: 5G; Base Station (BS); QoS; data rate, Radio Access Network (RAN)

I. INTRODUCTION

At the beginning of wireless mobile communication, it starts with the voice communication system only, i.e. the first generation (1G). With the significant advancement in wireless communication systems, there was a steady improvement in the wireless mobile communication which in result provide the second (2G), third (3G) and fourth-generation (4G) wireless networks respectively. Due to excessive use of multimedia and internet utilizing applications along with the use of voice features, some new technologies need to be introduced by focusing increment in capacity, better data rate, minimum latency and exceptional QoS. 5G networks are the one which provides the above-mentioned features that are highly required by future networks. Some of the essential requirements of 5G systems are data rate, latency, energy utilization and cost [1]. Utilization of energy is always a challenging aspect of designing and operation of all wireless communication systems and the same goes for 5G networks.

II. EVOLUTION OF WIRELESS TECHNOLOGIES

Wireless communication technologies have been evolving from time to time to fulfill the demand of wireless network users such as high data rate, high throughput, minimum delay and best quality as well as to provide the network accessibility everywhere and for everyone. In this section, we take the overview of wireless technologies from 1st generation to 5th generation. As the generation of technologies growing from 1G to 5G their efficiency also increasing in terms of utilization power, mobility, range spectrum sharing. Some of the old version of the wireless technology that includes 1st generation networks and 2nd generation networks use circuit switching. Packet switching was introduced from 4th generation and onwards. However, 2.5G and 3G use both types of switching technology. These technologies use two types of spectrum license and unlicensed spectrums. [2]

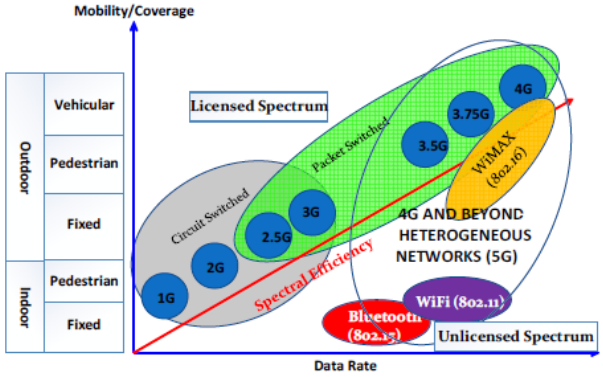

Fig. 1. Evolution of Wireless Technologies [2]

A. 1st Generation (1G)

It was introduced in the 1980s and based on various different standards such as Nordic Mobile Telephone (NMT), Advanced Mobile Phone Service (AMPS) and Total Access Communication System (TACS) [2]. 1G used for transmitting voice signals with the data rate of 2.4kbps and uses frequency modulation technique. A lot of disadvantages have been monitored in this generation in which improper hands-off, no security and capacity issues are the main. Since in this analog technique data security is not reliable. Voice call data could be stolen easily by hacking a user's password [3].

B. 2nd Generation (2G)

1990 is the era of 2G. It introduced digital technology in mobile phones. The first system of 2G was GSM for voice communication, Short Message Service (SMS) and email. Its data rate is higher than 1G up to 64Kbps. It saved battery time by using low power radio signals. 2.5G is an enhanced version of 2.5G. It used the

framework of the 2G system and merged General Packet Radio Services (GPRS) with 2G technology to increase the data rate up to 144 Kbps. It uses circuit switching as well as packet switching.

C. 3rd Generation (3G)

It was introduced at the end of 2000. It has various best features to accommodate the increasing requirement of wireless communication systems and provides data rates up to 2Mbps. It allows IP based internet on mobile access. This generation brought remarkable changes in wireless communication by maintaining QoS. There are several technologies that can be found in 3G these technologies are, namely Universal Mobile Telecommunications Systems, Code Division Multiple Access and Wideband Code Division Multiple Access [2]. Long Term Evolution (LTE) and Worldwide Interoperability for Microwave Access (WiMAX) is considered to be the technology that will be a future of radio network with improving data rate, capacity network coverage and cost [4-7].

D. 4rth Generation (4G)

4G networks are IP based communication systems launched in the last few years. As sometimes high data rate with minimum latency is the requirement of the system. So, it facilitates users by providing transformation of voice, data, and multimedia everywhere and every time on high data rates and with minimum latency. 4G introduced the latest applications in the world of the wireless network; among these applications, some examples are Multimedia Messaging Service (MMS), video chat, Mobile TV, etc. [4-6].

E. 5th Generation (5G)

5G is known as the network technology for the future. Due to the increasing number of users, it has been deploying commercially and replacing 4G systems to 5G systems. 4G systems have not the ability to deal with the massive amount of data and not defined a different strategy for indoor and outdoor uses. Channel interference may also make the system unreliable. While 5G has introduces to support spectrum utilization, provide ubiquitous computing and minimize the latency up to zero [8]. 5G networks offer higher capacity as compared to earlier generations but it faces many challenges such as higher capacity, lower delay, and high data rate, low cost and best quality of service for all users. Different standards of IEEE have introduced and they are accommodating in the deployment of 5G. 802.11 an, 802.11 ac, 802.11 ads and 802.11 of our recently introduced standards which are different from each other on the basis of bandwidth, frequency, modulation techniques, range, data rate and many more. Table 1 shows the brief details regarding the evolution of wireless technology and table 2 represents the technical comparison of 802.11 standards.

III. CHALLENGES IN-MIGRATION FROM 4G TO 5G

5G has been a hot research topic in the last few years. As the whole system is deployed on 3G and 4G so, it's not an easy task to migrate from 4G to 5G. Huge manpower is required to deploy this system as billions of devices are using 4G technology right now. Some of the significant challenges in-migration from 4G to 5G are as follow;

A. Multi-mode user terminals

There are multi-mode terminals used in 4G, so there is a need to design a system consists of the single user terminal to get rid of size limitations, power utilization, and cost and also to operate wireless networks of different types by using the approach of software radio.

B. Selection of wireless systems among others

In wireless communication, every system has its own pros and cons. The selection of the wireless system is very much dependent on the QoS requirement from the customer. This is the choice of appropriate technology at the required place at a specific time.

C. Security

Security is an essential part of any network. A mechanism should be designed which provides a lightweight mechanism and should be adaptive and reconfigurable.

D. Billing

Consumer billing is also a big challenge. It is challenging to handle account information of consumers of many service providers.

E. Attacks on Application Level

New software applications can be deployed to support the 5G network, but it can have bugs or security threats.

F. Jamming and spoofing

Spoofing is the term used for a fake GPS signal and the receiver treats these signals as the real signal. Attackers take advantage by using this technique and jamming occurs due to the transmission of signals from the transmitter at the same frequency shifts a GPS signal. The consumer should use the data which is encrypted. [9]. Some other challenges are to provide a high data rate with optimization of energy, Scalable and flexible network with low latency. Handling interference among channels, functional impact on economic growth and many more. Table 3 represents the details regarding 5G technologies.

Table 1. Evolution of Wireless Technology

Generation and Time Period		Protocol Family	Protocol RAT	MIMO Techniques	Bandwidth	Switch	Frequency Band	Standard Tech.	Core N/W	Tech. Mediums
1G	1980	IS-95, TIA-EIA 95, CDMA One	FDMA	FSK and FM	30KHz	Circuit	800MHz	AMPS NMT TACS/ JTACS PSTN	PSTN	Analog Cellular Technology
2G	1992-1997	CDMA One	CDMA, TDMA, FDMA	GMSK	200KHz		850/900/ 1800/1900 MHz	GSM		Digital Cellular Technology
2.5G	1998	3GPP Release 97	CDMA, TDMA	GMSK	200KHz	Packet/ Circuit		GPRS	PSTN/ Packet N/W	
3G	2000-2001	CDMA2000 3GPP 3GPP Release 4IMT-2000 Release 99 (R99)	WCDMA, TDMA, TDSCDMA CDMA, EV-DO Rev A and B	QPSK	1.25MHz to 5MHz	Packet/ Circuit	800/850/900 /1800/1900/ 2100 MHz	UMTS		CDMA 2000, UMTS, EDGE
3.5G	2002-2007	3GPP Release 5 and 6	EV-DO	QPSK (HSDPA) DL: 16QAM		Packet		HSPA: HSDPA HSUPA	Packet N/W and Internet	
4G	2011-2015	3GPP Release 10 and 11 IMT-Advanced	UL: SC-FDMA DL: OFDMA	UL: SU-MIMO (4x4) DL: MU-MIMO (8x8) FDD and TDD	1.4MHz to 20MHz		1.8GHz to 3.5GHz	LTE-A	Internet	WiMax, LTE Wi-Fi
5G	2016 to ahead	3GPP release 14, 15, and 16 ITU/IMT-202	BDMA NOMA Multi-RAT	Advanced MIMO Massive MIMO FBMC FQAM	60GHz		1.8, 2.6 GHz and expected 30-300GHz	NR?		WWWW

Table 2. Technical Comparison of 802.11 standards

Technical Specification	Modulation Scheme	Channel Bandwidth	Single Stream, Nominal Data Rate	EIRP	Range	World-Wide Availability
802.11an	OFDM	20.4MHz	Up to 150Mbps	22-36 dBm	12-70m indoor	✓
802.11ac	OFDM	20, 40, 80MHz	Up to 4333 Mbps – 867 Mbps	22-29 dBm	12-35m indoor	✓
802.11ad	OFDM, Low power single carrier, single carrier	2GHz	4.6 Gbps	1-10 dBm	60m indoor, and outdoor 100m	✓
802.11af	OFDM	5, 10, 20, 40 MHz	54Mbps	16-20 dBm	<100m indoor <outdoor 5Km	✓

Table 3. 5G Specification Table

Performance	10000 times the capacity of the current network	Parameters	Network capacity
	20Gbps downlink and 10Gbps uplink		Peak data rate
	100 Mbps		Cell edge data rate
	< 1 ms		Latency
	1 million connected devices per square km (0.38 sq. miles)		Connection density
	500km/h high speed		5G mobility
	30bits/Hz downlink and 15 bits/Hz uplink		Spectral efficiency

IV. FEATURES OF 5G TECHNOLOGY

5G is the enhancement of earlier generation, so, it has more powerful features to provide a flexible and reliable network which can support the requirements of high data rate, low latency, and no interference. It will capture the market in the coming few years as it has remarkable features and you can access any global information from your handset at any time. Some of the features are list down in below:

- It is expected that it is a complete wireless communication that has no limitations that's why it is known as "REAL wireless world".
- It also provides multimedia features to provide the facility of review newspapers watching T.V programs anywhere and at any time.
- Due to the high data rate, it reduces the transmission time as compared to earlier generations.
- It also supports the concept of artificial intelligence (AI) by providing access to the internet everywhere for every object. It also offers wearable devices.
- IPV6 is used to assign unique IDs to every object.
- Cognitive Radio is the latest technology that is deploying gradually. It allows radio technologies of different types for sharing the unused spectrum. This approach depends on Software Defined Radio (SDN).
- It also provides high uploading and downloading speed and broadcasts its data in Gigabits.

If we analyze all the features of 5G deeply so, we can conclude that it has changed the world of telecommunication by offering the latest features that were not available in earlier generations. It is a great blessing for a human being.

V. 5 G NETWORK'S EMERGING TECHNOLOGIES

Researchers have predicted by looking at the rapid growth in the technology that the time is near when the traffic of mobile radio and wireless will get exponentially increased. Billions of devices will be connected to the internet in order to share and access data without the limitation of time and place. Due to the exponential increase in the challenges of the connecting device like scalability, power utilization, spectrum utilization, cost and many more will get arises. In [15], a technical aim is proposed that can target the current running networks by providing the system that can significantly enhance the performance and QoS of the network. For the 5G system, the following are the essential technologies components [15].

- Radio-links
- Multi-node transmission
- Multi-antenna transmissions,
- Network dimension
- Spectrum usage
- Device-to-Device (D2D) communications
- Massive Machine Communications (MMC)

Some of the most critical technologies that will be essential in upcoming wireless standards are as follows,

A. Massive MIMOs

This technology is the upgraded form of MIMO technology. In this technology, arrays of multiple antennas being used that utilize the same frequency, time slot, and server number terminals. A key goal is to utilize all the assets of that MIMO system. We can conclude the massive MIMO can be counted as a new era technology which provides a secure spectrum, energy efficiency, robustness etc. [16]

B. Interference management

In radio/ cellular wireless communication systems, channel or frequency reuses the critical concept for the efficient utilization of resources. Moreover, in such technology, user throughput, and efficient traffic capacity are also important aspects. With the concept of densification and reuse, there has been an advancement in a system in terms of load sharing in-between local access networks and microcells. However, due to the dramatic change in network load and in density, there exists a co-channel interference at the edges of cells. Therefore, the cochannel interface is a serious threat to the new radio technologies. Hence efficient interference management schemes are a must for next-generation networks. There are two critical techniques for interference management, and details can be seen in [17]

C. Spectrum Sharing

When it comes to focusing on the upcoming broadband system for mobile communication [18,19], wider bandwidths and broad-spectrum are required to monitor the performance of a system. The sharing system of the spectrum is possible in two ways i.e. vertical sharing or horizontal spectrum sharing. Components of the network which are using spectrum collectively work as a balancer [20]

VI. 5G NETWORK'S ARCHITECTURAL REPRESENTATION

As per the research of [21], it has been examined that 5G has been based on intelligent architecture although the architecture of 5G is complex due to the RAN (Radio Access Network) it is working effectively. Moreover, 5G also comes with the virtual and flexible RAN that also comes with new interfaces that create additional access to data points. 5G offers huge potential for consumers and industry, as well as the hope that it will be much faster than existing technologies. 5G is committed to high social and economic value, where mobile devices play an even more important role in the lives of those who want to connect. 5G-based architecture networks use a modern ecosystem of technology and business innovations. The 5G architecture supports thousands of new consumer

and business applications, including manufacturing, energy, medical care and automobiles. Therefore, basic 5G architecture has been illustrated below the development of relevant knowledge and information for the readers regarding the working of 5G.

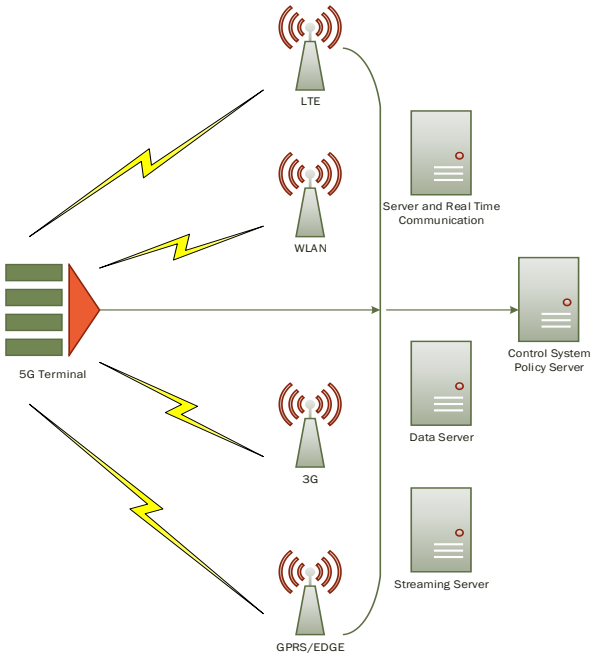

Fig. 1 5G Architecture [22]

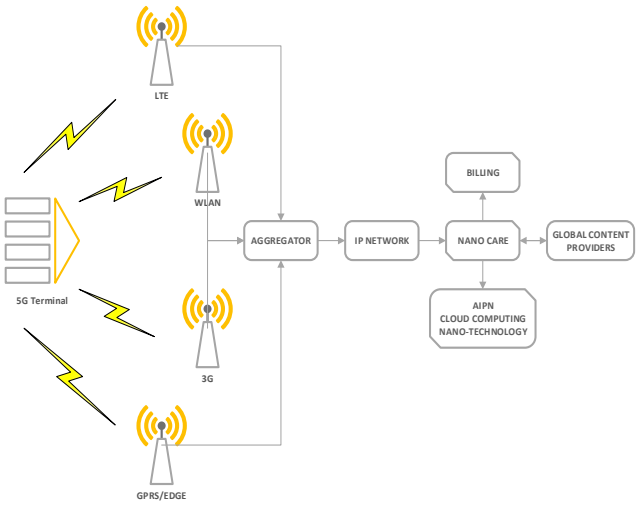

Fig. 2 5G Network Architecture

VII. CONCLUSION

In this paper, we have seen that there are two primary types of switching that takes place in wireless communication which is namely circuit switching and packet switching. The evolution of wireless technology took place from 1 generation networks and now it is on 5th generation networks. The differences in the generations are based on their data rate, frequency band, bandwidth, and forward error correction and application usage. 5G networks are much better than 4G networks in terms of data rates, frequency bands, and services. 5G networks are expected to provide a data rate of 10-50 Gbps with a bandwidth of 60 GHz. There are many other features of 5G networks among which the most highlighted are the usage of IPv6 and integration with Cognitive Radio and Software Defined Radio/Networks. A lot of work is still required in the domain of data privacy and security, energy utilization, spectrum management and utilization etc.

REFERENCES

[1] Andrews, Jeffrey G., Stefano Buzzi, Wan Choi, Stephen V. Hanly, Angel Lozano, Anthony CK Soong, and Jianzhong Charlie Zhang. "What will 5G be?." IEEE Journal on selected areas in communications 32, no. 6 (2014): 1065-1082.

[2] Gupta, Akhil, and Rakesh Kumar Jha. "A survey of the 5G network: Architecture and emerging technologies." IEEE access 3 (2015): 1206-1232.

[3] http://www.cleardoubts.com/technology/what-is-1g-or-first-generation-of-wireless-telecommunication-technology/

[4] J. G. Andrews, A. Ghosh, and R. Muhamed, Fundamentals of WiMAX, Prentice Hall, 2007.

[5] B. Furht and S. A. Ahson, Long Term Evolution: 3GPP LTE Radio and Cellular Technology. Boca Raton, FL: CRC Press, 2009, ch. 12, pp. 441–443.

[6] S. Sesia, I. Toufik, and M. Baker, Eds., LTE: The UMTS Long Term Evolution. John Wiley and Sons, 2009.

[7] K. R. Santhi, V. K. Srivastava, G. SenthilKumaran, and A. Butare,"Goals of true broad band's wireless next wave (4G-5G)," in Proc. IEEE 58th Veh. Technol. Conf., vol. 4. Oct. 2003, pp. 2317–2321.

[8] Panwar, Nisha, Shantanu Sharma, and Awadhesh Kumar Singh. "A survey on 5G: The next generation of mobile communication." Physical Communication 18 (2016): 64-84.

[9] Suk Yu Hui, Kai Hau Yeung, "Challenges in the Migration to 4G Mobile Systems", IEEE Communications Magazine, December 2003

[10] Gaikwad Vaibhav Vitthal, Bhor Pooja Vijay, "5G Future Wireless Communication Technology-A Survey", International Journal of Innovative Research in Computer and Communication Engineering, Vol. 5, Issue 1, January 2017

[11] Woon Hau Chin, Zhong Fan, and Russell Haines, "Emerging Technologies and Research Challenges for 5G Wireless Networks" Toshiba Research Europe Limited, Bristol, BS1 4ND, United Kingdom.

[12] Eduardo Casta˜neda, Ad˜ao Silva, At´ılio Gameiro, and Marios Kountouris, "An Overview on Resource Allocation Techniques for Multi-User MIMO Systems", 1553-877X (c) 2016 IEEE

[13] Mamta Agiwal1, Abhishek Roy2, and Navrati Saxena, "Next Generation 5G Wireless Networks: A Comprehensive Survey" 1553-877X (c) 2015 IEEE.

[14] Jing WANG & Chih-Lin, "Recent advances and future challenges for massive MIMO channel measurements and models", from science China February 2016, Vol. 59 021301:1–021301:16

[15] Osseiran, Afif, Federico Boccardi, Volker Braun, Katsutoshi Kusume, Patrick Marsch, Michal Materna, Olav Queseth et al. "Scenarios for 5G mobile and wireless communications: the vision of the METIS project." IEEE Communications Magazine 52, no. 5 (2014): 26-35

[16] Larsson, Erik G., Ove Edfors, Fredrik Tufvesson, and Thomas L. Marzetta. "Massive MIMO for next-generation wireless systems." IEEE Communications Magazine 52, no. 2 (2014): 186-195.

[17] Nam, Wooseok, Dongwoon Bai, Jungwon Lee, and Inyup Kang. "Advanced interference management for 5G cellular networks." IEEE Communications Magazine 52, no. 5 (2014): 52-60

[18] Fallgren, Mikael, and Bogdan Timus. "Scenarios, requirements, and KPIs for 5G mobile and wireless system." METIS deliverable D 1 (2013): 1.

[19] Ericsson, “5G Radio Access – Research and Vision,” Ericsson white paper, June 2013.

[20] T. Irnich et al., “Spectrum Sharing Scenarios and Resulting Technical Requirements for 5G Systems,” PIMRC 2013, London, Sept. 2013.

[21] Choi, Young-il, and Noik Park. "Slice architecture for 5G core network." In 2017 Ninth international conference on ubiquitous and future networks (ICUFN), pp. 571-575. IEEE, 2017.

[22] "5G - Architecture - Tutorialspoint". 2020. Tutorialspoint.Com. Accessed January 31 2020. https://www.tutorialspoint.com/5g/5g_architecture.htm.

2020 5th International Electrical Engineering Conference (IEEC 2020)
Feb, 2020 at IEP Centre, Karachi, Pakistan

Towards Novel biologically inspired Collision avoidance schemes for the Internet of Things (IoT) enabled self-driving cars in a controlled environment: A concept Paper

Zuhaib Ahmed Khan[1], Mubeen Rafaqat[2], Shabab Tariq[3] and Faisal Riaz[4*], Kamran Hameed[5], Iftikhar Ahmed[6], Abdul Ghafoor[7], Yasir Mehmood[8]

Control, Automotive and Robotics Lab affiliated lab of National Center of Robotics and Automation (NCRA HEC Pakistan), and with the Department of Computer Science and Information Technology, Department of Software Engineering, Mirpur University of Science and Technology (MUST), Mirpur-10250, AJK Pakistan (faisal.riaz@must.edu.pk)*

Abstract: This paper describes how collision in self-driving cars can be avoided using biologically inspired schemes. Self-driving cars can be considered as the best solution to avoid collision between vehicles. However, this collision avoidance capability can be increased if we use Internet-of-Things (IoT) based smart roads. The use of IoT is a growing technology and its use in self-driving cars is not explored at large. This research paper is a concept paper presenting the latest efforts in the Control, Automotive and Robotics lab, NCRA to implement IoT enable smart controlled environment to help AVs to avoid collisions more efficiently. In this regard concept of four novel schemes has been proposed in this paper along with their diagrams and pseudo codes. We have explored biological aspects in this regard. Our proposed models are Chameleon-inspired, Bat-inspired, and human Tactile-based collision avoidance schemes which further incorporate IoT concepts to envisage the next generation self-driving cars.

Keywords: Bat-inspired, Chameleon-inspired, IoT, Tactile-enabled, Test-Bed-Road-System, Autonomous Vehicles(AVs)

I. INTRODUCTION

Self-driving cars are considered as the best solution to avoid collision in vehicles. According to Sun et al. [1] human drivers are not good enough to avoid collision between vehicles. In another paper Kallioinen et al. [2] defined that self-driving cars have a potential to improve public safety. According to Nees [3] self-driving cars are much safer than human driven cars. So we can reduce the number of accidents by applying IoT based smart Cars.

IoT is a combination of different computing as well as mechanical devices. Luigi Atzori et al. [4] have defined that IoT is the connection of different devices around us as mobile phones, sensor Radio-Frequency Identification (RFID) tags, etc. Felix Wortmann Kristina and Flu¨chter [5] explained that there is no common definition for IoT that encompasses IoT. This term was originated almost 20 years before. Shancang Li et al. [6] defined that ”5G” will provide a new interface for the connectivity of IoT application and up to 20.4 billion devices will be in connection by 2020. From the above discussion, it is concluded that the use of IoT in self-driving car is an under-researched area. The great potential of this field in context of self-driving cars are yet to be explored.

IoT based smart road infrastructure improves the efficiency of self-driving cars. According to Gerla et al. [7] the vehicular network of IoTs improves the traffic flow in highways as well as in congested roads completely eliminated human control. Prasada et al. [8] stated that to make smart roads effective, it is necessary to employ advanced technology to handle the issues related to normal roads by collecting, processing and analyzing all the data related to it and find an alternative solution within a small fraction of time. From these facts, it can be implied that IoT based smart road infrastructure can avoid the collision in self-driving cars in an effective way.

The paper is organized as follows: Section 2 is about Literature Review. Section 3 is describing about the proposed solution. Section 4 is showing Experiments and Results and Section 5 is giving the Conclusion.

II. LITERATURE REVIEW

The safety of school children is very challenging while moving through public or school transport. Keeping in view the safety of students, Awad and Mohan [9] have investigated a mechanism to track transport through a global positioning system (GPS) and Assisted-GPS (AGPS). AGPS helps to improve the performance (Time-to –first-fix (TTFF)) of the system that calculates the position through GPS satellite. The worst case of TTFF calculation through autonomous GPS is 360 sec. and the worst case of AGPS is 13 sec. The proposed system also determines the route map which is the same as determined by GPS. Hardware is composed of Raspberry Pi with 4G Shield and IoT platform Ubidots. C and Python programming languages are used to write 4G Module and middleware code respectively.

Data processing is becoming a challenging task for the researchers due to the rapid increase in smart devices for the past few decades. Keeping in view the data processing challenges Babar and Arif [10] have proposed a system for smart transport using Big Data analytics. The proposed system is capable of managing and organization of Big Data. The proposed system identifies the obstacle of the road by considering the road traffic and the average speed of vehicles. The proposed system is very useful in case of emergency when citizens have to predict the estimated time to

reach the destination Apache Spark over Hadoop is used for data processing. After testing and analyzing different data sets it is found efficient in terms of data processing and size.

Chameleon is an animal that has a remarkable capability to change skin color. Ho-Hsiu Chou et al. [11] have successfully demonstrated electronic skin (e-skin) that can change skin color by sensing pressure as well as tactile sensing property. This skin was prepared by using Pressure Sensor (PS) and organic electrochromic devices (ECDs). The key parameter for this skin is weight, to make weight sensitive so that it may become capable to behave well on lightweight. The authors used ultrathin 1.2-mm-thick polyethylene naphthalate (PEN).

The safety of passengers in any vehicle is most important aspect. IoT based smart vehicles are facing problems of privacy. Phil Laplante [12] has proposed a concept of smart roads and highways. Ahmed et al. [13] have designed a GPS based Model Intelligent Vehicles System (MIVS) using real-time communication to overcome the collisions at T and Y-junctions. These smart roads could communicate with vehicles and make them more secure. The author has suggested three steps to make smart road. First step is on the initial stage of roads construction. In first step wireless or wired IoT sensors of various kinds can be placed in the field. The second step is installation of wearables, hand-held scanners, and tracking devices, along with the supporting software that helps in location tracking, collision avoidance, and communication intent, etc. The last step is to enable communication with smart roads and smart vehicles. Moreover there are many challenges like IoT devices installation, maintenance, and protection, etc. but this article is not describing about road infrastructure for Self-Driving Cars.

The world is switching towards the smart transportation system. So Franzò et al. [14] have presented the idea of smart roads in Italy. Before this smart roads were not present in Italy. So authors took initiative to make the roads smarts. It also addressed the problems of regulatory work of smart roads. Author also considered Humburg (Germany) as an example that is a specified area for the smart Vehicles. He was also inspired by some other smart roads examples that were working quite efficiently in the field. Authors used the agile method for this purpose and did not suggest any plan for self-driving vehicles roads infrastructure.

As the accuracy in sensors and processing power of controllers is getting improved, we can improve the awareness of road situations and the maneuvers in difficult traffic conditions of AVs. Dong et al. [15] used deep learning and computer vision algorithms to plan and make choices on the driving direction. The vehicle driving simulator based on the model predictive control is also used to collect, control and train the method. Finally, the method can be proved practically from the experience and the road scene in actual life. It is very helpful and effectively improves the reliability and safety of self-driving cars.

Nowadays use of ethics in self-driving cars is a hot topic. According to Riaz et al. [16] the role of social norms is important in robots and self-driving cars. The main focus is on ethical difficulties evolving from an individual vehicle that is an important but insufficient step to determining how technology will influence society and human lives. Kabeer et al. [17] have proposed a system that is empowered with emotion of fear, so the system can respond to avoid an accident.

The current research is focused on system-level of analysis how cars will communicate with each other and on the socio-technical systems in which they are embedded. While the Borenstin et al. [18] have used two traffic scenarios to propose the communication of self-driving cars to the system level that designers, policymakers and other should consider. While the authors also mentioned some alternatives, such as light rail. He recognized that the momentum behind the autonomous private passenger vehicle is happening almost inevitably. The author focused on a framework “Moral Responsibility for Computing Artifacts:

The limitation in the existing work is that the IoTs are not explored in area of biologically inspired schemes at large.

Contribution:

The existing work does not explore IoT at large in collision avoidance of self-driving cars. Worth of a vehicle depends on its safety. So that our aim was to provide safe and sound self-driving cars. The main contribution of our paper is as follows.

- Biologically inspired models for self-driving cars.
- Use of IoT in self-driving cars to avoid collision.
- Collision avoidance at blind curves in controlled environment.

The Rules that provide understanding to solve ethical issues related to AVs.

III. PROPOSED SMART ROAD SOLUTIONS

In this section we are proposing four biological schemes which can be helpful to avoid collision between vehicles at blind curve.

A. Chameleon Inspired Scheme:

The proposed model as shown in fig 1 is inspired from the chameleon. This model contains skin pigment cell board on the blind curve used for communication between the vehicles. In this model, the road contains a pressure sensor acting as a tactile sensor that detects the type of vehicle by calculating the weight of the vehicle. After detecting the vehicle the board changes the color depending on the type of vehicle and by changing colors. On the other hand it will also give information about the type and speed of the vehicle to all other vehicles who are present on that blind curve.

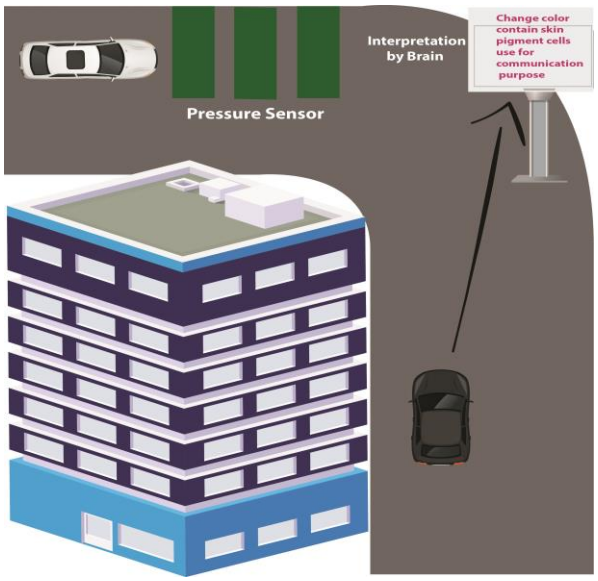

Fig: 1 Chameleon inspired model for vehicle collision avoidance

Vehicleidentification() method identifies the type of vehicle and sends threat to the chameleon inspired skin. Colorchange( ) method changes the color of skin and alerts other vehicles about the danger level.

Pseudo code: 1 Chameleon Inspired Scheme

1. Vehicleidentification (weight)
2. IF (weight>8,845 kg) THEN
   2.1 Return danger level high
3. END IF
4. IF (weight>1600 kg) THEN
   4.1 Return danger level medium
5. END IF
6. IF (weight>400 kg) THEN
   6.1 Return danger level low
7. END IF
8. IF (weight>150 kg) THEN
   8.1 Return danger level normal
9. END IF
10. Colorchange (danger level)
11. IF (danger level==high) THEN
    11.1Chameleon_inspired_skin = Red
    11.2Stimulation=”high danger”
    11.3 Action= Break
12 END IF
13 IF (danger level==medium) THEN
    13.1Chameleon_inspired_skin = green
    13.2Stimulation=”medium danger”
    13.3Action= slow speed
14 END IF
15 IF (danger level==low) THEN
    15.1 Chameleon_inspired_skin = blue
    15.2Stimulation=”low danger”
    15.3Action= keep moving in your lane medium
    15.4speed
16 END IF
17 IF (danger level==normal) THEN
    17.1Chameleon_inspired_skin = blue
    17.2Stimulation=”low danger”
    17.3Action= keep moving in your lane in normal
    17.4speed
   END IF

B. Tactile Enabled Model:

Our proposed project is inspired by tactile system which is explained in fig 2. Where we will make our whole road smart. We will attach the tactile sensors beneath the road and with fiber optics, we will connect smart roads with our server. As in our Nervous System, an external stimuli generates the electric impulse. That electric impulse follows the usual procedure to deliver a normal message. Interneurons are used for all urgent message. So here we are also using two types of messages.1st type of message is to send the normal messages to check the location and to make communication. Second type of message will automatically send on the server for an emergency case. Like vehicle is in danger or distance from collision is too short. For normal messages we are using tactile sensors for predictable communication and for alert messages we are using thermistor sensor. The server will lead autonomous cars to their destination and protect them from any type of collision. For double-check, we are also using V2V.

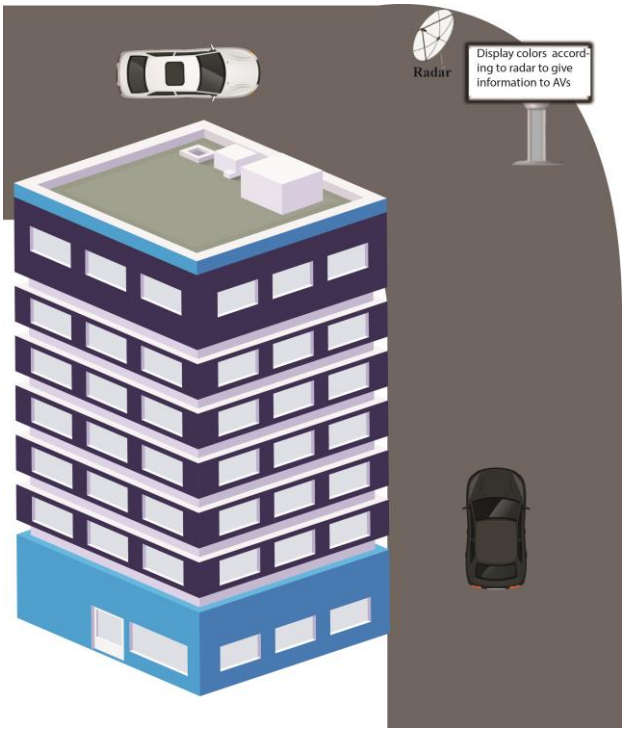

Fig: 2 Tactile Enabled Model communication for collisi on avoidance.

We are taking (c1, c2, c3…. cn) as Self-Driving ca rs and d is the distance between cars. Continuous i nformation on a car's position is coming from tactil e sensors. When distance d is decreasing between t wo cars c1 and c2, sensors will give different alar ming messages at different stages and will automati cally apply breaks when d is less than 1 meter.

Pseudo code: 2 Tactile enable Scheme

1. Self-driving Cars are (c_1, c_2, c_3…. c_n), distance between Self-driving Cars is d
2. Cars info → Server Room (continues)
3. c_1, c_2 → Travelling
4. If {
   - 4.1 Distance >= 10 meters
   - 4.2 Stimulation = "warning"
   - 4.3 Action ="Slow the Speed"

5 End if
6 }
7 If {
   - 7.1 Distance >=5 meters and < 10 meters
   - 7.2 Message = "alert"
   - 7.3 Action ="Leave Accelerator"

8 End If
9 }
10 If {
   - 10.1 Distance >=1 meters and < 5 meters
   - 10.2 Message = "red alarm"
   - 10.3 Action = Start pressing Break

11 End If
12 }
13 If {
   - 13.1 Distance < 1 meter
   - 13.2 Message = "Deadly Close";
   - 13.3 Action = Full Break

14 End If
}

C. Test bed Road System:

We are proposing a structure in which car will passes through a test-bed road system cameras, these cameras will assess the speed and behavior of the car and it will inform this information to a lamppost where lamppost is acting as a server. Also, a DRIPS screen will be attached to the Lamppost. That screen will show the instructions which are given to the self-driving car.

For example when 2 cars are traveling in opposite directions on a blind corner. Our server that is lamppost (in this case) will inform both cars to reduce their speed to avoid collision. A test-bed Road System will give information about the car's direction and speed. Which will help the server to indicate the required speed and direction to both cars

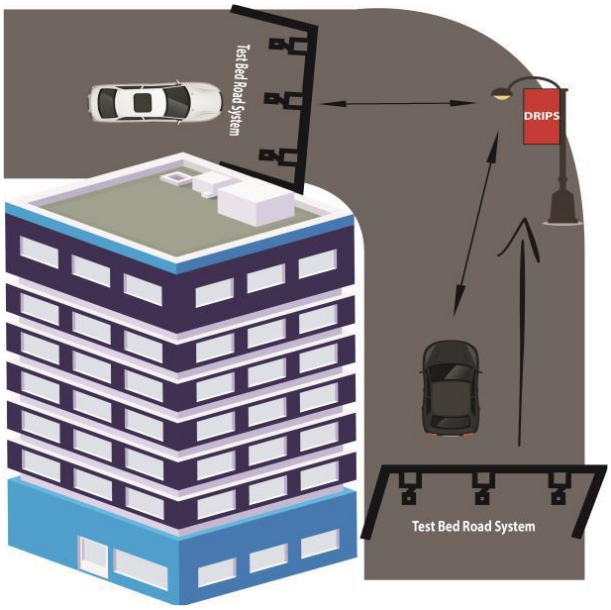

Fig: 3 Test Bed Road System

D. Bat Inspired Scheme:

The figure 3 shows that how bat inspired smart road infrastructure helps to avoid collisions of self-driving cars on blind spots. Two vehicles v1 and v2 are approaching to each other on blind curve. These vehicle take action on blind curve like speed change or applying break by looking at screen color. Controller takes input from the radar and calculate dimension and speed of vehicle that is approaching from other side and changes the color of screen accordingly.

Fig: 4 Bat inspired model for vehicle collision avoidance

This pseudocode takes inputs namely speed and dimensions of vehicles from radar, calculate warning level and shows that notification on screen by changing color.

Pseudo code: 3 Bat inspired Scheme

1. If (speed <=20 km and dimension = 3 square feet)
   - 1.1 Screen color ← Green
2. If (speed >20 km and dimension = 3 square feet)
   - 2.1 Screen color ← Yellow
3. If (speed <=20 and dimension 4>=6 square feet)
   - 3.1 Screen color ← Yellow
4. If (speed >20 and dimension 4>=6 square feet)
   - 4.1 Screen color ← Red
5. If (speed <=10 and dimension 7>=10 square feet)
   - 5.1 Screen color ← Yellow
6. If (speed >10 and dimension 4>=5 square feet)
   - 6.1 Screen color ← Red

IV. EXPERIMENTS AND RESULTS

Simulation is performed in a controlled environment using NetLogo simulation tool and found that when the heavyweight vehicle and low weight vehicle are at bind curve on the same time, heavyweight vehicle alerts high danger level to other vehicle and all other vehicles reduce their speed or apply break at that time depending upon the danger level. High, medium and low weight vehicles alert high medium and normal danger levels depending upon this danger level other vehicles take their actions. We performed 1000 test cases on different types of vehicles and found appropriate results as discussed above. Fig 5 shows the result of vehicle v1 and v2 danger level alerts.

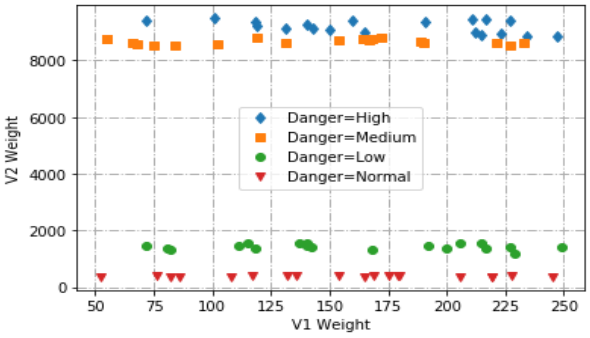

Fig: 5 vehicle v1 and v2 danger levels

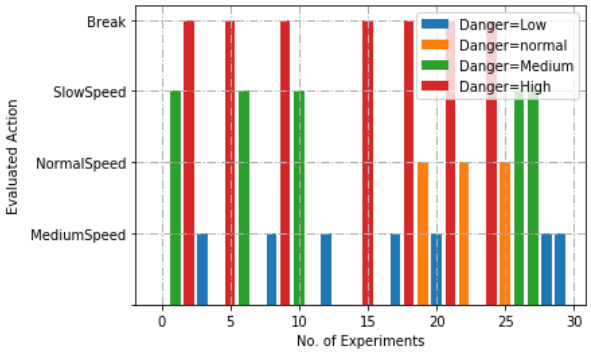

Fig: 6 Describes Evaluated action by vehicles depending upon danger level.

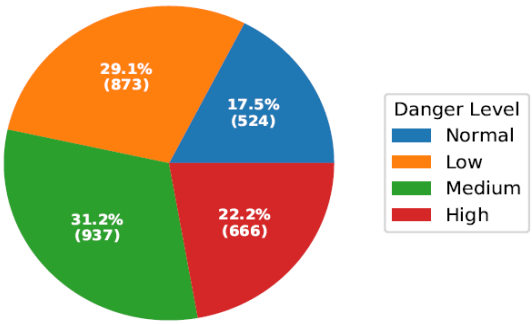

Fig: 7 shows percentage of normal high medium and low alerts.

V. CONCLUSION

In this paper, we have proposed novel collision avoidance schemes for self-driving cars in a controlled environment. These schemes are inspired by the biological system. As our body is working efficiently with the biological system, on the road by applying these schemes we are getting massive positive results in simulation. When the heavyweight vehicle and low weight vehicle are on a blind curve at the same time, heavyweight vehicle sends alert message “high danger level” to other vehicle and all other vehicles reduce their speed or apply break at that time. Danger level will depends on type of vehicle. Large numbers of experiments on vehicles are giving results by avoiding collision through following these schemes in a controlled environment. We are getting maximum results but it is expected that in the future when will complete mathematical modeling of our scheme, we may face some negative results.

REFRENCES

1. Sun, L., et al. *Courteous autonomous cars*. in *2018 IEEE/RSJ International Conference on Intelligent Robots and Systems (IROS)*. 2018. IEEE.
2. Kallioinen, N., et al., *Moral Judgements on the Actions of Self-Driving Cars and Human Drivers in Dilemma Situations From Different Perspectives.* Frontiers in Psychology, 2019. **10**(2415).
3. Nees, M.A., *Safer than the average human driver (who is less safe than me)? Examining a popular safety benchmark for self-driving cars.* Journal of Safety Research, 2019. **69**: p. 61-68.
4. Atzori, L., A. Iera, and G. Morabito, *The internet of things: A survey.* Computer networks, 2010. **54**(15): p. 2787-2805.
5. Wortmann, F. and K. Flüchter, *Internet of things.* Business & Information Systems Engineering, 2015. **57**(3): p. 221-224.
6. Li, S., L. Da Xu, and S. Zhao, *5G Internet of Things: A survey.* Journal of Industrial Information Integration, 2018. **10**: p. 1-9.
7. Gerla, M., et al. *Internet of vehicles: From intelligent grid to autonomous cars and vehicular clouds*. in *2014 IEEE World Forum on Internet of Things (WF-IoT)*. 2014.
8. Prasada, P. and K.S. Prabhu, *Novel Approach in IoT-Based Smart Road with Traffic Decongestion Strategy for Smart Cities*, in *Advances in Communication, Signal Processing, VLSI, and Embedded Systems*. 2020, Springer. p. 195-202.
9. Awad, A.Y. and S. Mohan, *Internet of Things for a smart transportation system.* International Journal of Interdisciplinary Telecommunications and Networking (IJITN),

2019. **11**(1): p. 57-70.
10. Babar, M. and F. Arif, *Real-time data processing scheme using big data analytics in internet of things based smart transportation environment.* Journal of Ambient Intelligence and Humanized Computing, 2019. **10**(10): p. 4167-4177.
11. Chou, H.-H., et al., *A chameleon-inspired stretchable electronic skin with interactive colour changing controlled by tactile sensing.* Nature communications, 2015. **6**(1): p. 1-10.
12. Laplante, P., *" Smarter" Roads and Highways.* IEEE Internet of Things Magazine, 2018. **1**(2): p. 30-35.
13. Ahmed, W., et al. *Model Intelligent Vehicle System for Life Safety at T, Y-Junctions*. in *2018 IEEE 21st International Multi-Topic Conference (INMIC)*. 2018. IEEE.
14. Franzò, S., et al. *Towards the New Concept of Smart Roads: Regulatory Framework and Emerging Projects Overview*. in *2018 International Conference of Electrical and Electronic Technologies for Automotive*. 2018. IEEE.
15. Dong, D., X. Li, and X. Sun. *A Vision-Based Method for Improving the Safety of Self-Driving*. in *2018 12th International Conference on Reliability, Maintainability, and Safety (ICRMS)*. 2018.
16. Riaz, F., et al., *A collision avoidance scheme for autonomous vehicles inspired by human social norms.* Computers & Electrical Engineering, 2018. **69**: p. 690-704.
17. Kabeer, M., et al., *Emotion Enabled Cognitive Driver.*
18. Borenstein, J., J.R. Herkert, and K.W. Miller, *Self-driving cars and engineering ethics: the need for a system level analysis.* Science and engineering ethics, 2019. **25**(2): p. 383-398.

2020 5th International Electrical Engineering Conference (IEEC 2020)
Feb, 2020 at IEP Centre, Karachi, Pakistan

Solar Power: A Way Out of Energy Crisis of Pakistan

Muhammad Hassaan Qadeer[1], Urooj Fatima[2], Misbah Kashif[3], Syed Umaid Ahmed[4] and Riaz Uddin[5*]

[1] Department of Electrical Engineering, NED University of Engineering and Technology, Karachi, 75290, Pakistan (riazuddin@neduet.edu.pk) *Corresponding author

Abstract: Pakistan is facing a significant supply-demand gap due to limited energy production, resulting in power cuts that are blamed for the country's instability. For years, this has been a major hurdle in the country's economic growth. The country with a short-fall of about 6000 MW has to opt for load-shedding in order to fulfill the demands. This load-shedding occurs mostly for uncertain period which disturbs the life cycle of many citizens. This article discusses the energy scenario of Pakistan with facts and figures leading to the load-shedding issue. Moreover, it proposes solution to energy crisis of the country by aiming to the sustainable alternative in terms of renewable energy. Pakistan, enjoying a higher rank among countries with great potential of solar irradiance can explore this resource not only to fulfill its demands but also to play a part in cleaning the environment of the world. With proper infrastructure and policies, Pakistan can utilize this potential to achieve a better solution to its energy crisis as well as to its economic conditions.

Keywords: Energy, Renewable, Solar, Irradiance, Cosmic

I. INTRODUCTION

Pakistan had been facing energy-crisis from past many decades. This energy-deficient country has a supply of 0.30 Tons Oil Equivalent (TOE) per person [approx. 14 BTUs]. Due to supply-demand gap, most areas of the country are victim of black-outs for an un-defined period. Pakistan has 581 kWh of per capita electricity generation in contrast with the global mean of 2657 kWh which enlightens the fact that the country needs power resources to fulfill its public demand [1].

Pakistan is blessed with almost all the sources of renewable energy including solar, hydel, biomass and wind. Among these sources, solar is the most abundantly available energy resource. This plethora has placed the country among the top ranked countries with the highest potential of solar energy. In Pakistan, the annual irradiance hits around 1900-2200 kWh/m^2 which provides a fast and effective short-term solution for the country to fulfill its demand by proper planning and efficient utilization of this solar potential. With solar power plants, Pakistan will not only fulfill its power demands but will also play its role in tackling the environmental threat to the world due to excessive green-house gas emissions [6].

II. ENERGY SCENARIO OF PAKISTAN

With the country's growing age, Pakistan is getting more dependable on imported energy which leads to major setback to its economy due to high oil prices in the international market. Although a major part of the country's budget is used for energy production, yet, the country is unable to meet the demands. Fig. 1 indicates the supply-demand gap of the country [3].

Currently, the country's deficit is 3000 MW to 6000 MW. This shortage of power leads to long hours of load-shedding, which badly affects all sectors including agriculture, industry, transportation, domestic and

	2012	2013	2014	2015	2016
Supply	12320	14600	16170	16500	17261
Demand	18940	18827	20576	21701	22559
Surplus/Deficit	-6620	-4427	-4406	-5204	-5298

Fig. 1 Electricity demand and supply during 2012–16

energy generation, hence, resulting in country's major economic loss. The country's total generating capacity is around 23,600 MW where as the country's total demand is approximately 27,000 MW [5]. Unfortunately, with growing industrialization and technology, the demand of energy will increase further thus, creating a greater difference between the supply and demand. Fig 2. shows the expected supply-demand curve from 2010-2030 which is considered to be increasing at 8-10% annual rate [12].

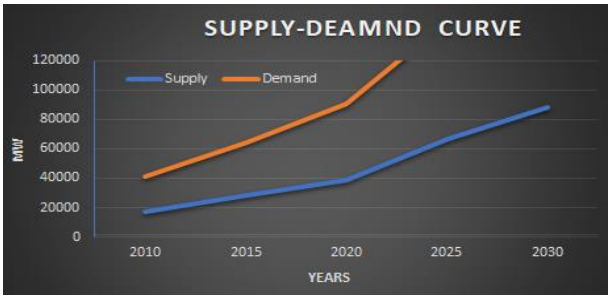

Fig. 2 Pakistan's supply-demand curve from 2010-2030

Acknowledging the fact that Pakistan is an energy deficient country, related authorities have been planning for improvements in this sector. Although non-renewable sources constitute the most in the energy production cycle of Pakistan, yet, the government has begun to utilize the renewable sources. As per the 2017 NEPRA State of Industry Report, Table 1 indicates the electricity generated from various sources in Pakistan whereas Table 2 refers to the energy mix ratio of the country [9].

Table 1 Electricity generated in Pakistan

SOURCE OF GENERATION	PAKISTAN
Oil (MW)	6785
Natural Gas (MW)	8868
Coal (MW)	810
Hydro Electricity (MW)	7116
Nuclear (MW)	1142
Renewables (MW)	1465

Table 2 Power mix ratio

RESOURCE	% OF PAKISTAN
Coal	3.09
Hydro Energy	27.17
Nuclear Energy	4.36
Oil	25.91
Natural gas	33.87
Renewables	5.59

Renewable energy resources are sufficient to satisfy global energy demands. Long-term reliable and pollution free power supplies can be guaranteed using these resources. Fig. 3 shows the technological capacity of Pakistan for multiple sources of renewable energy. Pakistan has 167.7 GW potential of sustainable energy, being 8 times higher than Pakistan's current demand for electricity, i.e. 21 GW [10].

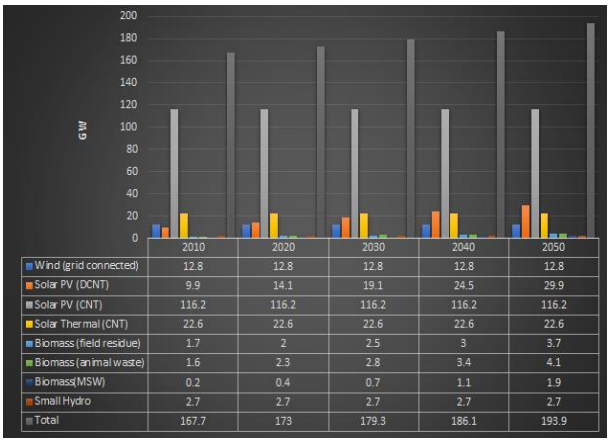

	2010	2020	2030	2040	2050
Wind (grid connected)	12.8	12.8	12.8	12.8	12.8
Solar PV (DCNT)	9.9	14.1	19.1	24.5	29.9
Solar PV (CNT)	116.2	116.2	116.2	116.2	116.2
Solar Thermal (CNT)	22.6	22.6	22.6	22.6	22.6
Biomass (field residue)	1.7	2	2.5	3	3.7
Biomass (animal waste)	1.6	2.3	2.8	3.4	4.1
Biomass(MSW)	0.2	0.4	0.7	1.1	1.9
Small Hydro	2.7	2.7	2.7	2.7	2.7
Total	167.7	173	179.3	186.1	193.9

Fig. 3 Different renewable sources projected potential for energy production in Pakistan (2010–2050)

From the figure, it is evident that the country has great potential for solar production and with the installation of solar plants, Pakistan can soon wipe out the load-shedding affair.

III. SOLAR POTENTIAL IN PAKISTAN

Being the sixth most wealthy country in terms of cosmic radiations with the planes of Southern Punjab, Sindh and Baluchistan enjoying around 8-10 hours of daily sunshine makes Pakistan's geography favorable for utilization of solar power. The intensity of solar energy in Pakistan's Sun Belt ranges in between 1800-2200 KWh/m^2 per day which again favors the exploitation of this renewable resource [12,13]. Figure 4 indicates the solar irradiations that fall in the country's major cities [6]. By some estimates, Pakistan's potential capacity of cosmic power is 1600 GW i.e. 40 times more than current consumption. When talking about off-grid systems, the country can fulfill 30% of its daily need as the sunshine is available during morning period only. Solar PV's average life expectancy is 25 years and has no maintenance costs. If solar photovoltaic panels were set up only on country's area of 100 km with an efficiency of 14 percent, 30 million tons of oil equivalent (MTOE) energy could be generated in the country and energy crises could be overcome [11].

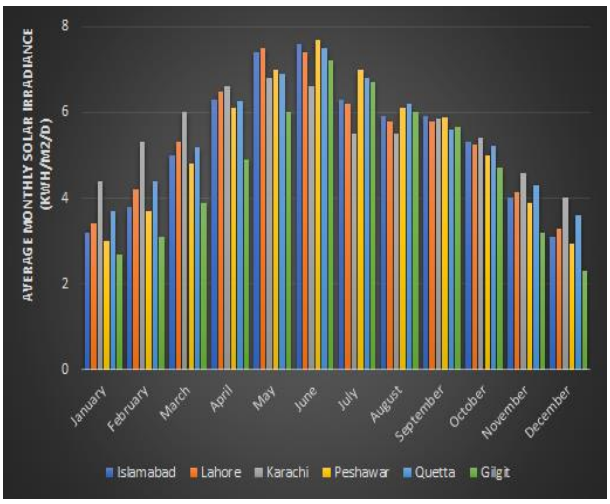

Fig. 4 Average monthly solar insolation

AEDB has calculated that Pakistan has an estimated potential of 2900 Gigawatt of cosmic power. On yearly basis Pakistan's solar energy production is 2.334 million Megawatts [4]. A research shows that 0.23 KW of electricity can be produced from 1 KW of solar PV which can considerably help to minimize load shedding in Pakistan.

Pakistan's solar potential (especially the provinces of Balochistan and Sindh) is the second highest in world. The average daily solar global plane radiation recorded under ESMAP is 5.67 kWh/m^2. The yearly mean everyday solar radiation (GHI) in the state was recorded in between 4.4 to 6.0 kWh/m^2 with an average of 5.3 kWh/m^2. Periodic maps of insolation (GHI) informed that yearly mean everyday solar radiation of the nation

is found to be 5.5 kWh/m^2. Pakistan's lowest yearly mean everyday solar insolation (4.3 kWh/m^2) is greater than world's yearly mean everyday insolation (3.6 kWh/m^2), that shows the marvelous solar power potential of the republic [5]. In Pakistan, Sindh and the province of Balochistan receives around 440 cal/cm^2 per day, while provinces of KPK and Punjab are obtaining an insolation of about 440 cal/cm^2 every day. The solar radiation owned by Kashmir is fewer than 400 cal/cm^2 per day [3]. In Pakistan, the mean universal irradiation dwindling on horizontal plane per day is approximately 200–250 watt for each m^2 [13].

With solar energy, electricity can be easily provided to rural areas without the fear of deforestation and energy safety [13]. In Islamabad, on 29th of May' 2012, Pakistan installed its first on grid solar power plant, especially contracted with Japan International Cooperation Agency (JICA) under Earth cooling project. This project has a capacity of 178.08 KW for PEC and Planning Commission of Pakistan (P block). The two bodies have shared production capability of 356.16 Kilowatts. The project permits the inheritors to sell of additional generation to the national grid. Pakistan installed the first huge scale Solar Park in Bahawalpur (Quaid-e-Azam Solar Park), which has the size of 1000MW and solar energy each year was 2000kWh/m^2. The accessibility of solar radiation is comparatively steady throughout the nation state, which calls upon the uses of solar power application like solar water heating, solar based crop drying, photovoltaics and desalination with solar. It was conveyed that nearly 7 solar stations having 234 KW of capacity were fitted in territory of Hindu Kush mountains (i.e. Himalayan region). DGNRER had mounted 18 solar setups throughout the state with 434 KW of total capacity. PCSIR had planned, established and fitted 5 solar desalination systems, 4 having capability of 250 gallons per day in Therparker and 1 having a size of 6000 gallons per day in Gwadar [5]. The table 3 represents the under-construction solar projects with their desired capacities [6].

Table 3 Projects of Solar PV under development

CONTRACTOR	CAPACITY (MW)	LOCATION	PROVINCE
Asia Petroleum	30	Chakwal	Punjab
First Solar Ltd.	2	Sindh	Sindh
Act Solar Ltd.	50	Nooriabad	Sindh
Jafri Associates	50	Nooriabad	Sindh
Solar Blue Ltd.	50	Punjab	Punjab
Adamjee Power	10	Thatta	Sindh
ET Solar Ltd.	25	Attock	Punjab
ET Solar Ltd.	50	Sialkot	Punjab
Crystal Energy	2	Thatta	Sindh
Forshine	50	Thatta	Sindh

IV. PAKISTAN AND SOLAR BASED TECHNOLOGY

Being commercially accessible technology, Solar PV energy has an important potential for longstanding progress. According to the Punjab Energy Subdivision, private businesspersons are performing work on solar plants in several regions, with an overall capacity of 90 MW [5]. Few applications of solar energy are being discussed below.

A. Solar water heating system

In Pakistan, this innovation has been broadly functionalized with yearly growth at 245 %. It was reported that about 9500 solar water heating divisions will be activated by 2015, and 24,000 divisions are expected to get operational by 2020. Exploiting solar water heating machinery as an alternative of natural gas or conservative source, has major advantages of cost-effective, environmental, and collective sustainability [12].

B. Solar liquid desalination

These technologies can be utilized to desalinate and cleanse saline water, which is not suitable for drinking, household and cleaning besides causing illnesses. These technologies are inexpensive, low tech and can be effortlessly implemented in these zones [13]. It desalts seawater or brackish water by means of solar distillation or by transforming the solar power into warm heat. The management of Baluchistan has mounted two solar projects in Gawadar, encompassing 240 stills where every plant can deal up-to 6 Kg of sea water on daily basis. Plans to progress with similar projects had been introduced for further areas of Pakistan [12]. In Gawadar, setup of two solar desalination projects have been finalized which can purify 6000 gallons of sea water. [13].

C. Solar PV

Solar grid plant fitted by the Pakistan Engineering Council and Planning Commission has a capacity of 178.08 Kilowatts, which fulfills its personal requirements and can even sell excess electricity to the Islamabad Electric Supply Company (IESCO). Likewise, the National Assembly of Pakistan installed a roof mounted solar project of 2 MW. The surplus production is fed back to the grid [11]. Solar Park, a super power project was built with the support of Chinese government at Bahawalpur City. It became purposeful in 2016 having an over-all capacity of 100 Megawatts. AEDB has provided LoI to additional 17 self-governing energy producers (IPPs) having total capacity of 484 Megawatt.

V. CONCLUSION

In Pakistan, mostly the energy is generated by fossil fuels creating loads of burden on country's economy due to costly imports of fossil fuels. Due to high

numbers of nation's population, huge gap between energy demand and supply has been created, resulting in power shortfalls. Since this supply gap has grown tremendously, therefore, all the industrial and other sectors of the country have been affected enormously. Our paper focuses on the minimization to the contribution of fossil fuels and to enhance renewable energy share (especially solar energy) to the country's power mix ratio. Solar energy technologies especially in Pakistan can be made well established and can be implemented to a vast scale due to the numerous amounts of solar energy availability. Solar energy is undoubtedly the most promising form of sustainable energy which can be game-changer in meeting the present and future energy demands. This is because it is the cheapest form of renewable energy, does not require a huge maintenance as compare to other means of energy production and has a greater life span. Moreover, Pakistan's topography, geographical location as well as its climatic conditions are well accurate and appropriate for the implementation of solar technologies to the maximum possible extent. The paper discussed the solar applications like solar PV, Solar water heating system and Solar liquid desalination but many more can still be discovered which can solve the country's energy deficiency and may become the gate-way of foreign investments with investors investing their money for the solar development in Pakistan. With this the paper concludes that if the country shifts towards solar energy-based technologies, the nation can get rid of energy crisis in a short time period.

REFERENCES

[1] S. M. N. Nawaz and S. Alvi, "Energy security for socioeconomic and environmental sustainability in Pakistan," 2018.

[2] Dr. S. R. Malik and M. A. Maqbool, "Energy Potential of Pakistan".

[3] S. Akhtar, M. K. Hashmi, I. Ahmed, and R. Raza, "Advances and significance of reflectors in solar energy technology in Pakistan," *Energy &Environment*, vol. 0, no. 0, pp. 1-21, 2018.

[4] F. Muhammad, M. W. Raza, S. Khan, and F. Khan, "Different Solar Potential Coordinates of Pakistan," 2017.

[5] Z. R. Tahir and M. Asim, "Surface measured solar radiation data and solar energy resource assessment of Pakistan: A review," 2017.

[6] F. Yazdan and M. N. Khan, "Identifying and Addressing Barriers to Solar PV Technology Indigenization in Pakistan," vol. 8, no. 1, pp. 1-3, 2018.

[7] "A Promising Future: Solar Energy to Become Cheapest Power Source in 10 Years," available at https://www.herox.com/blog/222-a-promising-future-solar-energy-to-become-cheapest.

[8] Q. A. U. Haq, "Design and Implementation of Solar Tracker to Defeat Energy Crisis in Pakistan," *I.J. Engineering and Manufacturing*, vol. 2, pp. 31-42, 2019.

[9] "NEPRA, National electric power regulatory authority. State of industry report 2017". Available at https://nepra.org.pk/industryreports.htm; 2019 [accessed 06-09-2019]

[10] M. M. Rafique and S. Rehman, "National energy scenario of Pakistan – Current status, future alternatives, and institutional infrastructure: An overview," *Renewable And Sustainable Energy Reviews*, vol. 69, pp. 156-157, 2017.

[11] M. Irfan, Z. Y. Zhao, M. Ahmad, and M. C. Mukeshimana, "Solar Energy Development in Pakistan: Barriers and Policy Recommendations," 2019.

[12] A. Raheem, S. A. Abbasi, A. Memon, S. R. Samo, Y. H. T. Yap, M. K. Danquah, and R. Harun, "Renewable energy deployment to combat energy crisis in Pakistan," *Energy, Sustainability and Society*, 2016.

[13] F. Bakhtiar and A. Ahmed, "A Review of Solar Energy in Pakistan: Current Status and Future Prospects," *Science, Technology and Development*, vol. 36, no. 3, pp. 189-195, 2017.